ABSTRACT

Title of Dissertation:	APPLICATION OF RECLAIMED WASTEWATER FOR AGRICULTURAL IRRIGATION: DEVELOPING A DECISION SUPPORT TOOL USING SPATIAL MULTI-CRITERIA DECISION ANALYSIS
	Manashi Paul, Doctor of Philosophy, 2020
Dissertation directed by:	Assistant Professor, Dr. Masoud Negahban-Azar, Environmental Science and Technology

Intensified climate variability, depleting groundwater, and escalating water demand create severe stress on high-quality freshwater sources used for agricultural irrigation. These challenges necessitate the exploration of alternative water sources such as reclaimed water to reduce the pressure on freshwater sources. To do so, it is key to investigate the spatial pattern of areas that are more suitable for water reuse to determine the potential of reclaimed wastewater use for irrigation. This study provides a systematic decision-analysis framework for the decision-makers using an integrated process-based hydrologic model for sustainable agricultural water management. The outcomes of this study provide evidence of the feasibility of reclaimed wastewater use in the agricultural sector.

The two objectives of this study were to: 1) identify the locations that are most suitable for the reclaimed wastewater use in agriculture (hotspots); and 2) develop the watershed-scale models to assess the agricultural water budget and crop production using different water conservation scenarios including reclaimed wastewater use.

To achieve the first objective, a decision-making framework was developed by using the Geographic Information System and Multi-Criteria Decision Analysis (GIS-MCDA). This framework was then tested in the Southwest (California), and the Mid-Atlantic (Maryland) regions. Based on WWTPs' proximity, sufficient water availability, and appropriate treatment process of the treated wastewater, the "Most Suitable" and "Moderately Suitable" agricultural areas were found to be approximately 145.5 km^2, and 276 km^2 for California and, 26.4 km^2 and 798.8 km^2 for Maryland, respectively.

These results were then used to develop the hydrologic models to examine water conservation and water reuse scenarios under real-world conditions, using the Soil and Water Assessment Tool (SWAT). In California, the combination of auto irrigation (AI) and regulated deficit irrigation (RDI) resulted in higher WP for both almond and grape (> 0.50 kg/m^3). Results also suggested that the wastewater reuse in almond and grape irrigation could reduce groundwater consumption more than 74% and 90% under RDI and AI scenarios, respectively. For Maryland, model simulations suggested that the green water productivity (only rainfall) can be improved up to 0.713 kg/m^3 for corn and 0.37 kg/m^3 for soybean under the reclaimed wastewater use scenario.

APPLICATION OF RECLAIMED WASTEWATER FOR AGRICULTURAL IRRIGATION: DEVELOPING A DECISION SUPPORT TOOL USING SPATIAL MULTI-CRITERIA DECISION ANALYSIS

by

Manashi Paul

Dissertation submitted to the Faculty of the Graduate School of the
University of Maryland, College Park, in partial fulfillment
of the requirements for the degree of
Doctor of Philosophy
2020

Advisory Committee:
Assistant Professor Masoud Negahban-Azar, Chair
Professor Adel Shirmohammadi
Associate Professor Hubert Montas
Associate Professor Kaye L. Brubaker
Professor Puneet Srivastava

© Copyright by
Manashi Paul
2020

Dedication

I would like to dedicate this dissertation to my parents, Ma and Baba. Anita Paul and Hari Narayan Paul are two pillars of my life, whose unconditional love and support have been a constant source of my strength and inspiration.

Acknowledgments

I would like to express my sincere gratitude to my advisor, Dr. Masoud Negahban-Azar, for his constant encouragement, support, and guidance throughout the journey for last four years. I would also like to express my gratitude to my entire advisory committee, Dr. Adel Shirmohammadi, Dr. Hubert Montas, Dr. Kaye Brubaker, and Dr. Puneet Srivastava, for their valuable advice and support.

I would like to acknowledge the Maryland Department of Environment (MDE), Maryland Geological Survey (MGS), Department of Environmental Science and Technology (ENST), UMD Global STEWARDS, Graduate School, and United States Department of Agriculture (USDA), for providing the resources, assistantship, fellowship, and funding for this research.

Thanks to all of my friends and colleagues in our ENST department, especially to Tuana Phillips, Amr Keshta, Sarah Ponte, Farshid Shoushtarian, Emily Keller, and Rahat Sharif, who kept their door open for many spontaneous conversations and encouraged me during my confusing times. Thanks to all 2019 UMD Global STEWARDS fellow, especially Sijal Dangol, for helping me during the critical research process. Thanks to Dr. Adnan Rajib, who always motivates me to pursue big dreams and be ambitious.

Finally, I am grateful to my support system, Ma, Baba, and my brother Tamal Paul, for their endless love and support. To Abu Sufian Mohammad Asib, thank you for your countless sacrifices and for walking this journey with me for the last seven years. Thank you for always believing in me even before I believed in myself.

Table of Contents

List of Tables

Chapter 2

Chapter 3

Chapter 4

Chapter 5

Chapter 6

Chapter 7

Chapter 8

List of Figures

Chapter 1

Chapter 2

Chapter 3

Chapter 4

Chapter 5

Chapter 6

Chapter 7

Chapter 8

List of Abbreviations

AHP	Analytical Hierarchy Process
CDL	Crop Data Layer
CR	Consistency Ratio
CWNS	Clean Watersheds Needs Survey
DSS	Decision Support System
FAO	Food and Agricultural Organization
FDA	Food and Drug Administration
FSMA	Food Safety Modernization Act
GIS	Geographical Information Systems
GLUE	Generalized Likelihood Uncertainty Estimation
GPD	Gallon Per Day
HUC	Hydrologic Unit Code
HRU	Hydrologic Response Unit
KGE	Kling-Gupta efficiency the (R^2),
LAI	Leaf Area Index
MCDA	Multi-Criteria Decision Analysis
MDE	Maryland Department of Environment
MGD	Million Gallon Per Day
NASS	National Agricultural Statistics Services
NPDES	National Pollutant Discharge Elimination System
NSE	Nash-Sutcliffe Efficiency

PABIAS	Percentage of Bias
ParaSol	Parameter Solution
PDSI	Palmer Drought Severity Index
POTW	Publicly Owned Treatment Works
R^2	Coefficient of Determination
RMSE	Root Mean Square Error
RSR	Ratio of Standard Deviation of Observations to RMSE
SUFI-2	Sequential Uncertainty Fitting
SWAT	Soil and Water Assessment Tool
SWAT-CUP	SWAT Calibration and Uncertainty Programs
USDA	United States Department of Agriculture
USGS	U.S. Geological Science
WHO	World Health Organization
WP	Water Productivity
WWTP	Waste Water Treatment Plant

Chapter 1: Introduction

1. Background

Water is constantly recycled through the hydrologic cycle. Climate change, such as changes in seasonal precipitation or temporal distribution, and magnitude of hydroclimatology, results in increases in either extreme drought or flooding (USGCRP 2018). In addition to climate variabilities, continuing growth in water demand among the agriculture, industry, and energy production sectors have put severe pressure on high-quality freshwater sources (Fant et al. 2016, Gohar and Cashman 2016, Taylor et al. 2013).

The agricultural sector is the largest consumer of freshwater globally, which consumes more than 70% of total freshwater withdrawals for food production (Jaramillo and Restrepo 2017, Pimentel and Pimentel 2007, Water 2009). The ongoing climate change, coupled with increasing water demand for human uses, have significant effects on water availability and water stresses in the agriculture sector (Ashraf Vaghefi et al. 2014, Nobre et al. 2016, Paul 2016, Paul et al. 2017), which adversely impacts the food security, at both regional and global scales (Anane et al. 2012, Montgomery et al. 2016). Within the current century, climate change is likely to further improve productivity in some areas and diminish it in others. For example, in Northern Europe, Denmark and Morocco, temperature increases have been shown to reduce grain yields of cereals due to shortening of the grain-filling period. At the same time, the combined effect of climate change is predicted to be beneficial in, e.g., Canada (Ali et al. 2017, Smith et al. 2013). For moderate changes in climate, the

adverse effects of increased temperature on grain yield are expected to be offset by the increased carbon dioxide (CO_2) concentration (Deligios et al. 2019). As a result, the deviations in crop production severely affect the regional economy, farm value, and socioeconomic development (Montgomery et al. 2016, Schmidhuber and Tubiello 2007). For example, observed historical data showed that extreme weather events caused significant corn yield reductions in U.S. (Karl et al. 2009).

Water scarcity is one of the most significant consequences of climate change, which suggests a necessity to explore alternative water sources to sustain food production in various countries across the world. To overcome this challenge, coupling reclaimed water to blue (water that flows through or below the land surface and stored in lakes, reservoirs, and aquifers) and green water (part of precipitation that infiltrates and is stored as soil moisture and then returns to the atmosphere via transpiration and evaporation) framework has the potential to significantly improve the water management for the agricultural areas (Falkenmark et al. 2004, Rees 2018). Reclaimed water resources may include reclaimed wastewater from wastewater treatment plants (WWTPs), return flows, desalination of seawater and highly brackish groundwater, and stormwater harvesting (Chen et al. 2016, Hurlimann and Dolnicar 2011, Rygaard et al. 2011). Previous studies show that agricultural irrigation with reclaimed wastewater has multiple advantages such as reducing pressure on freshwater sources (Jaramillo and Restrepo 2017, Rahman et al. 2016), improving nutrient management and recovery (Hanjra et al. 2015, Miller-Robbie et al. 2017), and producing higher reliability due to constant yields (Chen et al. 2012, Rahman et al. 2016). In both developed and developing countries, the most established water

reuse practice is the application of treated municipal wastewater for irrigation and other purposes (Angelakis et al. 2018, Jaramillo and Restrepo 2017). For example, many countries like China, India, Australia, Israel and the U.S. (e.g., California and Florida) have been using treated or partially treated wastewater for crop production (Hussain et al. 2002, Jimenez and Asano 2008, Keraita et al. 2008, Kivaisi 2001).

However, before the implementation of a water reuse project at the watershed scale, the potential (quantity and quality) and economic viability (cost-benefit analysis) of the recycled water sources should be assessed for the various irrigated crops (food/non-food crops). It is also necessary to analyze other key factors such as the technical feasibility (e.g., closeness to WWTPs), economic feasibility (e.g., water productivity), social acceptability (e.g., public acceptance and consumer response), and regulatory considerations (e.g., compliance with treatment requirements) (Ackerman 2012, Bixio et al. 2008, Jaramillo and Restrepo 2017, Saliba et al. 2018, Urkiaga et al. 2008). Thus, multiple quantitative and qualitative criteria need to be considered to plan for the reclaimed wastewater use for irrigation. It is necessary to identify the influential criteria and sub-criteria of the complex multi-criteria decision-making process and to analyze how these factors interact with each other. Identifying the most suitable locations considering all of the decision factors will be helpful to outline appropriate management strategies within a watershed.

Due to growing demands from industrial, hydropower generation, and urban sectors, the global water demand is projected to increase by 55% by 2050. These competing demands impose difficult water allocation decisions and limit sustainable development among users, particularly for food production and energy sectors.

According to the 2015 United Nations World Water Development report, agriculture will need to produce 60% more food globally by 2050 (Connor 2015). Therefore, appropriate evaluation of water allocation and water use management is required for developing strategies to cope with water scarcity. This complex network among various water users has led to extensive exploration of appropriate methodologies to describe and evaluate the rate of water consumption and available water flow within the watershed. Moreover, the effectiveness of managing reclaimed wastewater depends strongly on the hydrological system of the river basin, where the water reuse project is implemented. For decision-making process, an integrated approach of hydrological, economic, and environmental systems is required. Overall, understanding the consequences of wastewater reuse in irrigated agricultural watersheds is essential to seek the attention of policymakers and water resource managers so that the decision is selected in a manner to minimize risks to water quality and quantity, public health, and farmers' livelihoods.

2. Statement of the Problem

In the 2015 USGS water use report, reclaimed wastewater was reported as a source of irrigation water for 10 States (California, Florida, Arizona, Texas, Utah, Nevada, New Mexico, Colorado, Kansas, and Illinois), which accounted for less than 1% (669 MGD) of the total irrigation water used. Although a very small amount of reclaimed wastewater is used for irrigation purposes, its amount has increased from 472 MGD in 2010 to 669 MGD 2015 (Dieter et al. 2018). California, Florida, and Arizona are the leading users of reclaimed wastewater for irrigation with 289, 195, and 106 MGD, respectively. These numbers show that there is still great potential for

reclaimed wastewater use in agriculture that has not been fully exploited. However, long term data should be analyzed to project the future water demand and identify areas for additional reclaimed wastewater use (Urkiaga et al. 2008). Specifically, spatial mappings are needed to investigate the water demand (e.g., irrigation consumption) and freshwater shortage (e.g., groundwater).

To promote wastewater reuse in agriculture, the main challenge is to identify the available reclaimed wastewater sources in terms of quantity, quality, and accessibility, considering the different types of crops in certain locations. In addition, regulations, public health risks, and environmental impact must be evaluated for safe and rational implementation of wastewater reuse in agricultural use. Many researchers have acknowledged the advantage of knowledge-driven Decision Support Systems (DSSs) to derive the decision rules from existing knowledge to solve the area selection issues (Rajabi et al. 2014, Rikalovic et al. 2014, Saarikoski et al. 2016). However, most of the studies have been devoted only to farmers' and stakeholder's perceptions of treated wastewater use and its environmental and public health risk assessment (Ackerman 2012, Jaramillo and Restrepo 2017, Saliba et al. 2018). Also, past studies have assessed the feasibility of reclaimed wastewater use at small scales (e.g., only including few farms and treatment plants) (Anane et al. 2012, Neji and Turki 2015). As such, minimal attention has been paid to evaluate the potential of reclaimed wastewater use in agriculture and its economic viability for a variety of crops at larger scales (e.g., at a regional scale or for an entire state).

Although treated wastewater is used globally, the characterization of hydrological processes of these systems is not evaluated enough. It is important to address where

additional water is required and how crop production is affected by direct treated effluent use from a WWTP. It is also necessary to analyze the environmental and ecological effects of recycled water use and evaluate multiple scenarios to choose the best option. As a result, model-based DSS is required for the policy-makers and water resource managers to have adequate information about the benefits and challenges of water reuse options. Therefore, systematic interdisciplinary research is needed to understand the interaction between the driving factors for the reclaimed wastewater use in agriculture, the influential factors for irrigation in different crops, and the effects of direct water reuse on the water balance of the watershed.

Therefore, for the successful implementation of water reuse projects, three knowledge gaps should be addressed:

(i) lack of integral data and knowledge (such as water reuse guidelines and regulations, quality and quantity of treated wastewater, supply and demand ratio of reclaimed wastewater) of the multiple decision criteria for water reuse in spatially heterogeneous agriculture land;

(ii) absence of hydrologic model application to evaluate irrigation scenarios with treated wastewater; and

(iii) missing connection between model-based information and governing policy at the regional scale (impact of regulations on use of reclaimed water for various types of crops).

Therefore, key question was-

How to address all the challenges through interdisciplinary research that can enable the safe and successful use of recycled water for irrigation and provide recommendations for the policymakers?

More specifically, this research aims at addressing the following questions:

1) What are the main decision criteria and sub-criteria to assess the potential of reclaimed wastewater use for irrigation?

2) How to identify and classify suitable agricultural land for reclaimed wastewater use?

3) How to integrate all the decision criteria with hydrologic models as the driving engine?

4) And, to what extent can a hydrologic model be used to evaluate the irrigation water management considering different wastewater reuse and irrigation scenarios?

3. Objectives and Approach

The main objectives of this research were:

Objective 1: *To develop a framework for the identification of the most suitable areas (hotspots) for water reuse in agriculture.*

To obtain the first objective, a knowledge-driven DSS was developed using the Geographical Information Systems (GIS) combined with Multi-criteria Decision Analysis (MCDA) approach to assess the suitable agricultural land for reclaimed wastewater use. For this objective, the goals were:

- ➔ to evaluate the feasibility and suitability of reclaimed wastewater for irrigation considering multiple criteria.

➔ to apply the GIS-MCDA approach to identify the agricultural hotspots that are best suited for the use of reclaimed wastewater for agricultural irrigation.

Objective 2: *To develop a watershed-scale model to assess the agricultural water budget and crop production using different water conservation scenarios including reclaimed wastewater use.*

For the second objective, two agriculture-based watersheds were selected within the agricultural hotspots identified in the previous objective. Afterward, model-driven DSS was developed for two hydrologic models for further exploration of the appropriateness of sustainable reclaimed wastewater use in agricultural irrigation. The goals were:

➔ to develop sustainable irrigation scenarios to save freshwater, including direct reclaimed wastewater use.

➔ to estimate the crop water productivity for the irrigation scenarios and provide the best solution for the dry years.

A holistic conceptual framework was developed for this study, ensuring the transition from data to information and knowledge, to develop the decision support system (Figure 1). This framework was applied for two case studies representing two regions of the USA- California (Southwest) and Maryland (Mid-Atlantic) (Figure 2). Where, California has five major climates and mainly dominated by Mediterranean (Csa, Csb) and Semi-arid (BSk) climate. While, Maryland is dominated by Humid Subtropical (Cfa) and Continental (Dfa, Dfb) climate.

4. Dissertation Outline

This dissertation covers the transition between the steps of developing the decision framework for two study areas, the states of California and Maryland. These steps are described in the subsequent chapters, for California (Chapter 3-6) and Maryland (Chapter 7-8), respectively. Of note is, two of these chapters have already been published as peer-reviewed journal articles (chapters 3 and 4), and are included here in slightly modified forms. The rest of the chapters are included as separate manuscripts to be submitted to journals.

Chapter 2 presents the literature review on the climate change impact of freshwater and how this influenced to use reclaimed wastewater needs for agricultural irrigation. This chapter also provides a detailed description of two key components of the decision framework, GIS-MCDA, and hydrologic model.

Chapter 3 is titled "*Assessment of Agricultural Land Suitability for Irrigation with Reclaimed wastewater Using Geospatial Multi-Criteria Decision Analysis."* It presents the detailed assessment of merging GIS and AHP to enhance the predictive ability of the MCDA approach for the identification of hotspots that are more suitable for water reuse in the Southwest region (California).

Chapters 4-6 present different phases of the hydrologic model application to evaluate the model predictability in California agricultural water management, including reclaimed wastewater irrigation. Due to the complexity of California's hydrology, this task expanded into 3 chapters.

Chapter 4 is titled "*Sensitivity and uncertainty analysis for streamflow prediction using multiple optimization algorithms and objective functions: San Joaquin*

Watershed, California." This chapter portrays the evaluation of the model calibration performance and sensitivity and uncertainty analysis for streamflow prediction of a California watershed.

Chapter 5 is titled "*Agricultural water management decisions in ungauged semi-arid watersheds: the value of remote sensing integrated hydrologic modeling."* This chapter illustrates the remote sensing application to improve model performance for evapotranspiration and crop yield prediction.

Chapter 6 is titled "*Assessing the water productivity of the efficient irrigation strategies in a water-stressed agricultural watershed: San Joaquin Watershed, California."* This chapter presents the assessment of different irrigation management scenarios, including reclaimed wastewater use for almond and grape production.

Chapter 7 is titled "*Multi-criteria Decision Analysis to Evaluate Reclaimed Wastewater Use for Agricultural Irrigation: The case study of Maryland."* This chapter presents the GIS-MCDA application to evaluate the potentiality of irrigation with reclaimed wastewater use from Maryland's WWTPs.

Chapter 8 is titled "*Assessment of Sustainable Irrigation Water Resource Management Practices using the Hydrologic Model in Maryland."* This chapter describes the hydrologic model application to assess the potentiality reclaimed wastewater use for corn and soybean as the two most dominant crop production.

Finally, Chapter 9 summarizes the findings of this research study and presents the conclusion and directions for future research.

5. *Figures*

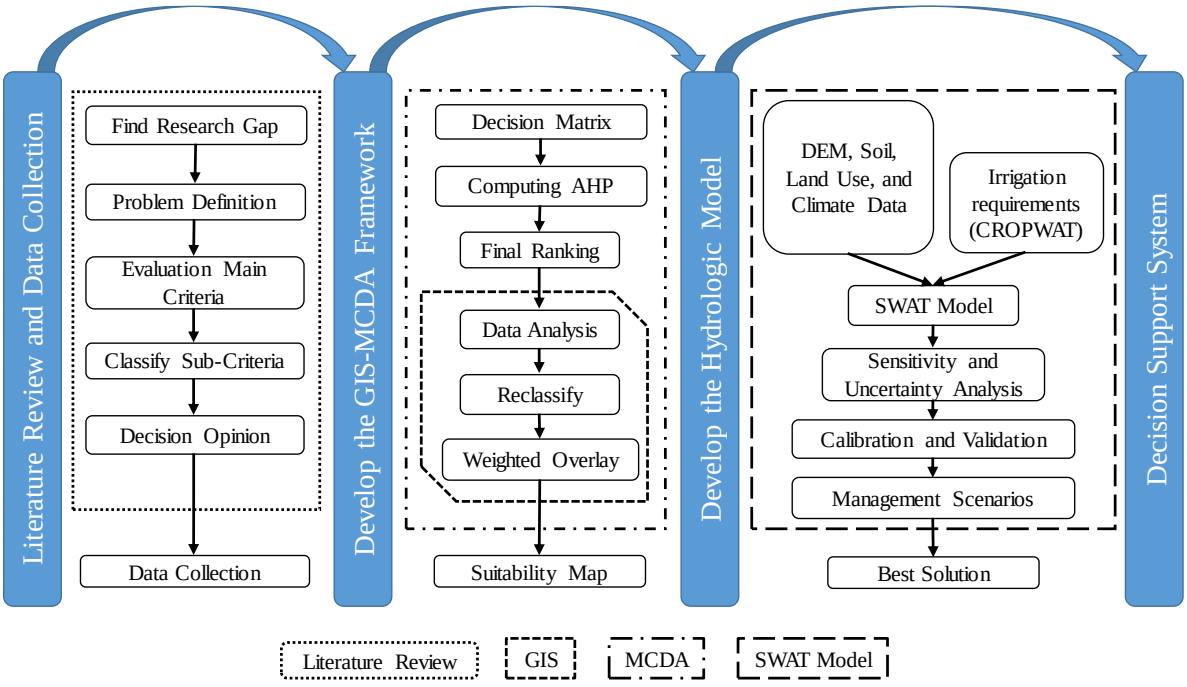

Figure 1: Schematic representation of the conceptual framework applied in this research.

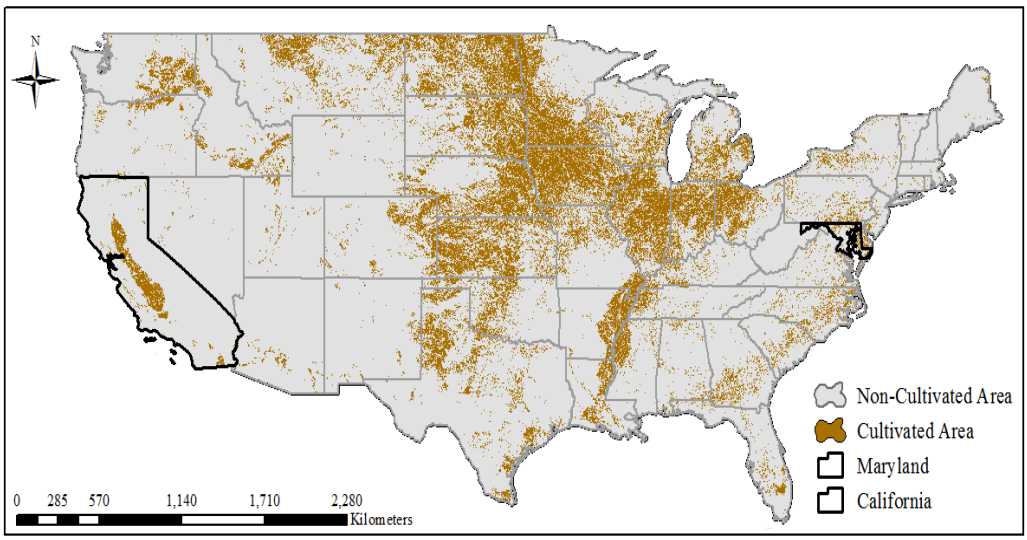

Figure 2: Locations of the case study areas (outlined in black) representing the Southwest and Mid-Atlantic region.

Chapter 2: Literature Review

1. *Climate Change and Overuse Impact on Freshwater and Agriculture*

Each year produced crops, livestock, and seafood contribute more than $300 billion to the U.S. economy (USGCRP 2014). According to the 2017 United States Department of Agriculture Economic Research Service (USDS-ERS), 21.6 million full and part-time jobs (11% of US employment) were related to agriculture and food industries which contributed almost $1.053 trillion (5.4% share) to U.S. gross domestic product (GDP) (USDA-ERS, 2018).

Extreme Events: Since 1980, the U.S. has endured 219 weather and climate disasters where the cumulative damage costs exceed $1.5 trillion (Smith 2018). Each disaster has a distinct footprint of impact such as- wildfire impacts on the west of the Plains and Southeast states, high-frequency inland flooding events in the adjacent states to large rivers or the Gulf of Mexico, drought impacts in the Southern and Plains states where billions of dollars' worth of agriculture and livestock assets are established. California's recent near-record high temperatures and low precipitation caused severe drought conditions, including low reservoir levels in the state (NOAA 2016). As a result of the intense drought conditions in 2015, California's irrigated acres decreased by 10% from 2010, and irrigation withdrawals declined 4,070 MGD (18% of total irrigation use).

Overuse: Nationwide, 70% of fresh groundwater (82,300 MGD) withdrawal is used for irrigation (Dieter et al. 2018). Only 5 states -California, Arkansas, Nebraska, Idaho, and Texas are accounted for 46% of the total groundwater (freshwater) withdrawals for all categories nationwide. According to USGS 2015, only California

accounted for almost 9% of the total withdrawals and 9% of freshwater withdrawals in the United States, which are predominantly used for irrigation. This freshwater was mainly provided from six major water distribution systems, where the Colorado River is a critical source for this state. To meet the high demand for irrigation and urban water demand in Southern California, Colorado River provides 55 to 65% of the total supply (CRWUA, n.d.). Due to the combined effect of climate change and overuse, a significant storage drawdown has resulted in the Colorado River Basin, which resulted in water delivery shortage and decreased hydropower production (Sheikh 2019). Currently, 15% of the Colorado River's supply is used by cities with a population of 40 million, and 70% is used to irrigate 5.5 million acres of land (Sheikh 2019). It is estimated that by 2060 the number of people supported by the Colorado River could double, which will increase water withdrawals from the river ("Three Reasons", 2017). If farms are not expanding, and water demands are not expecting to increase, still, farmers have to compete with the growing cities to buy water rights to maintain their growth.

Unlike the Southwest region of the U.S., the Mid-Atlantic region is experiencing higher temperatures during winter and summer and heavy precipitation in spring and fall (Boesch, 2008; Mallakpour and Villarini 2017). Despite heavy precipitation, the Mid-Atlantic region experiencing intermittent rainfall with higher temperatures, especially during the growing season. As a result, recurrent short-term droughts are becoming more frequent, and the evaporation rate increased during the summer. This higher temperature during the growing season leads to more evaporation loss and a decrease in soil moisture (Boesch, 2008). Based on 100 years (1901-2001) historical

data, only in Maryland the average annual precipitation was 1092.2 mm (43 in) or 25,000 MGD (million gallons per day) while water lost by evapotranspiration was about 711 mm (28 in) or 17,000 MGD (NOAA, 2002).

In addition, rapid urbanization and population growth resulted in a complex set of changes in water consumption among different sectors. For example, industrial and commercial use declined over the years, while domestic use, public supply, and irrigation use significantly increased. This water demand is expected to rise in the future with increasing suburban land development that affecting the groundwater recharge area and increasing irrigation needs on agricultural land during summer droughts (Boesch, 2008). As a result of higher freshwater demand and climate change, Maryland's aquifers are experiencing several challenges such as declining water table, salt-water intrusion, poor water quality, lack of productive aquifer, etc. (Figure 1 and Table 1). The long-term observation records from many of the monitoring wells located in the coastal plain are also showing the declining trend of groundwater table (Figure 2).

2. Influential Criteria of Reclaimed Wastewater Use for Irrigation

One of the main important aspects of reclaimed wastewater use is the economic feasibility of the project, which is mainly driven by the treatment plant's capacity and the water distribution cost from the source to the point of use (Bixio et al., 2008; Hernandez et al., 2006; Urkiaga et al., 2008). Therefore, the proximity of the wastewater treatment plants to its point of use (agricultural land) and the volume of treated water are the two important criteria to consider.

However, it is also crucial to maintain the treatment level to reduce the risk of pathogens presence on the soil and crop (Bixio et al., 2008; Jaramillo and Restrepo, 2017; Urkiaga et al. 2008). The Food and Agriculture Organization of the United Nations (FAO) has developed the guidelines for the agricultural reuse of treated water. However, to allow irrigation with reclaimed wastewater for edible crops, the US Food and Drug Administration (FDA) Food Safety Modernization Act (FSMA)'s Produce Rule provides stricter guidelines. The FSMA's Produce Rule applies to most agricultural producers of food crop, especially a strict microbial quality standards for irrigation water for fresh produce crops, especially which consumed as raw (Allende et al. 2018, Astill 2018, Dougherty 2016). According to California's Water Recycling Criteria-Title 22, the Category 3 reclaimed wastewater meets the FSMA rule requirement for coliform assay (Figure 3) (Sheikh, 2015). This requirement is emerging the necessity to categorize the existence of crop patterns and create a map of their spatial distribution.

3. Developing Decision Analysis Framework

To obtain the objectives of this study, both Knowledge-driven and Model-driven DSSs are required (Jha 2010, Power 2000). Knowledge-driven DSS provides management advice or to choose the best option based on expert knowledge and historical record. Model-driven DSS employs the complex systems that help in formulating alternatives, analyzing impacts of alternatives, and interpreting and selecting appropriate options. A reliable assessment needs to include comprehensive multiple decision criteria interactions and address the challenge of capturing the complex hydrologic and irrigation system. Based on relevant literature review,

existing research gaps are identified regarding the development of integrated framework (coupled knowledge-based and model-based DSSs), which can be a useful tool for understanding the interaction of multiple criteria for water reuse and quantifying the hydrologic and economic effects of changing irrigation policies and management decisions. Therefore, the literature review of this study was focused on finding the best solution of knowledge-driven DSS for mapping the suitable agricultural land for irrigation with reclaimed wastewater use and model-driven DSS to evaluate the complete water budget for water reuse management.

3.1. Multi-Criteria Decision Analysis

To effectively assess the feasibility and suitability of agricultural land for reclaimed wastewater irrigation, spatial analytical and optimization methods are needed to evaluate multiple spatial criteria and objectives. To solve this multidisciplinary problem, MCDA is required, which can consider multiple objectives, criteria, and constraints. In the MCDA process, the required inputs are scores across several dimensions associated with different alternatives and outcomes; and weights relating to tradeoffs across these dimensions (Huang et al., 2011). The total value score (*V*) for an alternative is calculated as a linear weighted sum of its scores across several criteria (Eq.1).

$$V_i = \sum_{j=1}^{n} W_j X_{ij} \quad \text{(i)}$$

where X_i represents the score on a single value scale. The weights Wi sum to 1.

The assessment of irrigated agricultural land suitability for reclaimed wastewater use is a spatial decision problem, which involves spatially variable decision criteria.

This complex geospatial problem leads to the necessity of using Geographical Information Systems combined with Multi-criteria Decision Analysis (GIS-MCDA). Many researchers have acknowledged the advantage of knowledge-driven approaches like GIS-MCDA method in data-sparse situations, where decision rules derived from existing knowledge are used to solve the area selection issues and potential mapping problems (Harris et al., 2001; Machiwal et al., 2015; Rajabi et al., 2014; Stevens and Pfeiffer, 2011). The GIS-MCDA method has been widely used in several environments and water-related research to improve the transparency, adaptability, and analytical accuracy of decision making in water resource management (Akıncı et al., 2013; Assefa et al., 2018; Montgomery et al., 2016). Worldwide, many water resource managers and decision-makers have applied the GIS-MCDA method in agriculture, water resources management, and environmental science (Anane et al., 2012; Assefa et al., 2018; Assefa et al., 2015; Nketiaa et al. 2013; Rikalovic et al., 2014).

There are several methods of combining multiple criteria for optimal decisions: multi-criteria value function methods such as pairwise comparison method (Saaty, 1977). This is also known as the Analytical Hierarchy Process (AHP) (Saaty, 1978). It is developed as a general theory of measurement based on obtaining preferences or weights of importance to the criteria and alternatives (Saaty 1987). This approach allows to represent the full range of human decision-making logic and to evaluate decision-making objectives and to handle multiple criteria and compensating both qualitative and quantitative data (Assefa et al., 2018; Opricovic 2011; Woltersdorf et al., 2018).

In the AHP method, a hierarchy structure is formulated to organize the complex multi-criteria problem in a number of levels. In this decision hierarchy, the first level corresponds to the general purpose of the problem, the second level to the criteria, and the third level to the sub-criteria (Kabir, 2012; Kabir et al., 2014; Saaty, 1980). The criteria are weighted on a scale from 1 to 9, where the 9 indicates "Extremely Importance" and 1 indicates "Equal Importance" (Saaty, 1977). Once the judgments or the weights of the criteria have been entered into the comparison matrix, the consistency of the pairwise matrix is checked using the consistency ratio (CR). The CR of the pairwise matrix is used as an indicator of the degree of consistency or inconsistency (Feizizadeh and Blaschke, 2014; Feizizadeh et al., 2014; Saaty, 1977). CR compares a consistency index (CI) of the matrix with the consistency of a random-like matrix (RI).

$$CR = \frac{CI}{RI} \tag{ii}$$

Where random index (RI) is the average of the consistency index of the randomly generated pairwise comparison matrix (Assefa et al., 2018). The CI is the consistency index calculated from the pairwise matrix and can be expressed as:

$$CI = \frac{\lambda_{max} - n}{\mathrm{n} - 1} \tag{iii}$$

Where λ_{max} is the largest eigenvalue of the pairwise comparison matrix, n is the order of the matrix. For CR value ≤ 0.10 indicates that judgments are consistent and are suitable for the implementation of the AHP analysis (Saaty, 1977). For CR values greater than 0.10, the pairwise comparisons matrix needs to be adjusted, and the weighting values should be modified.

AHP has been applied for solving a wide variety of water resources problems, where complex criteria across different levels are involved (Assefa et al., 2018; Hamouda et al., 2012; Machiwal et al., 2011; Srdjevic et al., 2012; Woltersdorf et al., 2018). Few studies have been found which used integrated GIS-MCDA technique with the AHP method to assess the land suitability and allocation regarding non-traditional water use for irrigation (Aldababseh et al., 2018; Anane et al., 2012; Assefa et al. 2018). However, these studies explored the feasibility of reclaimed wastewater use in agricultural land either at a small scale or for an existing crop pattern. No study was found that considers the spatial distribution of existing diverse crop patterns for a large number of water sources with the combination of their proximity, capacity, and different treatment processes.

3.2. Hydrologic Models

The hydro-ecosystem structures (i.e., land use and land cover, vegetation, soils, hillslopes, water bodies, infrastructure, etc.) spatially controls the effects of the climate on functions (i.e., crop production, evapotranspiration, water use decision and management, irrigation, etc.) (Childers et al., 2014; Eshtawi et al., 2016; O'Keefe et al., 2012). Therefore, water resources assessment within a watershed scale should focus on the flow of water between different hydrologic components in a climate-water nexus. A model-based DSS approach could evaluate this climate-nexus with the long term historic records. A Model-driven DSS has analytical capabilities to answer "what if" scenarios and to choose the best option among a set of alternatives. Figure 4 conceptualizes the relationship between water resources (water inputs), water consumptions (withdrawal), and the role of treated wastewater application

(reuse) in the water system in a watershed. It reflects the synergies and symbiosis between water resources, human decisions, and biophysical processes at a watershed scale, showing the water budget components (vertical and horizontal), climate functions, and hydro-ecosystem structure. This figure also indicates that as an additional source to the natural flow, the non-traditional water sources (e.g., desalinated water, treated wastewater, and harvested stormwater) have impacts on the watershed hydrology. Both horizontal and vertical water components are dominated by water supply and drainage, which influence the quantities of treated wastewater as a non-traditional water resource. In addition, since the successful implementation of sustainable water resources policies depends on the long-term hydrological assessments, a hydrologic model is required, which allows historical time series in the system. In this case, the hydrologic modeling approach has proven as an effective tool in such a physical interpretation.

Hydrologic models are effective tools to understand and simulate the hydrologic processes (including streamflow and water budget components), and to evaluate the effects of agricultural management practices, conservation scenarios, and help make watershed management decisions (Paul 2016, Paul et al. 2017, Shao et al. 2017, Wang et al. 2016). The watershed hydrologic model uses a set of mathematical descriptions to simulate the hydrologic cycle. Numerous physically-based hydrologic models have been developed and applied across the world to assess the different hydrologic processes (Borah and Bera 2003, Devia et al. 2015, Li et al. 2015). The critical question for hydrological model studies is to select the most appropriate model. One of the most important issues that need to be considered is the spatial scale

that incorporated in the study and how much physical detail can be included. Figure 5 illustrates the relation between the spatial scale and physical detail of the available hydrologic models.

Computational efficiency of the models is another important key for choosing the right model for a particular study. Worldwide researchers applied various hydrologic models to study the hydrologic phenomena and cycle like empirical/metric models, conceptual/parametric models, physically-based models, etc. Conceptual models like Variable Infiltration Capacity (VIC) and Hydrologiska Byrans Vattenavdelning (HBV) are a semi-distributed model that performs efficiently for flood regimes while TOPMODEL in shallow soil and moderate topography (Dettinger et al. 2011, Devia et al. 2015). Compared to other models physically-based models, like Mike-SHE and SWAT, are performs better where these required significant amounts of data and empirical parameters (Devia et al. 2015, Golmohammadi et al. 2014).

A suitable model also can be chosen based on its range of applications in a complex hydrologic system. Borah and Bera (2003) reviewed 11 hydrologic models based on their various application and performance on different watersheds and found that Hydrological Simulation Program –Fortran (HSPF) performed well for long-term continuous simulations in mixed agricultural and urban watersheds and Soil and Water Assessment Tool (SWAT) in predominantly agricultural watersheds. While Dynamic Watershed Simulation Model (DWSM) is capable of simulating storm events (rainfall) for agricultural and suburban watersheds.

Among these models, SWAT is extensively used as an effective tool for agricultural water resource management (Panagopoulos et al. 2014, Sorando et al.

2019, Uniyal et al. 2019, Van Liew et al. 2003). This model also used by many water resource managers and policymakers for decision-making process in watershed management (Baker et al. 2013, Giri and Nejadhashemi 2014, Senent-Aparicio et al. 2017, Sulis et al. 2009). SWAT is a watershed model (Arnold et al. 1998), which is developed to evaluate the impact of land management practices and climate on the water in large and complex watersheds over long periods. In SWAT, different water balance components, and water resources (e.g., blue and green waters) are calculated through an explicit calculation at the subbasin level. In this model, a watershed is divided into a number of subbasins and based on homogeneous soil types, land-use types, and slope classes categorized into hydrological response units (HRUs) that allow a high level of spatial detail simulation.

SWAT simulates the hydrologic cycle based on water balance equation:

$$SW_t = SW_o + \sum_{i=1}^{t}(R_{day} - Q_{surf} - E_a - w_{seep} - Q_{gw}) \quad \text{(iv)}$$

Where SW_t and SW_0 are the soil water storage at time t and 0 respectively, R_{day} is the precipitation, E_a is the actual evapotranspiration, Q_{surf} is the surface runoff flow, Q_{gw} is the groundwater flow, and w_{seep} is the deep aquifer recharge.

For the water budget, SWAT differentiates the solid (snow/freezing rain) and liquid (rain) precipitation based on the mean daily air temperature. If the air temperature is lower than snowfall temperature, then precipitation is considered solid (i.e. snow), which will accumulate until melt. In SWAT, snowmelt in the model was estimated through a mass balance approach:

$$SNO = SNO + R_{day} - E_{sub} - SNO_{mlt} \quad \text{(v)}$$

Where, SNO is the total amount of water in the snowpack on a given day (mm H2O), E_{sub} is the amount of sublimation (mm H_2O), and SNO_{mlt} is the amount of snowmelt (mm H_2O). Changes in snowpack volume depend on additional snowfall or release of meltwater in the basin. A more comprehensive description of the equation used by SWAT can be found in Neitsch et al. (2011).

Precipitation may be infiltrated into the soil surface or intercepted and held in the vegetation, and excess water moved as runoff towards the stream channel. SWAT provides two methods for the surface runoff estimation- through an empirical model like SCS curve number procedure and the Green & Ampt infiltration method which is a physical-based equation. While water intercepted by vegetation, it can be held as canopy storage and made available for evapotranspiration. According to Penman (1956), the potential evapotranspiration is defined as "the amount of water transpired by a short green crop, completely shading ground, of uniform height and never short of water". For the potential evapotranspiration (PET) estimation, three methods have been incorporated into SWAT: the Penman-Monteith method, the Priestley-Taylor method, and the Hargreaves method. After the PET estimation, the actual evapotranspiration is determined. SWAT calculates the actual amount of transpiration and soil evaporation or snow sublimation. Actual soil evaporation is calculated using exponential functions water content and soil depth (Neitsch et.al., 2011).

The SWAT model has gained international acceptance as a robust interdisciplinary watershed modeling tool, as evidenced by hundreds of SWAT-related papers (Dietrich and Funke 2009). A distributed watershed model like SWAT aims to support policy

and decision-makers to take the spatial distribution of relevant natural and socio-economic characteristics of the watershed and water uses into account. SWAT is not only a hydrologic model to simulate the hydrologic processes; it also uses a plant growth sub-model to simulate all types of land cover (Wang et al. 2016). This plant growth sub-model is used to assess the removal of water and nutrients from the root zone, transpiration, and biomass/crop yield. Therefore, worldwide SWAT is being extensively used to simulate crop growth, hydrologic balance, soil erosion, and other environmental responses by numerous researchers. Its applicability for the predictions of flows, water budget including hydrologic components, and crop water use has been verified by the various studies (Ahmadzadeh et al. 2016, Ashraf Vaghefi et al. 2017, Paul 2016, Rajib et al. 2016, Shao et al. 2017). Researchers also applied the SWAT model to investigate the potential of non-traditional water resources for different crop irrigations. For instance, treated wastewater for paddy irrigation (Jeong et al. 2016), desalination and stormwater harvesting (Eshtawi et al. 2016), and wastewater reuse for cotton (Panagopoulos et al. 2014), etc.

4. *Figures*

Figure 1: Locations of different aquifers within Maryland State. Map is collected from Maryland Geological Survey (MGS) (http://www.mgs.md.gov/groundwater/gw-status.html)

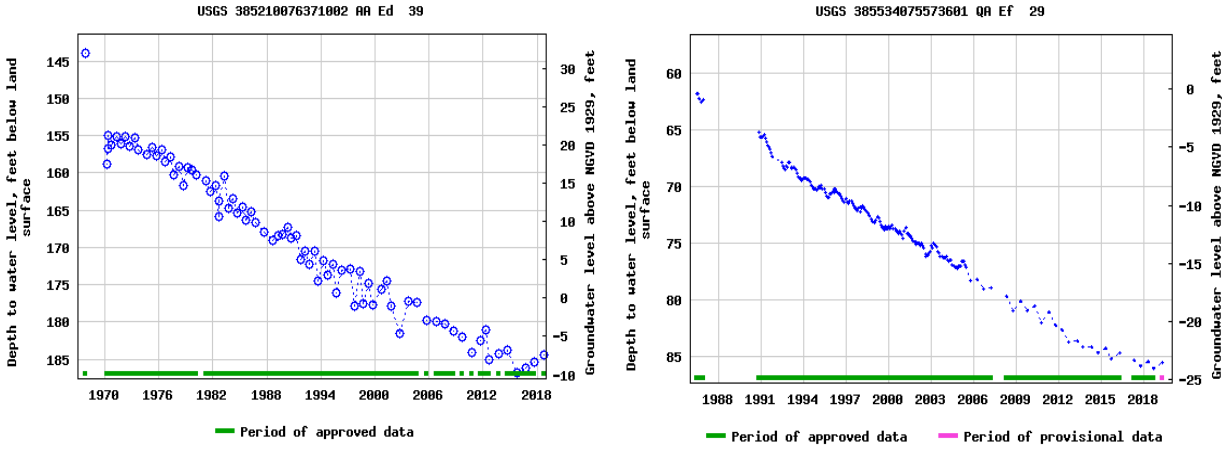

Figure 2: Declined groundwater trend of represented wells a) Western shore (Magothy aquifer) and b) Central Eastern shore (upper Patapsco aquifer).

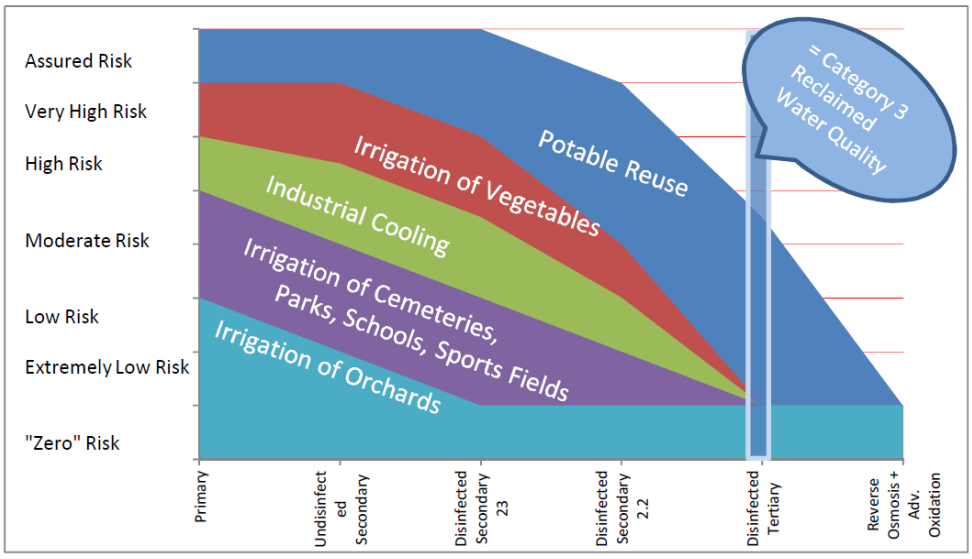

Figure 3: Illustration of different risk levels vs. different wastewater treatment levels for five uses of recycled water (adapted from (Sheikh 2015)).

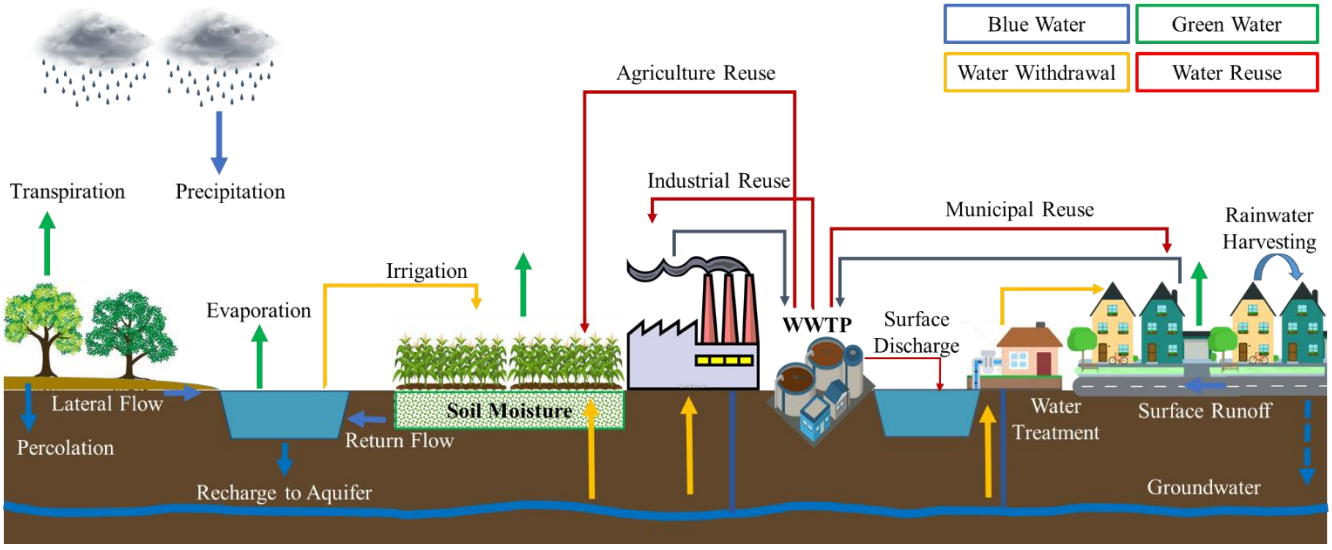

Figure 4: Illustration of the hydrologic cycle, including the wastewater reuse component.

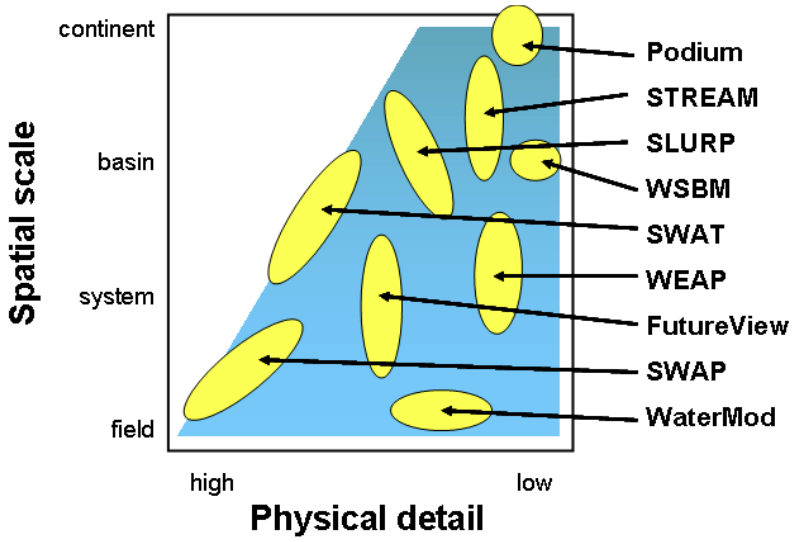

Figure 5: Spatial and physical detail of hydrologic models, adapted from Droogers and Immerzeel (2008).

5. *Tables*

Table 1: The cumulative impact of the wells pumping from Maryland's aquifers. This table was created based on information from the Maryland Geological Survey (MGS) website (http://www.mgs.md.gov/groundwater/gw-status.html).

Region	Reduction in baseflow to streams threatening aquatic habitat	Lack of productive aquifers	Well interferences causing conflict between users	Water levels exceeding management levels	Salt-water intrusion	Arsenic	Nitrates	Pesticides	Radioactivity	Deep pumping levels resulting in high energy costs
Fractured Rock	X	X				X	X	X	X	
Upper Chesapeake Bay		X	X	X		X				
Western Shore		X		X	X	X			X	X
Central Eastern Shore			X	X	X	X	X	X		
Lower Eastern Shore		X	X		X		X	X		

Chapter 3: Assessment of Agricultural Land Suitability for Irrigation with Reclaimed Water Using Geospatial Multi-Criteria Decision Analysis

Abstract

Water scarcity, climate variability and continuing growth in water demand have put severe pressure on high-quality freshwater sources. This challenge exacts the necessity to explore alternative water sources for agricultural irrigation. The objective of this study was to implement the integrated geospatial Multi-Criteria Decision Analysis (MCDA) with the Analytical Hierarchy Process (AHP) to evaluate the potentiality of reclaimed water use for agricultural irrigation in California. Five evaluation criteria included in this study were agricultural land (crop type), climate conditions, water policies, irrigation status, and proximity to wastewater treatment plants (WWTPs) respectively. The suitability maps for reclaimed water use were generated for three cases in terms of accessibility to WWTPs, their discharge volume and appropriate treatment processes respectively. In addition, a composite suitability map was produced using the hybrid model considering all three cases together. Results from this study led to a better understanding of sustainable reclaimed water use for crop irrigation at a regional level. It provided supporting evidence of the applicability of the GIS-MCDA method integrated with AHP technique for a larger geographical scale with a diverse crop pattern. This study established the importance of using both knowledge-based and data-driven criteria and sub-criteria in the decision framework. The results also highlighted how the spatial distribution of suitable areas for reclaimed water reuse is closely linked to the agricultural areas.

This chapter has been published in *Agricultural Water Management.*
Paul, M., Negahban-Azar, M., Shirmohammadi, A., & Montas, H. (2020). Assessment of Agricultural Land Suitability for Irrigation with Reclaimed Water Using Geospatial Multi-Criteria Decision Analysis. Agricultural Water Management, 231, 105987. https://doi.org/10.1016/j.agwat.2019.105987

1. Introduction

The agricultural sector is the largest global consumer of freshwater, which accounts for about 70 percent of total freshwater consumption (FAO, 2017). Uncertain water availability, climate variability, and continuing growth in water demand have put severe pressure on high-quality freshwater sources for irrigation (Fant et al., 2016; Gohar and Cashman, 2016; Taylor et al., 2013). The growing global water shortage has contributed to agricultural production reduction, which adversely impacts the food security, and severely affect the regional economy, farm value, and socioeconomic development (Anane et al., 2012; Montgomery et al., 2016). The water scarcity exacts a necessity to explore additional or alternative water sources to sustain food production in various countries across the world, especially in water-scarce environments. Alternative water resources may include reclaimed water from wastewater treatment plants (WWTPs), return flows of irrigation water, desalination of seawater and highly brackish groundwater, and stormwater harvesting (Chen et al., 2016; Hurlimann and Dolnicar, 2011; Rygaard et al., 2011). Many countries like Australia, Chile, China, Cyprus, India, Israel, Italy, and Mexico have been using some of their treated or partially treated wastewater for crop production (Angelakis et al., 2018; Jaramillo and Restrepo, 2017; Jimenez and Asano, 2008; Keraita et al., 2008). In the U.S., growing agricultural water reuse projects (e.g., in Florida and California) also provides evidence that reclaimed water can be effectively used for agricultural irrigation (Bischel et al., 2011; Exall et al., 2008).

Worldwide, most of the water reuse projects were driven by the immediate needs to increase the water supply in agriculture to overcome the crisis of recurrent and

long-term drought conditions (Bixio et al., 2008; Jaramillo and Restrepo, 2017). Agricultural irrigation with reclaimed water provides multiple benefits including reducing pressure on freshwater (Jaramillo and Restrepo, 2017; Rahman et al., 2016), nutrients management and recovery (Hanjra et al., 2015; Miller-Robbie et al., 2017), and higher reliability due to constant yields (Chen et al., 2012; Rahman et al., 2016). However, wastewater needs to be adequately treated to be reused in agricultural irrigation, especially for food crops due to potential health and environmental risks. Other limiting factors that need to be considered in reclaimed water use in agricultural irrigation include technical feasibility (e.g. closeness to WWTPs), economic factors (e.g. ability to meet the water demand), social and environmental factors (e.g. public acceptance and consumer response), and regulatory considerations (e.g., compliance with treatment requirements) (Ackerman, 2012; Bixio et al., 2008; Jaramillo and Restrepo, 2017; Saliba et al., 2018; Urkiaga et al., 2008). As a result, before the implementation of water reuse projects, it is very important for the policy-makers and water resource managers to have the adequate information regarding the availability (quantity and quality) and economic viability (cost-benefit analysis) of the reclaimed water sources for irrigation of different type of crops (food/non-food crops). Thus, multiple quantitative and qualitative decision criteria should be considered to plan for the use of reclaimed water for irrigation. Of note is some of these criteria cannot be easily quantified in numbers or expressed into monetary values (Kiker et al., 2005).

In addition, the assessment of irrigated agricultural land suitability for irrigation with reclaimed water is a spatial decision problem which involves spatially variable

decision criteria. This complex geospatial problem leads to the necessity of using Geographical Information Systems (GIS) combined with Multi-criteria Decision Analysis (MCDA). Although this approach is more subjective, it has the advantage of incorporating the expertise and knowledge of the decision-makers in the modeling process (Harris et al., 2001; Rikalovic et al., 2014; Saarikoski et al., 2016). The GIS-MCDA solves the complex decision-making problem based on evidence of varying quantity, quality, guidelines, and experts' opinions, and considering a wide range of decision criteria and constraints (Akıncı et al., 2013; Assefa et al., 2018; Montgomery et al., 2016). Of note is, any implemented project dynamically changes the environmental conditions (Saparauskas et al., 2011; Zavadskas et al., 2009), which highly influence the feasible solutions (Kalibatas and Turskis, 2008) and determine the set of critical criteria (Streimikiene et al., 2016). For example, efficient waste utilization alternative selection could influence waste reuse efficiency in terms of social, economic, and environmental aspects (Turskis et al., 2012). Thus, proper site selection depends on its sustainability characteristics (Peldschus et al., 2010) and available technologies to use (Sivilevicius et al., 2008; Zavadskas et al., 2013c). Stakeholders in the modern world should find a reliable solution considering the effective investments and both global and local perspectives of the outcomes (Zolfani et al., 2013).

Worldwide, some researchers have applied the MCDA framework for the evaluation of feasible wastewater reuse for irrigation (Ganoulis, 2003; Kalavrouziotis et al., 2011; Lee et al., 2018; Woltersdorf et al., 2018). However, very few scientific papers demonstrated the use of integrated GIS- MCDA approach for the agricultural

land suitability assessment for irrigation with reclaimed water (Aldababseh et al., 2018; Anane et al., 2012; Neji and Turki, 2015). Most of these studies assess the feasibility of reclaimed water use in agricultural land at a small scale (e.g. only including few farms and a limited number of treatment plants). For instance, Anane et al. (2012) considered only two WWTPs to rank the suitable sites for irrigation with reclaimed water, while Neji and Turki (2015) evaluated the alternatives for three WWTPs in Tunisia. In another study, Aldababseh et al. (2018) assessed an ex-ante land suitability analysis for the irrigation of seven critical crops with desalinated and treated wastewater in the Emirate of Abu Dhabi. To the best of our knowledge, there is no study that considers the spatial distribution of diverse crop patterns with a combination of a large number of WWTPs and their proximity, capacity, and different treatment processes.

The aim of this study was to develop a decision support system for agricultural irrigation with reclaimed water from WWTPs using an integrated framework of GIS-MCDA. The main objectives of this study were to: (1) develop a GIS-MCDA framework to identify the agricultural hotspots that are best suited for irrigation with reclaimed water; (2) evaluate the feasibility of reclaimed water use for irrigation considering proximity to WWTPs, discharge volume, and treatment processes respectively; and (3) produce a composite map using a hybrid model identifying the hotspots combining all of the decision criteria. In addition, a sensitivity analysis has been carried out with variable criteria weights to better explain the consistency of the best solution given by the MCDA.

2. *Methodology*

2.1. Study Area

The study area for this research was the entire state of California (Fig. 1). California is the leading state in agricultural production in the United States. It has the highest irrigated farm acreage and uses about one-fourth of the total irrigation water in the United States (Johnson and Cody, 2015). The Central Valley of California is known as its productive agricultural heartland due to its well-suited condition for vegetables and fruit cultivation. Four counties of Tulare, Kern, Fresno, and Merced in Central Valley, and Monterey in Central Coastal region of California are ranked as the leading agricultural counties in the nation. About 77,100 irrigated farms generated an overall agricultural production value of $42.6 billion in 2017 (USDA-ERS, 2018). The state produces over 400 different commodities including over one-third of the country's vegetables and two-thirds of its fruits and nuts. According to USDA National Agricultural Statistics Services (NASS), 26% of agricultural lands were orchards, 52% were cultivated alfalfa, hay, pastureland, rice, corn, and cotton, and 11% were vegetables in 2017.

The demand for alternative water supply sources is increasing among the farmers in California as a way to continually meet their irrigation demands in the face of growing water scarcity (Schulte, 2016). The ongoing growth provides evidence that the demand for alternative water sources such as reclaimed water to irrigate the agricultural lands is increasing (Bischel et al., 2011; Schulte, 2016). According to USGS estimation, in 2015, California used 289.4 million gallons of reclaimed water per day (MGD) for irrigation including 217.7 MGD for crop-irrigation (Dieter et al.,

2018). However, only in California, approximately 2,210 MGD of wastewater is being treated including all publicly, non-publicly, and federally owned WWTPs (EPA, 2019). Thus, there is still great potential for reclaimed water use in agriculture that has not been fully exploited.

2.2. Multi-Criteria Decision Analysis (MCDA)

In the MCDA framework, the weights or scores are defined to check the performance of alternative decision options against multiple criteria that are measured in different, and sometimes in incommensurable units (i.e., a combination of quantitative and qualitative criteria). In general, the required inputs in the MCDA process include scores across several dimensions associated with different alternatives and outcomes, and weights relating to tradeoffs across these dimensions (Huang et al., 2011). The total value score for an alternative is calculated as a linear weighted sum of its scores across several criteria (Eq.1).

$$V_i = \sum_{j=1}^{n} W_j X_{ij} \tag{1}$$

Where V_i is the overall score for alternative i; W_j denotes the relative weight for criteria j; and X_{ij} is the priority of alternative i with respect to criteria j.

Numerous techniques have been developed to define the weights for criteria and combine them to solve the complex decision-making process. Different MCDA methods have different robustness when assessing choices in specific problems (Zavadskas et al., 2013a; b). Major MCDA approaches include multi-criteria value functions methods such as weighted summation (Hajkowicz and Higgins, 2008);

outranking approaches such as PROMETHEE (Brans and Vincke, 1985; Vetschera and De Almeida, 2012) and ELECTRE (Kumar et al., 2016; Roy, 1978); distance to ideal point methods such as TOPSIS (Dong et al., 2016; Yoon, 1980) and compromising programming (CP) (Ballestero and Romero, 1996; Martin et al., 2017); soft computing concept such as logic scoring of preference (LSP) (Dujmovi'c, 1996; Montgomery et al., 2016); pairwise comparison methods such as Analytical Hiearchy Process (AHP) (Hou et al., 2016; Saaty, 1978); prioritization technique such as DEMATEL(Azarnivand and Chitsaz, 2015; Fontela and Gabus, 1976); fuzzy set analysis (Kosko, 1992; Mirajkar and Patel, 2016); mathematical approach like linear programming (LP) (Srinivasan and Shocker, 1973); and compromising ranking method such as VIKOR (Opricovic, 1998), etc. In the modern era, stakeholders may need newer MCDA methods (Keshavarz Ghorabaee et al., 2016), or integrated MCDA approaches (Bagocius et al., 2014) to solve complicated problems (Ruzgys et al., 2014; Xu, 2001). For instance, improved AHP method like Analytical Network Process (ANP) (Aminu et al., 2017; Saaty, 1996), an integrated ranking method such as superiority and inferiority ranking (SIR) (Xu, 2001), Fuzzy AHP (Anagnostopoulos and Petalas, 2011; Buckley, 1985; Elshaikh et al., 2018), Fuzzy ANP (Mikhailov and Singh, 2003; RazaviToosi and Samani, 2016) and Fuzzy TOPSIS (Chen, 2000; Kim et al., 2013) are used to solve the complex problem.

AHP method, which was first introduced by Saaty in 1978, is still a widely used MCDA method (Saaty, 1978; 1979; 1980). AHP gets its popularity due to its good understandability, ease of implementation, and interpretability of the results by both modelers and decision-makers. It allows the researchers to represent a full range of

human decision-making logic considering both qualitative and quantitative data and combines them by decomposing complex problems into systematic hierarchies to rank alternatives based on different criteria (Assefa et al., 2018; Opricovic, 2011; Woltersdorf et al., 2018). For this reason, several studies have applied the AHP for solving a wide variety of water and environmental problems, including water resource allocation (Zhang et al., 2019), selection (Grum et al., 2016), feasibility evaluation (Cozzi et al., 2015), resolving conflicts (Mainuddin et al., 1997), and priority and ranking (Hassani et al., 2019). Of note is, well-backgrounded goals are essential to define the problem and should be included in any decision-making model (Turskis et al., 2019d). Therefore, when stakeholders use MCDA methods, one of the critical tasks is to determine the importance of criteria. The AHP method is the most widely used method for this purpose (Zavadskas et al., 2016). In addition, researchers have developed other techniques to assign criteria weights based on their importance (Eckenrode, 196; Delbecq and Vandeven, 1971; Kersuliene et al., 2010; Linstone and Turoff, 2002; Turskis et al. 2019b).

In the MCDA process, the criteria and weighting can be modelled as crisp as well as fuzzy or grey (Turskis et al., 2019a; Turskis et al., 2019c). This may vary based on the nature of the criteria or the modelling preference. In case of land allocation problems, cropland and forest land could be assigned with crisp boundaries (either one or the other) or fuzzy boundaries (with one or more classification levels where the land is partially forest and partially cropland). Thus, in the decision-making process, it is sometimes difficult to choose between alternatives with multiple attributes. AHP has the ability to simplify the complicated decision-making process

by using pairwise comparison technique and reducing the number of comparisons and confirming consistency by comparing objects with multiple attributes. The pairwise comparison technique provides a powerful, simplified, and relatively unbiased ranking criterion (Assefa et al., 2018; Saaty, 1980; Worqlul et al., 2015).

Few of the MCDA techniques were integrated with GIS to assess the land suitability and allocation for water resource management (Table 1), where AHP is the most applied to solve the complex decision-making processes regarding water reuse for irrigation. In the presented study, the process of a suitability assessment and identifying hotspots for reclaimed water use involves two main steps (Fig. 3). In the first step, the influential geospatial decision criteria and sub-criteria were evaluated. Then, a GIS-MCDA model was developed using the AHP technique to solve the spatial decision-making process. The MCDA method was implemented using geospatial data and ArcGIS 10.1 software (ESRI, 2012). In GIS-MCDA, a spatial decision alternative is defined as a single raster of a specified size or a combination of multiple rasters. The following subsections describe the procedure for the development of GIS-MCDA in this research in more detail.

2.2.1. Defining Criteria and Sub-criteria

Decision criteria and sub-criteria are labeled as either factors or constraints. A factor is a criterion that amplifies or reduces the suitability of a specific alternative for the activity under consideration, while a constraint serves to limit the alternatives under consideration. Based on the existing literature, data availability, and expert opinions five main influential criteria as factors and one as a constraint were selected for the assessment of the suitable agricultural land for the reclaimed water irrigation.

The five selected criteria are: 1) land cover (crop type); 2) reclaimed water sources; 3) irrigation status; 4) groundwater priority; and 5) climate. Each of these criteria is individually evaluated using different sub-criteria. Sub-criteria were processed separately depending on their discrete and continuous form. The detailed rationale behind the selection of these criteria and sub-criteria are explained hereafter.

I. Land Cover (Crop Type)

According to NASS-CDL (2017), the total harvested area in California was 46,741 km2 with a planted area of 16,591.7 km2 in 2017. To assess the suitable agricultural land for reclaimed water irrigation, all of the agricultural lands were included in the land cover criteria. The main concern regarding reclaimed wastewater use is the effect on the human and health environment. Thus, California's Water Recycling Criteria-Title 22 was followed strictly during the classification (NWRI, 2012; Schulte, 2016; Sheikh, 2015). The detailed information can be found from Title 22 of the California Code of Regulations, Division 4, Chapter 3: Water Recycling Criteria. But briefly, according to the regulations, both nonfood crops/processed food crops and food crops can be irrigated with reclaimed water depending on the treatment process (Table 1). Therefore, all the existing crops within California were categorized into six classes as alternatives based on the reclaimed water sensitivity and tolerance: non-food crops fiber, non-food crops fodder, non-food crops oil crops, food crops grains and legumes, food-crops orchards, and food-crops vegetables.

II. Reclaimed wastewater Sources

In this study, treated wastewater from the wastewater treatment plants (WWTPs) has been considered as the alternative water source for agricultural irrigation. Only

the publicly owned treatment works (POTWs) were considered since these are mainly designed to treat the domestic sewage from residential and commercial communities and are owned and operated by the local government agencies. POTWs' data was collected and combined from the 2012 Clean Watersheds Needs Survey (CWNS) and Enforcement and Compliance History Online (ECHO) datasets (EPA, 2012). After collecting the data, the POTWs were screened and categorized using a three steps process (Fig. 2). The step by step rationale behind selecting and categorizing the WWTPs are described hereafter.

First: Each treatment facility discharges its treated wastewater (effluent) into the environment through many different methods (i.e., Outfall to Surface Waters, Discharge to Ground Water, or Reuse: Potable, etc.). In this research, five discharging ways were considered as high reuse potential for agriculture including Evapotranspiration, Ocean Discharge, Spray Irrigation, Reuse Irrigation, and Outfall to Surface Waters (Fig. 2). Discharging method "Evapotranspiration" is a system to dispose the treated wastewater into the atmosphere through evaporation from the soil surface and/or transpiration by plants, without discharging wastewater to the groundwater reservoirs or surface water. Thus, all the WWTPs which discharge their treated wastewater through evapotranspiration were considered as a source for agricultural irrigation. It is reported that more than 80% of treated wastewater (3,440 Mm3/year) is being discharged to the ocean in California (Angelakis et al., 2018). This large volume of treated wastewater can also be used for irrigation purposes, therefore, WWTPs discharging to the ocean were included here as a high potential source of water for irrigation. The successful application of treated water for

irrigation mainly depends on the farmers' acceptability. Therefore, the existing reusing practice nearby like "Spray Irrigation" and "Reuse: Irrigation" can represent a positive economic and social impact and were included in this study. In addition, "Outfall to Surface Waters" discharging method was considered only for those WWTPs located in the coastal regions and counties, which have low surface water consumption according to USGS estimation, and there is no downstream user.

Second: Reclaimed water is a reliable source to meet part of the demand for irrigation water, and to minimize the dependency on freshwater sources. It is apparent that since larger treatment plants discharge higher volumes of reclaimed water, they can be considered as more reliable sources. In this study, the projected design flow of individual WWTPs was used to classify them depending on their treated effluent discharge capacity.

Third: The quality of the treated wastewater plays a very important role in reclaimed water applications. Title 22 of the California Code of Regulations states that the level of treatment impacts the reclaimed water use in agriculture. For example, if treated water contacts the edible portion of the crop, (i.e., vegetables or root crops), tertiary treatment and disinfection are required (Table 1). In this step, we classified the WWTPs based on their treatment methods and included it as a decision criterion.

III. Irrigation Status

According to the 2015 USGS data, California is the largest freshwater consumer in the U.S. (18,983 MGD), mainly due to irrigation (Dieter et al., 2018). California consumes 80% of the total water to produce food (Mount and Hanak, 2014). Under

this decision criteria, county-wise data of the total agricultural freshwater withdrawals (surface and groundwater) was considered to classify the study (e.g. counties with highest irrigation water use were assigned higher priority for reclaimed water use).

IV. Groundwater Priority

While surface water is the primary source of irrigation in California, groundwater is also being used to meet the irrigation demand in many areas. Based on the California Statewide Groundwater Elevation Monitoring (CASGEM) data, the Department of Water Resources (DWR) has identified 518 groundwater basins in California and categorized them into four prioritization groups of high, medium, low, and very low priority. The groundwater basins prioritization was made using the following eight criteria: population, population growth rate, the total number of wells and irrigated acreage, the degree of dependency on the groundwater, documented impacts on groundwater like overdraft and saline intrusion, and any other relevant documented adverse impacts. In this study, we considered the statewide groundwater prioritization as a decision criterion and assigned higher priority to watersheds that are considered high priority groundwater watersheds.

V. Climate

Agricultural production in California is very sensitive to climate change (Pathak et al., 2018). Change in amounts, distribution, and frequency of precipitation and temperature intensify the water availability for agricultural and reduce crop areas and yields (Pathak et al., 2018; Tanaka et al., 2006). Therefore, in this study climate was selected as a criterion for suitable agricultural land evaluation. Climate criteria decomposed with the climate region and historical drought information for different

watersheds within the state. Each watershed was ranked and weighted based on their severity of climate and drought conditions together through a two-step process:

a) Climate Region: According to the California Emergency Management Agency (CEMA), California is divided into 11 major climate impact regions (Fig. 1). Coastal and southern regions of California state have a Mediterranean climate, with slightly rainy winters and dry summers. The coastal region has a moderate temperature, warmer winters, and cooler summer due to the ocean in the west. Northern California has a moderate oceanic climate, which receives higher annual precipitation compared to the southern part of the state. California's deserts have little water, few plants, and very hot summers situated on the east side. The central valley has a semi-arid climate with a distinct dry summer season and a cool, foggy, rainy season, which is suitable for crop production. The Sierra Nevada and the Coastal region form a ring around the Central Valley where half of the country's fruits, vegetables, and grains grow due to the rich soil and long growing season. Rest of California covered by the Mountain ranges, which include the Klamath Mountains and the Cascade Range in the north.

b) Drought Index: Since a drought can adversely affect agricultural crop productions, use of reclaimed wastewater for irrigation can conserve food security by providing a drought-proof source of additional water. To incorporate the drought information into the Climate criteria, the Palmer Drought Index, or the Palmer Drought Severity Index (PDSI) was considered as an indicator of drought. In this study, PDSI was collected from the West Wide Drought Tracker (https://wrcc.dri.edu/wwdt/) for 35 years (1981-2015), where PDSI was calculated based on the precipitation and temperature, and a supply-and-demand model of soil

moisture (Abatzoglou et al., 2017). It assigns 0 as normal, and negative number as drought condition (e.x., negative 2 is moderate drought, negative 3 is severe drought, and negative 4 is extreme drought).

2.2.2. Developing the AHP Model

The AHP technique (Saaty, 1978) was applied in the GIS-MCDA structure, where a hierarchical mechanism is used to rank criteria and alternatives according to their importance (Cozzi et al., 2015; Feizizadeh and Blaschke, 2014). The AHP uses pairwise comparisons between the criteria to help decision-makers to evaluate the relative importance of criteria. Through this process, the weights and ranking of the criteria were determined for the GIS-MCDA model (Fig. 3). The development of the AHP model for this study is described in the following steps:

i. Formulating Hierarchy

After defining all the selected criteria and evaluation of sub-criteria, they were used to formulate the hierarchy structure (Fig. 4). The hierarchy structure was articulated based on the AHP method to organize the complex multi-criteria problem in a number of levels. The decision hierarchy is containing a goal, the main criteria, the sub-criteria, and the options. The first level of the hierarchy corresponds to the general purpose of the problem, the second level to the criteria and the third level to the sub-criteria (Saaty, 1980). Fig. 4 shows that the main criteria and sub-criteria were outlined in the first and second levels of the hierarchy, based on their priority (described above) to reclaimed water use in the agriculture land. In this study, the hierarchy is structured into four levels (Fig. 4).

ii. Weighting the Criteria and Sub-criteria

The AHP theory was applied to assign the criterion weight is a fundamental step in the MCDA process. The pairwise comparison technique derives the weights by comparing their relative importance between two criteria. As a result, the comparison matrix was established considering the relative importance of each criterion and comparing one-to-one based on pairwise scale. The sub-criteria were weighted according to Saaty's 1 to 9 scale, where the highest value (9) indicates "Extremely Important" while the reciprocal (1/9) indicates "Extremely Insignificant" (Table 3). The weights of each sub-criterion were assigned based on the rationale described in Table 4.

iii. Evaluating Consistency

Once the judgments or the weights of the criteria have been entered into the comparison matrix, the consistency of the pairwise matrix is checked using a consistency ratio (CR) to check the degree of consistency or inconsistency (Saaty, 1980). CR compares the consistency index (CI) of the matrix with the consistency of a random-like matrix (RI).

$$CR = \frac{CI}{RI} \tag{2}$$

Where random index (RI) is the average of the consistency index of the randomly generated pairwise comparison matrix. RI is varied with the numbers of criteria (n) (Saaty, 1980).

The CI is the consistency index calculated from the pairwise matrix and can be expressed as:

$$CI = \frac{\lambda_{max} - \mathrm{n}}{\mathrm{n} - 1} \quad (3)$$

Where λ_{max} is the largest eigenvalue of the pairwise comparison matrix, n is the order of the matrix. CR value of less than 0.10 indicates that judgments are consistent and are suitable for the implementation of the AHP analysis (Saaty, 1978). For CR values greater than 0.10, the pairwise comparisons matrix needs to be adjusted, and the weighting values should be modified.

iv. Ranking and Prioritizing the Criteria

From the pairwise comparison matrix, the values of each cell were divided by the total of its column. The resulting matrix is called a ‘‘normalized matrix’’ (Saaty, 1978). From this normalized matrix, the final priorities were obtained, which are indicated as “Weights” and “Ranks” columns of Table 2-4. Thus, the final AHP outputs are: (i) a relative priority of each criterion presented in percentages, and (ii) a relative rank of each criterion.

In this study, three separate robust maps were produced considering the proximity, discharge flow rate, and acceptable treatment process, to minimize the dependence between different crop types and treated water quality. For all other alternatives and criteria, we assumed that there is no dependency between them. Therefore, three pairwise matrices computed separately for: (1) all WWTPs with acceptable discharge methods (Case 1-Table 5); (2) WWTPs categorized with flow volume (Case 2-Table 6); and (3) WWTPs considering the treatment processes (Case 3-Table 7).

2.2.3. Creating Thematic Layers and Model Setup

In the GIS-MCDA method, the data is needed in spatial nature for i) the geographical data models, ii) spatial extent for the criteria evaluation, and iii) the spatial dimension of the decision problem. Six major datasets were collected and generated in spatial nature including Crop Data Layer (CDL) for land use and land cover (LULC); the location of WWTPs for reclaimed wastewater sources; groundwater basin prioritization maps; county wise freshwater consumption map for irrigation status; and drought index map and climate zone map for climate criteria. A complete list of datasets that were used in this study is provided in Table 8.

After collecting the required data, the spatial analysis was done to obtain the MCDA criteria maps. Spatial analysis was made with the quantifiable data regarding single-objective decision making with an optimized number of criteria. Spatial analysis to identify a suitable area for reclaimed wastewater irrigation starts with representing each selected sub-criterion by a thematic layer in which each point takes a value according to that sub-criterion (Figure 4). Each main criteria or thematic layer was obtained in a raster format and evaluated using GIS and geo-statistical tools. Crop Data Layer (CDL 2017) was used to perform the agricultural land classification in the ArcGIS environment. WWTP information including locations, discharge method, flow and treatment units were collected from CWNS 2012 and NPDES data source and processed into a raster format. The sub-criteria of each main criterion was assigned with the scale (according to Table 4) using the Spatial Analysis tool named "Reclassify" in the ArcGIS platform and reclassified maps were produced for each criterion (Figure 5a-5e). All the thematic layers were converted into raster layers with

a uniform 30*30 m resolution. One constraint map (Figure 5f) was created which indicates the unsuitable land use for irrigation, (e.g., urban areas, barren land, forests, wetlands, water bodies, and shrublands).

The weights based on the final matrix (Table 5-7) were distributed to individual criteria and then combined using the Weighted Sum Overlay tool in ArcGIS. Total of five criteria layers for Case 1, seven criteria layers for Case 2, and six criteria for Case 3 were combined to produce the single suitability map. The interval classification was used to obtain the suitability for all generated maps and represented in four classifications of Most Suitable, Moderately Suitable, Low Suitable, and Least Suitable respectively.

2.3. Sensitivity Analysis

In the AHP technique, criteria weights represent the influence of each criterion in the model distribution (Feizizadeh and Blaschke, 2014; Robinson et al., 2010). The final ranking of options is dependent on the choice of performance scoring scales. Therefore, criteria weights can be sources of uncertainty and may considerably impact the decision outcomes (Belton and Hodgkin, 1999; Feizizadeh and Blaschke, 2014). To address this issue, the sensitivity analysis was performed as the final check for the whole process, and to assess the robustness of the model. In this study, the One-at-a-Time (OAT) approach was applied for the sensitivity analysis, which provides a good balance between efficiency and efficacy (Bertolini et al., 2004; Bertolini et al., 2006).

Through the analysis, three aspects of criteria weight sensitivity were examined by (1) investigating the stability of the evaluation by implying a known amount of

change to one weight and observing changes in the rankings of criteria; (2) identifying most sensitive criteria to weight changes; and (3) visualizing the changes in the spatial dynamics. In this study, a 10% change of weights for each main criterion was applied to analyze the model's response.

3. Results and Discussion

3.1. Evaluation of Main Criteria

3.1.1. Agricultural Land Classification Mapping

The agricultural land use was delineated using the Boolean map, where all the croplands were considered for the analysis and other types of land use/cover were discarded (Fig. 5a and 5f). According to CDL (2017), more than sixty different types of food and non-food crops were recorded in 30*30m resolution. Based on Table 4, the agricultural lands were reclassified and mapped into six classes. These classes are Fodder Crops (49,424 km^2), Non-food Crops- Fiber (1,089 km^2), Non-food Crops-Oil (490 km^2), Food Crops- Grains and Legumes (7,135 km^2), Food Crops- Orchard (22,294 km^2), and Food Crops- Vegetables (1,610 km^2) (Fig. 5a).

3.1.2. Proximity Mapping of Reclaimed Wastewater Sources

The location of WWTPs and their proximity to the point of use are very important factors in the decision process. Agricultural land close to WWTPs or downstream of treatment plants can get easier access to reclaimed water compared to areas that are further from the treatment plants or are located upstream. However, the upstream or downstream direction from WWTP to agricultural land was not analyzed during the proximity mapping. From each of the WWTP, Euclidean Distances (i.e., distance raster) were calculated and then reclassified into three classes: 0-5 km, 5-15 km and

>15 km (Fig. 4 and Fig. 4b). In this study, three proximity maps were produced for the three cases (Case 1, 2, and 3). The CWNS 2012 database contains 905 records of WWTPs within California. It includes the projected flow for only 488 of the WWTPs. The database also includes information about the treatment process for only 53 WWTPs. Of note is those 53 WWTPs are large facilities and their combined treated effluent comprises about 73% of total recorded effluent. After the reclassification, three different proximity maps were created. Fig. 5b shows the proximity map of the reclaimed water sources considering acceptable discharge methods.

3.1.3. Mapping of Agriculture's Freshwater Consumption

The groundwater and surface water extraction per county were mapped using the USGS 2015 dataset. All the 58 counties in CA were assessed in terms of their annual freshwater consumption in the agricultural sector, and the weighted county maps were generated. These maps present the priority zones for using reclaimed water for irrigation. Results showed that, Imperial County extracted the highest amount of freshwater for irrigation (1,850 MGD), followed by Kern (1,617 MGD), Fresno (1,616 MGD), Tulare (1,396 MGD), San Joaquin (1,190 MGD), and Stanislaus (1,034 MGD) respectively. These six counties have the largest freshwater consumption in agriculture, therefore, were given the highest score in the evaluation (Fig. 5c). Other counties were also classified according to their total freshwater use in agriculture respectively (Table 4 and Fig. 5c).

3.1.4. Groundwater Basin Prioritization Mapping

According to the CASGEM data, a total of 43 basins were categorized as a high priority, and 84 basins as medium priority regarding groundwater basin prioritization.

The rest of the groundwater basins were categorized as low or very-low priority (total of 391). After reclassification, different scores were assigned to groundwater basins, where high priority basins received the highest and low priority basins received the lowest scores (Fig. 5d). The groundwater basin prioritization mapping shows that the highest priority zones consisted of 51814.5 km^2 and were mainly outlined in the Central Valley. The low (17247 km^2) and very low priority (55976 km^2) were mapped to the eastern part of the California desert due to the insignificant agricultural activity.

3.1.5. Watershed Prioritization Mapping

All the watersheds in California were classified based on their drought severity and local climate conditions using the method described before. These drought severity classifications include Very High, High, Medium, Low, Very low, and Normal conditions. For instance, the coastal region of Southern California receives the lowest PDSI (-6.9) with maximum years (11 years) followed by the California Desert Region (PDSI -6) with maximum years (8 years). Watersheds were assigned different scores according to their PDSI, in which watersheds with the lowest PDSIs received the highest priority for reclaimed water use in agriculture (Fig. 5e).

3.2. Factors Weight and AHP Assessment

Three pairwise matrices were formulated and the weight of the criteria was computed separately for Case 1 (Table 5), Case 2 (Table 6), and Case 3 (Table 7), respectively. During the pairwise comparison, the consistency was evaluated simultaneously to check if the judgments were rational. If the CR (Eq. 2) exceeds

10%, the inconsistencies of the judgments were rechecked, and the criteria evaluations were readjusted.

The final consistency of pairwise matrices was checked and found to be 0.051, 0.056 and 0.051, for three Cases of 1, 2, and 3, respectively. In Case 1, proximity to WWTPs had the highest priority with a score of 0.529 followed by the land cover (crop type) (0.265) and Watershed Prioritization (0.114) as the second and the third influential criteria (Table 5). In Case 2, the WWTPs which treated more than 100 MGD wastewater scored the largest (0.359) considered as the highest priority to irrigate the agricultural land followed by the WWTPs with the capacity of 25 < Flow ≤ 100 MGD (0.249) and Flow ≤ 25 MGD (0.171) (Table 6). Similarly, in Case 3 regarding the acceptable treatment process, the WWTPs having advanced or secondary treatment with the disinfection method scored the highest (0.540) compared to the other WWTPs which treated the wastewater with Secondary treatment process (Table 7).

3.3. Agricultural Land Suitability Mapping for Irrigation with Reclaimed Wastewater

Three suitability maps were produced for three Cases, based on selected discharging methods, discharge volumes, and different treatment processes. Case 1 was constituted to assess the accessibility of each WWTP to the nearest agricultural land. Therefore, the generated suitability map shows the most suitable agricultural areas that are in close proximity to the WWTPs (Fig. 6a). Case 2 was established to evaluate the suitability in terms of flow (Fig. 6b). Fig. 6b shows the most suitable

agricultural areas that are close to the WWTPs with a large volume of discharge. The last suitability maps were generated based on Case 3, which includes the treatment process of WWTPs (Fig. 6c). For instance, reclaimed water from WWTPs with advanced treatment processes can be used for all types of crops, but undisinfected secondary recycled water can only be used for non-food crops and process food crops.

3.3.1. Case 1: Considering Selected Discharging Methods

Based on the selected discharging methods, a total of 352 WWTPs were included in the generation of the suitability maps. The final suitability map based on the five main criteria and their sub-criteria is presented in Fig. 6a. Results show that "Most Suitable" agricultural areas comprise 36.7% (6515 km2), and "Moderately Suitable" areas comprise 23.3% (4138.7 km2) of the total agricultural areas (Fig. 6a). Of note is in this study, the CWNS database was used as the primary source to obtain treated discharge characteristics, discharge volumes, and treatment processes for all POTW-WWTPs. The Non-POTW facilities that often treat wastewater from industries (e.g., manufacturing or processing foods and beverages) could be additional sources of reclaimed water for irrigation. However, due to the lack of effluent information and treatment processes, Non-POTW facilities were not included in this study.

3.3.2. Case 2: Considering Treated Discharge Volume

Since most of the high capacity WWTPs are located near the coastal regions where agricultural land is minimal, agricultural areas within close proximity to WWTPs are limited. The suitable areas for irrigation with reclaimed water within close proximity of large WWTPs (>100 MGD) occupy a total of 735.3 km^2, which

corresponds to 6% of the total agriculture land (Figure 6b). On the other hand, WWTPs with low capacity (100> Flow> 25 MGD) were found to be accessible to about 1021.2 km^2 of lands in the state. Of note is the CWNS 2012 database contains projected discharge volume data for 488 (out of 905) WWTPs. The complete dataset of recorded flow data for all of 905 WWTPs could produce more comprehensive suitability maps for the GIS-MCDA model.

3.3.3. Case 3: Considering the Appropriate Treatment Processes

Treatment processes were only reported for 53 WWTPs in the CWNS database. But because they are all larger facilities, they discharged 73% of the total treated effluent. Among those WWTPs with treatment process data, only 5 WWTPs are located in the Central Valley. Therefore, minimal agricultural lands (3830 km^2) were found as suitable areas for irrigation with the reclaimed water close to those WWTPs. The majority of WWTPs with treatment process information is located in the Southern California Coastal Region and San Francisco Bay Area (34 and 13 respectively). They treat more than 3018.75 MGD of wastewater. However, these regions have minimal agricultural activities (1.2% of total agricultural land) compared to other regions. As a result, only 14 km^2 of agricultural area is marked as "Most Suitable" and 484.1 km^2 as "Moderately Suitable" in Southern California Coastal Region and San Francisco Bay Area respectively (Fig. 6c).

3.3.4. Composite Maps Considering All Three Cases

In the end, a hybrid model was built to evaluate the feasibility and suitability of treated water for agricultural irrigation considering proximity, availability, and appropriateness of the treated flow from municipal WWTPs. According to this, "Most

Suitable" agricultural areas occupy a total of 145.5 km^2, and "Moderately Suitable" areas occupy a total of 276 km^2 respectively. The final suitability map from the hybrid model was then superimposed with the CDL layer for the verification of the suitability map (Fig. 7). The discharge flow volume and agricultural land classes of the surrounding area were checked by the visual interpretation and using attribute data from the CDL layer. To assess the accuracy of the classified suitability map, a random WWTP was selected for verification. For instance, a treatment plant (Fresno-Clovis Regional WRF) situated in Fresno county was selected with a projected treated flow of 118 MGD with advanced treatment. Fresno county uses approximately 2492.77 MGD freshwater for irrigation. There are approximately 43 km^2 of Orchard (Almond, Grapes, Pistachio, and Walnuts), 6 km^2 of Alfafa, 5 km^2 of Pasture and 2 km^2 of Cotton are located within 5 km distance from this facility, that may use reclaimed water as an additional irrigation water source. Of note is verification with the filed data is recommended in future studies when suitability classifications from different sources are compared.

3.3.5. Further Discussion

The focus of this study was to develop and apply a systematic geospatial decision framework using the GIS-MCDA method for the assessment of suitable agriculture land for reclaimed water use. Of note is many researchers have acknowledged the advantage of knowledge-driven approaches like GIS-MCDA method in data-sparse situations where decision rules derived from existing knowledge to solve the area selection and potential mapping problem (Harris et al., 2001; Machiwal et al., 2015; Rajabi et al., 2014). It has been observed that for the cases with limited data, Saaty's

systematic decision approach, AHP, will give similar results to much more complex MCDA methods like PROMETHEE, TOPSIS, or ELECTRE (Kabir et al., 2014; Tscheikner-Gratl et al., 2017). It should be noted that AHP is often used in crisp decision applications, where the alternatives are compared with respect to the criteria, and for each criterion, a crisp value is assigned as the weight of alternatives. This crisp value provides a sharp and rigid boundary. However, in the real world, it is difficult to assign scores with crisp values for the assessment of complex water resource systems. Another limitation of the AHP approach is, it becomes a lengthy task for analysis when there is a large number of criteria and sub-criteria involves (Macharis et al., 2004). Considering the number of criteria and sub-criteria in this study, the AHP method was still relatively easy to implement.

Additionally, in some cases, the final decision or ranking of options are dependent on the choice of performance scoring scales. To address this issue, a sensitivity analysis was performed using the OAT approach, and the relationship between criteria weights and performance scoring scales were examined. It should be noted that the weights were changed only for the main criteria to evaluate the main effects one-at-a-time, and the interaction effects between two or more criteria had been ignored to keep the procedure simple (Bertolini et al., 2006; Chen et al., 2013; Sun et al., 2012).

3.4. Sensitivity Analysis

Six scenarios were performed for the sensitivity analysis to determine the robustness of the GIS-MCDA method developed in this study. To perform the sensitivity analysis, the assigned weights to each criterion were altered with 10%

increments from the initial input values. The weight change was applied to one criterion at a time (keeping the other criteria constant), using the OAT analysis method (Aldababseh et al., 2018; Paul and Negahban-Azar, 2018). The pixel numbers of each main criterion were evaluated in each scenario for per land suitability class (Fig. 8). The relative sensitivity also calculated to interpret the output for the different scenarios to show how the weight change in one criterion affects the suitability classes in the output (Table 9). Results show that 10% weight increase to five main criteria (one at a time) had an obvious change (increasing or decreasing) in the pixel numbers per land suitability class (Fig. 8). Sensitivity analysis showed that land suitability patterns change respective to the weight change under each scenario. Pixel numbers in "Most Suitable" areas were relatively stable with the weight increase in all main criteria except agricultural land classification. The pixel numbers were decreased in "Low Suitable" class for all scenarios whereas a noticeable increase in the number of pixels found in the "Moderately Suitable" class (Table 9).

The deviation in the decision weights (e.g., proximity to WWTPs) has a substantial impact on the pixel number of the "Low Suitable" (0.02 to -0.86) and "Least Suitable" (-0.24 to -0.66) class. The largest variation of the pixel number found for the "Moderately Suitable" when the weight was changed for the groundwater basin prioritization (relative change 1.24). There is a dramatic change in the number of cells in "Moderately Suitable" and "Low Suitable" classes. The noteworthy shifts between "Moderately Suitable" and "Low Suitable" take place in all scenarios. For scenario 1, when weight was changed for the distance of the WWTPs, the change of the pixel number was minimal compared to other scenarios.

Thus, the proximity of the WWTPs to the agricultural point of use plays an important role in the suitability mapping.

4. Conclusion

This study successfully implemented an integrated and comprehensive GIS-MCDA approach to evaluate the agricultural land suitability for irrigation with reclaimed water. To demonstrate how this GIS-MCDA model performs under realistic conditions, a case study was presented for the State of California. This study appears to be the only study to model the agricultural hotspot identification for reclaimed water use in agriculture at the state-wide scale considering several quantitative and qualitative decision criteria using the AHP method. The ultimate goal was to produce prescriptive suitability maps showing the agricultural areas that are most suitable for irrigation with reclaimed water.

Three separate robust maps were created at three stages considering the proximity to WWTPs, discharge flow rates, and acceptable treatment processes respectively. In addition, a composite suitability map was produced using the hybrid model considering all three cases together. Accordingly, the agricultural areas in the study area were classified spatially ranging from “most suitable” to “least suitable” areas for reclaimed water irrigation. Among the decision criteria, proximity to WWTPs and crop types were the most influential. Results also highlighted how the spatial distribution of suitable areas is closely linked to the agricultural areas. Of note is the assumption was that all criteria were independent, and there was no possible dependency influence in the decision-making process. As discussed before, there might be a dependency on some of the decision criteria. For instance, the irrigation of

different types of crops might be influenced by the appropriateness of the treatment process. For future research, it is suggested that other decision analysis methods such as ANP can be applied to consider the potential dependency in decision criteria and sub-criteria.

In conclusion, results from this study lead to a better understanding of sustainable reclaimed water use for crop irrigation at regional levels by developing a decision framework to prioritize agricultural areas for reclaimed water use. The main contribution of this study was to develop a GIS-MCDA framework and to test the framework at a large geographical scale (state of California) with diverse crop patterns. While the GIS-MCDA framework was specifically developed for the study area, the proposed approach can be easily applied to other areas with some modifications (e.g. revising the decision criteria and sub-criteria). Thus, results from this study provide a useful tool for decision-makers and stakeholders (e.g farmers) and help them with the development and expansion of reclaimed water for agricultural irrigation.

5. Figures

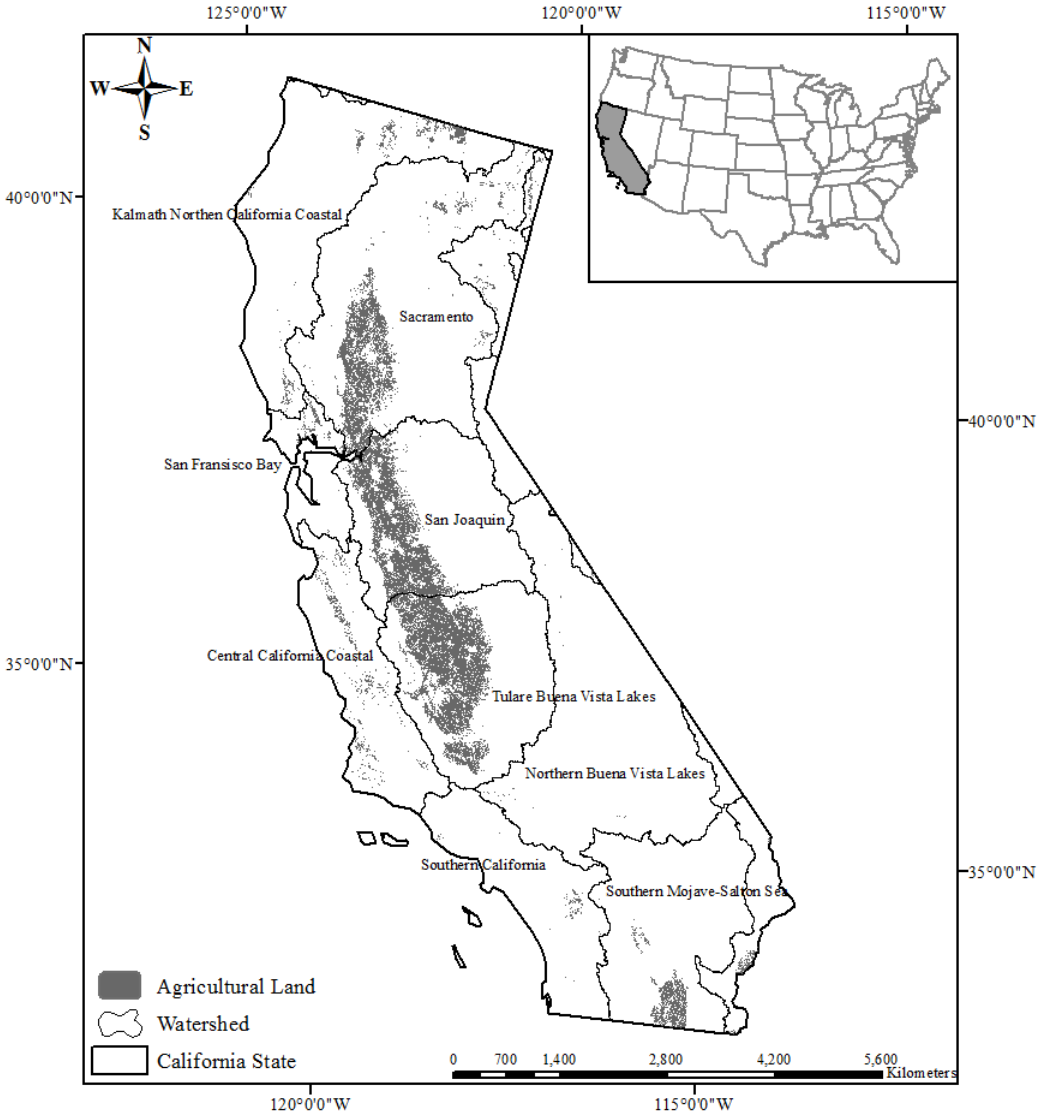

Figure 1: Agricultural lands and major watersheds in State of California as the study area.

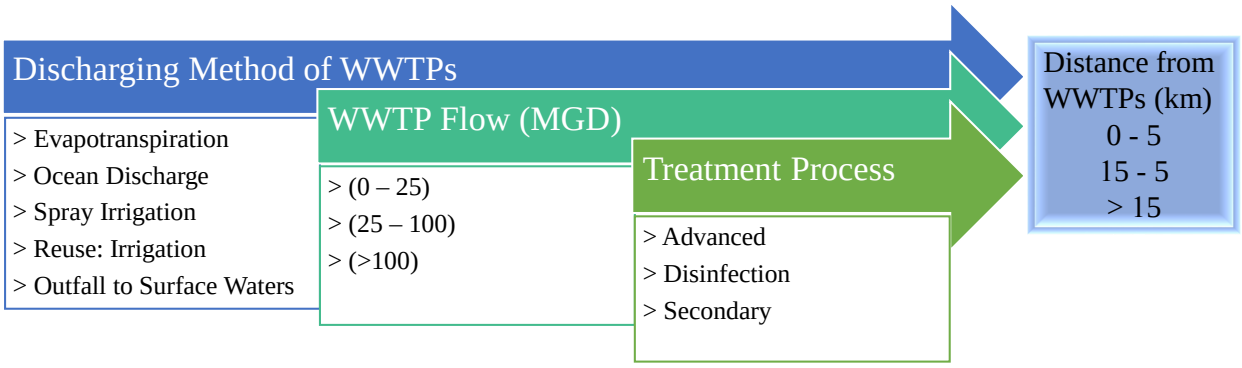

Figure 2: Three-stage classification process for wastewater treatment plants.

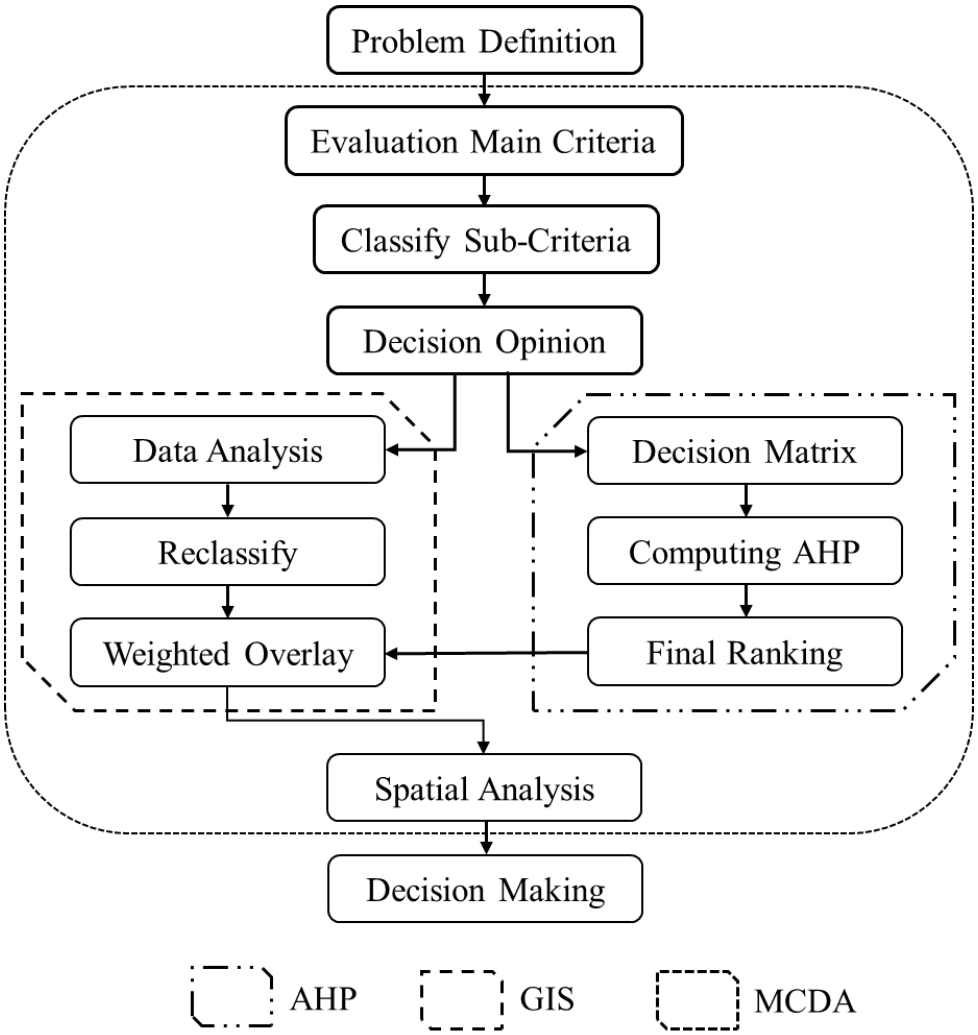

Figure 3: The Integrated Geographical Information System and Multi-criteria Decision Analysis (GIS- MCDA) framework developed in this study using the Analytical Hierarchy Process (AHP) technique.

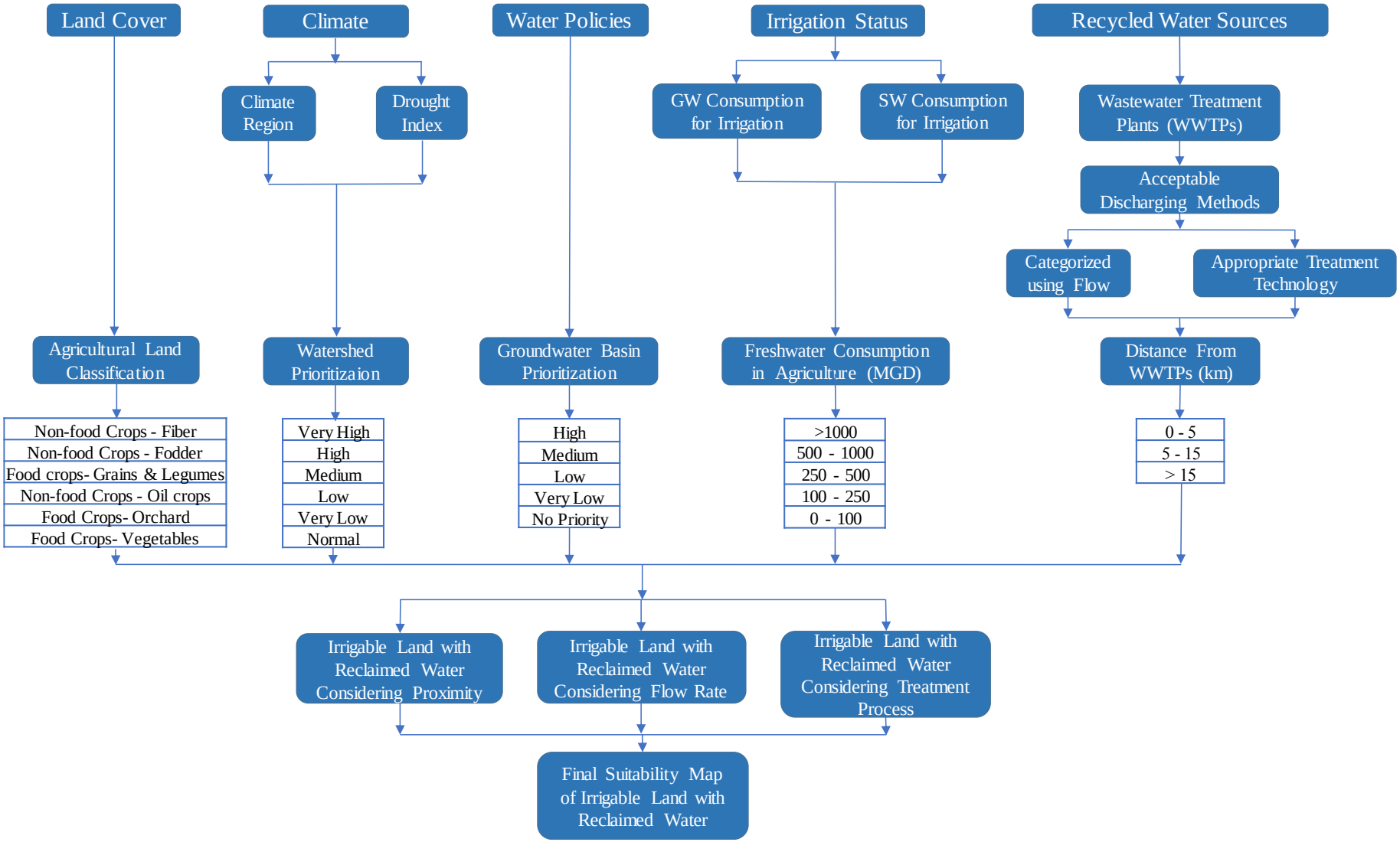

Figure 4: Developed decision framework for the assessment of suitable agricultural land for irrigation with reclaimed wastewater.

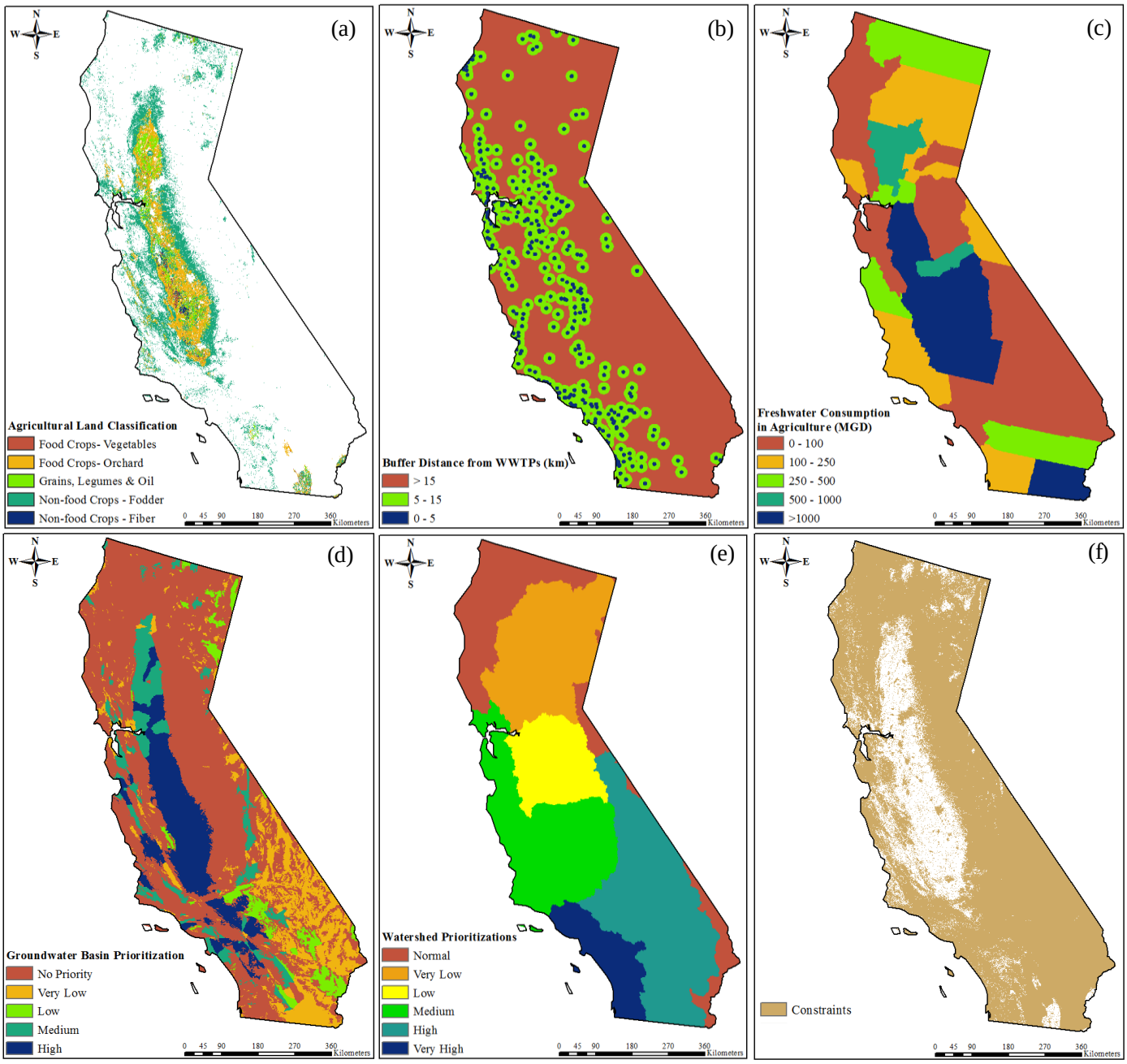

Figure 5: Thematic layers for main decision criteria and land use constraints: a) agricultural land classification; b) proximity to wastewater treatment plants (WWTPs); c) freshwater consumption; d) groundwater basin prioritization; e) watershed prioritization; and f) Boolean map for agricultural land use constraint.

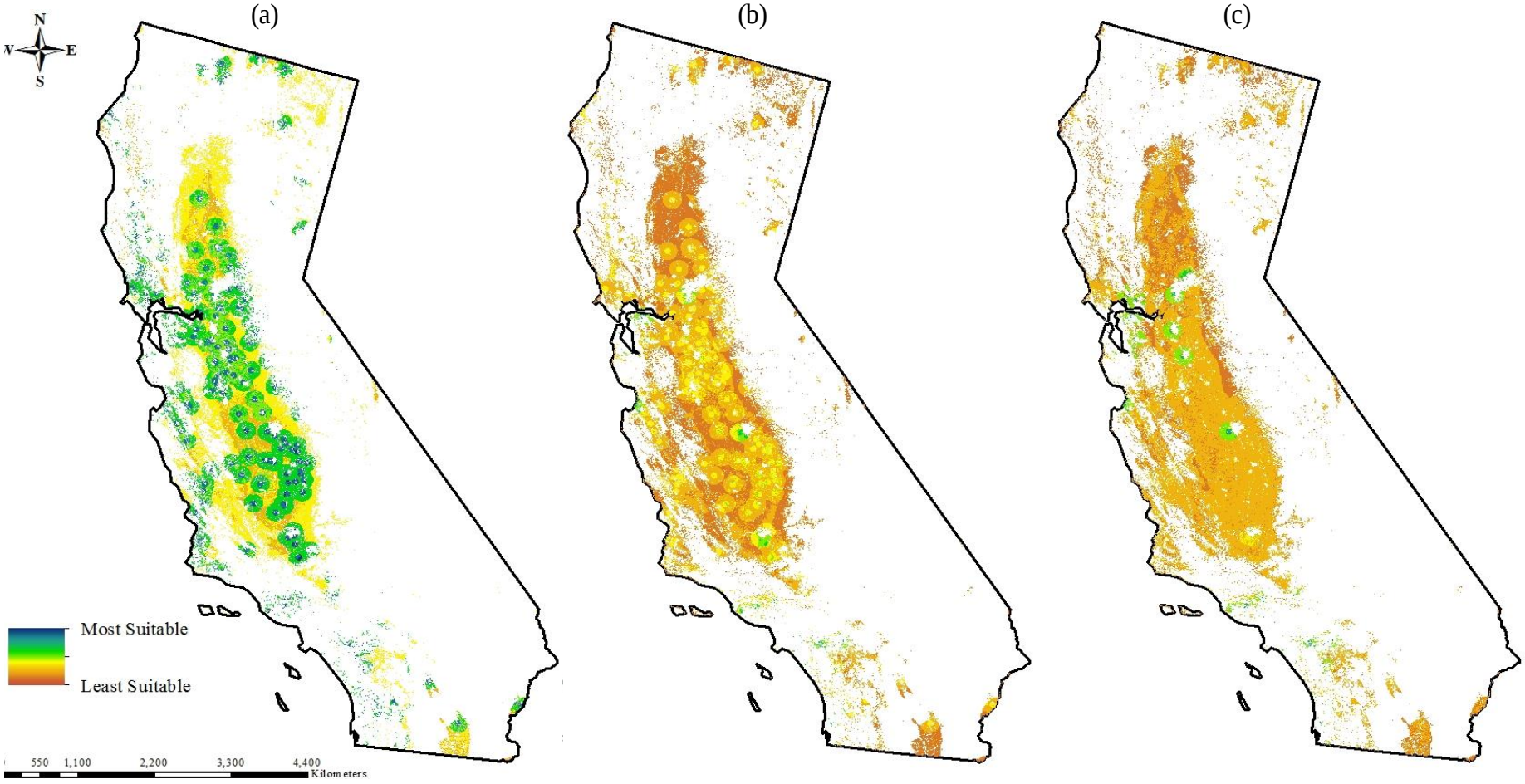

Figure 6: Suitability maps of the agricultural land for recycled water irrigation: a) stage 1 considering all WWTPs with acceptable discharge methods; b) stage 2 considering WWTPs with categorized flow volume, and c) stage 3 considering WWTPs with appropriate treatment processes.

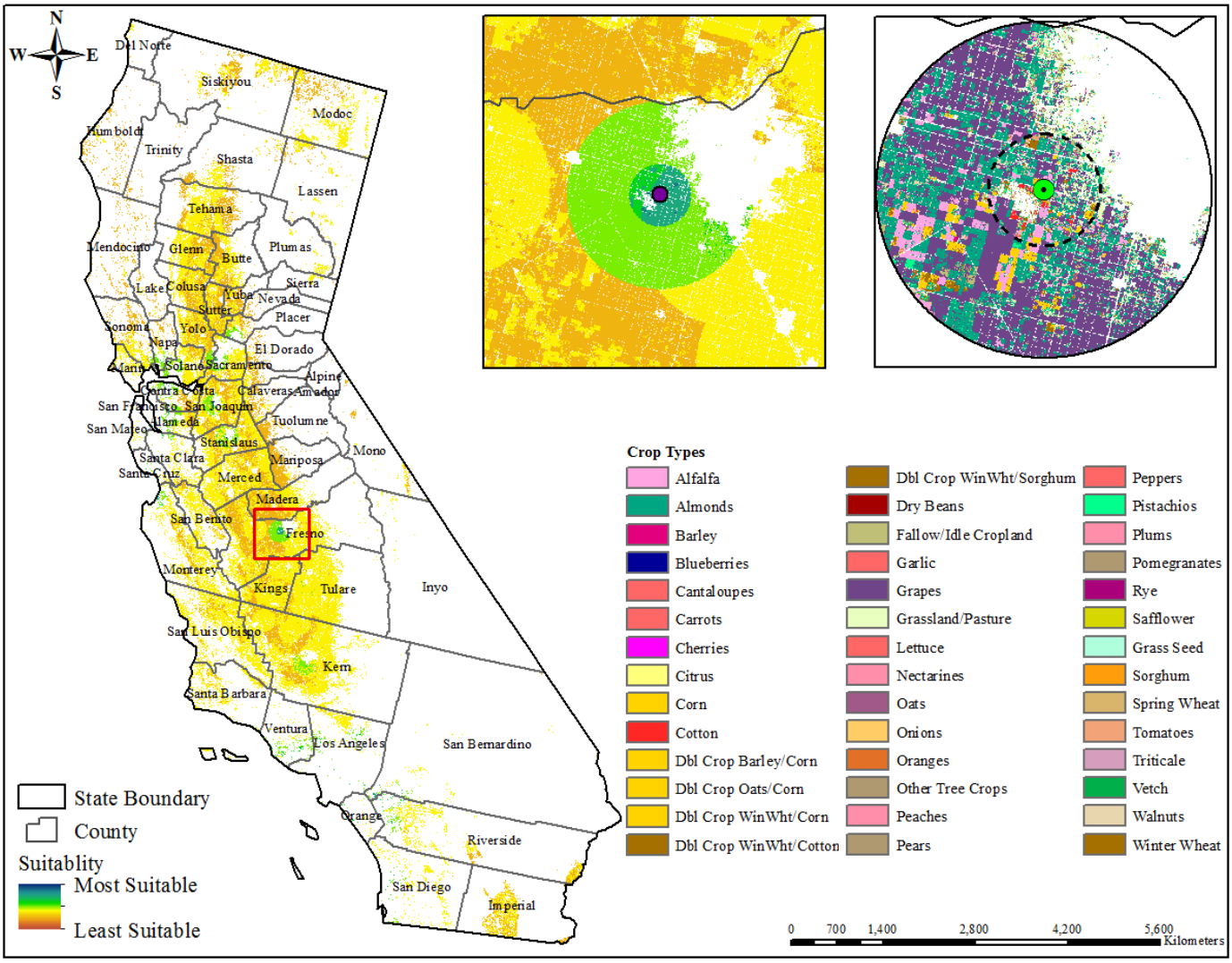

Figure 7: Final suitability map showing the location of the suitable agricultural lands ranging from “most suitable” to “least suitable” for recycled water irrigation. a) an example suitability map for a wastewater treatment plant in Fresno County; b) different types of crops within 5 and 15 km of the wastewater treatment plant.

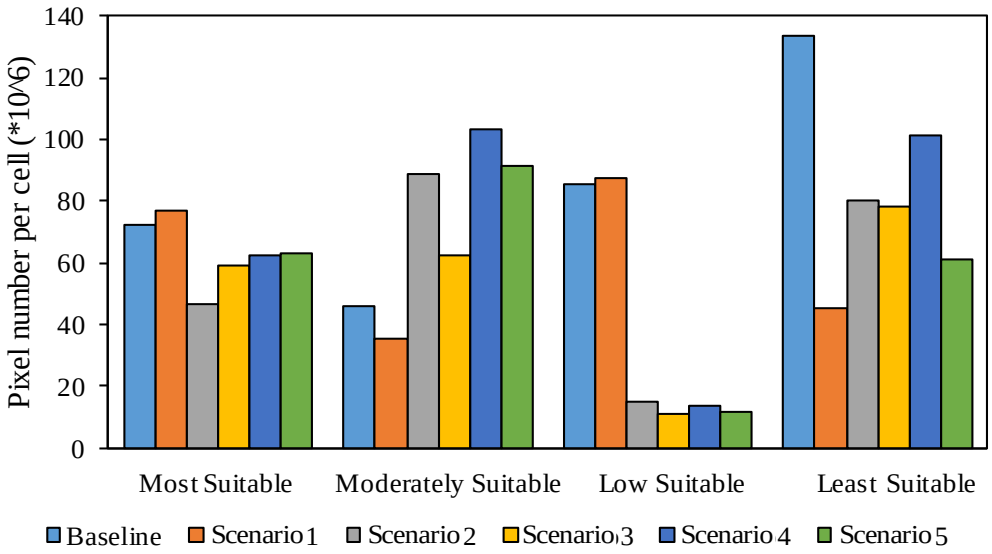

Figure 8: One-at-a-Time (OAT) sensitivity results showing the changes in pixel numbers per land suitability classes under five scenarios compared to the baseline condition.

6. Tables

Table 1: Use of different scoring techniques in the development of the GIS-MCDA framework.

Objectives	Study Area	MCDA Technique	Reference
To map and rank suitable sites for irrigation with treated wastewater	Nabeul-Hammamet catchment, Tunisia	Fuzzy-AHP	(Anane et al., 2012)
To identify the variety of interactions, dependencies and feedback between higher and lower level factors, and the impact of these interacting factors on sustainable citrus production	Ramsar District, Iran	ANP	(Zabihi et al., 2015)
To assess land suitability for tobacco production in tobacco zone	Shandong Province, China	Fuzzy-AHP	(Zhang et al., 2015b)
To evaluate agricultural water reuse practices for the improvement of irrigation	Cebala, Tunisia	CP	(Neji and Turki, 2015)
To incorporate a larger number of criteria into a flexible and adaptive structure for evaluating agricultural land capability and suitability	Boulder County, Colorado, USA.	LSP	(Montgomery et al., 2016)
To assess agricultural land suitability to achieve food security in an arid environment	Emirate of Abu Dhabi, UAE	AHP	(Aldababseh et al., 2018)
To identify benefits and challenges of different nutrient and water reuse systems	Town of Outapi, Namibia	AHP	(Woltersdorf et al., 2018)
To assess potentially irrigable areas for home gardens, water availability, and feasibility of water-lifting technologies	Lake Tana Basin, Ethiopia	AHP	(Assefa et al., 2018)
To present a methodology using MCDA procedure for the selection of constructed wetlands in tile-drained agricultural catchments	Lithuania, Europe	ELECTRE	(Punys et al., 2019)

Table 2: The current regulation for agricultural water reuse in California.

Category	Treatment	Reclaimed wastewater Quality
Food Crops (edible portion get contacts with recycled water)	Disinfected tertiary recycled water ✓ Oxidization ✓ Coagulation ✓ Filtration ✓ Disinfection	✓ Total Coliform bacteria (last 7 days) <2.2 MPN/100ml[1] ✓ Total Coliform bacteria (max. in 30 days) <23 MPN/100ml ✓ Total Coliform bacteria (at any time) <240 MPN/100ml ✓ Turbidity < 2 NTU[2] (average, within 24-hour period) ✓ Turbidity < 5 NTU (maximum, within 24-hour period) ✓ Turbidity < 10 NTU (maximum, at any time) ✓ BOD[3] & TSS[4] < [5]NS
Surface-irrigated Food Crops (above-ground edible portion, not contacted with recycled water)	Disinfected secondary 2.2 recycled water ✓ Oxidization ✓ Disinfection	✓ Total Coliform bacteria (last 7 days) <2.2/100ml ✓ Total Coliform bacteria (in any 30 days) <23/100ml ✓ Turbidity <NS ✓ BODs & TSS < NS
Pasture (used for dairy productions and consumed by human)	Disinfected secondary 23 recycled water ✓ Oxidization ✓ Disinfection	✓ Total Coliform bacteria (last 7 days) <23/100ml ✓ Total Coliform bacteria (in any 30 days period) <240 MPN/100ml ✓ Turbidity <NS ✓ BODs & TSS < NS
Orchards and Vineyards Fodder, Seed and Fiber Crops Processes Food Crops	Un-disinfected secondary recycled water ✓ Oxidization	

[1]MPN/100ml- bacterial count in most probable number per 100 milliliters
[2]NTU- Nephelometric turbidity units
[3]BOD- Biological Oxygen Demand
[4]TSS- Total Suspended Solid
[5]NS- Not specified by state regulations

Table 3: Pairwise scale that is used in the Analytical Hierarchy Process (AHP) based on (Saaty, 1978).

Intensity of Importance	Definition	Explanation
1	Equal Importance	Two activities contribute equally to the objective
3	Weak Importance	Experience and judgment slightly favor one activity over another activity over another
5	Strong Importance	Experience and judgment strongly favor one
7	Very Strong Importance	An activity is favoured very strongly over another; its dominance demonstrated in practice
9	Extremely Importance	The evidence favoring one activity over another is of the highest possible order of affirmation
2, 4, 6, and 8	Intermediate Values Between Adjacent Scale Values	Compromise is needed between two judgement

Table 4: Weights assigned for each criterion and sub-criterion.

Criteria-Thematic Layer	Sub criteria-Feature Class	Rank	Justifications
Agricultural land Cover	Non-food Crops-Fiber	9	The non-food crops like fiber crops (i.e. cotton) and fodder crops (i.e. alfalfa) are allowed to be irrigated with undisinfected secondary treated wastewater (Title 22). Cotton is also tolerant to exchangeable Sodium, and salt and very tolerant to Boron with low sensitivity to the water supply. Therefore, cotton was considered as a high priority crop to irrigate with reclaimed wastewater. Fodder crops like alfalfa or pasture need 800-1600 mm of water during the growing period, which has low to medium sensitivity to water supply quality (Pescod, 1992). These Non-food crops were also given high priority to be irrigated with reclaimed wastewater. Grains and legumes/oil like safflower are not consumed directly by humans or animals. Thus, all the Food crops (grains & legumes) and Non-food crops (Oil) were given as medium priority for irrigation with reclaimed wastewater. Food crop like orchard has limited contact to irrigation water compared to vegetables, thus, orchards were given lower priority than grains but higher than vegetables. Finally, vegetables that are eaten raw considered as "high risk" since the edible portion may have direct contact with reclaimed wastewater. Therefore, vegetables were given the lowest priority for irrigation with reclaimed wastewater.
	Non-food Crops-Fodder	8	
	Food Crops-Grains & Legumes	7	
	Non-food Crops-Oil crops	7	
	Food Crops-Orchard	5	
	Food Crops-Vegetables	3	
Distance from WWTP (km)	0 – 5	9	In the case of WWTP capacity, the assumption was larger treatment plants that discharge higher volumes of reclaimed wastewater are more reliable sources. In case of appropriateness, WWTPs were categorized based on Title 22 of the California Code of Regulations. The highest priority was assigned to the WWTPs, which have advanced treatment with disinfection unit processes. In case of accessibility, the WWTPs within 5 km proximity to agricultural activities were given the highest priority.
	5 – 15	5	
	>15	1	
Watershed Prioritizations	Very High	9	Drought Index: The PDSI of each watershed was evaluated and categorized based on the annual and seasonal trend, frequency, maximum and minimum drought condition for the last 30 years (1987-2017). Results show that the most frequent and chronic
	High	8	

	Medium	7	drought condition was sustained in Southern California; thus this region was given the high priority for the reclaimed wastewater irrigation. Climate Region: Since most of the agricultural lands are located in the Central Valley, it is selected as a high priority zone for the reclaimed wastewater irrigation. The northern mountains get lots of rain and snow that feed streams and rivers which flow through Central Valley and represent a primary source of freshwater (Pathak et al., 2018). Therefore, despite of less agricultural activities, a medium-high priority was given for the reclaimed wastewater use for irrigation in these regions.
	Low	6	
	Very Low	5	
	Normal	3	
Groundwater Basin priority	High	9	The groundwater basin prioritization information was incorporated as a decision criterion. The assumption was high priority groundwater basins are most preferred for the reclaimed wastewater use in agriculture to reduce the pressure on groundwater extraction.
	Medium	7	
	Low	5	
	Very Low	3	
	No priority	1	
Fresh Water Consumption in Agriculture (MGD)	>1000	9	The assumption was the reclaimed wastewater use as an additional water source is more favorable in the heavily irrigated counties. Therefore, counties were categorized into five groups and ranked based on their total freshwater consumption in agriculture. For instance, the counties that extract more than 1000 MGD water for irrigation were considered as the highest priority for the reclaimed wastewater use.
	500 – 1000	8	
	250 – 500	7	
	100 – 250	5	
	0 – 100	2	

Table 5: Pairwise comparison and ranking of decision criteria for all the WWTPs with the acceptable discharging method.

Recycled Water Irrigation for Agricultural Land Pairwise Matrix							
	Proximity to WWTPs	Agricultural Land Cover	Watershed Prioritization	GW Basin Prioritization	Counties Prioritization	Weights	Rank
Proximity to WWTPs	1.0	3.0	6.0	8.0	9.0	0.529	1
Agricultural Land Cover	0.33	1.0	4.0	5.0	6.0	0.265	2
Watershed Prioritization	0.17	0.25	1.0	4.0	3.0	0.114	3
GW Basin Prioritization	0.12	0.20	0.25	1.0	2.0	0.053	4
Counties Prioritization	0.11	0.17	0.33	0.50	1.0	0.039	5

Table 6: Pairwise comparison and ranking of decision criteria for the WWTPs considering their flow volumes (in MGD).

Recycled Water Irrigation for Agricultural Land Pairwise Matrix									
	Proximity to WWTPs			Agricultural Land Cover	Watershed Prioritization	GW Basin Prioritization	Counties Prioritization	Weights	Rank
	Flow > 100	25< Flow ≤100	Flow ≤ 25						
Flow > 100	1.0	2.0	3.0	5.0	6.0	7.0	8.0	0.359	1
100 < Flow ≤ 25	0.5	1.0	2.0	4.0	5.0	6.0	7.0	0.249	2
Flow ≤ 25	0.33	0.5	1.0	3.0	4.0	5.0	6.0	0.171	3
Agricultural Land Cover	0.2	0.25	0.33	1.0	4.0	5.0	6.0	0.111	4
Watershed Prioritization	0.17	0.2	0.25	0.25	1.0	2.0	3.0	0.050	5
GW Basin Prioritization	0.14	0.17	0.2	0.2	0.5	1.0	2.0	0.035	6
Counties Prioritization	0.12	0.14	0.17	0.17	0.33	0.5	1.0	0.025	7

Table 7: Recycled Water Irrigation Suitability Criteria Weight Calculation for the WWTPs with Acceptable Treatment Units.

Recycled Water Irrigation for Agricultural Land Pairwise Matrix								
	Proximity to WWTPs							
	Advanced and Disinfection Treatment	Secondary Treatment	Agricultural Land Cover	Watershed Prioritization	GW Basin Prioritization	Counties Prioritization	Weights	Rank
Advanced and Disinfection Treatment	1.00	6.0	5.0	7.0	8.0	9.0	0.540	1
Secondary Treatment	0.17	1.00	2.0	3.0	4.0	5.0	0.173	2
Agricultural Land Cover	0.20	0.50	1.00	3.0	5.0	5.0	0.140	3
Watershed Prioritization	0.14	0.33	0.33	1.0	2.0	3.0	0.069	4
GW Basin Prioritization	0.12	0.25	0.25	0.50	1.0	2.0	0.046	5
Counties Prioritization	0.11	0.20	0.20	0.33	0.50	1.0	0.032	6

Table 8: Summary of the datasets used in this study.

Data Type	Sources	References
Land Cover	USDA National Agricultural Statistics Service-Cropland Data Layer (NASS-CDL) 2016	https://nassgeodata.gmu.edu/CropScape/
Climate	U.S. Geological Science Watershed Boundary Dataset (USGS-WBD)	https://viewer.nationalmap.gov/basic/
	Climate Zones Areas in California	https://hub.arcgis.com/datasets/CAEnergy::california-building-climate-zones
	The West Wide Drought Tracker	https://wrcc.dri.edu/wwdt/about.php
Water Sources	Groundwater Consumption in Irrigation (MGD)	http://ca.water.usgs.gov/water_use/index.html
	Surfacewater Consumption in Irrigation (MGD)	
Water Policy	CASGEM Groundwater Basin Prioritization	https://gis.water.ca.gov/app/gicima/
	Areas Adjudicated for Groundwater Use	https://gis.water.ca.gov/app/boundaries/
Location of Wastewater Treatment Plants (WWTPs)	Clean Watersheds Needs Survey (CWNS) 2012	https://www.epa.gov/cwns
	National Pollutant Discharge Elimination System (NPDES)	https://www.epa.gov/npdes

Table 9: Relative sensitivity of the model criteria under five scenarios compared to the baseline condition.

	Scenario1	Scenario2	Scenario3	Scenario4	Scenario5
Most Suitable	0.06	-0.35	-0.19	-0.14	-0.13
Highly Suitable	-0.23	0.93	0.35	1.24	0.98
Moderate Suitable	0.02	-0.83	-0.87	-0.84	-0.86
Least Suitable	-0.66	-0.40	-0.42	-0.24	-0.54

Chapter 4: Sensitivity and Uncertainty Analysis for Streamflow Prediction Using Multiple Optimization Algorithms and Objective Functions: San Joaquin Watershed, California

Abstract:

Uncertainty analysis prior to the model calibration is key to the effective implementation of the hydrologic models. The major application of sensitivity analysis is to indicate the uncertainties in the input parameters of the model, which affects the model performance. There are different optimization algorithms developed and applied in the hydrologic model, which can be performed with different objective functions to calibrate and quantify the uncertainties in the system. The purpose of this study was to evaluate the model calibration performance and sensitivity of parameters using three optimization algorithms and five objective functions for predicting monthly streamflow. First, Sequential Uncertainty Fitting (SUFI-2), Generalized Likelihood Uncertainty Estimation (GLUE), and Parameter Solution (ParaSol) were used to calibrate the monthly streamflow for the semi-arid San Joaquin Watershed in California by using Soil and Water Assessment Tool (SWAT) model. The best performance metrics (R^2, NSE, PBIAS, P-factor, and R-factor) were obtained by SUFI-2 while using NSE as the objective function. Afterward, the coefficient of determination (R^2), Nash-Sutcliffe Efficiency (NSE), the percentage of bias (PBIAS), Kling-Gupta efficiency (KGE) and Ratio of the standard deviation of observations to root mean square error (RSR) were used as an objective function to assess the monthly calibration performance. KGE is found to be a suitable objective function to

This chapter has been published in Modeling Earth Systems and Environment.
Paul, M., & Negahban-Azar, M. (2018). Sensitivity and uncertainty analysis for streamflow prediction using multiple optimization algorithms and objective functions: San Joaquin Watershed, California. Modeling Earth Systems and Environment, 4(4), 1509-1525.
https://doi.org/10.1007/s40808-018-0483-4

calibrate this complex and snowmelt-dominated watershed. The findings from this study will serve as a guideline for hydro-ecological researchers to achieve further watershed management goals.

1. Introduction

Hydrologic cycle has close interactions with the surface and subsurface processes by the integration of climate, land use and land cover (LULC) and ocean systems (Kumar et al., 2017; Paul et al., 2017; Zhang et al., 2017a). To identify the potential impacts of LULC changes, soil degradation, and climate changes on the ecosystem, it is necessary to study the hydrological parameters, such as surface runoff, soil moisture, evapotranspiration (ET), groundwater, streamflow etc. (Kumar et al., 2017; Paul, 2016; Talib and Randhir, 2017). Assessment of hydrology has been a long-standing research topic in studying agricultural management, flood forecasting and inundation mapping, soil degradation, nutrient losses, and biodiversity conservation practices (Morton and Olson, 2014; Paul, 2016; Paul et al., 2017; Rajib et al., 2016a; Schilling et al., 2014).

Hydrologic models are effective tools to understand and simulate the hydrologic processes to evaluate the impact of climate and LULC changes, to investigate water quality, and to plan the water resources management (Paul, 2016; Paul et al., 2017; Shao et al., 2017; Wang et al., 2016). However, the successful application of distributed hydrologic models depends on proper calibration-validation and uncertainty analysis to capture the existing complex environmental condition (Abbaspour et al., 2015a; Kouchi et al., 2017). Calibration is performed by the appropriate selection of the model input parameters regarding suitable ranges to

simulate the hydrological process accurately which is assessed by comparing model outputs for a given set of observed data (streamflow, sediment, etc.) (Arnold et al., 2012; Kouchi et al., 2017). The accurate calibration of the hydrological models is a challenging task due to the uncertainties in hydrological modeling. According to several studies, the main sources of uncertainties are the input errors due to inaccurate and interpolated measurements; inaccuracy due to over-simplification of the model; errors in model structure or hypothesis and algorithms; inaccuracies of observation used to calibrate the model; and errors in parameterization and output ambiguity (Abbaspour, 2008; Khoi and Thom, 2015; Kouchi et al., 2017; Singh et al., 2013; Xue et al., 2013). Therefore, sensitivity analysis is crucial to quantify the uncertainty of the system, determine the effect of input parameters on the outputs, the integral knowledge of data, and optimize the design of a system.

Although model uncertainty is difficult to quantify, using a suitable calibration method can manage to control these large uncertainties (Khoi and Thom, 2015; Kouchi et al., 2017; Rostamian et al., 2008; Wu and Chen, 2015a). A number of optimization algorithms have been developed in the literature and applied in hydrologic models to calibrate the model, quantify the uncertainty of the system, and rank the influence of various parameters on the system. For instance, the Sequential Uncertainty Fitting procedure (SUFI-2) (Abbaspour et al., 2004), Generalized Likelihood Uncertainty Estimation method (GLUE) (Beven and Binley, 1992), Bayesian Inference (Box and Tiao, 2011), Parameter Solution (ParaSol) (van Griensven and Meixner, 2006), Particle Swarm Optimization (PSO) (Eberhart and Kennedy, 1995; Kennedy and Eberhart, 1995), etc. have been developed and applied

to many hydrological studies. Several studies, evaluate the uncertainty of the model systems and input parameters using different optimization techniques. For example, (Khoi and Thom, 2015) applied four uncertainty techniques (SUFI-2, GLUE, ParaSol and PSO) to evaluate the parameter uncertainty analysis of streamflow simulation at the Srepok River watershed in Vietnam, they reported that the SUFI-2 method has the advantages to provide more reasonable simulated results compared to other three techniques. (Yesuf et al., 2016)(2016) have investigated SUFI-2 and GLUE techniques for the Maybar Watershed in Ethiopia, and found that both techniques were able to produce reasonable simulated results for uncertainty analysis, calibration, and validation of the hydrologic model (Yesuf et al., 2016).

The optimization algorithms differ based on the assessment strategies, determination of the set of parameter ranges, and examination of the desired threshold for a particular objective function (Kouchi et al., 2017). Model simulation performance is evaluated graphically (to compare how well the simulated values fit with the observed data), and statistically (referred as goodness-of-fit criteria, and performance or efficiency criteria). The efficiency criteria can also be used as objective function during the calibration process to help identify an optimal parameter that means parameter sets are adjusted according to a specific search scheme to optimize certain calibration criteria (objective functions) (Madsen, 2003; Muleta, 2011). Different objective functions rely on different features of the variable that is targeted for calibration, especially when several sites and/or different variables are being calibrated. For Example, Nash-Sutcliffe efficiency tends to rely on the peaks (Nash and Sutcliffe, 1970), while mean absolute error relies more on average

deviations, or least-square errors aim to fit the hydrograph for high flows. Therefore, the relevance and choice of an objective function is an important decision to calibrate a watershed model because an inappropriate objective function can give a good output in statistical terms while it is conflicting from the reality (Abbaspour, 2013; Molina-Navarro et al., 2016; Muleta, 2011). For instance, (Garcia et al., 2017) identified the best objective functions to calibrate the parameter set and estimate the robustness and sensitivity of the rainfall-runoff model in 691 French watersheds. (Molina-Navarro et al., 2017) assessed the impact of the objective function for multi-site and multi-variable calibration using a hydrologic model in the Odense catchment in Denmark. (Muleta, 2011) examined the sensitivity of hydrologic model performances to the objective function during automated calibrations in the Little River Experimental Watershed (LREW) in Georgia.

Looking at these recent studies, it is evident that the capability of using different optimization algorithms in relation to different objective functions needs to be verified in different regions. Despite this importance, there is no study that exclusively focuses on the semi-arid region like the Central Valley of California. In this study, the San Joaquin watershed located in the central valley of California was selected where water management activities are intense. It is an agricultural watershed where the watershed hydrology affected by several reservoirs and dams which are operated for extensive agricultural irrigation. A hydrologic model will be the basis of developing the strategies for sustainable water resources management for such complex hydrology to watershed managers, agricultural producers, and policymakers. However, before the development of the water resource management,

it is necessary to identify and quantify the large uncertainties subjected to the distributed hydrological modelling using different optimization algorithms and objective functions within the same hydrologic modeling framework. The aim of this study is to (1) evaluate hydrologic model performances and calibration results using three different optimization algorithms (SUFI-2, GLUE, and ParaSol), and (2) evaluate the impact of five objective functions (R^2, NSE, PBIAS, KGE and RSR) on the monthly streamflow simulations. To achieve these objectives, SWAT-CUP (SWAT Calibration and Uncertainty Programs) (Abbaspour, 2008) was used for model calibration-validation and sensitivity analysis coupled with the distributed hydrological model the Soil and Water Assessment Tool (SWAT) (Arnold et al., 2012) in the San Joaquin Watershed. SWAT is one of the most widely used distributed models, and it has been applied worldwide for hydrologic and water quality simulations. In recent years, many studies compared the performance of SWAT models under different optimization algorithms coupled with SWAT-CUP to calibrate the streamflow and uncertainty analysis (Kumar et al., 2017; Molina-Navarro et al., 2017; Uniyal et al., 2015; Yesuf et al., 2016; Zhang et al., 2015a), that establish its applicability and scientific acceptance under many different circumstances.

2. *Methodology*

2.1. Study Area

The San Joaquin watershed is located in central California and located on the highly agricultural region of the Sacramento-San Joaquin Delta (Figure 1). The watershed has a drainage area of 15357.7 km^2 approximately (USGS Hydrologic Unit

Code 18040001). The land use is primarily dominated by agricultural land (37.4%) and the remaining area consists of grass/pasture (29.7%), shrubland (7.9%), fallow/idle cropland (7.8%), urban (7.3%), forest (6.8%), and water (3.1%) (Table 1). Based on the USDA National Agricultural Statistics Service-Cropland Data Layer (NASS-CDL) 2016, agricultural land mainly dominated by almond (10.35%), followed by vineyard (8.2%), alfalfa (4.2%), winter wheat (2.6%), tomatoes (2.4%) and cotton (2.3%). The San Joaquin River originates from the high Sierra Nevada Mountains and flows through the northwest of the central valley before reaching the Sacramento-San Joaquin Delta. The Sacramento-San Joaquin Delta has an arid-to-semiarid climate, where average annual precipitation is 323 mm (12.5 inches), and the average annual temperature is 17.1°C with minimum and maximum of 9.7 and 24.5°C respectively (Service, 2017). Soils in the San Joaquin Delta are composed of mainly ultisols in the high Sierra Nevada ecoregion and recent alluvial soil in the Central Valley ecoregion (Gronberg and Domagalski, 1998). A United States Geological Survey (USGS) gauging station 11261500 was used as an outlet at Fremont in California. In addition, another USGS station 11254000 at Mendota was used in the upstream during calibration. One watershed inlet was defined at the USGS station 11251000 below the dam on the San Joaquin River at Friant, California (Figure 1).

2.2. Hydrologic Model

In this study, the SWAT model (version 2012 with its ArcSWAT interface) was used to delineate the San Joaquin Watershed. SWAT is a physically-based semi-distributed and time-continuous hydrologic model (Arnold et al., 1998). SWAT is a

watershed scale model, was developed to evaluate the impact of land management practices and climate on the water in large and complex watersheds over long periods of time. In SWAT, different water balance components, and water resources (e.g., blue and green waters) are calculated through an explicit calculation at the subbasin level. In this model, a watershed is divided into a number of subbasins and based on homogeneous soil types, land-use types, and slope classes categorized into hydrological response units (HRUs) that allow a high level of spatial detail simulation.

2.3. Model Setup

The SWAT model requires input data include Digital Elevation Map (DEM), land use map, soil map, and weather/climate data as the main input data (Neitsch et al., 2011). A 30 m resolution DEM data derived from the USGS National Elevation Dataset (USGS-NED, 2013) was used to delineate the watershed boundary. A 30 m resolution of land use data from the NASS-CDL 2016 and soil data from the State Soil Geographic (STATSGO) database were used. Daily precipitation and daily maximum and minimum temperature data for 15 years (2002-2016) were obtained from the National Climatic Data Center (NCDC) website for 18 weather stations (Figure 1). The multiple HRU options were used to represent the soil and land use types where a single HRU represents a unique combination of soil type and land use. This watershed was discretized into 3902 HRUs in 73 subbasins. Surface runoff is determined using the modified Soil Conservation Service (SCS) Curve Number (CN) method (Arnold et al., 1998; Neitsch et al., 2011; Service, 1972; Wu et al., 2012). The Penman-Monteith method (Monteith, 1965) was used to estimate the potential

evapotranspiration (PET). Channel routing is calculated using the Muskingum routing method or variable storage routing method (Arnold et al., 1998).

2.4. Calibration / Uncertainty Analysis Programs

2.4.1. SUFI-2

Based on the Bayesian framework, the sequential and fitting process is used in SUFI-2 for calibration, validation, and sensitivity and uncertainty analysis (Khoi and Thom, 2015; Kouchi et al., 2017). In SUFI-2, all sources of parameter uncertainties (e.g., model input, model structure, and measured data) are accounted and described as uniform distributions (Abbaspour, 2013). The model's goodness-of-fit and uncertainty are determined by two indices: P-factor and R-factor. Latin hypercube sampling is used to obtain the propagation of the uncertainty and known as P-factor. The P-factor is the percentage of observed data bracketed by the 95% prediction uncertainty (95PPU) (determined at the 2.5% and 97.5% levels of the cumulative distribution of output variables). The R-factor is quantifying the strength of a calibration/uncertainty analysis by the average thickness of the 95PPU band divided by the standard deviation of the observed data (Abbaspour, 2013). The value of the P-factor ranges between 0 and 100% and R-factor ranges between 0 and infinity. Theoretically, where the simulation exactly corresponds to the observed data, the P-factor, and R-factor incline to be 1 and 0, respectively. The aim of the SUFI-2 is bracketing most of the observed data with the smallest possible uncertainty band that means good results with a relatively large P-factor and small R-factor. An objective function is defined before uncertainty analysis and assigned with a required stopping rule.

2.4.2. GLUE

The GLUE is relatively simple and widely used in hydrology. GLUE was first introduced by (Beven and Freer, 2001) to allow the equifinality of parameter sets during the estimation of model parameters in over parameterized models. The GLUE depends on the Monte Carlo method where a large number of simulations are performed with randomly chosen parameter values selected from prior parameter distributions. In this method, a likelihood value is assigned to each set of parameter values to compare the predicted simulation and observed data and evaluate the simulated parameter combination into the real system. However, GLUE rejects the concept of a unique global optimum parameter set within some particular model structure used in the most calibration procedures in the hydrological modeling. GLUE is different from other optimization algorithms because of its acceptability of different parameter sets which can produce fit model predictions with similarly good performance. The objective of GLUE is to identify a set of behavioral models within the universe of the possible model or parameter combinations (Abbaspour, 2013; Blasone et al., 2008; Kouchi et al., 2017). Similar to SUFI-2, all sources of uncertainty are also accounted in GLUE for parameter uncertainty (Beven and Freer 2001).

2.4.3. ParaSol

The ParaSol method combines the objective functions into the global optimization criterion and the modified Shuffle Complex (SCE-UA) algorithm is used for uncertainty analysis to find the optimum solutions (Abbaspour, 2013; Duan et al., 1992; van Griensven and Meixner, 2006). Similar to GLUE methodology, a threshold

or criterion value is used to divide the performed simulations into ‘good’ and ‘not good’ simulations after the optimization of the modified SCE-UA. However, unlike GLUE, the threshold value can be defined by the χ^2-statistics where the selected simulations correspond to the confidence region (CR) or Bayesian statistics which could point out the high probability density (HPD) region for parameters or the model outputs (Abbaspour, 2013; Wu and Chen, 2015b). Through the global SCE algorithm, the minimization of a single function can be done up to 16 parameters (Abbaspour, 2013; Duan et al., 1992).

2.5. Objective Functions

The coefficient of determination (R^2), Nash-Sutcliffe Efficiency (NSE), the percentage of bias (PBIAS), Kling-Gupta efficiency (KGE), and Ratio of the standard deviation of observations to root mean square error (RSR) were used as objective functions to assess the agreement between simulated and observed streamflow hydrographs.

2.5.1. Coefficient of Determination

Standard regression R^2 (Krause et al., 2005) is an indicator in which the model explains the total variance in the observed data (the squared ratio between the covariance and the multiplied standard deviations of the observed and predicted values.). R^2 describes the degree of collinearity between the observed and simulated values. Therefore, large R^2 value can be obtained with a poor model that consistently overestimates or underestimates the observations. However, this SWAT-defined statistic, albeit non-standard, is used in this work to allow comparison with previous literature on this model (Montas et al., 2019).

2.5.2. Nash-Sutcliffe Efficiency

Dimensionless NSE (Nash and Sutcliffe, 1970) is addressing the temporal dynamics and the most widely used statistics for hydrologic calibration. The values range from negative infinity to 1, where 1 shows a perfect model; zero implies that observed mean is as good as predicted model; and less than zero means observed mean is a better predictor than the model. NSE is sensitive to extreme values due to the squared differences between observed and simulated values (Krause et al., 2005).

2.5.3. Percentage of Bias

PBIAS (Yapo et al., 1996) is robust and commonly used to determine how well the model simulates the average magnitudes for the output response of interest. According to Moriasi et al. (2007), error-index PBIAS is one of the measures that should be included in the model performance reports. PBIAS measures the tendency of the simulated values to be larger or smaller than their observed counterparts. Positive PBIAS values indicate a tendency of the model simulations to overestimate and negative values indicate to underestimate the observations respectively.

2.5.4. Kling-Gupta Efficiency

NSE uses the observed mean as baseline, which can lead to the overestimation of model skill for highly seasonal variables(e.g., runoff in snowmelt-dominated basins). To overcome this problem associated with NSE, (Gupta et al., 2009) proposed an alternative performance indicator KGE, based on the equal weighting of three sub-components: linear correlation (r), bias ratio (β) and variability (α), between simulated and observed discharge (Eq. 4).

2.5.5. Ratio of Standard Deviation of Observations to RMSE

RSR standardizes the root mean square error (RMSE) using standard deviation of the observations. (Moriasi et al., 2007) developed RSR based on the recommendation by (Singh et al., 2005). Moriasi et.al. (2007) mentioned that RSR providing a normalized value to compare model performances across watersheds or various constituents. The corresponding performance efficiency criteria for these five objective functions were established according to a recent review of (Moriasi et al., 2015) and (Thiemig et al., 2013) (Table 2). The formulations of these five objective functions are as follows:

$$R^2 = \frac{[\sum_i (Y^{obs,i} - Y^{obs}_{mean})(Y^{sim,i} - Y^{sim}_{mean})]^2}{\sum_i \sqrt{(Y^{obs,i} - Y^{obs}_{mean})^2} \sum_i \sqrt{(Y^{sim,i} - Y^{sim}_{mean})^2}} \quad (1)$$

$$NSE = 1 - \frac{\sum_i (Y^{obs} - Y^{sim})^2}{\sum_i (Y^{obs} - Y^{obs}_{mean})^2} \quad (2)$$

$$PBIAS = \frac{\sum_{i=1}^{n} (Y^{obs} - Y^{sim})}{\sum_{i=1}^{n} Y^{obs}} x\, 100 \quad (3)$$

$$KGE = 1 - \sqrt{(r-1)^2 + (\alpha-1)^2 + (\beta-1)^2}\ ;\ \alpha = \frac{\sigma_{sim}}{\sigma_{obs}}\ ;\ \beta = \frac{Y^{obs}_{mean}}{Y^{obs}_{mean}} \quad (4)$$

$$RSR = \frac{RMSE}{STDEV} = \frac{\sqrt{\sum_{i=1}^{n} (Y^{obs} - Y^{sim})^2}}{\sqrt{\sum_{i=1}^{n} (Y^{obs,i} - Y^{obs}_{mean})^2}} \quad (5)$$

Where Y^{obs} is the observed data, Y^{sim} is the simulated output, and Y^{obs}_{mean} is the mean of observed data, Y^{sim}_{mean} is the mean of simulated output, r is the linear regression coefficient between simulated output and observed data;, where σ_{sim} and σ_{obs} are the standard deviation of simulated output and observed data.

2.6. Calibration, Validation and Sensitivity Analysis

The calibration protocol presented by (Abbaspour et al., 2015b) was followed to calibrate the SWAT model. The SWAT model was calibrated for monthly streamflow from 2009 to 2016 with one-year warm-up period (2008) and validated from 2002 to 2007. The following paragraphs describe the calibration procedure used in this study in a step-by-step process.

SWAT Model Parameters: SWAT model contains over 200 hydrological parameters, and clearly all of them may not contribute significantly to the output. Therefore, it is necessary to identify the most sensitive input parameters and their ranges for streamflow simulation. In this study, initially, 32 parameters and their initial value ranges were selected based on the literature review on and nearby Central Valley watersheds (Burke and Ficklin, 2017; Chen et al., 2017a; Luo et al., 2008).

Local Sensitivity: Local sensitivity process was taken, where a single parameter was allowed to change in the input parameters and other parameters kept constant. It is also called as one-at-a-time analysis since it is an indicator only for the addressed point estimates instead of the entire distribution.

Global Sensitivity: the second approach to sensitivity analysis is the global sensitivity analysis, where a global set of samples are used to explore the design space. SWAT-CUP uses t-stat (high absolute values suggest more sensitivity) and p-value (values close to zero suggest a high level of significance) to identify the relative significance of individual parameters. For the global sensitivity process, 1000 numbers of iterations were selected to identify the most sensitive input parameters. Total of 18 sensitive parameters were identified by Hypercube One-at-a-time (LH-

OAT) and global sensitivity analysis using the SUFI-2 (Table 3). These parameters were used for the streamflow simulations at two stream gauge stations (Figure 1). Table 4 shows that the sensitive parameters yielded by the three optimization techniques (SUFI-2, GLUE, and ParaSol) are the same. However, there are variations in the ranking of the sensitive parameters. This variation in the sensitivity ranking of the parameters is attributed due to the difference in the sampling techniques used for selecting the random samples. Similar results were found by (Uniyal et al., 2015) and revealed that any of the techniques (GLUE, SUFI-2, ParaSol, etc.) could be used for the sensitivity analysis.

Rainfall and Snowmelt: Rainfall and snowmelt both are driving variables in the watershed hydrology. Therefore, it is better to abstain to calibrate simultaneously with other model parameters (Kouchi et al., 2017). To avoid this identifiability problems with other parameters, the snow parameters and their values were fixed initially in the model. Then, rest of the parameters were used to calibrate the model.

Optimization Algorithms: To compare the three optimization algorithms, similar conditions were used regarding calibration parameters and their initial ranges, and statistical criteria. In SUFI-2, the sample size for one iteration could be set in the range of 500–1000 simulations (Abbaspour, 2013; Wu and Chen, 2015a; Xue et al., 2013), however, 500 is recommended by (Abbaspour, 2013). In this study, three iterations with 500 simulations in each iteration (total 1500 simulations) were conducted for uncertainty analysis with a preset threshold value NSE=0.5. Initially, like SUFI-2, same 1500 simulation runs were used for GLUE and ParaSol to compare the sensitivity of calibration performance of the model. However, fewer runs could

not produce satisfactory results regarding P-factor and R-factor (results not shown here) while using GLUE and ParaSol as optimization algorithms. Moreover, different studies and literature reviews recommended that GLUE and ParaSol need higher simulations (Abbaspour 2013; Khoi and Thom 2015; Wu and Chen 2015). In the GLUE, generally a wide physically meaningful ranges are used for each parameter to cover more possible behavioral solution. This requires one iteration with a large number of simulation runs (maximum 10,000). (Yang et al., 2008) performed the GLUE with 1000, 5000, 10,000 and 20,000 runs and best performance found for a sample size of 10,000 runs. In this study, the parameters range has been selected based on the literature review (mentioned above), therefore, a small simulation runs of 5000 was used with same initial parameter ranges used in SUFI-2. To keep consistency with SUFI-2, the NSE=0.5 was selected as the objective function to screen the behavioral and non-behavioral simulations for GLUE. ParaSol optimization technique also requires a larger number of simulations (>5000). However, similar to GLUE a smaller sample size of 3000 runs and same initial parameter ranges used to conduct uncertainty analysis.

Evaluating Objective Functions: To evaluate the effect of different objective functions on the streamflow simulation, same initial parameter ranges were used (Table 3). Total of five objective functions were used separately (one objective function per calibration run) to optimize the parameter ranges to calibrate the monthly streamflow. In each iteration, the behavior threshold of each objective function was set based on Table 2 (as example, for NSE it was 0.5) to get satisfactory results.

Finally, the performance of each calibration results was compared using the five efficiency criteria (Table 2).

3. Results and Discussion

3.1. Performance Sensitivity to Optimization Algorithms

3.1.1. SUFI-2

The results from the third iteration were used for uncertainty analysis. SUFI-2 found 384 behavioral simulations in last 500 simulations. The 95PPU for the simulated monthly discharge after the third iteration shown in Figure 2. It is found that 70% measurements at the Fremont station and 60% measurements at the Mendota station were bracketed by the 95PPU during the calibration period and 78% and 62% during the validation period. The relative width of 95% probability band (R-factor) was near 1 during both calibration and validation period (Table 5). These results indicated that SUFI-2 was capable of capturing the observations during the calibration and validation periods. In the Fremont station, the values of the performance measures of the best simulation were within the criteria suggested by (Moriasi et al., 2015), except PBIAS during the calibration period (Table 5). However, Mendota station did not have satisfactory results during both calibration and validation periods, except R^2 (Table 5). At the outlet (Fremont station), for the best simulation the values of R^2, NSE, and PBIAS were 0.91, 0.84, and -40.45% respectively during the calibration period; and 0.88, 0.84, and -7.33% respectively during the validation period.

3.1.2. GLUE

Like SUFI-2, the same threshold value (NSE = 0.5) was used in the GLUE. However, GLUE achieved only 285 behavioral simulations out of 5000 simulation runs. Figure 3 shows the 95PPU plot with 2.5% and 97.5% of the accumulated distribution of prediction uncertainty from the behavioral simulations. The small P-factor (21%- 30%) indicated that the GLUE optimization algorithm was not able to predict the reasonable observations at both Fremont and Mendota Stations (Table 5). In Figure 3 it is also shown that the 95PPU region from GLUE was narrower (R-factor = 0.74 and 0.45 at Fremont and Mendota Station respectively) than the SUFI-2 (R-factor = 1.02 and 0.85) during the calibration period. However, similar to SUFI-2, calibration and validation results were "very good" in terms of R^2 and NSE at the outlet (Table 2 and 5). At the Fremont Station, for the best simulation R^2, NSE, and PBIAS were found to be 0.89, 0.83, and -40.41% respectively during the calibration period; and 0.88, 0.84, and -4.17% respectively during the validation period. However, at the Mendota station performance criteria did not meet except R^2 (Table 5).

3.1.3. ParaSol

ParaSol algorithm was applied last to compare the sensitivity performance with the other two optimization algorithms. Unlike GLUE, the ParaSol achieved 2002 behavioral simulations in 3000 simulation runs. The statistical summary of behavioral simulation results is presented in Table 5 and the hydrograph of the observed and best-simulated streamflow with 95PPU in Figure 4. Figure 4 showed that ParaSol algorithms obtained a very narrow uncertainty region and only 61-63% observed

streamflows at the Fremont station, and 17-16% observed streamflows at the Mendota station were covered by the 95PPU (Table 5 and Figure 4). At the outlet (Fremont station) for the best simulation the values of R^2, NSE, and PBIAS were found to be 0.90, 0.83, and -47.44% respectively during the calibration period; and 0.88, 0.87, and -14.87% respectively during the validation period (Table 5).

3.1.4. Comparison Among Three Optimization Algorithms

The comparison among the SUFI-2, GLUE, and ParaSol was conducted in three aspects: model performance, uncertainty prediction, and computational efficiency.

Model Performance: Amongst three optimization algorithms, there are quite small differences in model performances in the streamflow simulation during both calibration and validation periods (Table 5). Using all the three algorithms, the R^2 and NSE values were ranked as "very good" at the watershed outlet during both calibration and validation periods (Table 2 and 5). However, using all the algorithms, the calibrated model always overestimated the streamflows (-ve PBIAS) to capture the peak flow in 2011. Model performance at Mendota station was not satisfactory based on performance criteria (Table 2), except R^2. In the previous study, (Chen et al., 2017a) also found similar results for the Mendota station using the SUFI-2 algorithm. This may be attributed to insufficient and uneven spatial distribution of the weather stations and due to the influence of the reservoir in the upstream (Figure 1). Another possible reason for the mismatch could be the caused by the intense human activities in the upper reaches of the watershed including irrigation channels or small hydropower dams (Figure 1). In this study, the model performance during the validation period revealed the model capability to encompass the variation of

observed streamflow in magnitudes (Figure 2-4) and according to the statistical performances sometimes showed better than calibration periods (Table 5). This demonstrates the ability of the model to reproduce the discharge in the San Joaquin Watershed, which can serve as a base model for management and future scenarios analysis.

Model Prediction Uncertainty: The SUFI-2 achieved satisfactory simulations of the streamflow, and indicating a reasonable uncertainty in the calibration and validation results. The SUFI-2 algorithm yielded the similar R^2 (0.91) and NSE (0.84) from the best simulation compared to other two algorithms (GLUE and ParaSol), and generated more balanced prediction uncertainty ranges (R-factor 0.85 to 1.02) with the best coverage of measurement (P-factor 0.60 to 0.78) at the same time (Table 5). However, GLUE and ParaSol barely showed the improvement on P-factor (ranges from 0.16 to 0.63) and R-factor (ranges from 0.22 to 0.74) comparing the SUFI-2. The R-factors for the streamflow of SUFI-2 showed a better performance than GLUE and followed by ParaSol (Table 5). This revealed that the prediction uncertainty range from the SUFI-2 algorithm was wider than that from the GLUE and ParaSol. The ParaSol algorithms generated very narrow prediction uncertainty bands (R-factor 0.22 to 0.33) which were not distinct from the best prediction. This may have resulted from a violation of the statistical assumption of independent and normally distributed residuals. Overall, in this study, the R-factor values found quite small for GLUE and ParaSol that generated the small bands of the 95PPU, and thus small number of observed streamflows were bracketed by the 95PPU (small P-factors) (Figure 3-4). Small values of P and R factor in Fremont and Mendota station, indicated that GLUE

and ParaSol were not successful in capturing the uncertainty (95PPU, R-factor, P-factor) based on the defined conditions (i.e., initial parameter ranges, number of simulation runs, and behavioral threshold value).

Model Computational Efficiency: The last aspect of the comparative analysis was the model computational efficiency. In this study, an intensive computation was applied for GLUE (5000 simulation runs) and ParaSol (3000 simulation runs) compared to SUFI-2 (total 1500 simulation runs in three iterations). The SUFI-2 algorithm succeeded to get 384 behavioral solutions in last 500 simulations, while GLUE and ParaSol found 285 and 2002 behavioral simulations in 5000 and 3000 simulations, respectively. Although GLUE and ParaSol used a larger number of simulations, the P-factor and R-factor of SUFI-2 showed a better performance than GLUE and ParaSol. Therefore, SUFI-2 was easy to implement compared to other algorithms because the high efficient Latin Hypercube (LH) sampling method can reduce the sampling sizes within a certain space (Khoi and Thom, 2015; Wu and Chen, 2015a). In the ParaSol, another high efficient sampling method SCE-UA was applied to localize the global optimum of the parameter ranges (Wu and Chen, 2015a; Yang et al., 2008; Zhang et al., 2015a). The GLUE required large intensive computations (5000 runs) due to use of relatively simple Monte Carlo sampling algorithm, although the application of the GLUE was easier than the other two methods on the sensitivity analysis and global optimization calculation. Therefore, GLUE has the low computational efficiency for high dimensional and complex models which required more computational resources and time for estimating the uncertainty. The correlation matrix among the best simulation of the streamflows

from three optimization algorithms also concluded that the GLUE was less efficient for uncertainty analysis than the SUFI-2, and ParaSol (Table 6).

This study has been done for the semi-arid to the arid climate in the Central Valley of California. These findings were similar to the study conducted by (Kouchi et al., 2017), where the SUFI-2, GLUE, and PSO were used to assess the uncertainty estimates for the Karkheh River Basin and Salman Dam Basin (Iran) located in the semi-arid and arid regions respectively and indicated the advantages of using the SUFI-2. Chen et al. (2017) also applied the SUFI-2 algorithm for the uncertainty analysis and the monthly streamflows calibration in the San Joaquin watershed. In general, it can conclude that the SUFI-2 technique is the promising technique in the calibration and uncertainty analysis in the semi-arid to arid regions.

3.1.5. Sensitivity of Model Parameters to three Optimization Algorithms

Table 7 and Figure 5 show the best estimates and 95% uncertainty ranges of all parameters resulting from the GLUE and ParaSol, and posterior parameter ranges resulting from SUFI-2. Each calibrated parameter range has large overlaps by all three algorithms, although SUFI-2 showed the narrower ranges compared to other two optimization algorithms. The reason behind this is, SUFI-2 creates a combination of all calibrated parameters values for each simulation, and after each iteration, the parameter ranges expressed to narrower distribution from the initial wider distribution.

3.2. Performance Sensitivity to Objective Functions using SUFI-2

SUFI-2 allows to use different objective functions and to modify the threshold individually to optimize the calibration parameters. To identify the best objective

function, five objective functions (R^2, NSE, PBIAS, KGE, and RSR) were evaluated to calibrate the model using SUFI-2. Table 8 and Figure 6 shows the model performance by five objective functions using SUFI-2 in the San Joaquin Watershed.

3.2.1. Robustness of Model Performance

Figure 6 and Table 8 show that all five objective functions performed well at the outlet (Fremont station). Table 8 shows that R^2, NSE and PBIAS values remain almost consistent, while KGE and RSR values showed more variability by all objective functions. The calibration results yielded from different objective functions showed "very good" R^2 and NSE values, while PBIAS values were "unsatisfactory" (Table 8). Only "satisfactory" PBIAS (-14.93%) found at the Fremont station while PBIAS was used as an objective function in the iteration (Table 8). However, a small number of behavioral simulations (56) found compared to the other objective functions (474, 329, 251, and 323 for R^2, NSE, KGE, and PBIAS respectively). In addition, from the hydrograph, it is revealed that the best-simulated streamflow from each objective function (R^2, NSE, KGE, and RSR) captured the observed streamflow satisfactorily, while it seemed to have slightly underestimated for PBIAS (Figure 6). Based on the comparative analysis between Figure 6 and Table 8, the final calibration results suggest that using KGE as objective function might be the best option to obtain a good calibration in a complex watershed.

3.2.2. Sensitivity of Model Parameters

Unlike the different optimization algorithms, the parameters obtained by each objective function showed different ranges (Figure 7) for the San Joaquin Watershed since different objective functions solve different problems (Kouchi et al. 2017).

Figure 7 also presents that the identified optimal values for the calibrated parameters were different to each other. However, any clear dominance was not detected among the objective functions with regard to producing optimum parameters values. These results explained the concept of parameter "non-uniqueness" and the concept of "conditionality" of the calibrated parameters where an unconditional parameter range is defined as parameter range to calibrate the model (Kouchi et al., 2017). Therefore, the unconditional parameter range of CN2 for San Joaquin Watershed would be the range indicated by the dashed line in Figure 7. This also indicated a large parameter uncertainty associated with the choice of objective functions regarding parameter ranges.

However, the optimal parameter values were very different from each other while simulated streamflow was not different from each other (Table 9) and considered as "very good" when judged by 4 different performance criteria (R^2, NSE, KGE, and RSR) (Table 2 and 8). These results were consistent with the equifinality concept (Beven and Freer, 2001; Muleta, 2011), which illustrates that multiple sets of parameters can simulate different and acceptable representations of the watershed characteristics. Relative robustness of the performance criteria was also examined using the correlation matrix (Table 9). Table 9 shows the inter-correlation among the best-simulated streamflows determined from five different objective functions for the calibration period. Table 9 indicates that except PBIAS, the best-simulated streamflows from other four objective functions were well correlated ($r = 0.95 \sim 0.99$).

4. Importance of Study

Successful calibration of the distributed hydrologic models is important for future analysis for watershed or crop managements, and evaluation of impacts of climate and land use changes on the hydrology. Prior to calibration, it is critical to assess the model uncertainties. According to (Abbaspour, 2013), reporting the model uncertainty is necessary otherwise the calibration will be "meaningless" and "misleading". The key application of sensitivity analysis is to indicate the uncertainties in the input parameters of the model. Another application of sensitivity analysis is in the utilization of models by managers and decision-makers, which helps to understand the uncertainties, and pros and cons with the limitations and scope of a hydrologic model.

It is also necessary to test the sensitivity of the hydrologic models to different optimization algorithms. However, most applications are only reporting a single optimization algorithm. One of the main reasons is some of the uncertainty analyses techniques are difficult to apply (e.g., the need for testing statistical assumptions). In addition, for a complex hydrologic model, another restriction is the number of simulation runs required for the uncertainty analysis, which needs high CPU speed and parallel computation technology.

This study provides an insight into a hydrologic model response to three different optimization techniques (SUFI-2, GLUE, and ParaSol) for streamflow simulation. The findings show that SUFI-2 is more suitable for the semi-arid San Joaquin watershed to estimate the parameter uncertainty of the streamflow. This study also revealed that all three techniques produced acceptable calibration results, however, with different parameter ranges. This is an important step toward the development of strategies for

sustainable water resources management in such semi-arid region with heavy agricultural activities like Central Valley, California.

The second objective of this study was to find a suitable objective function for the streamflow simulation. In most of the studies, NSE used as the objective function, however, in this study it was clear that KGE was more efficient than NSE. One of the reasons could be since KGE was developed (Section 2.5.4 and Eq. 4) to overcome the problem associated with NSE where observed mean used as a baseline, which can lead to overestimation of model skill for highly seasonal variables (e.g., runoff in snowmelt-dominated watersheds). Therefore, in a snowmelt-dominated watershed like San Joaquin watershed (Lettenmaier and Gan, 1990) KGE could be the more suitable to use as the objective function.

The results presented in this manuscript were developed for both low flow (Year 2015) and high flow (Year 2011) simulations, and proved to be suited for both low and high flow simulations. Hydrological models are generally used to simulate the streamflow at ungauged sites by transferring model parameters from gauged to ungauged subbasins. In this study, available streamflow was found for only 2 gauge stations- at the outlet (Fremont station) and at the upstream (Mendota station), despite of having a very large drainage area (15,357.7 km^2). The choice of the objective function used for gauged watersheds might influence the simulation of the regionalized models on ungauged sites. There is a high probability that the model parameter, transfered from gauged to ungauged watersheds, will carry much more uncertainty than the choice of the objective functions used in gauged watersheds.

Therefore, there is a need to test the sensitivity of the objective functions in a smaller gauged watersheds.

5. Summary and Conclusion

The objectives of this study were to evaluate the different optimization algorithms and multiple objective functions to simulate the monthly streamflow with the calibration of the parameter set of a distributed hydrologic model. The SWAT hydrologic model was developed for a large semi-arid watershed in Central Valley, California (San Joaquin). Three different optimization algorithms (SUFI-2, GLUE, and ParaSol) were evaluated for monthly streamflow simulations. The optimization algorithms were implemented in the SWAT-CUP 2012. The calibration performance and sensitivity of parameters of these algorithms were compared through evaluating the P-factor, R-factor, R^2, NSE, and PBIAS of the best simulation. Afterward, model calibration performance and sensitivity of parameters were evaluated by five objective functions (R^2, NSE, PBIAS, KGE, and RSR) using SUFI-2. The following conclusion can be drawn:

1) By comparing the results from three optimization algorithms, the SUFI-2 performed better than the other two algorithms due to the good R^2 and NSE values of the best simulation results and the best prediction uncertainty ranges (P-factor), and the relative coverage of measurements (R-factor).
2) Different objective functions presented different range of the parameters with distinct optimal values while simulating similar streamflow with satisfactory performance criteria.

3) In case of conducting hydrological simulation for streamflow, the SUFI-2 algorithm with KGE as objective function coupled with SWAT model is preferred for the semi-arid and snowmelt-dominated watersheds like San Joaquin watershed.

The calibration and validation performance are not sensitive to the choice of optimization algorithm and objective function, but the obtained parameters are different. Therefore, using the calibrated optimal parameter sets achieved in this study, the local water resource managers and decision makers can obtain more confident prediction intervals for the streamflow simulation.

6. Figures

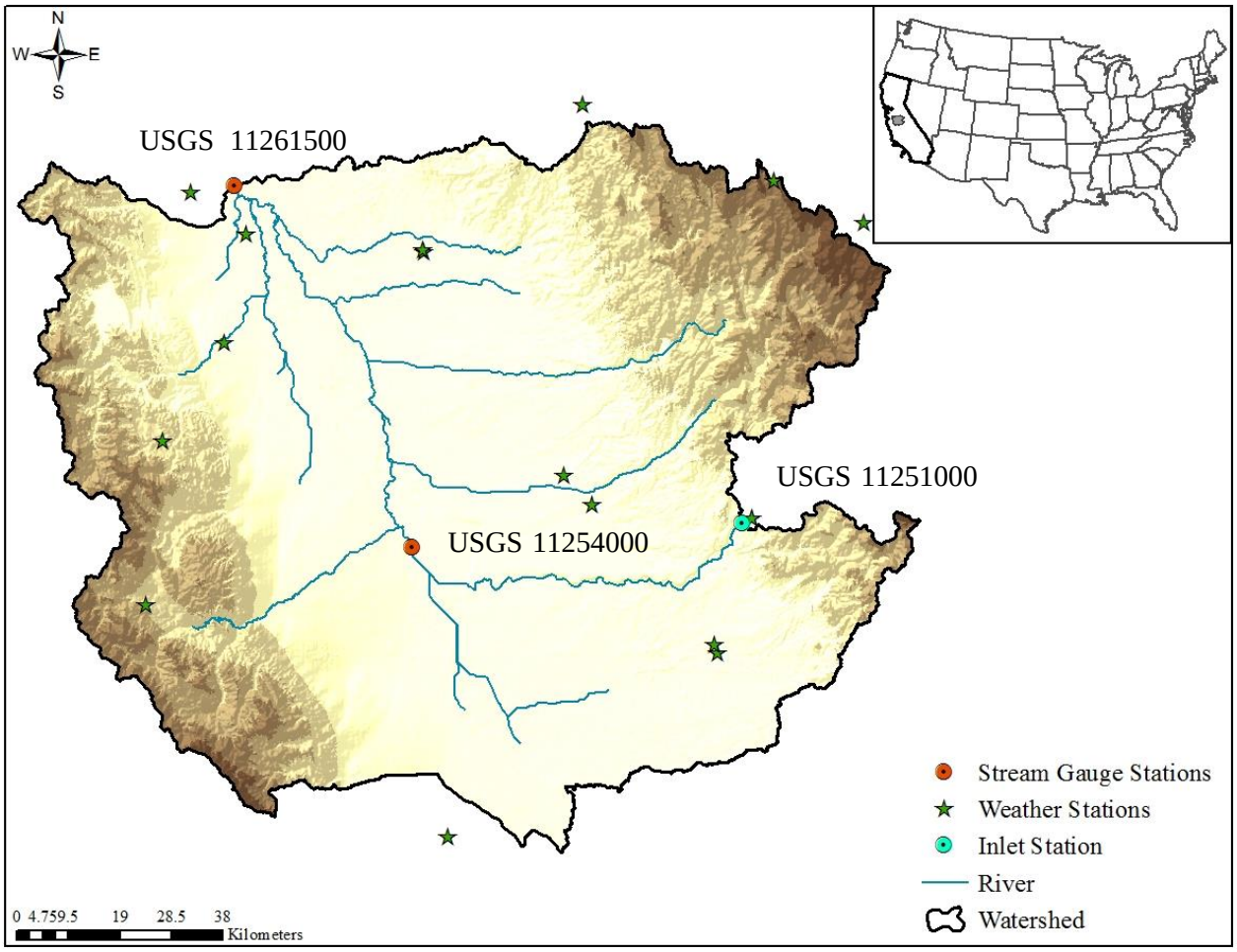

Figure 1: Location of San Joaquin watershed in California, with selected weather stations and the United States Geological Survey's streamflow gauge stations at respective watershed outlets and inlets.

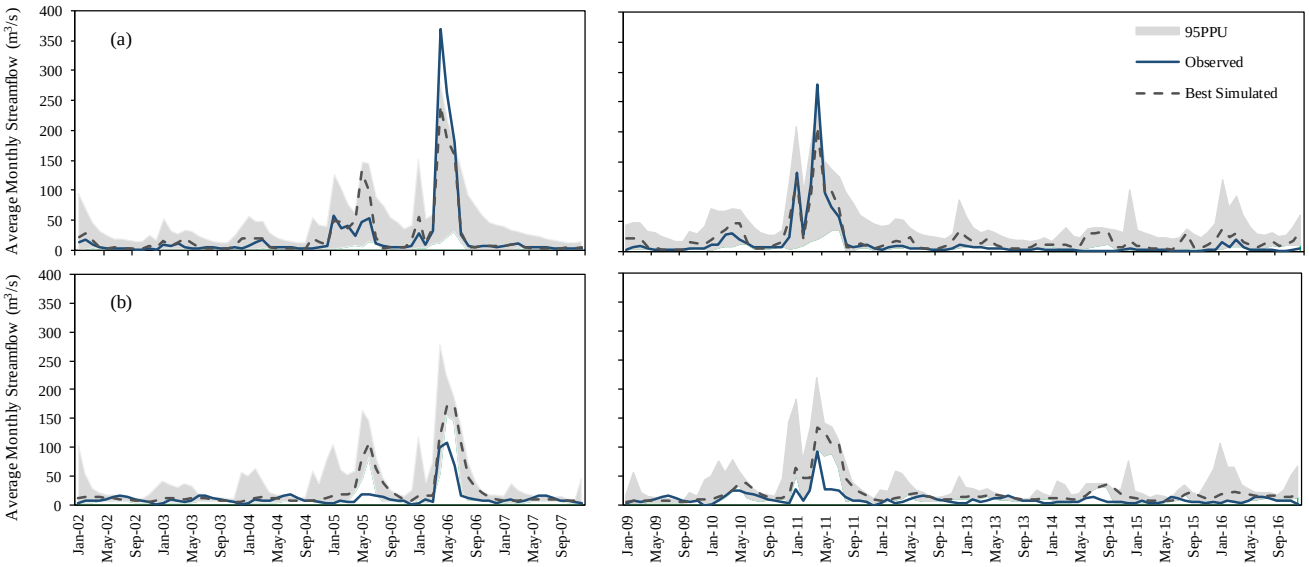

Figure 2: The best simulated and observed monthly streamflow with 95PPU for calibration (2009-2016) and validation (2002-2007) periods at a) Fremont station and b) Mendota station by using the SUFI-2.

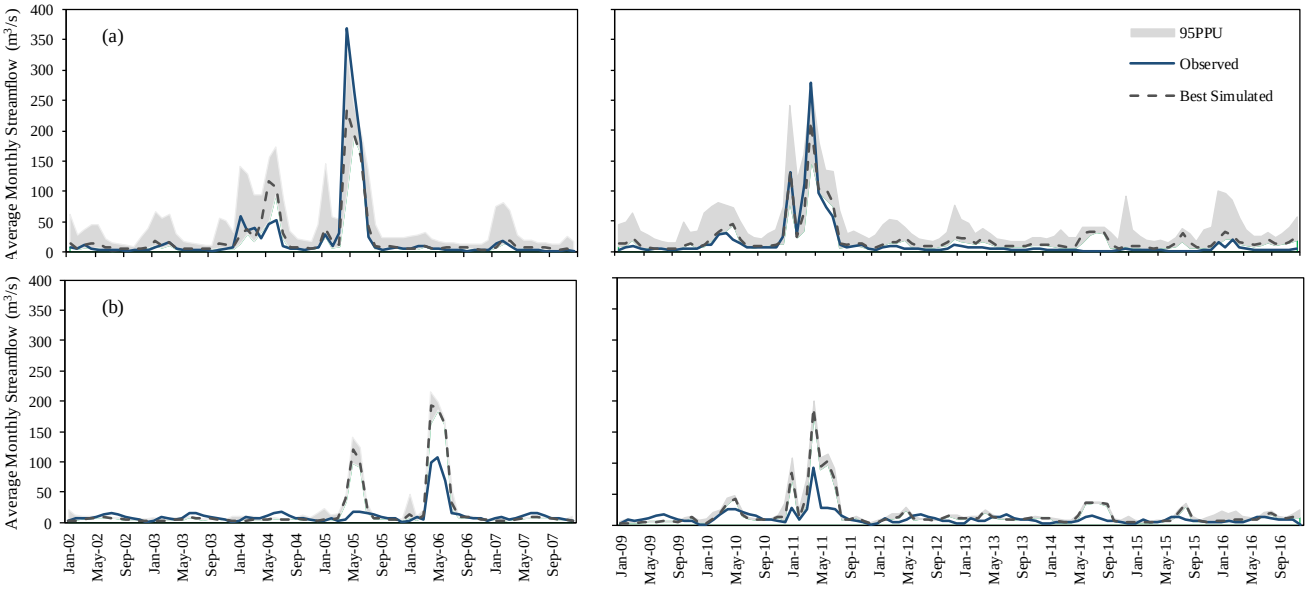

Figure 3: The best simulated and observed monthly streamflow with 95PPU for calibration (2009-2016) and validation (2002-2007) periods at a) Fremont station and b) Mendota station by using the GLUE.

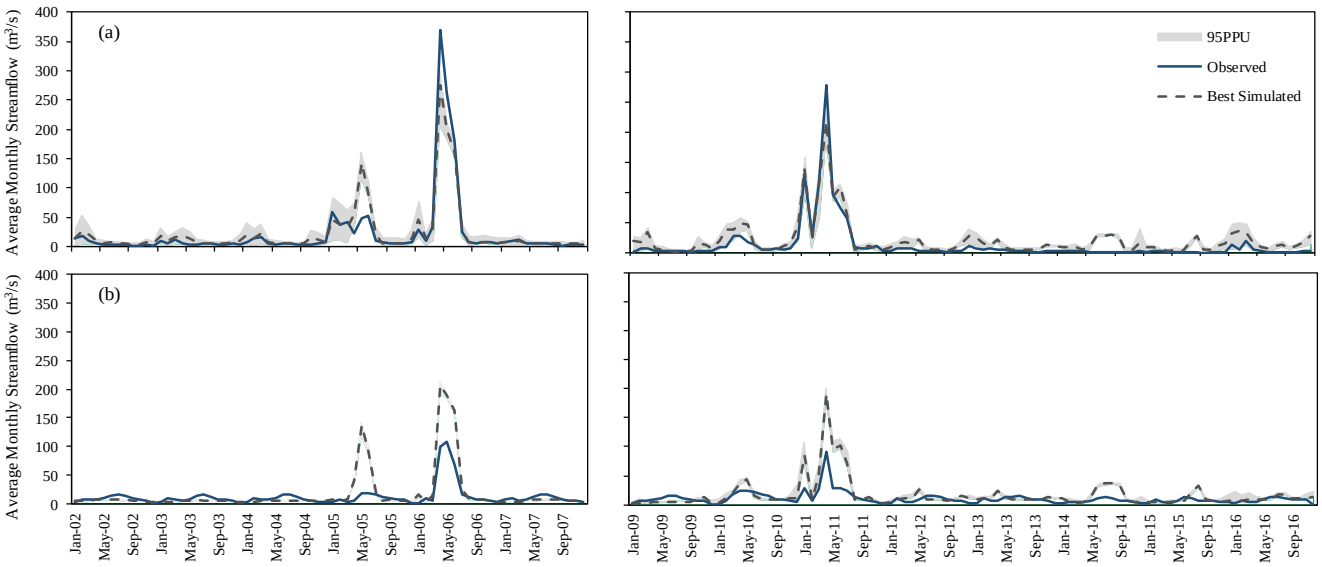

Figure 4: The best simulated and observed monthly streamflow with 95PPU for calibration (2009-2016) and validation (2002-2007) periods at a) Fremont station and b) Mendota station by using the ParaSol.

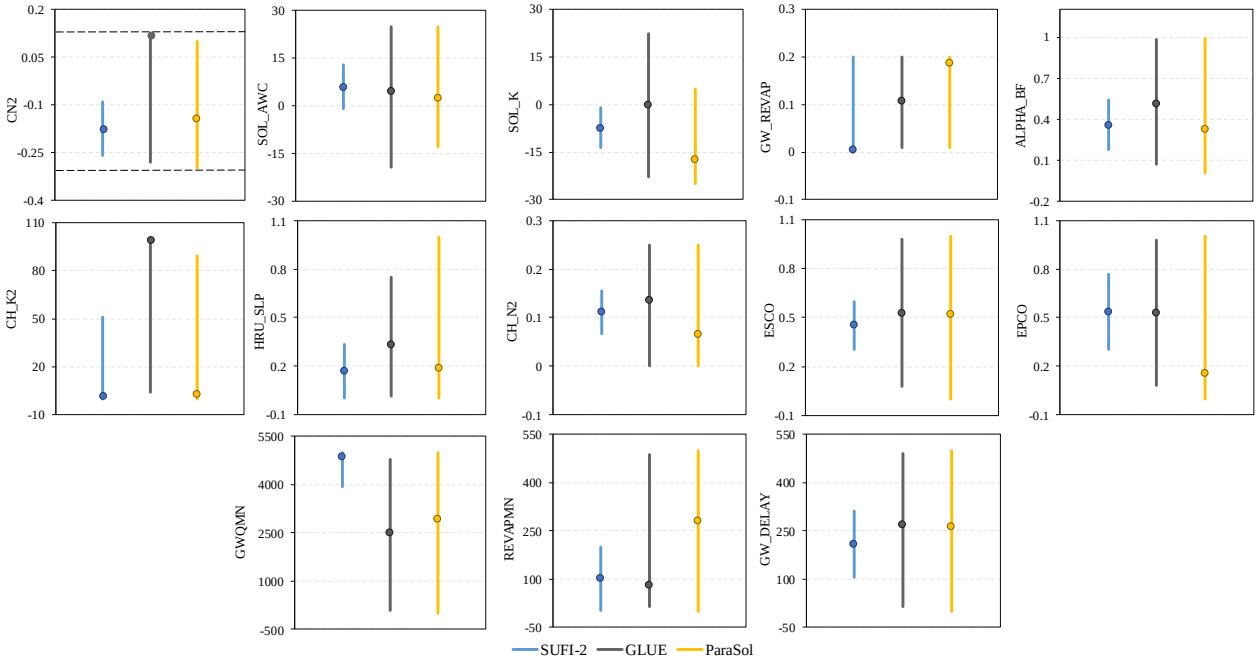

Figure 5: Final parameter uncertainty ranges with best estimates (points in each line) of the calibrated parameters by three optimization algorithms in San Joaquin watershed.

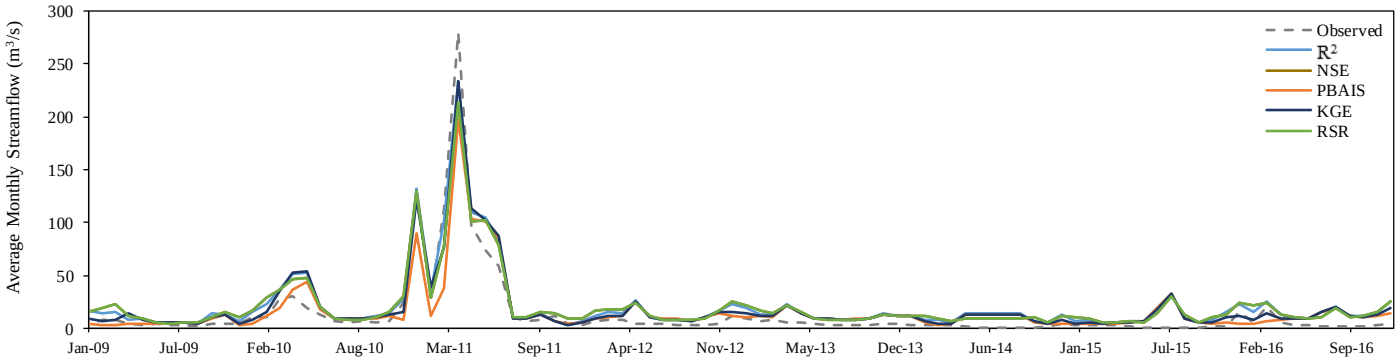

Figure 6: Comparison of the monthly observed and best simulated streamflow obtained at Fremont station when R2, NSE, PABIAS, KGE, and RSR used as objective function.

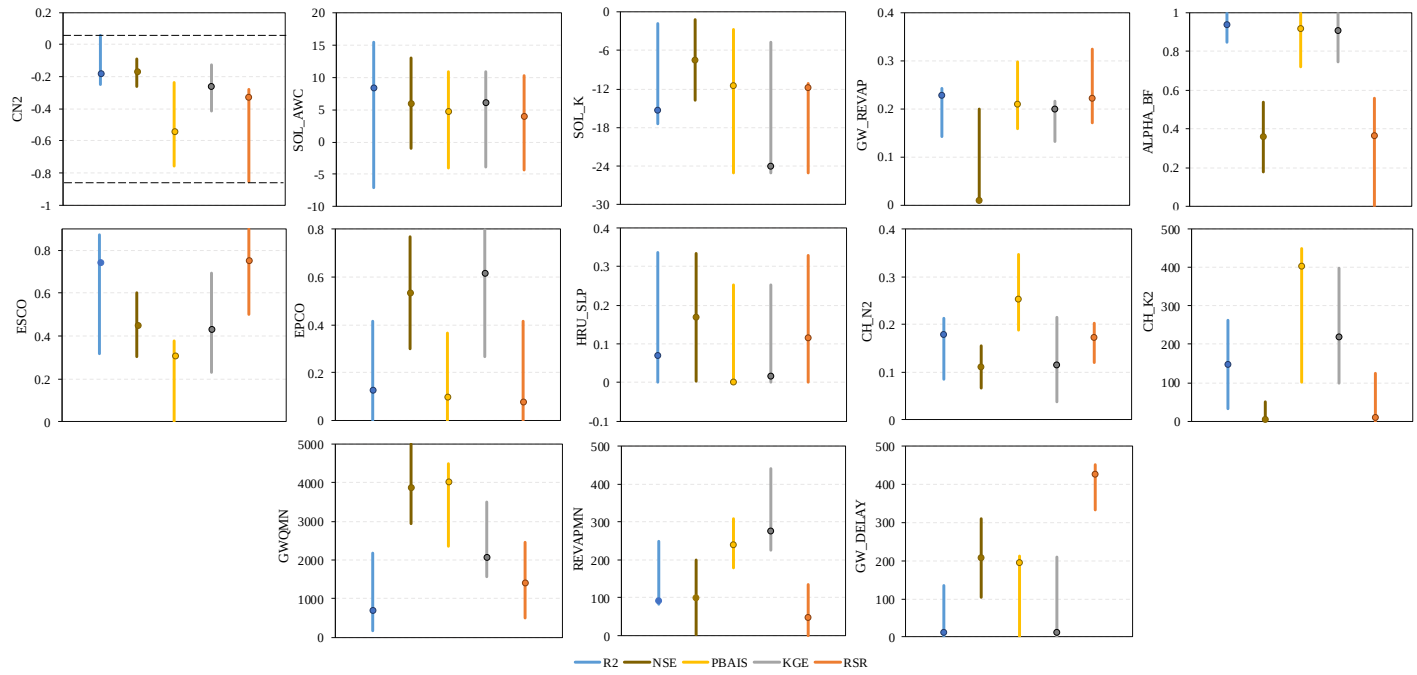

Figure 7: Final parameter uncertainty ranges with best estimates (points in each line) of the calibrated parameters by five objective functions using SUFI-2 in San Joaquin watershed.

7. Tables

Table 1: Characteristics of land use and land covers in San Joaquin watershed.

	Area (km^2)	Area (Acre)	% Watershed Area
Agricultural Land	5744.7	1419548	37.4
Grass/Pasture	4560.9	1127017	29.7
Shrubland	1214	300014.4	7.9
Fallow & Barren	1192.3	294629.3	7.8
Urban	1128	278742	7.3
Forest	1041.7	257412	6.8
Water &Wetland	475.9	117600.7	3.1

Table 2: Performance evaluation criteria for flow measures for watershed scale models (adapted from Kouchi et al. (2017), Moriasi et al. (2015), and Thiemig et al. (2013).

Measure	Temporal Scale	Very Good	Good	Satisfactory	Not Satisfactory
R^2	D-M-A[1]	$R^2 > 0.85$	$0.0.75 < R^2 \leq 0.85$	$0.60 < R^2 \leq 0.75$	$R^2 \leq 0.6$
NSE	D-M-A	NSE >0.80	$0.70 < NSE \leq 0.80$	$0.50 < NSE \leq 0.70$	$NSE \leq 0.50$
PBIAS (%)	D-M-A	$PBIAS < \pm 5$	$\pm 5 \leq PBIAS < \pm 10$	$\pm 10 \leq PBIAS < \pm 15$	$PBIAS \geq \pm 15$
KGE	M	$0.9 \leq KGE \leq 1$	$0.75 \leq KGE < 0.9$	$0.5 \leq KGE < 0.75$	$KGE < 0.5$
RSR	M	$0 \leq RSR \leq 0.5$	$0.5 < RSR \leq 0.6$	$0.6 < RSR \leq 0.7$	$RSR > 0.7$

[1]D, M and A denoted daily, monthly, and annual temporal scales, respectively

Table 3: Descriptions and initial ranges of the most sensitive parameters used for model calibration for San Joaquin watershed.

Parameter	Definition[a]	Scale of input	Adjustment[b]	Initial Range
Groundwater				
ALPHA_BF	Baseflow recession constant (days)	Watershed	1	0.01-1
GW_DELAY	Groundwater delay (days)	Watershed	2	1-500
GW_REVAP	Groundwater "revap" coefficient	Watershed	1	0.01-0.20
REVAPMN	Re-evaporation threshold (mm H_2O)	Watershed	1	0.01-500
GWQMN	Threshold groundwater depth for return flow (mm H_2O)	Watershed	1	0.01-5000
Soil water				
SOL_K	Soil saturated hydraulic conductivity (mm/hr)	HRU	3	-15-15
SOL_AWC	Available soil water capacity (mm H_2O/mm soil)	HRU	3	-15-15
Channel Flow				
CH_N(2)	Main channel Manning's *n*	Reach	1	0.01-0.15
CH_K(2)	Main channel hydraulic conductivity (mm/hr)	Reach	1	5-100
Surface Runoff				
CN2	Curve number for moisture condition II	HRU	3	-0.3-0.1
EPCO	Plant uptake compensation factor	HRU	1	0.75-1
ESCO	Soil evaporation compensation factor	HRU	1	0.75-1
Lateral Flow				
HRU_SLP	Average slope steepness (m/m)	HRU	1	0-1
Snow				
SFTMP	Snowfall temperature (^oC)	Watershed	1	0-5
SMFMN	Melt factor for snow on December 21 (mm H_2O/ ^oC-day)	Watershed	1	0-10
SMFMX	Melt factor for snow on June 21 (mm H_2O/ ^oC-day)	Watershed	1	0-10
SMTMP	Snow melt base temperature (^oC)	Watershed	1	-2-5
TIMP	Snow pack temperature lag factor	Watershed	1	0-1

[a] Source: Neitsch et al., 2001

[b]Type of change to be applied to the existing parameter value: '1' means the original value is to be replaced by a value from the range, '2' means a value from the range is added to the original value, '3' means the original value is multiplied by the adjustment factor (1+ given value within the range)

Table 4: Sensitivity of the model parameters for monthly streamflow simulation generated by the three optimization algorithms.

	SUFI-2			GLUE			ParaSol		
Parameters	Ranking	t-stat	P-value	Ranking	t-stat	P-value	Ranking	t-stat	P-value
r__CN2.mgt	1	-26.82	0	1	-39.90	0	1	22.71	0
r__SOL_K().sol	2	-14.08	0	2	-34.00	0	2	21.63	0
r__SOL_awc().sol	3	13.10	0	3	25.11	0	3	-16.88	0
v__ESCO.hru	4	-5.23	0	6	-4.35	0	13	0.13	0.90
v__ALPHA_BF.gw	5	-3.56	0	5	-5.61	0	9	2.15	0.03
v__HRU_SLP.hru	6	-2.68	0.01	4	-16.06	0	4	8.90	0
v__REVAPMN.gw	7	2.26	0.02	10	0.84	0.40	6	-3.45	0
v__GWQMN.gw	8	2.03	0.04	7	3.84	0	8	-3.35	0
v__GW_REVAP.gw	9	0.99	0.32	9	1.90	0.06	5	-4.46	0
v__CH_K2.rte	10	-0.52	0.60	11	-0.36	0.72	7	3.39	0
v__EPCO.hru	11	0.43	0.67	13	0.11	0.91	11	0.58	0.56
a__GW_DELAY.gw	12	0.29	0.77	8	2.77	0.01	10	0.82	0.41
v__CH_N2.rte	13	-0.26	0.79	12	-0.29	0.77	12	-0.26	0.80

Table 5: Performance of the three optimization algorithms for the calibration and validation periods in San Joaquin watershed. Cal-Calibration and Val-Validation

Optimization Techniques	**Stations**		**R^2**	**NSE**	**PBIAS**	**P-factor**	**R-factor**
SUFI-2 500+500+500 runs 384 behavioral simulations	Fremont	Cal.	0.91	0.84	-40.45	0.70	1.02
		Val.	0.88	0.84	-7.33	0.78	0.98
	Mendota	Cal.	0.76	-1.97	-55.54	0.60	0.85
		Val.	0.81	-0.96	-32.13	0.62	0.87
GLUE 5000 runs 285 behavioral simulations	Fremont	Cal.	0.89	0.83	-40.01	0.29	0.74
		Val.	0.88	0.84	-4.17	0.30	0.71
	Mendota	Cal.	0.75	-2.00	-43.02	0.23	0.45
		Val.	0.81	-0.95	-66.31	0.21	0.43
ParaSol 3000 runs 2002 behavioral simulations	Fremont	Cal.	0.90	0.83	-47.44	0.61	0.33
		Val.	0.88	0.87	-14.87	0.58	0.32
	Mendota	Cal.	0.75	-2.04	-61.62	0.17	0.24
		Val.	0.80	-1.22	-45.26	0.16	0.22

Table 6: The correlation matrix among the best simulated streamflow obtained by three optimization algorithms.

Sensitivity Techniques	**SUFI-2**	**GLUE**	**ParaSol**
SUFI-2	1	0.97	0.99
GLUE		1	0.96
ParaSol			1

Table 7: List of best estimates and the final parameter uncertainty ranges of the parameters based on all three optimization algorithms applied in San Joaquin watershed.

Parameter	Initial Rang	Uncertainty Range and Best Parameter Estimate[1]		
		SUFI-2	GLUE	ParaSol
ALPHA_BF	0.01-1	0.359 (0.1, 0.6)	0.511 (0.07, 1)	0.046 (0.01, 1)
GW_DELAY	1-500	207.25 (1, 250)	269.145 (15, 490)	263.00 (0, 500)
GW_REVAP	0.01-0.20	0.006 (0.01, 0.1)	0.108 (0.01, 0.2)	0.188 (0.01, 0.2)
REVAPMN	0.01-500	101.1 (0.01, 250)	81.342 (13.5, 487)	279.23 (0.01, 500)
GWQMN	0.01-5000	4886 (3000, 5000)	2502.745 (100, 4780)	2941.6 (0.01, 5000)
SOL_K	-25-25	-7.42 (-10, 5)	-0.212 (-22.7, 22.29)	-15.416 (-25, 4.8)
SOL_AWC	-25-25	5.975 (-5, 10)	4.574 (-19.454, 25)	2.562 (-12.96, 25)
CH_N(2)	0.01-0.25	0.112 (0.07, 0.14)	0.135 (0, 0.25)	0.065 (0, 0.25)
CH_K(2)	5-100	5.3 (5, 50)	99.21 (4, 100)	2.506 (0, 89.12)
CN2	-0.3-0.3	-0.176 (-0.35, -0.01)	0.018 (-0.28, 0.12)	-0.142 (-0.3, 0.1)
EPCO	0.01-1	0.534 (0.25, 0.75)	0.526 (0.08, 0.98)	0.154 (0, 1)
ESCO	0.01-1	0.453 (0.25, 0.75)	0.525 (0.08, 0.98)	0.522 (0, 1)
HRU_SLP	0-1	0.169 (0, 0.5)	0.334 (0.01, 0.75)	0.190 (0, 1)

[1]c (a, b) for each parameter means: c is the best parameter estimate, (a, b) is the 95% parameter uncertainty range except SUFI-2 (in SUFI-2, this interval denotes the final parameters distribution)

Table 8: Calibration results for best simulated and observed monthly streamflow by five different objective functions using the SUFI-2 in San Joaquin watershed.

Objective Function in Iterations	No. of Behavioral Simulations	Stations	R^2	NSE	PBIAS	KGE	RSR
R^2 (0.60)	474	Fremont	0.91	0.82	-53.36	0.56	0.37
		Mendota	0.78	-1.52	-54.60	-0.45	1.59
NSE (0.50)	384	Fremont	0.91	0.84	-40.45	0.62	0.40
		Mendota	0.76	-1.97	-55.54	-0.36	1.51
PBIAS (±15)	56	Fremont	0.80	0.77	-14.93	0.70	0.48
		Mendota	0.78	-1.48	-42.80	-0.44	1.58
KGE (0.50)	251	Fremont	0.89	0.85	-32.93	0.74	0.38
		Mendota	0.78	-1.50	-53.50	-0.45	1.58
RSR (0.70)	323	Fremont	0.91	0.84	-51.41	0.60	0.40
		Mendota	0.79	-1.28	-52.30	-0.37	1.51

Table 9: The correlation matrix among the best simulated streamflow obtained by five different objective functions using the SUFI-2.

Objective Function	R^2	NSE	PBIAS	KGE	RSR
R^2	1	0.98	0.91	0.95	0.98
NSE		1	0.94	0.94	0.99
PBIAS			1	0.98	0.94
KGE				1	0.98
RSR					1

Chapter 5: Agricultural Water Management Decisions in Ungauged Semi-arid watersheds: Value of Remote Sensing in Integrated Hydrologic modeling

Abstract

Central Valley of California is a region with diverse and heterogeneous landscape, with limited water resources, variable climate and intensified human activities. It has a semi-arid environment with uneven distributions of water and temperature, where evapotranspiration (ET) plays a major role in controlling surface water balance components and hydrologic regimes. ET and biomass/crop yield are influenced by the leaf area index (LAI). It is also challenging to predict its complex hydrological processes and biophysical dynamics with limited observation. Remotely sensed data could provide a great source of data to study vegetation indices and hydrologic dynamics for this complex hydrologic system. The objective of this study was to develop a methodology to improve plant growth through direct assimilation of remotely sensed leaf area index (LAI) data for a large complex watershed. Remotely sensed LAI data was integrated into the SWAT (Soil and Water Assessment Tool) model for San Joaquin Watershed, California. The impact of direct LAI assimilation was evaluated for hydrology (streamflow and ET) and crop yield. Results showed that direct LAI assimilation into the SWAT model was able to capture actual vegetation dynamics and estimate more accurate ET and biomass/crop yield at each Hydrologic Response Unit (HRU). The outcomes of this study serve as a decision support tool in this regard by providing quantitative information for crop water use and estimating crop production.

This chapter will be submitted for publication in *Remote Sensing*.

1. *Introduction*

Efficient water resource management through accurate prediction of hydrologic components is the most decisive issue for the arid and semi-arid regions as limiting freshwater impacts the crop productivity and food security for a watershed (Ashraf Vaghefi et al., 2014; Ficklin et al., 2009; Teixeira et al., 2013). Hydrological modeling has become an essential part for the decision making process, such as improving irrigation water use (Udias et al., 2018), predicting water demand (Zou et al., 2018), water productivity (Ahmadzadeh et al., 2016), and crop yields (Wang et al., 2016) at the local and regional scales. However, water resource managers often face enormous difficulties related to shortage and uncertainty of climate data, vegetation growth and management information at the regional scale. Continuous and long-term data are required to calibrate the hydrologic model to obtain feasible results for accurate decision making. The difficulties often arise during upscaling the field scale data to regional scales in illustrating complex water supply network and landscape heterogeneity.

Remote sensing provides a great source of data to study vegetation indices and hydrologic dynamics from multi-spectral bands. Studies showed that model estimates could be improved using the remotely sensed data and data assimilation method for its continuous long-term temporal and high spatial resolution (Alemayehu et al., 2017; Chen et al., 2017b; Ma et al., 2019). However, most of these studies used remotely sensed soil moisture (Liu et al., 2017; Patil and Ramsankaran, 2017; Rajib et al., 2016b) or ET (Ha et al., 2018; Jhorar et al., 2011; Zhang et al., 2017b) data for hydrological model improvement; little attention has been focused on assimilating

remotely sensed vegetation indices. Remotely sensed vegetation data are mainly used for calibrating/validating a hydrological model to understand the hydrological process at the plot scale (Trombetta et al., 2016) or at large scale considering particular land/crop pattern such as forest, grassland, shrubland (Alemayehu et al., 2017; Ma et al., 2019; Sun et al., 2017a). Very few studies showed an enhanced representation of the vegetation and biophysical dynamics to improve the predictive capability of a hydrologic model at large landscapes (e.g., regional scale) with diverse crop patterns.

Land-surface characteristics such as vegetation growth, plant types, and water consumption by plants influence both biophysical and hydrological processes (Siad et al., 2019). Vegetation growth and plant phenology affect the water balance by controlling ET and interception and alters the spatial and temporal dynamics of streamflow and crop yield (Siad et al., 2019). Canopy properties such as the leaf area index (LAI) indicates the vegetation growth cycle and plant activity in terms of water consumption and transpiration (Bhattacharya, 2018). Therefore, LAI influences the ET rate and its partitioning into transpiration (T) and interception (I). At the same time, LAI has a significant impact on photosynthesis and radiation interception, which contributes to biomass production (Yildirim et al., 2017).

Scientific methods and approaches are needed to capture these complex and real-time hydrological processes at a local to regional scale (Gao, 2002; Rostamian et al., 2008; Thakur et al., 2017). Worldwide researchers are applying the integrated hydrologic and crop growth models to simulate watershed dynamics, including hydrologic process and biomass production (Chen et al., 2017c; Dokoohaki et al., 2016; Ramos et al., 2018).

In the most physically-based hydrological models, LAI is computed based on quantitative tools (Sun et al., 2017b) or obtained externally, such as measured from the field (Ramos et al., 2018) or through remote sensing products (Alemayehu et al., 2017). Accurate data can be found at the field scale, where influential factors for crop development (i.e., soil properties, radiation use efficiency, and water use) can be monitored properly (Chen et al., 2017c; Han et al., 2018). Researchers showed that the accurate LAI reflects the field variability of soils and crops in different phases of the plant cycle which are essential in precision agriculture (Bellvert et al., 2018; Chen et al., 2017c; Gebbers et al., 2011) and to calculate the optimum yield (Almeida Carina, 2011; Ramos et al., 2018).

The main goal of this study was to predict hydrologic and biophysical dynamics for a complex and data-limited watershed in Central Valley, California, by improving its vegetation growth module. This region has a semi-arid environment with uneven distributions of water and temperature (Lund, 2016), where ET plays a major role in controlling surface water balance components and hydrologic regimes (Tanaka et al., 2006). To predict its complex hydrologic dynamics with limited observation data, the objectives of this study were: (i) to develop a methodology to improve the plant growth sub-model of a hydrologic model through direct assimilation of remotely sensed LAI data ii) to calibrate and quantify the hydrologic processes for a large ungauged watershed, and iii) to evaluate the crop yield estimation using the modified plant growth sub-model.

2. *Methodology*

2.1. Soil and Water Assessment Tool (SWAT) Overview

The Soil and Water Assessment Tool (SWAT) is a physically-based, semi-distributed model, running on a daily, monthly or annual time step (G. Arnold et al., 2012; Neitsch et al., 2011). The SWAT model is such a model that utilizes a plant/crop growth module to simulate many types of land cover. SWAT is widely used to assess the impact to of climate variability on hydrology (Ahiablame et al., 2017; Ficklin et al., 2009; Mango et al., 2011) and crop production (Bauwe and Kahle, 2019; Srinivasan et al., 2010; Wang et al., 2016). As a process-based model, SWAT can be extrapolated to a broad range of conditions that may have limited observations (Sun et al., 2017c). Therefore, it is widely used to study the impacts of environmental change for a wide range of scales and environmental conditions across the globe.

During model development, a watershed is partitioned into a number of sub-basins according to the topography and they are connected by a stream network. Each sub-basin is further divided into several homogeneous Hydrological Response Units (HRUs), which represent a unique land cover, soil, slope, and management combinations. SWAT predicts water budget dynamics, as well as crop yields in different HRUs, identified within the watershed.

In SWAT, evapotranspiration occurs from each HRU area, which varies from day to day as a function of LAI (Ha et al., 2017; Neitsch et al., 2011). SWAT model has three options to estimate potential ET: Penman-Monteith, Hargreaves, and Priestley-Taylor methods. According to the Penman-Monteith method, the SWAT model

estimates both potential soil evaporation and plant transpiration as a function of potential ET and LAI (Neitsch et al., 2011; Ritchie, 1972). Thus, the potential ET computed as:

$$ET_c = \frac{\Delta\,(H_{net} - G) + \rho_{air} * c_p - [e_z^o - e_z]/r_a}{\Delta + \gamma(1 + \frac{r_c}{r_a})} \quad (1)$$

$$r_c = \frac{1}{0.5 * g_l * LAI} \quad (2)$$

Where, ET is the maximum transpiration rate (mm/d), Δ is the slope of the saturation vapor pressure-temperature curve (kPa/ºC), H_{net} is the net radiation (MJ/m^{2}d), G is the heat flux density to the ground (MJ/m^{2}d), ρ_{air} is the air density (kg/m^3), C_p is the specific heat at constant pressure (MJ/kgºC), e_z^o is the saturation vapor pressure of air at height z (kPa), e_z is the water vapor pressure of air at height z (kPa), γ is the psychrometric constant (kPa/ºC), r_a is the diffusion resistance of the air layer (aerodynamic resistance) (s/m), r_c is the plant canopy resistance (s/m), and g_l is the maximum conductance of a single leaf (m/s).

SWAT model uses the simplified version of the Erosion Productivity Impact Calculator (EPIC) plant growth model to simulate the annual vegetation growth and assess the biomass/yield production (Neitsch et al., 2011; Williams et al., 1989). The plant growth module simulates the LAI as a function of canopy heights, which are required to calculate the canopy resistance and the aerodynamic resistance (Neitsch et al., 2011). In the initial period of plant growth, canopy height and leaf area development are controlled by the optimal leaf area development curve. The function of optimal leaf area development is listed as:

$$fr_{LAImx} = \frac{fr_{PHU}}{fr_{PHU} + \exp(l_1 - l_2 * fr_{PHU})} \quad (3)$$

$$fr_{PHU} = \frac{\sum_{i=1}^{d} HU_i}{PHU} \quad (4)$$

Where fr_{LAImx} is the fraction of the plant's maximum leaf area index for the plant; l_1 and l_2 are the shape coefficients, fr_{PHU} is the fraction of potential heat units for a certain period during the growing season, HU is heat units accumulated on a given day (d) and PHU is the potential heat units that required for plant maturity. PHU is given in model database and known before model running.

For perennial and annual plants, the increase of LAI on a day i is calculated as:

$$\Delta LAI_i = \left(fr_{LAI,i} - fr_{LAImx,i-1}\right) * LAI_{mx} * (1 - \exp\left(5 * (LAI_{i-1} - LAI_{mx})\right)) \quad (5)$$

In the end, LAI for the day is calculated as:

$$LAI_i = LAI_{i-1} + \Delta LAI_i \quad (6)$$

LAI influences transpiration and light interception, and at the same time, determines the amount of intercepted solar radiation (Figure 1). Here, LAI acts as an indicator of the degree of water and temperature stress and modifies crop growth in the crop model. Monteith (1977) established the empirical relationship between the accumulation of dry matter and the accumulation of solar radiation intercepted by a crop (Figure1) (G. Arnold et al., 2012; Neitsch et al., 2011). The potential biomass for a day is converted from intercepted radiation as a function of LAI and plant species-specific Radiation Use Efficiency (RUE) (Monteith, 1977; Neitsch et al., 2011). Thus, total plant biomass is estimated as:

$$\Delta bio = RUE * H_{phosyn} \quad (7)$$

Where, H_{phosyn} is the amount of intercepted photosynthetically active radiation (PAR) on a given day (MJm^{-2}) and calculated as:

$$H_{phosyn} = 0.5 * H_{day} * (1 - \exp(-k_l * LAI)) \quad (8)$$

Where, H_{day} is the incident total solar (MJm^{-2}), and k_l is the light extinction coefficient.

The crop yield is computed as a harvestable fraction (harvest index) of the accumulated biomass production from each HRU (Figure 1). Thus, crop yield is calculated as:

$$yld = bio_{ag} * HI \quad (9)$$

Where, yld is the crop yield (kg/ha), bio_{ag} is the aboveground biomass on the day (kg/ha), and HI is the harvest index on the day of harvest.

2.2. Study Area

San Joaquin watershed, a representative watershed dominated by agriculture is located in Sacramento-San Joaquin Delta of California (Figure 2). The San Joaquin River is the second-longest within California, which has a drainage area of 15357.7 km^2 (USGS Hydrologic Unit Code 18040001). The Sacramento-San Joaquin Delta has an arid-to-semiarid climate with an average annual precipitation of 323 mm (12.5 inches), and an average annual temperature of 17.1°C with minimum and maximum of 9.7 and 24.5°C respectively (Service, 2017). Approximately 65% of the precipitation is lost to evaporation or vegetation (Siebert, 2003). The soil of Central

Valley is mainly dominated by Alluvial depositions, including Fluvents, Alfisols, Inceptisols, Mollisols, and Vertisols (Davis, n.d.).

The San Joaquin watershed is a complex agricultural watershed with a diverse crop pattern in the valley surrounded by pastureland and upland forest where extensive irrigation and water regulations are practiced. The land use is primarily dominated by agricultural (37.4%) followed by grass/pasture (29.7%), shrubland (7.9%), fallow/idle cropland (7.8%), urban (7.3%), forest (6.8%), and water (3.1%) (Table 1). According to Crop Data Layer (CDL-2017), almost 70 types of crops are growing within this 37.4% agricultural land, including orchards, vineyard, grain, pasture, and vegetables. The most prominent crop types are pasture (32.1%), almond (11.4%), vineyard (8.5%), corn (7.4%), and alfalfa (4.2%) (Table 1).

2.3. SWAT Model Implication and Modification

Since LAI controls a series of critical parameters related to the hydrological (e.g., ET, Eq. 1-2) and biophysical (e.g., biomass and crop yield, Eq. 7-9) process, the amount of ET and biomass would be changed when LAI values are adjusted. Therefore, plant growth models can be improved by proper modeling of LAI distribution for a better estimation of ET rates or biomass/crop yield.

Two distinct approaches were considered for better understating the impact of direct LAI assimilation in the SWAT model simulations.

Approach A: conventional SWAT simulation (SWAT)- In this case, the conventional calibration technique was applied using the selected parameters (Table 2) to calibrate the daily discharge at the outlet. The stepwise model calibration and validation processes were adapted from Paul and Azar (2018). The outputs were used

as a baseline model to compare the outputs from the calibration technique using remotely sensed data.

Approach B: SWAT simulation with direct LAI insertion (SWAT-LAI)- Remotely sensed LAI time series was processed and replaced (Eq. 5-6) into the SWAT plant growth module. The objective was to capture the actual vegetation dynamics and the occurrence of canopy management during plant growth. Consequently, a specific approach to the MODIS LAI process and SWAT revision was developed in this study. The SWAT model was calibrated using daily LAI values extracted satellite data as inputs (LAI assimilation). Similar flow parameters were used to simulate the daily streamflow and ET.

Calibrating the hydrologic model for streamflow simulations was relatively straightforward since it used observed streamflow with well-established instrumentation with fewer measurement errors. Another approach for calibrating the model is to compare the observed and modeled ET and crop yield since LAI has a direct influence on the ET through transpiration (Eq. 2) and dry biomass (Eq. 7) (section 2.1). However, calibrating the model for simulating green water flow (ET) is not usually possible in large-scale watersheds due to the scarcity of monitoring locations for ET. Therefore, the model prediction of ET was compared with remotely sensed data, assuming that remotely sensed prediction of WT is more representative of the real-world scenario.

2.4. Data Processing and Model Setup

In SWAT, the hydrologic model was developed using the high-resolution spatial dataset (i.e., DEM, land use, soil maps) as input to ensure the detailed HRU

distribution (Table 3). A total number of 73 sub-basins were identified for SJW, and 3902 HRUs were defined. HRUs were delineated applying thresholds 2-2-2% for land use-soil-slope. The watershed was delineated for USGS 11261500 gauging station as an outlet at Fremont and defined USGS 11251000 as watershed inlet below the dam on the San Joaquin River at Friant, California (Figure 2). MODIS-LAI data with a 500 m spatial and 4-day temporal resolution and MODIS-ET data with a 500 m spatial and 8-day temporal resolution have been downloaded from which a daily average LAI value has been reconstructed for the period of 2009-2014. ET process is dependent on the local climate and land cover properties, and LAI is driven by the plant type. Therefore, both ET and LAI data were derived at the HRU scale and used as input into the model. A specific approach was developed in this study to revise the SWAT crop growth module and evaluate the model performance; details are described in the following subsections.

2.4.1. Irrigation and Crop Management

According to 2017 CDL, orchards, such as almond and grape, are the two most prominent cultivated crops in the SJW (Table 1). Therefore, this study simulated the crop yields for only almond and grape to evaluate the remotely sensed LAI use in the model.

SWAT simulates the potential plant phenological (leaf area) development based on the daily accumulated heat units or from the planting date to the harvest date. Plants uptake water from the soil through their roots as they grow. Thus, irrigation can be scheduled manually or applied automatically by the model in response to water deficit in the soil at the root zone level. Another approach is to calculate actual

crop evapotranspiration (ET_c) generated from reference crop evapotranspiration (ET_o) and crop characteristics coefficient (K_c) that is adjusted by environmental stressors including water availability for plant growth. In this study, irrigation was scheduled based on ET_c, (i.e., ET_o*K_c) according to the California Irrigation Management Information System CIMIS (https://cimis.water.ca.gov/) where the difference between precipitation and ET_c was considered as irrigation water to be applied. Irrigation length and frequency were adjusted throughout the irrigation cycle, taking into account the crop growth and precipitation events based on the CIMIS information.

2.4.2. Crop Yield Simulations

After flow calibration, the crop parameters (Table 4) from the SWAT database were used to simulate the crop yields. For crop yield simulations, parameters related to LAI, harvest index (HI), and radiation use efficiency (RUE) are commonly used in the model to simulate plant growth (Marek et al., 2017).

Observed crop yields were collected for 2009–2014 from the USDA National Agricultural Statistics Service (USDA-NASS) (http://www.nass.usda.gov). USDA-NASS reports crop yields at the county/state level in ton/acre (grape) or lbs/acre (almond) unit; however, the SWAT estimates in kg/ha (dry yield) at the harvest time (Srinivasan et al., 2010). Therefore, the unit conversion was done for both crop yields and presented here in kg/ha unit.

2.5. Evaluation of Model Performance

Model calibration and validation were performed by comparing model-simulated streamflow with measured daily streamflow. The SWAT model was calibrated for 8

years (2009-2016) with one-year warm-up period (2008) and validated for another 5 years (2002-2007). Both observed and simulated results were evaluated using four quantitative statistical parameters - the coefficient of determination (R^2), Nash-Sutcliffe Efficiency (NSE), the percentage of bias (PBIAS), and Kling-Gupta efficiency (KGE). The detailed descriptions of the model calibration and validation process for streamflow and the evaluation matrix were discussed in Paul and Azar (2018).

Since remotely sensed data had a different temporal coverage (2008 to 2014) for ET and LAI, the SWAT model was calibrated from 2009 to 2014 using LAI insertion and validated with remotely sensed ET with the same time period. The model performance for ET simulation with remotely sensed MODIS ET was evaluated by the R^2 and standard deviation (SD) parameters. And at the end, the model prediction for average annual crop yield was compared with the observed NASS data by relative yield reduction (RYR) and Root Mean Square Error (RMSE). The statistical equation for all the performance evaluation criteria is described in Table 5.

3. Results and Discussion

3.1. Model Calibration and Validation

Comparison of observed and simulated daily streamflow by both conventional SWAT and SWAT-LAI approach indicated that daily flows for (2009-2014) were well estimated with high R^2, NSE, KGE values of 0.82, 0.78, and 0.53 respectively. The higher values of R^2 (>0.80) indicate a "good" correlation between daily observed and simulated flows and higher NSE values (>0.75) demonstrated a "good" agreement between these (Moriasi et al., 2015; Paul and Negahban-Azar, 2018).

However, the PBIAS of simulated daily discharge from the observed discharge was high, where the model underestimated by −39.8% in daily streamflow. The peak flow was considerably underestimated during the wet years (2011) and overestimated during drought years (2013-2014). Although the model was simulated using one regulated reservoir flow data (as inlet), multiple unregulated reservoirs and extensive irrigation canals within the watershed might have made the higher bias at the outlet.

Simulated flow from SWAT-LAI matched the observed flow better during the calibration period (2009-2014) compared to conventional SWAT calibration outcome. This observation is supported by an apparent improvement in peak flows predictions (Figure 3). Differences between simulated daily streamflow from SWAT and SWAT-LAI was generated using a bar plot to understand the improvement in the temporal variability (Figure 3).

3.2. Model Performance for ET Prediction

The model performance was also checked between simulated ET with MODIS ET at the sub-basin scale and evaluated by R^2 and SD values between them (Figure 4). The R^2 values ranged from 0.02 to 0.43, and the SD values ranged from 0.39 to 0.78 during conventional SWAT simulation (Figure 4). A noticeable improvement was found while ET was simulated with MODIS LAI. Higher R^2 values with an increment of 0.002 to 0.19 and lower SD values with a reduction of -0.003 and -0.20 were found when SWAT integrated with the MODIS LAI, which indicates an improved agreement between simulated ET by SWAT-LAI and MODIES ET. A small improvement of the R^2 and SD found for the upland forested area (i.e., subbasins 24, 28), which are highly dominated by snowmelt and regulated reservoirs (Chen et al.,

2017a), while the dominant area of irrigated croplands (i.e., subbasins 32-45) showed a better performance for SWAT-LAI modeling approach.

3.3. Model Performance for Crop Yield Simulation

As explained earlier (section 2.1), the SWAT simulates crop growth using the incoming PAR absorbed by the crop canopy and uses the daily LAI to simulate the ET and crop yield. Therefore, parameters related to LAI were used to simulate the crop yield. In this study, three parameters are found most sensitive - potential maximum leaf area index for the plant (BLAI), the fraction of growing season at which senescence becomes the dominant growth process (DLAI), and radiation use efficiency (BIO_E). In addition to that, BIO_INIT (initial biomass), BIOMIX (biological mixing efficiency), PHU_PLT (number of heat units to bring the plant to maturity), and LAI_INT (initial leaf area index) was chosen to adjust management files (.mgt). In the case of SWAT-LAI, only radiation use efficiency (RUE) was used for crop yield simulation due to its direct effect on biomass simulations (Eq. 7). The default and calibrated parameters are shown in Table 4 for both SWAT and SWAT-LAI simulations. Table 4 is showing that considerable adjustment of the parameters was taken under the conventional SWAT simulation, while slight variations were found during SWAT-LAI simulation. Low LAI and RUE values during the SWAT simulations indicate high temperatures or water stresses on plants (Bat-Oyun et al., 2012) despite a high amount of irrigation application. However, considerable RUE (BIO_E) was found under the same irrigation application when MODIS LAI was used in the SWAT plant growth model. This outcome showed that MODIS LAI

insertion in the model could capture both real-world crop and irrigation management well.

Comparison of observed and simulated crop yields by SWAT and SWAT-LAI are presented in Figure 5. The average annual crop yields collected from the USDA-NASS report were compared to the simulated average annual yield for both almond and grapes for 2009–2014. From Figure 5, it is noticeable that direct insertion of LAI gives reasonable results for almond and grape yields compared to conventional SWAT simulation. The simulated average annual almond yields by SWAT (3180.2 kg/ha) and SWAT-LAI (2613.3 kg/ha) were higher than the observed yield (2104.7 kg/ha). However, the average annual almond yield for SWAT-LAI was closer to observed data than the results from the conventional SWAT model. As a result, the RMSE values decreased from 714.5 to 254.1 kg/ha, the relative yield values reduced from -21.51% to -4.23% when direct LAI insertion was applied.

Unlike almond, the conventional SWAT plant growth model underestimated the grape yields, especially in dry years (2013-2014). Grape yield predictions in SWAT-LAI showed similar underestimation tendencies compared to observed values, except for 2009. On the other hand, yield estimated from both modeling approaches were similar during dry years 2013-2014, with SWAT-LAI producing the best estimates. During 2009-2014, the average annual grape yields by SWAT and SWAT-LAI were 3715.5 kg/ha and 3631.7 kg/ha, respectively, which shows a small difference than the observed average annual yield (3648.4 kg/ha). Comparatively, the SWAT- LAI model estimated more accurate grape yield compared to the SWAT model, with the RMSE

values decreases from 429.3 kg/ha to 208.9 kg/ha, and the relative yield decline from -1.8% to 0.46%.

3.4. Deviation of Model Estimates

Almond and grape yields at the HRU scale were compared between two modelling approaches over the simulation years (2009-2014) (Figure 6). Compared to SWAT estimates, SWAT-LAI showed a great improvement in spatial details and captured the observed crop yield more reasonable, especially during droughts (2013-2014).

Almond crop yields ranged from 2941 kg/ha to 4314.6 kg/ha under SWAT simulation, while it varied between 2182.7 kg/ha and 3510.8 kg/ha under SWAT-LAI simulation. SWAT simulates higher almond yields compared to observed yield with less yield variations at the HRU scale (Figure 6). Although, errors of estimate were higher for SWAT simulation, which resulted in RMSE 458.8 kg/ha to 1072.8 kg/ha for 2009-2014. SWAT-LAI estimated more accurate almond yield at the HRU scale, with the reducing RMSE values of 208.8 kg/ha to 572 kg/ha during 2009-2014.

The dry grape yield showed a higher variation compared to almond yield, especially during dry years 2013-2014. SWAT simulated average annual grape yields around 3503.7 kg/ha and 3217.7 kg/ha during the 2013 and 2014 dry years, however, a larger variation was generated at the HRU scale (Figure 6). However, the range of variation of model estimates found relatively small when LAI assimilation was carried throughout the growing season. SWAT-LAI computed the average annual grape yields with 3626.2 kg/ha and 3451.5 kg/ha with a smaller variation in HRU scale which is closer to observed values during the 2013 (3946.4 kg/ha) and 2014

(3592.5 kg/ha) dry years, respectively (Figure 6). As a result, the RMSE for grape yields ranged from 592.8 kg/ha to 1554.3 kg/ha under SWAT simulation, minimizes for SWAT-LAI simulation with estimates ranges from 717.9 kg to 1136.1 kg/ha.

That gives the impression that plant growth in SWAT is more "weather-sensitive" than in the field. SWAT uses Fourier Series to convert stationary temperature data into a continuous function that is used to compute heat unit accumulation and LAI at a daily scale. Therefore, the impact of soil drought on plant growth and subsequent crop yield might be overestimated by SWAT. Other studies also have provided similar evidence from their research (Bauwe and Kahle, 2019; Sinnathamby et al., 2017).

4. Implications

Worldwide, researchers used various remote sensing data, such as soil moisture, ET, snow, and LAI in the SWAT model to predict the streamflow, sedimentation, crop yield for row crops, the biomass of forest etc. However, few studies have evaluated the model simulation for a better understanding of crop response to remotely sensed data used at a large scale diverse landscape.

Previous studies on this watershed showed that, although SWAT was able to simulate streamflow at the outlet, upstream streamgauge stations were rated as unsatisfactory due to lack of irrigation and water management data (Chen et al., 2017a). Through the enhanced method described in this study, it is clear that SWAT application in semi-arid regions with limited observations can be greatly benefitted from high-resolution MODIS LAI use. This study showed the positive consequence of daily MODIS LAI use in SWAT simulation for streamflow and ET prediction. The

results showed that both streamflow and ET are sensitive to modified LAI use, especially model improvement was noticeable for a spatial variation on ET computation. It also showed the evidence of the model's performance improvement by comparing SWAT-simulated crop yields with observed values, especially for critically dry years.

The relationship between LAI and crop yield varies with types of crops and at different growing-stages of a plant. Daily LAI simulates under ideal growing conditions, such as under sufficient water and nutrient supply, and suitable climate conditions (Figure 1) (Arnold et.al., 2012; Neitsch et.al., 2011). For perennial crops like orchard or vineyard, LAI comparisons between different years are a good way to monitor the water status and crop quality (Johnson et al., 2003). When the tree is younger, increasing LAI boosts the fruit yield. If the canopy gets too dense it prevents light penetration to lower levels and to developing fruits and affects the crop quality and quantity. This process is modified through crop vegetation management such as pruning to increase the yield. Since every tree or vine in the orchard or vineyard has a unique combination of plant phenology, it demands a systematic model to estimate water use. For orchard or vineyard, crop water uses, and productivity is driven primarily by radiation and varies by canopy development and training (Rosati et al., 2004; Teixeira et al., 2013). Therefore, accurate LAI measurement is crucial and important for computing/projecting crop yield.

The outcomes of this study provided evidence that remotely sensed LAI could be an alternative and advanced solution to predict the accurate crop water use for California's large, complex, and dynamic agricultural landscape to that of the

conventional SWAT. This improved model was used to predict accurate crop water use and crop yield and quantify crop water productivity for different irrigation scenarios.

5. Conclusion

The main objective of this study was to improve the vegetation growth module within the SWAT model to quantify the hydrological process and crop yield for JRW. Since ET and biomass/crop yield are depending on the LAI, a series of critical parameters related to hydrology and crop yield were determined. Remote sensing application could provide reasonably quick and accurate LAI information due to its higher sampling density, especially for a complex watershed where multiple crop types have existed. This study developed a methodology to estimate ET rates and crop yields using remotely sensed LAI data for complex and ungauged watersheds like JRW. Results also showed that proper modeling of the LAI distribution plant growth module was able to capture actual vegetation dynamics and estimate more accurate biomass/crop yield at the HRU scale than the SWAT model's internal algorithms using heat units. The outcomes of this study serve as a decision support tool in this regard by providing quantitative information for crop water use and estimating crop yield.

6. *Figures*

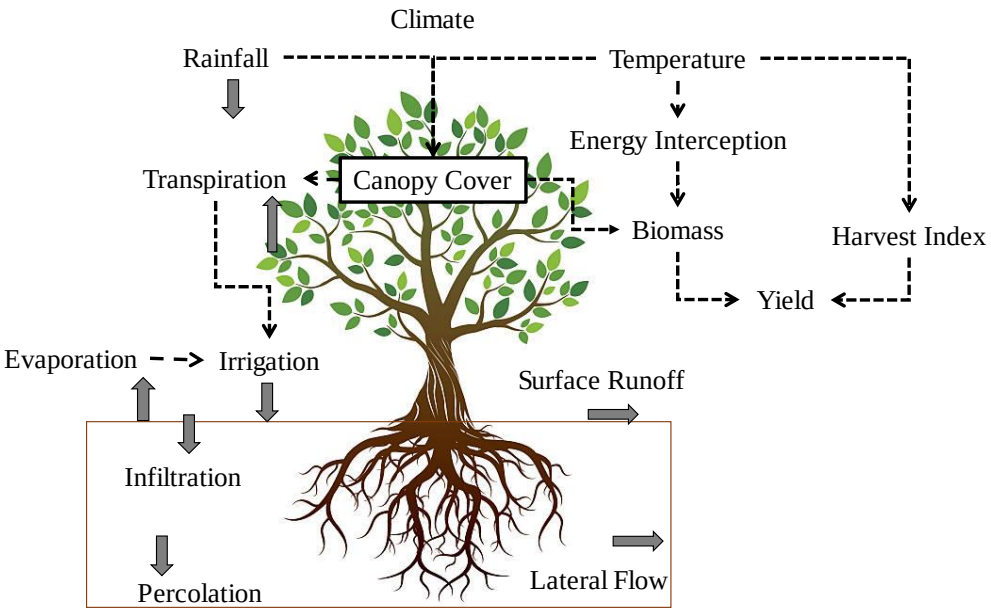

Figure 1: Main components of soil-water balance interaction with vegetation and climate. Continuous and dashed lines are indicating the direct and indirect links between the variables. For explanation, see section 2.1.

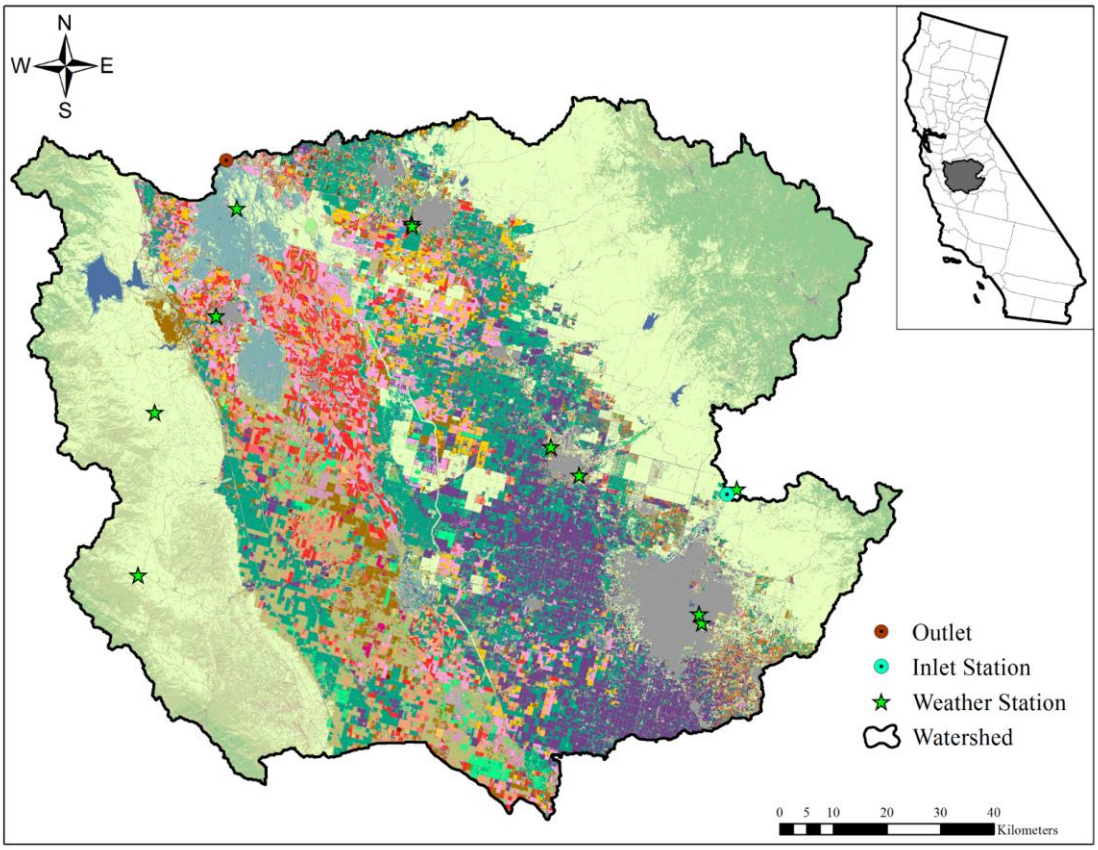

Figure 2: Map of the study area, showing the crop data layer 2017 for San Joaquin Watershed in California.

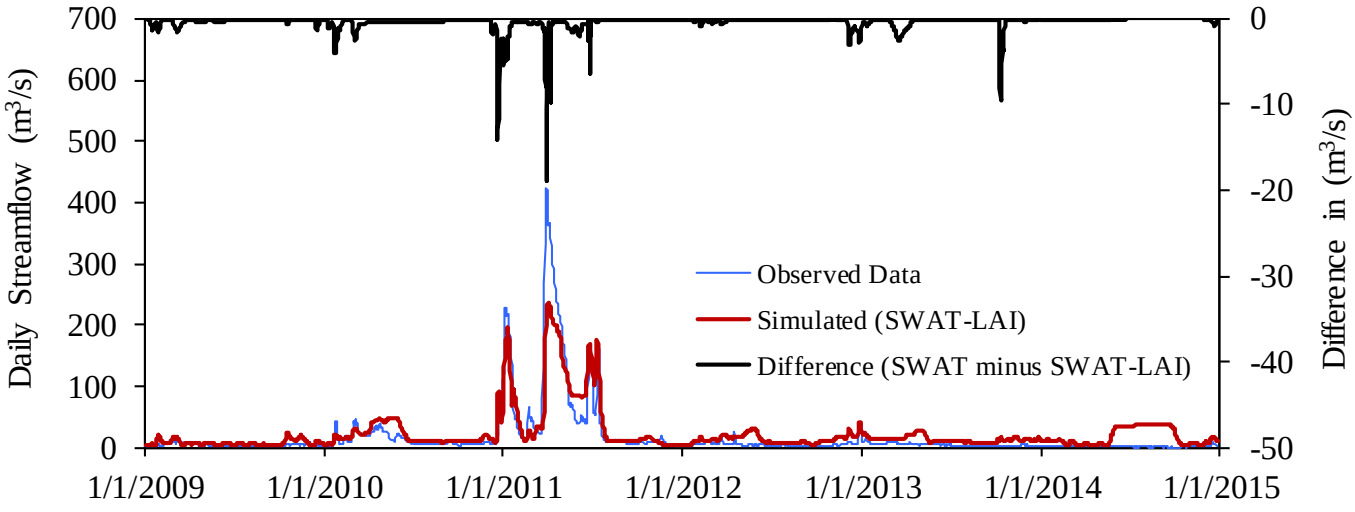

Figure 3: Temporal variability of observed daily streamflow with estimated values from conventional SWAT calibration (SWAT) and the SWAT calibration with remotely sensed LAI insertion (SWAT-LAI).

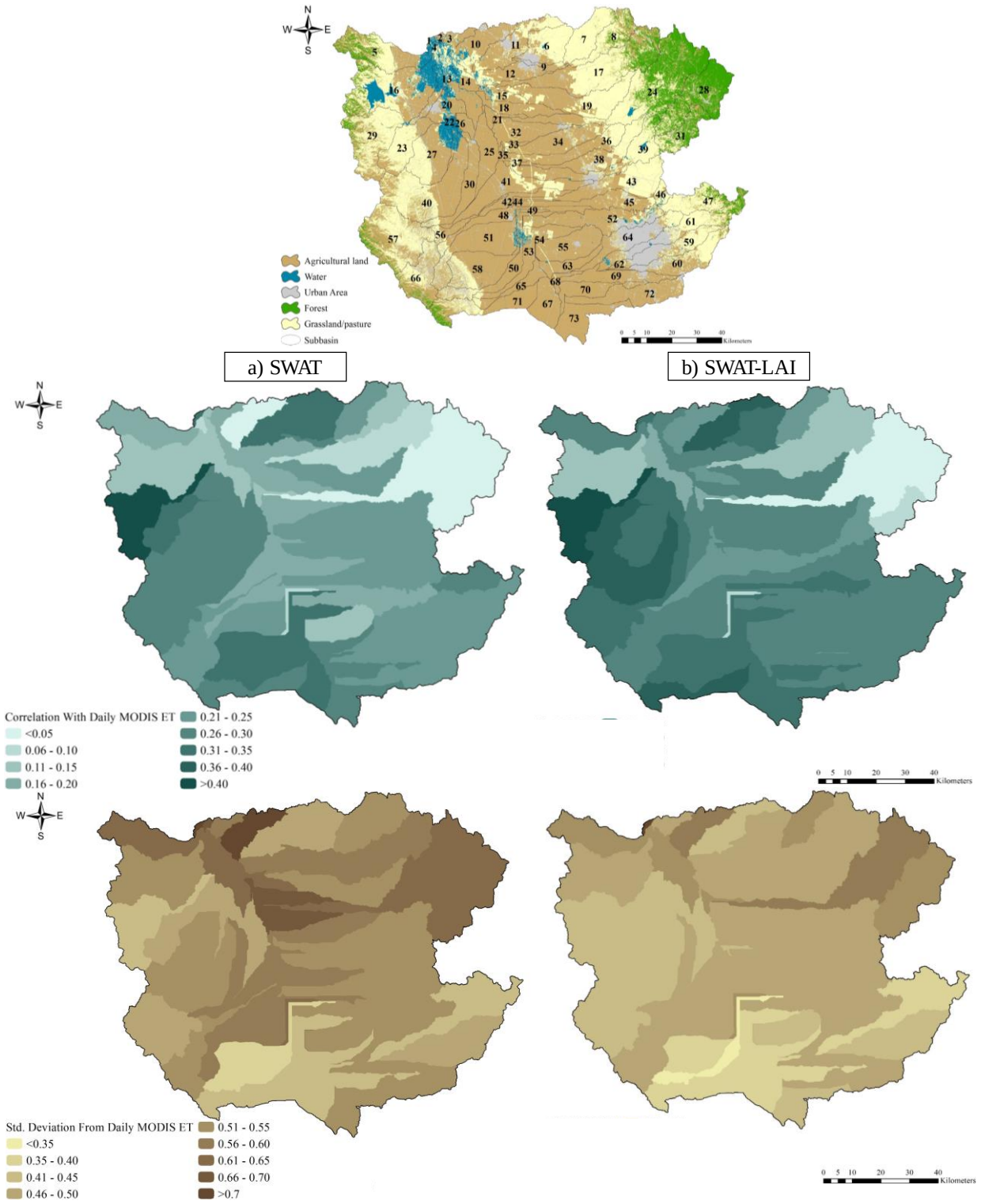

Figure 4: Spatial agreement between the remotely sensed daily ET with (a) SWAT and b) SWAT-LAI simulated daily ET at subbasin scale. At the top, the map is showing the location of delineated subbasins with major land cover (derived from 2017 CDL).

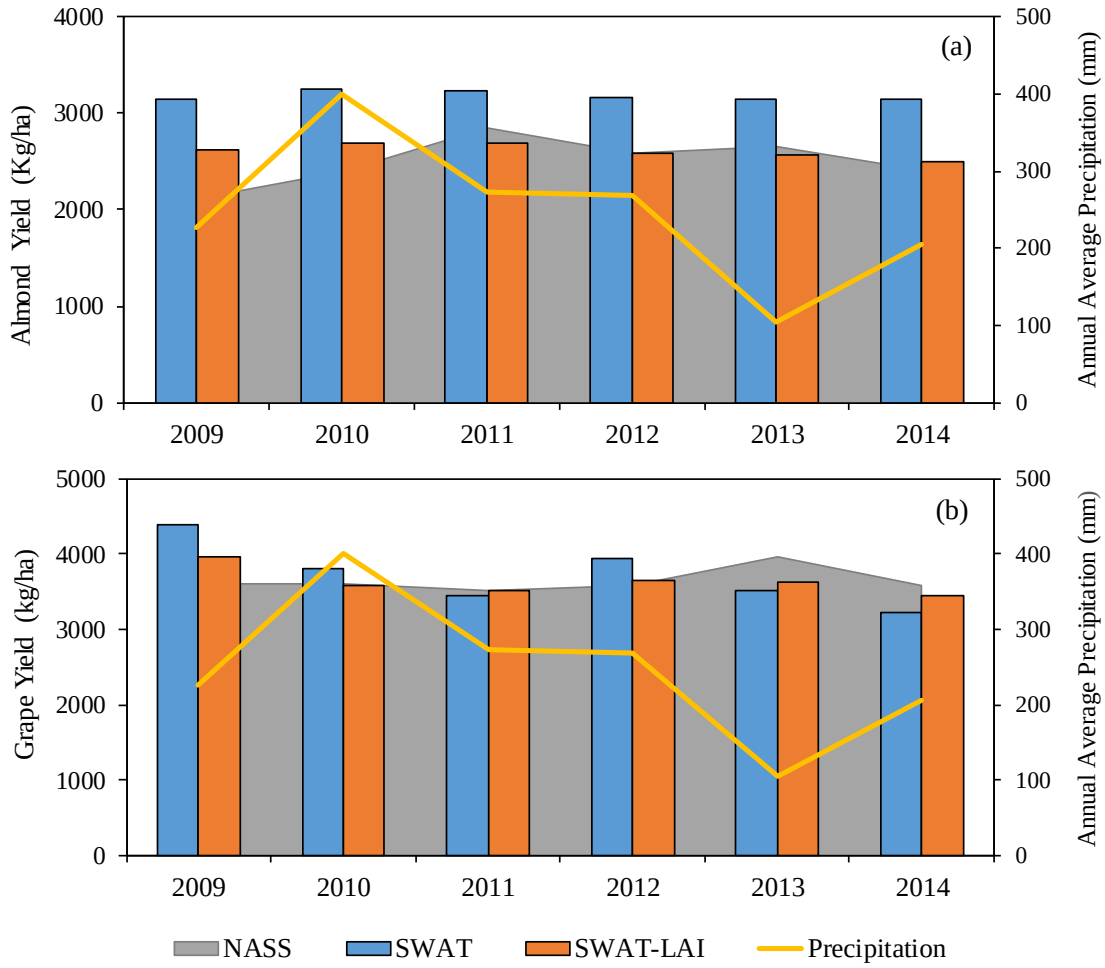

Figure 5: Comparison of observed (NASS) and simulated a) almond and b) grape yields under the SWAT and SWAT-LAI approaches. Average annual precipitation is showing on the secondary y-axis derived from model climate input.

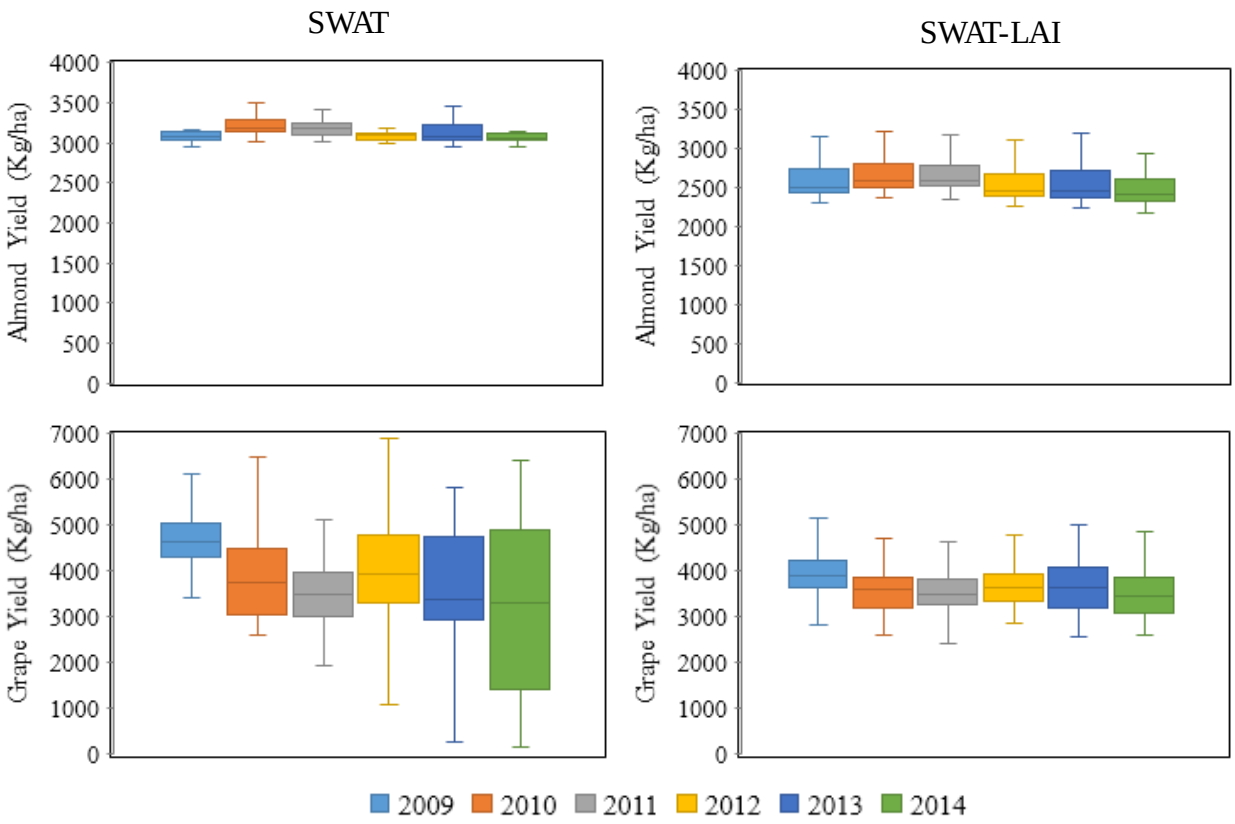

Figure 6: Uncertainty of model estimates on almond (top), and grape (bottom) yield for 2009-2014. Box-plots indicate maximum, minimum, and average values with first and third quartiles of the simulated crop yields at the HRU scale.

7. Tables

Table 1: Major land cover and land use data within study watershed.

Land Use/Land Cover	Area (Acres)	Area (km^2)	% Watershed Area
Agricultural Land	1649708.8	6676.13	43.5
Grass/Pasture	1127017.3	4560.9	29.7
Urban & Barren	320405.5	1196.6	8.4
Shrubland	300014.4	1214.1	7.9
Forest	280216.8	1134	7.4
Water &Wetland	117600.7	475.9	3.1
Major Crop Land			
Almonds	409015.2	1655.2	10.8
Vineyard	310374.2	1256.0	8.2
Corn	267791.7	1083.7	7.1
Alfalfa	159149.1	644.1	4.2
Winter Wheat	131367.7	531.6	3.5
Tomato	90269.5	365.3	2.4
Cotton	85585.2	346.4	2.3
Orchard	83757.5	339.0	2.2

Table 2: Selected parameters for daily streamflow simulation.

Parameter	Definition[a]	Scale of input	Initial Range
ALPHA_BF	Baseflow recession constant (days)	Watershed	0.01-1
GW_DELAY	Groundwater delay (days)	Watershed	1-500
GW_REVAP	Groundwater "revap" coefficient	Watershed	0.01-0.20
REVAPMN	Re-evaporation threshold (mm H_2O)	Watershed	0.01-500
GWQMN	Threshold groundwater depth for return flow (mm H_2O)	Watershed	0.01-5000
SOL_K	Soil saturated hydraulic conductivity (mm/hr)	HRU	-15-15
SOL_AWC	Available soil water capacity (mm H_2O/mm soil)	HRU	-15-15
CH_N(2)	Main channel Manning's *n*	Reach	0.01-0.15
CH_K(2)	Main channel hydraulic conductivity (mm/hr)	Reach	5-100
CN2	Curve number for moisture condition II	HRU	-0.3-0.1
EPCO	Plant uptake compensation factor	HRU	0.75-1
ESCO	Soil evaporation compensation factor	HRU	0.75-1
HRU_SLP	Average slope steepness (m/m)	HRU	0-1
SFTMP	Snowfall temperature (^oC)	Watershed	0-5
SMFMN	Melt factor for snow on December 21 (mm H_2O/ ^oC-day)	Watershed	0-10
SMFMX	Melt factor for snow on June 21 (mm H_2O/ ^oC-day)	Watershed	0-10
SMTMP	Snow melt base temperature (^oC)	Watershed	-2-5
TIMP	Snow pack temperature lag factor	Watershed	0-1

[a] Source: Neitsch et al., 2001

Table 3: Summary of inputs of the SWAT model and evaluation datasets.

Data Type	Spatial/Temporal Resolution	Source
Digital Elevation Model (DEM)	30m	USGS National Elevation Dataset (USGS-NED 2013)
Land Use and Land Cover	30m	USDA National Agricultural Statistics (USDA-NASS)- Crop Data Layer
Soil Data	250m	State Soil Geographic (STATSGO) database
Precipitation	Daily (2002-2016)	National Climatic Data Center (NCDC)
Temperature	Daily (2002-2016)	
Streamflow	Daily (2002-2016)	USGS 11261500 San Joaquin River at Fremont Ford Bridge
Leaf Area Index (LAI)	500m/4 days	MODIS Landsat
Evapotranspiration (ET)	500m/8 days	

Table 4: Default and calibrated values of selected crop parameters for almond and grape yield simulation.

Crop parameters	Parameters Description	Almond			Grape		
		Default Value	Calibrated Value		Default Value	Calibrated Value	
			SWAT	SWAT-LAI		SWAT	SWAT-LAI
BIO_E	Radiation use efficiency or biomass energy ratio (kg/ha)/(MJ/m^2)	16.1	10	25	30	18	35
BLAI	Maximum potential leaf area index (m^2/m^2)	1.2	1	1.2	2	1	2
DLAI	Fraction of growing season when growth declines	0.99	0.80	0.99	0.9	0.8	0.9
PHU_PLT	Number of heat units to bring plant to maturity	0	250	250	0	100	100
LAI_INIT	Initial leaf are index	0	3	3	0	3	3
BIO_INIT	Initial biomass (kg/ha)	0	1000	1000	0	250	250
BIOMIX	Biological mixing efficiency	0.2	0.25	0.25	0.2	0.25	0.25
HVSTI	Harvest index for optimal growing season (kg/ha)/(kg/ha)	0.02	0.02	0.02	0.05	0.05	0.05
WSYF	Lower limit of harvest index	0.01	0.01	0.01	0.01	0.01	0.01

Table 5: Description and formula of the performance evaluation criteria for streamflow, ET, and crop yield simulation.

	Evaluation Criteria	Equation
Streamflow Evaluation	Nash-Sutcliffe Efficiency (NSE)	$NSE = 1 - \frac{\sum_i (X^{obs} - X^{sim})^2}{\sum_i (X^{obs} - X^{obs}_{mean})^2}$
	Percentage of Bias (PBIAS)	$PBIAS\ (\%) = \frac{\sum_{i=1}^{n} (X^{obs} - X^{sim})}{\sum_{i=1}^{n} X^{obs}} x\ 100$
	Kling-Gupta efficiency (KGE)	$KGE = 1 - \sqrt{(r-1)^2 + (\alpha - 1)^2 + (\beta - 1)^2}$; $\alpha = \frac{\sigma_{sim}}{\sigma_{obs}}$; $\beta = \frac{X^{obs}_{mean}}{X^{obs}_{mean}}$
	Coefficient of Determination (R^2)	$R^2 = \frac{[\sum_i (X^{obs,i} - X)(X^{sim,i} - X^{sim}_{mean})]^2}{\sum_i \sqrt{(X^{obs,i} - X^{obs}_{mean})^2}\ \sum_i \sqrt{(X^{sim,i} - X^{sim}_{mean})^2}}$
ET Evaluation	Standard Deviation (SD)	$STDEV = \sqrt{\sum_{i=1}^{n} (X^{obs,i} - X^{obs}_{mean})^2}$
Crop Yield Evaluation	Relative Yield Reduction	RYR (%) $= \frac{Y^{obs} - Y^{sim}}{Y^{obs}} x\ 100$
	Root Mean Square Error (RMSE)	$RMSE = \sqrt{\sum_{i=1}^{n} (Y^{obs} - Y^{sim})^2}$

Chapter 6: Assessing the Water Productivity of the Efficient Irrigation Strategies in Water Stressed Agricultural Watershed: San Joaquin Watershed, California

Abstract

Intensified climate variability, depleting groundwater, and escalating water demand creates severe stress on high-quality water sources used for agricultural irrigation. The water scarcity exacts a necessity to explore the non-traditional water sources to sustain food production across the U.S. The objective of this study was to develop different water conservation scenarios, including sustainable wastewater reuse scenarios for an agriculture-based watershed. Regulated deficit irrigation (RDI), auto or precise irrigation (AI), wastewater reuse (WR), and their combinations were evaluated as different scenarios. The potential wastewater reuse scenario was developed through the treated wastewater capacity of the existing wastewater treatment plant as a valuable alternative for emergency agricultural water (e.g., drought years) and to reduce groundwater extraction. For each scenario, crop yield, irrigation consumption, and groundwater savings were estimated for almond and grape using the Soil and Water Assessment Tool (SWAT) model. The water productivity (WP) was calculated and compared at the Hydrologic Response Unit (HRU) for each crop under multiple efficient irrigation strategies. The results of groundwater improvement and deterioration under each scenario and WP ratios were presented. This study will enable modelers to combine process-based hydrological models into the decision-making process for agricultural water management.

This chapter will be submitted for publication in *Sustainability*.

1. Introduction

California receives approximately 200 million acre-feet (MAF) of precipitation in a non-drought year (Bureau of Reclamation, 2007). However, almost 65% of the total precipitation is lost to evaporation or vegetation. Remaining 71 MAF surface runoff and imported water are supplies for environmental, agricultural, and urban uses through California's complex water distribution system. In addition, groundwater used as an important source to meet the high water demand (Siebert, 2003).

California's central valley is the most productive and diverse agricultural land in the U.S. surrounded by pastureland and upland forest where extensive irrigation and water regulations are practiced. In spite of extreme climate-related trends over the past decades, including droughts and extreme weather, California has the largest number of irrigated farmed acres compared to other states and consumed the highest irrigated water per acre compared to other states. According to USGS, an estimated 61% (25.8 MAF) of total surface and groundwater is withdrawn for agricultural irrigation (Johnson and Cody, 2015). The availability of irrigation water has been a major factor in the development of California's agricultural production (Johnson and Cody, 2015).

Due to extreme water scarcity, cropping patterns in the central valley have shifted from forage and feed crops to permanent orchard and vine crops due to their higher crop value. Most vegetables and row crops (including grain and pasture crops) are planted and harvested during the same production year, sometimes more than once, and maybe fallowed in dry years. In contrast, California is prioritizing to grow more permanent orchard crops, and vineyard crops are planted once that require continuous

watering to reach maturation and cannot be fallowed during dry years without loss of investment. As a result, cash crops like almond and grape acreage increased at 5% annual growth in California within the 2004-2013 period (Johnson and Cody, 2015).

Therefore, the water distribution system, including both infrastructure and operating policies, evolved primarily to satisfy the needs of orchard crops. However, direct information is limited across the agricultural regions on how much groundwater is being used to supplement local irrigation demand (Matios and Burney, 2017). Data regarding groundwater use for irrigation are critical for ensuring long-term water and food security. Policymakers and stakeholders need enough information regarding water supply and water demand for each crop and the potential benefits of more-efficient irrigation management.

Improved water delivery strategies are needed to assess before implementation to satisfy the increasing irrigation needs of orchards and other specialty crops, particularly as they transition from surface irrigation to pressurized irrigation (micro-irrigation and sprinklers). In addition, benefits of direct wastewater reuse from wastewater treatment plant (WWTP) is also needed to evaluate as an addition or alternative water source for irrigation. Despite the wealth of studies on the subject of wastewater irrigation, few studies on the influence of effluent from a WWTP on irrigation water have been performed on the situation where direct wastewater reuse accounts for most of the wastewater reuse. Therefore, it is important to address how irrigation water is affected by effluent from a WWTP on irrigation water prior to any analysis of the impacts of direct wastewater reuse.

California has a long history of using recycled water mostly for agricultural irrigation as well as for groundwater recharge, environmental uses, industrial uses, landscape irrigation, etc. (Schulte, 2016). Most of the WWTPs discharged their treated water to the surface water bodies like rivers, irrigation canals, etc. Very few studies found that evaluated the model simulation for a better understanding of crop responses to different irrigation, including water reuse from WWTP at large scale watershed.

The purpose of this paper is to assess the effects of groundwater and direct wastewater reuse from a WWTP on orchard/vineyard irrigation. The objective of this study was to use a semi-distributed model to predict water productivity and groundwater consumption under different irrigation scenarios, including wastewater reuse for two major crops (almond and grape) of California. This study aimed to provide two benefits- (i) to choose a suitable irrigation strategy during droughts and (ii) to emphasize future research efforts that can allocate to key economic crops based on water productivity.

2. Methodology

2.1. SWAT Model Modification

The calibrated SWAT model from the previous study, described in chapter 4, was used here to evaluate the different irrigation scenarios on almond and grape water productivity. In the SWAT model, actual crop evapotranspiration (ET_c) generated from reference crop evapotranspiration (ET_o) and crop characteristics (K_c) are adjusted by environmental stressors including water availability for plant growth. Thus, the effects of applied water at various fractions of ET_c was evaluated on

almond and grape yield and water productivity. Net irrigation ($P\text{-}ET_c$) requirement was calculated and scheduled at the HRU level and assigned from the aquifer. The management files within the SWAT model were updated including SWAT-LAI results from the previous study and the crop yields for different irrigation scenarios was obtained by re-running the modified SWAT application.

In the SWAT model, irrigation water applied at the HRU level which can be obtained by five types of water sources: a reach, a reservoir, a shallow aquifer, a deep aquifer, or a source outside the watershed. Groundwater can be used as a source of irrigation by assigning either from the shallow or deep aquifer for each HRU. The detailed descriptions of the developed irrigation scenarios are described in the next section.

2.2. Best Management Scenarios (BMPs)

For each type of crop, two management practices were specified- irrigation operation after dormancy and harvest. Irrigation length and frequency were adjusted throughout the irrigation cycle, taking into account the crop growth and precipitation events based on the CIMIS information (https://cimis.water.ca.gov/). In addition to baseline, three regulated BMPs with different irrigation amounts and efficiency were defined for almond and grape and introduced into the SWAT model by changing the management (.mgt) files for each HRU.

Baseline: San Joaquin valley mainly relied on groundwater due to surface water shortages and water-conserving irrigation measures, such as micro-sprinkler and drip systems, are commonly used to irrigate. Thus, groundwater irrigation with micro-sprinkler was defined as a baseline scenario for this study. For almond, a sprinkler

irrigation system was used with 0.85 efficiency and a drip system for the grape with 0.90 efficiency (Table 1).

Regulated Deficit Irrigation (RDI): Deficit irrigation is applied to limit the excessive vegetative growth and improve fruit quality or limit water use during droughts. Regulated deficit irrigation (RDI) is a sustainable irrigation practice of regulating or restricting the application of irrigation water, limiting the vine water use to below that of a fully watered vine. RDI is a "standard" irrigation strategy that utilized commonly in drought-prone areas (Phogat et al., 2017; Pritchard, 2010). According to CIMIS, successful RDI is typically considered 50 to 60% of full ET_c for the orchard and vineyard. In this study, 75% of full ETc was used for both crops under the RDI scenario (Table 1).

Precise or Auto Irrigation (AI): If water availability is limited, growers can adjust by applying irrigation water when trees are most sensitive to stress. In SWAT, auto irrigation is triggered by using defined plant water stress and soil water deficit irrigation scheduling. Plant stress is defined as the ratio of actual to potential plant transpiration and varied from 0.40-0.95 (Allen et al., 1998). In this study, an average of 0.75 was used as plant stress assuming when the plant is experiencing 25% water stress, a fixed amount of water will be applied from the groundwater.

RDI-AI: This BMP is developed as a combination of RDI and AI, where auto irrigation was applied with regulated deficit irrigation amount during the growing season.

Wastewater Reuse (WR): In SWAT, WR from the existing WWTP was simulated by changing the source of irrigation from ‘aquifer’ to an outside the watershed. Based

on the WWTP capacity, the WR potentiality was accurately calculated for selected HRUs (Table 2). A total of four WWTPs are located within the San Joaquin Watershed (SJW) with different treated capacities that consumed by multiple users (Table 2). WR was applied for subbasin 11 and 59 only based on the treated water potentiality, including appropriated treatment and excluding conflicted users (Figure 1). Three WR scenarios were developed coupled with RDI, AI, and RDI-AI to evaluate the WR potentiality to reserve groundwater (Table 2, rightmost column).

2.3. Water Productivity and Water Saving Estimation

Water productivity (WP) (kg/m^3) is defined as the ratio of production (kg/ha) to water used (m^3) (Molden and Sakthivadivel, 1999). To analyze crop water productivity under different scenarios, two indices WP_{IP} (including irrigation and effective rainfall volume) and WP_{ET} (actual ET volume) were calculated. The WP was calculated for each HRU using calibrated SWAT model outcomes. For this study purpose, the average WP for almond and grape were presented for the particular subbasins which have WWTP within the subbasin and have the potentiality for water reuse. In this study, the HRU scale WP was calculated using simulated values of evapotranspiration (ET) and crop yield for almond and grape.

Water productivity of almond and grape were estimated by dividing simulated yield by the applied irrigation water, and actual evapotranspiration (ET) obtained from calibrated SWAT simulations for each BMPs.

$$WP = \frac{Y_i \, x \, A_i}{V_i \, x \, A_i} \tag{1}$$

Where Y is the crop yield per unit area (kg/ha), A is the area of the HRU (ha), V is the volume of consumed water by crops (m^3/ha). V can be expressed as applied irrigation water volume or as ETc volume to calculate WP_{IP} or WP_{ET}, respectively.

3. Results and Discussion

3.1. Irrigation Scenarios

Figure 2 is showing the difference in the WP indices, which is the result of different water allocation for crop irrigation. Irrigation water productivity (WP_{IP}) under stressed scenarios (RDI, AI, and RDI-AI) increased substantially as compared to full irrigation (Figure 2). The main point is the difference between WP_{IP} within the BMPs; higher WP for BMPs indicates the optimum ratio of water allocation for crop production.

The average annual almond and grape water productivity vary considerably across the subbasins. According to baseline scenarios, the average WP_{IP} is about 0.29-0.50 kg/m^3 for almond and 0.12–0.58 kg/m^3 for grape. From the model estimation, it is found that grape yields were quite sensitive to irrigation volumes used under different BMPs within the subbasins. Almond yield variability is also clearly affected by water irrigation scenarios within subbasins. Almond and grape yield sensitivity to irrigation amount was generated sufficient benefits for crop production to offset the irrigation costs in the irrigation scenarios. For example, under the RDI strategy, the crop yield of almond and grape is decreased while the overall WP_{IP} and WP_{ET} are increased (Figure 2). However, the combination of auto irrigation (AI) and regulated deficit irrigation (RDI) resulted in WP more than 0.50 kg/m^3 for both crops and subbasins except for almond in subbasin 59. However, a clear trend was found for both almond

and grape, a reduced water application increased water productivity (WP_{IP} and WP_{ET}). The RDI-AI scenario returning the highest WP_{IP} values for both almond and grape compared to the full irrigation scenario (baseline).

The WP_{IP} and WP_{ET} differences are significant under AI and RDI-AI, as the representative of auto or precise irrigation. For efficient irrigation scheduling, auto irrigation (AI) provides higher crop yields than conventional scheduled irrigation. Under auto irrigation management, the SWAT model triggered an accurate amount of water for irrigation under the assigned stress level, which resulted in high WP_{IP}. This indicates that auto irrigation would be the best option to utilize limited water and maintain high grape production during the drought years.

For almond, productivity related to ET losses (WP_{ET}) showed no clear pattern relative to BMPs and varied within a narrow range from 0.35 to 0.78 kg/m^3 across different irrigation applications. Higher WP_{ET} found for grape compared to almond, with a range of 0.31 to 1.1 kg/m^3. However, the magnitude of the WP increase was lower for upstream subbasin compared to downstream. After exhausting experimentation, it was found that subbasin in the upstream (ex., subbasin 59) are having less groundwater availability in the aquifer, which resulted in less water productivity for almond under the same irrigation amount and frequency.

These results were consistent with many filed scale experiments in a similar semi-arid region that showed minor crop water deficit has little effect on the crop yield. According to Williams and Phene (2010), over-irrigation reduced the buds' number in the vines and resulted in fewer grape yields. Sustained deficit irrigation application with moderate vine water stress is enough to maintain high water use efficiency and

yields of high quality (Pritchard, 2010; Williams et al., 2010). In contrast, other studies showed that a 35% reduction in irrigation caused up to 30% reduction in grape yield (Stevens et al., 2008; Stevens et al., 2010). Similar to grape, almond also showed better water use efficiency with deficit irrigation. For example, (Goldhamer et al., 2006) revealed that during the growing season, a uniform deficit irrigation treatment with 70% and 85% of full ET experienced little almond yield loss compared to the full ET treatment. Another note is calculated WP in this study was much lower than field measured values. Researchers mentioned that, low water productivity of almond and grape indicating large undesirable water loss under large basin irrigation systems (Atroosh et al., 2013; Phogat et al., 2017)

3.2. Benefits of Water Reuse

Wastewater reuse applications were combined with advanced, water-saving, and drip irrigation technologies, including RDI, AI, and RDI-AI irrigation strategies, to maintain the overall crop production and evaluate the impacts on groundwater conservation. Three optimal water-saving strategies were developed for the WR scenario (Table 2). Table 3 is highlighted the selected HRUs and their model delineated areas for almond and grape within subbasin 11 and 59. RDI, AI and RDI-AI irrigation scenarios were applied with assigned “outside” source for those specific HRUs. Based on the WWTP capacity treated wastewater applied for almond (case 1), grape (case 2), and almond-grape together (case 3) (Table 2).

The model simulation showed that wastewater reuse in separate almond and grape irrigation could reduce groundwater consumption more than 74% and 90% under RDI and AI scenarios, respectively. In subbasin 59, the total 1.7 MGD wastewater reuse in

almond and grape irrigation could save 45.53%, 83.12%, and 84.05% groundwater consumption under RDI, AI, and RDI-AI, respectively. This analysis suggests that more efficient irrigation management (RDI-AI) can save more groundwater consumption without losing current agricultural production and benefits.

However, it should be noted that the projected impact of the generated BMPs on crop yields should be verified in the field. Despite its water stress resistance, almond's quantitative and qualitative production depends on proper irrigation management. Also, the feasibility of direct wastewater transfers across the farms should be assessed properly. Despite these limitations, the large potential water savings highlighted in the analysis indicate that cost-effective optimal irrigation strategies could be implemented in water-scarce regions like California.

4. Conclusion

This study outlined a simple approach to evaluate the best water-saving strategies by targeting specific cash crops. Results showed that reducing irrigation in almond and grape could provide higher water use efficiency and increase water productivity. Precise or auto irrigation (AI) provides more efficient agriculture management in the high water-scarce watershed. Coupled regulated deficit irrigation with auto irrigation (RDI-AI) provides considerable increases in water use efficiency in the same areas. Treated wastewater reuse to the adjacent areas to WWTP with regulated deficit irrigation is recommended for almond in the downstream of the watershed as well as for grape. It can be concluded that treated wastewater reuse for the cash crop irrigation, such as almond and grape, could be benefitted for groundwater saving without major adverse impacts on these crops' quality. The obtained information

from this study can be utilized for developing better irrigation management practices for orchard and vineyard in California.

5. *Figures*

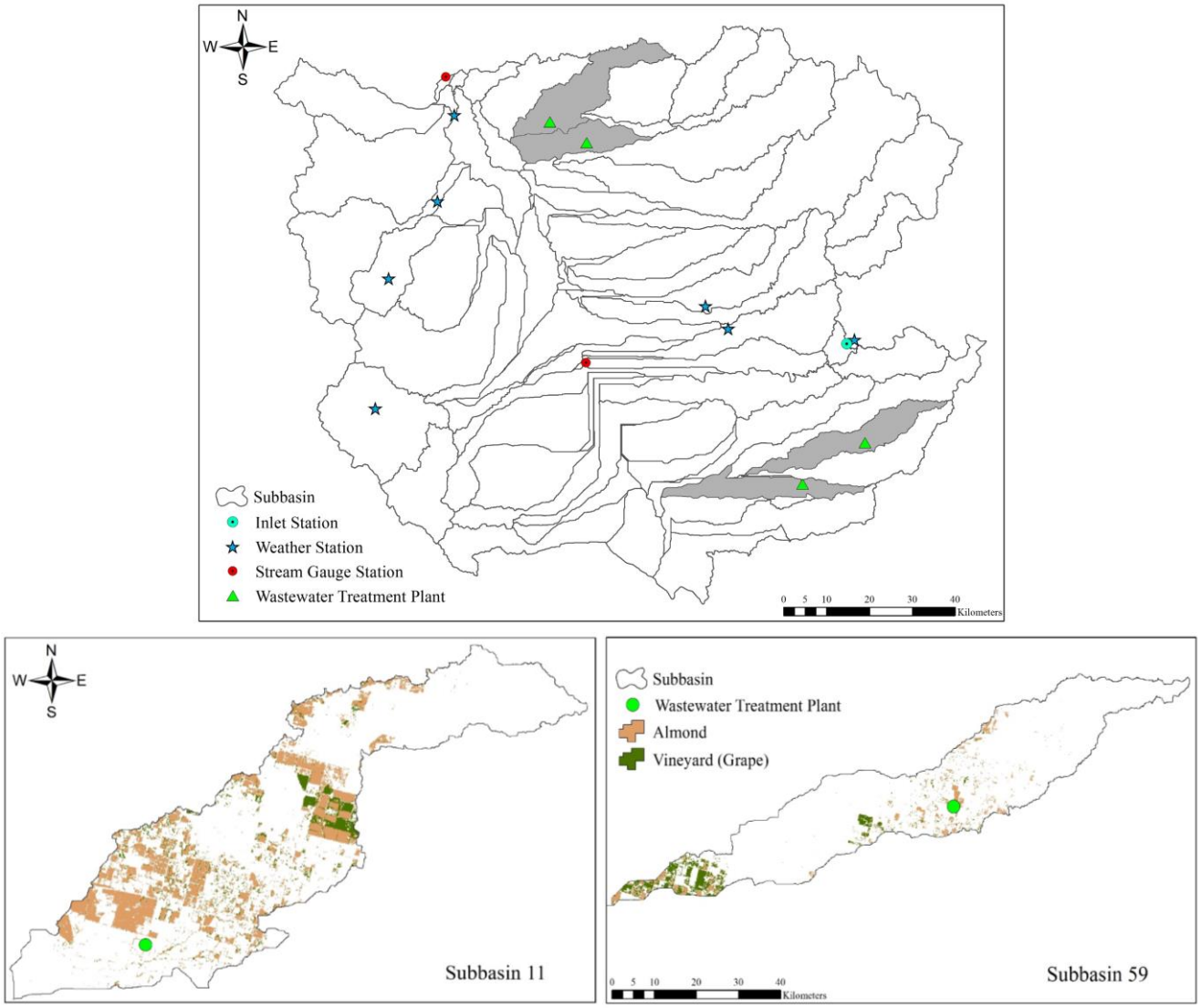

Figure 1: Map is showing the location of WWTP with almond and grape HRU within the San Joaquin Watershed- a) subbasin 11 and b) subbasin 59.

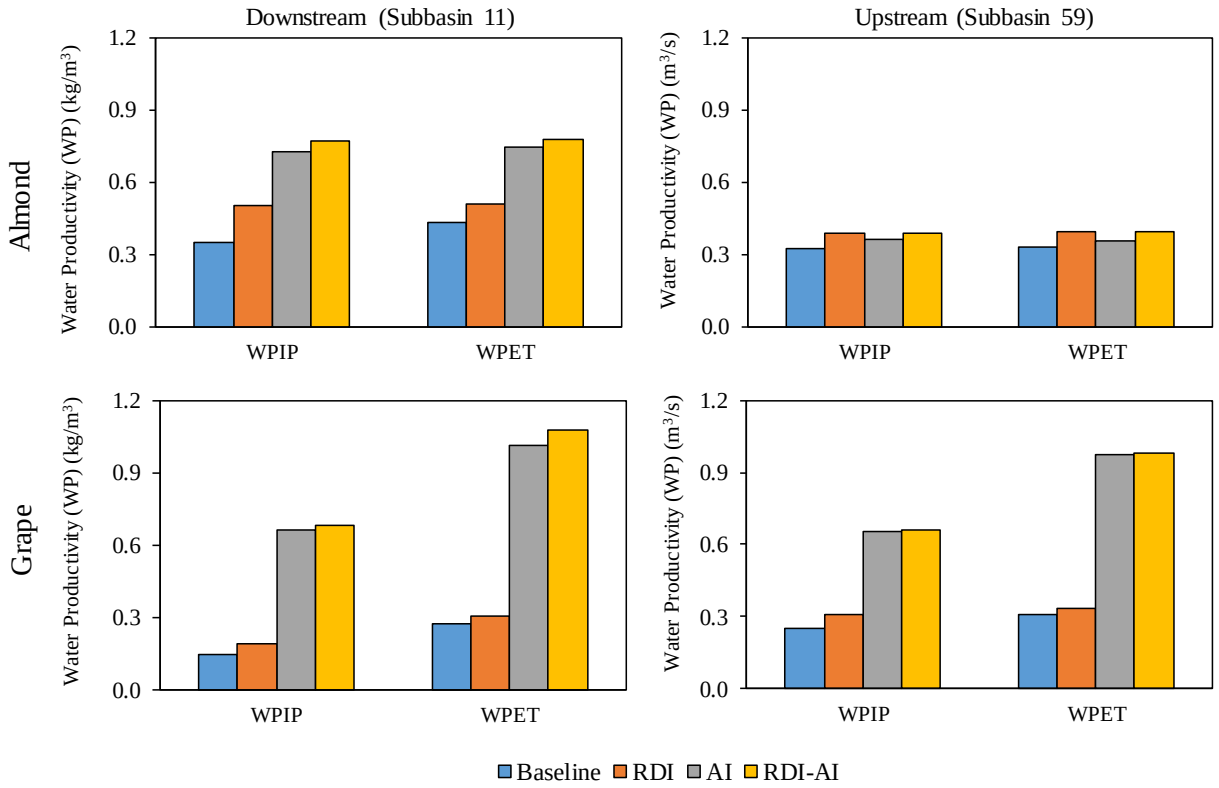

Figure 2: Model simulated average values of WPIP and WPET for almond and grape in the i) downstream (subbasin 11) and ii) upstream (subbasin 59).

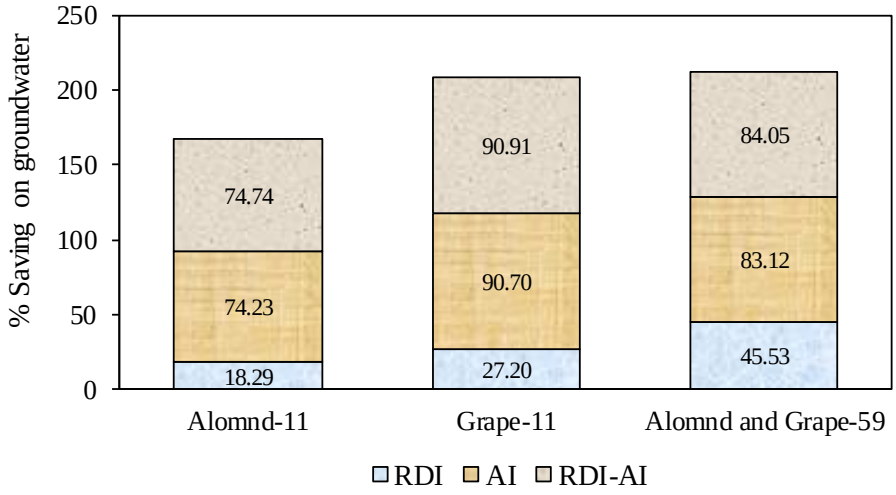

Figure 3: Percentage of groundwater saving due to direct wastewater reuse for irrigation. Values were calculated for selected HRUs where WR was applied.

6. *Tables*

Table 1: List of Best Management Practices developed for the analysis of water productivity.

BMPs		*Description*	*Irrigation Efficiency*		*Runoff Loss*
			Almond	*Grape*	
Baseline		Water extract from aquifer and amount calculated by ET_c (ET_o*K^c) for each crop	85%	90%	10%
BMP 1	RDI	Regulated deficit irrigation applied during crop growth. A uniform reduction of full ET (e.g. 75%) was applied for each period			
BMP 2	AI	Auto or precise irrigation applied with 0.75 plant stress			
BMP 3	AI-RDI	Auto irrigation applied with 0.75 plant stress and regulated deficit irrigation during growing season			
BMP 4	WR	Set the irrigation source as "Outside" in the .mgt files			

Table 2: List of the existing WWTPs within SRW and description of the treated wastewater use potentiality for almond and grape irrigation.

Subbasin	WWTP Name & Description	Effluent Description	Receiver	Wastewater Reuse Capacity	Assigned BMPs
11	**Atwater WWTF** Average 3.3 MGD discharges to surface water	Disinfected Tertiary Treated Municipal Wastewater	Receiving Water Peck/Atwater Drain	850.5 acres 3.44 km^2	Case 1 - Applied only to Almond Case 2 - Applied only to Grape
12	**Merced WWTF** Average 6.8 MGD discharges to surface water, including 5.7 MGD directly to agricultural fields	Secondary effluent	Hartley Slough, MUN, AGR, PRO, REC-1, WARM, MIGR, SPWN, WILD	1752.6 acres 7.1 km^2	Since treated water is consumed by agriculture and other consumers, wasn't considered for this study
		Tertiary effluent			
		Disinfected Secondary effluent	Merced Wildlife Management Area REC-2, WARM, WILD		
		Secondary effluent	Land Application Area MUN, AGR, IND, and PRO		
59	**Colvis WWTF** Average 1.7 MGD discharges surface water	Disinfected Tertiary, Municipal Wastewater	Fancher Creek	411.9 acres 1.7 km^2	Case 3- Applied to Almond and Grape together
		Disinfected Tertiary, Municipal Wastewater	Diversion Channel from Big Dry Creek Reservoir to Little Dry Creek		
		Disinfected Tertiary, Municipal Wastewater	Groundwater underlying recycled water use sites		
69	**Malaga WWTF** No longer discharges to surface water. All treated wastewater is sent to land disposal ponds	Disinfected Tertiary-treated Municipal Wastewater	Fresno Irrigation District Central Canal	242.3 acres 0.98 km^2	Since appropriate treated water discharge to an irrigation canal and consumed for irrigation, was not considered for this study
		Un-disinfected Secondary-treated Municipal Wastewater	Groundwater		

Note: PRO- Industrial process supply; REC1- Water contact recreation; REC2- Non-contact water recreation; WILD- Wildlife habitat; MUN- Municipal supply; IND- Industrial service supply; AGR- Agriculture supply; SPWN- Spawning reproduction and/or early development; WARM- Warm freshwater habitat; MIGR- Migration of aquatic organisms

Table 3: Selected HRUs no and area within subbasin 11 and 59. Wastewater was applied to the selected HRUs, marked with grey color.

Subbasin	HRU No	Area (km^2)	
		Almond	Grape
11	357		0.307
	358		0.044
	359		2.836
	360		0.117
	361		4.500
	362		0.214
	363		1.820
	364		0.318
	365		0.048
	366	1.700	
	367	0.057	
	368	0.300	
	369	4.673	
	370	33.132	
	371	1.866	
	372	5.468	
	373	1.533	
	374	0.366	
59	3240		8.546
	3241		0.544
	3242		0.020
	3243	0.353	
	3244	6.709	
	3245	0.403	
	3246	2.492	

Chapter 7: Multi-criteria Decision Analysis to Evaluate Reclaimed Wastewater Use for Agricultural Irrigation: The case study of Maryland

Abstract

Groundwater is the largest source of irrigation for Maryland, which also plays a vital role in the sustainable and healthy aquatic system by supplying water to streams and rivers. However, Maryland's aquifers are experiencing several challenges such as overuse, salt-water intrusion, lack of productive aquifer, etc. The Chesapeake Bay is also facing the problem of water pollution due to pollutant runoff, including fertilizers and pesticides from the agricultural fields. To alleviate the pressure on groundwater and reduce the pollutants loading from the agricultural land it is necessary to explore the potentiality of recycled water for irrigation use. To effectively address this issue, spatial analysis based on optimization methods is needed to evaluate the multiple spatial criteria. The objective of this study is to implement the integration of Geographical Information Systems (GIS) and Multi-Criteria Decision Analysis (MCDA) to evaluate the potentiality of recycled water from wastewater treatment plants (WWTPs) for Maryland state. Evaluation criteria included agricultural lands, water consumption by counties, groundwater wells density, groundwater level, and locations of the WWTPs as a source of recycled water sources. The WWTPs are categorized based on their distances, flows, and treatment process information. The Analytical Hierarchy Process (AHP) approach is used for the prioritization of both qualitative and quantitative data to evaluate decision-making objectives. The study produces realistic agricultural land capability and suitability maps to make it a useful

This chapter will be submitted for publication in *Sustainability*.

tool for integrated regional land-use planning. The results also highlight how the spatial distribution of suitable areas is closely linked to the agricultural land.

1. Introduction

Increasing population and continuous development resulted in increased demands for freshwater in the Mid-Atlantic region. Despite abundant precipitation, water supplies in this region are limited by the intermittent droughts and contamination by agricultural and industrial sources (Masterson et al., 2016). Like other Mid-Atlantic states, groundwater is a vital source of fresh drinking water in Maryland, as well as the main source for irrigation, commercial and industrial uses, and some of the power plants. Groundwater from the confined aquifer is mainly used for domestic purposes including drinking water and public water-supply (Masterson et al., 2016). Groundwater also provides baseflow to streams, rivers, and wetlands and maintain a healthy and sustainable aquatic habitat and ecosystem.

Recently, the Mid-Atlantic region experiencing uncertain rainfall events with a warmer climate during the growing season. Due to more intermittent rainfall and increased evaporation with warmer temperatures, recurrent short-term droughts are becoming more likely to occur during the summer (Boesch, 2008). The climate models projected an increase in the growing season coupled with reductions in soil moisture for this region, which might increase the water demand for crop and landscape irrigation (Boesch, 2008). Therefore, groundwater demand for agricultural irrigation will be increased to maintain high crop production. These changes will require adaptation by Maryland's agricultural industry, including changes in crop varieties and increased irrigation.

Current pumping records indicate that in response to extensive development, intermittent drought conditions and to maintain high crop productivity, irrigation withdrawals are increasing in the region especially in coastal areas. These increased irrigation pumping and higher withdrawals contribute to the decline in water levels in confined aquifers. The long-term observation records from many monitoring wells in the region are showing the declining trend of groundwater table, especially in the coastal plain (Masterson et al., 2016). In addition, Maryland's groundwater system is vulnerable to sea-level rise, especially in the coastal plain where the unconfined surficial aquifers are thin and are not hydraulically connected with the underlying aquifer. Considering all of these issues, regional water resource managers face various challenges to meet local water demands due to increasing rates of groundwater withdrawals, lack of productive aquifers and saltwater intrusion.

Each day billions of gallons of wastewater are generated across the Chesapeake Bay region (CBP, 2020). To safely and effectively treat this large amount of wastewater and to reduce the excess amount of nutrients discharged into the bay, hundreds of treatment facilities in this region are being upgraded with advanced wastewater treatment technologies. As a major state in the Chesapeake Bay region, Maryland is also seeking a sustainable solution to reduce nutrient loading to the Bay. As a result, Maryland's Restoration Fund has provided more than $1.25 billion to upgrade its 67 WWTPs which are expected to reduce 10 million pounds of Nitrogen and 1 million pounds of Phosphorus per year (EPA, 2016).

To overcome these water quantity and quality issues, coupling reclaimed and/or greywater to blue (surface and groundwater) and green water (soil moisture and

evapotranspiration) framework has the potential to significantly improve the water management for the agricultural area (Falkenmark et al., 2004; Rees, 2018).

1.1. Scope and Objectives

Studies have shown that agricultural irrigation with reclaimed wastewater has multiple advantages such as providing high reliability due to constant yields (Chen et al., 2012; Rahman et al., 2016), reducing pressure on freshwater (Jaramillo and Restrepo, 2017; Rahman et al., 2016), improving nutrient management and recovery (Hanjra et al., 2015; Miller-Robbie et al., 2017), etc. In both developed and developing countries, the most established water reuse practice is the application of treated municipal wastewater for irrigation and other purposes (Angelakis et al., 2018a; Jaramillo and Restrepo, 2017). Currently, the water reuse capacity in Maryland is very limited. In Maryland, there are 32 spray irrigation sites of treated wastewater onto land surfaces as one of the alternatives for wastewater disposal. However, the full potential use of Maryland's reclaimed wastewater has not been explored yet considering the water demand-supply zones, spatial distribution of existing crop patterns and treatment facilities, and water reuse regulations. At the same time, understanding how limited freshwater sources have been affected by natural (drought condition) and human stresses (increasing water demand) is key to sustainable management of groundwater sources in Maryland. This situation is also leading to the need for a comprehensive assessment of non-traditional water sources availability for irrigation in Maryland.

The main focus of this study was to outline the critical groundwater zones in and then to identify suitable agricultural areas (hotspots) for reclaimed wastewater use for

irrigation. To generate the agricultural hotspot maps, the main objectives of this study were to: 1) generate a groundwater vulnerability map that crucial for irrigation use, 2) identify the influential criteria for irrigation with reclaimed wastewater; and 3) develop an integrated geospatial Multi-Criteria Decision Analysis (MCDA) framework to identify the agricultural areas that are best suited for recycled water use. The results from this study provide useful information to decision-makers and stakeholders and help them with the development and expansion of reclaimed wastewater use in agriculture.

2. *Methodology and Data*

2.1. Study Area

Maryland is located in the Mid-Atlantic region of the United States. Maryland's climate is classified as humid subtropical with an average annual precipitation of about 45 in/yr (EPA, 2012a). In this region, spring and fall seasons are warm and the winter season is cold with an average annual snowfall of 14.6 in and an average temperature of 38 ^{o}F (3.3 ^{o}C). Summer season is generally hot and humid with an average temperature of 79.2 degrees F (26.2 degrees C). Recently, Maryland is experiencing higher temperatures during winter and heavy precipitation in spring, summer, and fall (Mallakpour and Villarini, 2017).

Maryland can be divided into three regions of western mountainous, Piedmont, and coastal plain (Western and Eastern Shore) (Figure 1). Groundwater in Maryland's coastal plain is derived from rain and snow that falls within the outcrop area of the aquifers (the area where the aquifers reach the surface). These outcrop areas are normally under unconfined conditions and are the principal recharge zones for the

aquifers. Water from rain and snowmelt infiltrates through the soil until it reaches the water table. The saturated zone forms the water-table (or surficial) aquifer and flows slowly towards areas of discharge (streams, rivers, and ponds) and the rest of water to the deep confined aquifer systems. On the other side, most aquifers in Piedmont are unconfined aquifers (also called water-table aquifers) with no overlying impermeable layer to protect groundwater from surface-based sources of contamination.

In the Eastern Shore, where aquifers are unconfined (Columbia or Surficial aquifers) the majority of water withdrawn is used for seasonal irrigation (agriculture) (Andreasen et. al., 2013; MDP, 2019). Most of the shallow unconfined groundwater is discharged to streams or the Bay or through evapotranspiration. Only a very small fraction of the water reaches the deeper aquifers, and as a result, the extreme irrigation practices would have a negative effect on the recharge (Masterson et al., 2016). In addition, if the saturated thickness of a surficial coastal plain aquifer is less than 25-30 feet or so and is underlain by a confining unit, it becomes challenging for a farmer to develop water from shallow on-site wells.

2.2. MCDA Framework

MCDA is a valuable decision analysis tool, being used to explicitly evaluate a large set of alternatives and conflicting criteria in the decision-making process. It provides a systematic approach to structure the decision problems, evaluating the benefit/cost information and decision-maker or stakeholder views to rank the alternatives (Kabir, 2012; Kabir et al., 2014; Paul et al., 2020; Sadiq and Tesfamariam, 2009). In the MCDA process, the required inputs are scored across

several dimensions associated with different alternatives and outcomes; and weights relating to tradeoffs across these dimensions (Huang et al., 2011).

Identification of the agricultural hotspots for water reuse is a spatial decision problem, which needs geospatially based decision analysis involving multiple criteria and sub-criteria. To consider the spatial decision alternatives and evaluation criteria, an integrated framework of the MCDA process with Geographic Information System (GIS-MCDA) has been used in this study. GIS-MCDA method is an emerging approach for the assessment of suitable agricultural land, which considers multiple spatially variable criteria. Worldwide, many studies have applied GIS-MCDA method to achieve the optimal decision-making from multiple spatially variable criteria (Aldababseh et al., 2018; Assefa et al., 2018; Ayalew, 2014; Paul et al., 2020; Rikalovic et al., 2014; Yalew et al., 2016). To develop the GIS-MCDA framework, previously developed method by the research team has been followed with some modifications (Paul et al., 2020). The following subsections describe the decision criteria and sub-criteria in more detail.

2.3. Criteria and Subcriteria Selection

Based on the existing literature, data availability, and expert opinions five main influential criteria as factors and one as a constraint were selected for the assessment of the suitable agricultural land for reclaimed wastewater irrigation. The four selected factor criteria are: 1) agricultural land cover (crop type); 2) reclaimed wastewater sources; 3) water policy: groundwater vulnerability zone; and 4) climate impact: watershed prioritization.

2.3.1. Reclaimed Wastewater Sources

The proximity of the wastewater treatment plants to the agricultural land is the most important criteria to maintain the cost-effectiveness of water reuse in agriculture. In this research, only publicly owned treatment works (POTWs) were considered which are designed to treat the domestic sewage and owned and operated by the local government agencies. Among these POTW facilities, seven discharging methods were selected considering their reuse potential for irrigation, including spray irrigation, reuse: irrigation, land application, overland flow, outfall to surface waters, discharge to groundwater and another facility (Figure 2). While most of the existing spray irrigation sites are close to the WWTPs, there are some spray sites that are 2 to 4 miles away from the facilities. Based on this existing practice, four distance classes were considered. In the next step, selected WWTPs were classified into four categories based on their discharge capacity (Figure 2). Of note is the design capacity of the WWTPs was considered in this study.

To promote the reuse of reclaimed wastewater, the Maryland Department of Environment (MDE) amended a water reuse guideline in 2009 to include the irrigation with highly treated Classes I and II effluent quality. In 2010, a new amendment allowed Class IV water reuse in irrigation for food crops (with no contact with the edible portion of the crop). Based on this, all selected WWTPs were classified into two groups based on their treatment process including advanced and secondary treatment processes (Figure 2).

2.3.2. Agricultural Land

According to MDE guidelines, reclaimed wastewater is prohibited for fruit and vegetable irrigations that are eaten raw and are not commercially processed. Based on the 2010 revised amendments, Class IV water is allowed to reuse for food crop irrigation, especially when there is no contact with the edible portion of the crop (EPA, 2012a). Therefore, two types of crops are selected for recycled water use: Food Crops including grains, legumes, oils and orchard; and Non-food Crops including pasture for foraging livestock, sod farms, commercial crops (Christmas tree).

2.3.3. Water Policy: Groundwater Vulnerability Zone

Groundwater vulnerability zones were generated and assessed to identify the potential of using recycled water for irrigation. The assumption was that the areas that are facing groundwater decline have higher priority for water reuse. To generate the groundwater vulnerability maps, controlling factors like groundwater withdrawals information, geomorphology, aquifer depth, and recharge potential were considered. According to Maryland Code 2005, under Environment Section 5-502 (b)(2)- users need to obtain permit approval for withdrawing an annual daily average of 10,000 gallons per day (GPD) or more. Spatial distribution of the permitted groundwater withdrawal indicated that most of the groundwater well situated on the agricultural land and higher withdrawal amount is allocated in the Coastal Plain Shore. Maryland's Shore also facing saltwater intrusion problems due to lower aquifer depth and climate change. To integrate these issues, the spatial distribution of groundwater well density, water extraction and aquifer information was considered here to generate a groundwater vulnerability map. Groundwater vulnerability zones have

been identified by integrating these factors and classifying them into six categories of very high, high, medium, low, very low and normal in terms of their vulnerability level.

2.3.4. Climate Impact: Watershed Prioritization

To plan for decadal-scale planning and adaptation, decision-makers need to incorporate the information regarding changes in future water supply and demand induced by climate change and economic development in the decision-making system. According to climate projection models, under the higher emissions scenario, summer droughts and heat stresses are expected to increase in the Mid-Atlantic region, which might increase the water demand for crop and landscape irrigation (Boesch 2008). In addition, a higher population and economic development are expected in this region which will increase the water demand in the future. Luck et.al. (2015) developed the worldwide Aqueduct Water Stress projections data including the potential changes of water supply and demand, water stress, and seasonal variability at the HUC4 watershed level. Here, indicators of water supply, water demand (withdrawal and consumptive use), water stress (ratio of water withdrawal to supply), and intra-annual (seasonal) variability were considered for 2040 and under RCP8.5 climate scenarios (Luck et al., 2015). Based on these long-term projections of future water availability, Maryland's watersheds were categorized into five vulnerability classes: extremely high, high, medium-high, low-medium, and low.

2.4. Weighting of Criteria and Sub-criteria

Analytical Hierarchy Process (AHP) (Saaty, 1978) was used to weigh and rank the criteria and sub-criteria. The ranking process developed in Paul et al. (2020) was used in this research. But briefly, the whole process is done in four phases:

i) Formulating Hierarchy: A hierarchical mechanism is used in the AHP technique to organize the complex multi-criteria problem in a number of levels. Within the hierarchy structure, all the criteria and sub-criteria organize according to their importance. In this study, a decision hierarchy structure is articulated into four levels (Figure 3).

ii) Assigning Priorities: The AHP uses pairwise comparisons between the criteria to help decision-makers to evaluate the relative importance with each other. A comparison matrix is established (n x n matrix, where m is the number of criteria) considering the relative importance of each criterion and comparing one-to-one based on pairwise scale. All the criteria were weighed on a scale from 1 to 9 (Table 1).

iii) Weighting Criteria: In the next step, the pairwise comparison matrix is normalized and formed a "normalized matrix". In the normalized matrix, the values of each cell were divided by the total column values from the pairwise comparison matrix. Therefore, each entry of the normalized matrix can be computed as:

$$A_{j\,k} = \frac{a_{jk}}{\sum_{i=1}^{n} a_{j\,k}} \tag{1}$$

iv) Consistency Check: Saaty (1977) also introduced a consistency ratio (CR), which is a comparison between the consistency index and the random consistency index. The consistency ratio (CR) is computed to check the consistency of the conducted comparisons. The CR can be computed as:

$$CR = \frac{CI}{RI} \quad (2)$$

Where CI is the consistency index and RI is the random consistency Index. The consistency index is calculated from the pairwise matrix and estimated as:

$$CI = \frac{\lambda_{max} - n}{n - 1} \quad (3)$$

Where, λ_{max} is the largest eigenvalue of the pairwise comparison matrix and n is the order of the matrix.

For CR ≤ 0.1 or 10%, the judgments are considered as consistent and acceptable, and for CR > 0.1, the subjective judgment needs to be revised or modified.

2.5. Data Collection and Processing

For the GIS-MCDA method spatial data is needed which have spatial extent for the criteria evaluation, the spatial dimension of the decision problem and which can set in the geographical data models. Therefore, all the required data were collected or processed in spatial nature. Six major data types including here: Crop Data Layer (CDL) for land use and land cover (LULC); the location of WWTPs for reclaimed wastewater sources; aquifer and groundwater well permit information for groundwater prioritization map; and watersheds prioritization map for climate criteria.

The groundwater vulnerability map was created based on four components including groundwater wells density, permitted water withdrawal limit, aquifer thickness and aquifer's geological characteristics. The conceptual framework for groundwater vulnerability map assessment is shown in Appendix A. In this study, all the permit information regarding groundwater withdrawal for irrigation use were

collected from the MDE. Well number and average and maximum withdrawal information per tax map were integrated to generate the groundwater withdrawal heat map. A digital map produced by the USGS was used here that is showing the thickness of the surficial aquifer of Maryland (Denver and Nardi, 2016). Based on the aquifer maps collected from the Maryland Geological Survey (MGS), critical zones for groundwater extraction were identified. This aquifer map was used to identify the critical zone for reclaimed wastewater use. This layer displays the location of the outcrop and subcrop regions beneath the Surficial and Surficial Upland aquifers. Here, outcrop areas were generated by intersecting the aquifer and confining unit surfaces with land surface and bathymetry that means the top of the aquifer is the water table. Subcrop areas were generated by intersecting the aquifer and confining unit surfaces with the bottoms the Surficial and Surficial Upland aquifers that means this aquifer is situated under a blanket of surficial sediments. A complete list of datasets that were used in this study is provided in Table 2.

2.6. GIS Model Setup

The process of a suitability assessment and identifying hotspots for reclaimed wastewater use involves two main steps. In the first step, the MCDA method was applied using the AHP technique to evaluate the influential geospatial decision criteria and sub-criteria. In the second step, a GIS-MCDA model was developed using the weights and ranking of the criteria resulted from the previous step. In the GIS-MCDA method, a spatial decision is defined as a single raster of a specified size or a combination of multiple rasters. The normalized weights attributed to each criterion

were used to derive new raster datasets. In order to derive AHP values, the new raster files were incorporated into the following equation implemented in map algebra:

$$Suitability\ Map = W_{RWS} * RWS + W_{AL} * AL + W_{GVZ} * GVZ + W_{WP} * WP \quad (4)$$

Where, $W_{RWS,}$ $W_{AL,}$ $W_{GVZ,}$ and W_{WP} are the weight of Recycled Water Source (RWS), Agricultural Land (AL), Groundwater Vulnerability Zone (GVZ) and Watershed Prioritization (WP) respectively.

After the data collection, data were analyzed and evaluated using GIS and geo-statistical tools to obtain the MCDA criteria maps. Each selected sub-criterion was represented by a thematic layer that was assigned with the values according to Table 3. After that, each main criterion or thematic layer was converted into a raster format. All of the raster data then processed using a weighted overlay tool to identify the most suitable areas for irrigation with reclaimed wastewater (hotspots). In the end, all of the generated suitability maps was represented in six suitability levels including "very high" to "not suitable" respectively.

3. Results and Discussion

3.1. Criteria Evaluation

3.1.1. Reclaimed wastewater Sources

In this study, three proximity maps were produced for the three cases: Case 1- all WWTPs with acceptable discharge methods; Case 2- WWTPs categorized with flow volume; and Case 3- WWTPs considering the treatment processes. Based on CWNS 2012 and MDE databases total of 279 WWTPs were selected in the study area (Figure 4). According to the Clean Water Act, the projected flow was recorded for 195 out of 279 WWTPs. The database also completed with projected treated effluent

information. Projected treatment discharge information was documented for 140 facilities where 101 facilities have the advanced treatment and 39 have secondary treatment processes. Of note is all of large facilities (>10 MGD) are situated near the fall line where the urban areas are clustered and agricultural lands are minimal (Figure 4). Fig 5a shows the reclassified Euclidean distance map of the reclaimed wastewater sources considering all acceptable discharge methods.

3.1.2. Agricultural Land

The agricultural lands were reclassified into two classes of agriculture with food crops and non-food crops respectively. The highest priority was assigned to non-food crops such as fodder, oil, and commercial crops (sod farms, nursery, christmas trees, etc.). Based on the Maryland water reuse guideline, another class was selected for all suitable food crops such as grains, legumes & orchards which irrigation water doesn't have direct contact with the edible portion of the crop. From the reclassified maps (Fig 5b), it is found that most of the agricultural land is clustered in two regions of piedmont and Eastern Shore. Most food-crop farms (corn and soybean) are clustered in the Eastern Shore, and non-food crops like forage crops (alfalfa and hay/non-alfalfa) are clustered in the Piedmont region. In addition, orchards (apple and peaches) and commercial farms (Christmas tree) are scattered in the Piedmont region, which has high potentiality for reclaimed wastewater use.

3.1.3. Groundwater Vulnerability Zone

For effective water-resources planning, the cumulative impact of thousands of wells pumping on Maryland's aquifer is crucial. The State of Maryland controls its surface and groundwater uses to conserve, manage, and protect the State's water

resources. As a result, MDE processes a water appropriation permit application for surface or groundwater withdrawal. Total of 1354 (out of 1471) permitted wells, extracting water from groundwater aquifers to use for different types of irrigation practices, such as crop irrigation, nursery/sod farming irrigation, golf course or park irrigation etc. Most of the wells are used for crop irrigation, from which the average permitted discharge is <0.5 MGD (500,000 GPD) (Appendix B). They are mainly clustered in the Eastern Shore due to higher agricultural activities (Appendix C).

Most of the shallow unconfined groundwater is discharged to streams or the Bay or lost through evapotranspiration and a very small fraction is recharged to the deeper aquifers. Shallow groundwater zones in the outcrop or subcrop areas have quick recharge properties which also concern as potential conduits for contamination (Appendix C). Therefore, these zones are considered unsuitable for drinking water use and more preferable for agricultural irrigation. There was limited GIS data for the aquifers in the western side of the fall line, however, geologically deeper confined aquifers are situated in this region. Since deeper confined aquifers should be reserved for drinking water supply. In addition, deep pumping results in high energy costs. Therefore, this region was given higher priority for recycled water use for irrigation.

The produced groundwater basin prioritization map shows that low lying flat plain of the Eastern Shore is found more favorable for recycled water use, whereas upland plain of the western part is given as less priority for recycled water use. The highest priority zones consist of 814.5 km^2 and were mainly outlined to the Eastern Shore. The low (17,247 km^2) and very low priority (55,976 km^2) were mapped to the

western part of Maryland due to the insignificant well use and position for outcrop and subcrop area (Figure 5c).

3.1.4. Watershed Prioritization

Maryland's watersheds were classified based on their water stress severity and local climate conditions using the method described before (section 2.3.4). Based on this, watersheds were categorized into Very High, High, Medium, Low, Very low, and Normal watersheds according to water stress severity. For instance, the Patapsco River basin is expected to experience "very high" water stress by 2040 and "high" water stress in Gunpowder-Patapsco near the Chesapeake Bay and Chincoteague Bay near the Atlantic Ocean (Figure 5d). Watersheds were assigned different scores according to their water stress ranks, in which watersheds with the higher potentiality for water stress received the highest priority for reclaimed wastewater use in agriculture.

3.2. Criteria Ranking and AHP Assessment

The weights of each criterion and sub-criterion were assigned based on the rationale described in the previous section 3.1. In this study, three matrices were designed for three cases: 1) all WWTPs with acceptable discharge methods (Case 1-Table 4), 2) WWTPs categorized with flow volume (Case 2-Table 5), and 3) WWTPs considering the treatment processes (Case 3-Table 6).

From the normalized matrix, the final priorities were obtained, which are indicated as "Weights" and "Ranks". Thus, the final AHP outputs are: (i) a relative priority of each criterion presented in percentages, and (ii) a relative rank of each

criterion (Table 4-6). Table 4-6 shows all three pair-wise comparison matrices between all evaluating criteria as well as between their classes/categories.

From the pairwise matrix, it is evident that the location of WWTPs and their proximity to the point of use are very important factors in the decision process. Thus, the proximity to WWTPs, with a weight of 55.6%, has the most important influence on agricultural land suitability for reclaimed wastewater use. Agricultural land close to WWTPs or downstream of treatment plants can get easier access to reclaimed wastewater compared to areas that are further from the treatment plants or are located upstream. In terms of normalized weights, land use (25.9%) ranked the second, being followed by GW basin prioritization (17.2%), and watershed prioritization (4.9%). Similarly, the highest weights (33.4%) found for the larger facilities (>10 MGD) in Case-2 and 51.3% for the advanced treatment facilities in Case-3. The final CR values for all three matrices were checked and found to be 8.8%, 9.2% and 5.3%, for Case 1, 2, and 3 respectively.

3.3. Suitability Maps

3.3.1. Case 1: Considering selected discharging methods

Case 1 was constituted to assess the accessibility of each WWTP from the nearest agricultural land. Therefore, the generated suitability maps show the most suitable agricultural areas that are in close proximity to the WWTPs. The suitability maps indicate that the suitability of the agriculture irrigation with reclaimed wastewater influenced mainly by the proximity to the WWTP facilities (Figure 6a). The resulted suitability area categorized into five classes including very high suitable to low suitable classes (Figure 6). Based on the final weights (Table 4), the very high

suitable class constitutes only 1.2% (66.17 km^2) of the total agricultural area and the high, moderate and low suitable class constitutes 48.8% (2711.14 km^2), 42.6% (2354.73 km^2), and 6.6% (364.05 km^2) respectively. The "very high" suitable areas are clustered at the Eastern Shore and northwest of the Piedmont region where most of the agricultural lands are located (Figure 4 and 6a). Although most of the WWTPs are in the northeast Piedmont region, most of the grain crops (such as corn, soybean etc.) are clustered at the Eastern Shore. Thus, "very high" and "high" suitability found mostly on the Eastern Shore and near the Atlantic Ocean, where more agricultural lands are located within close proximity to wastewater treatment facilities.

Since there is no significant agricultural activity near large urban areas with large WWTP facilities (Figure 4), urban agriculture could be another potential use for reclaimed wastewater. Urban agriculture was out of the scope of this research but could be an option to put the reclaimed wastewater from large facilities into beneficial use. In addition, only POTW-WWTPs that treats the domestic sewages were considered as the primary source to obtain treated recycled water for irrigation. The other non-POTW facilities could be additional sources of reclaimed wastewater for irrigation that often treat wastewater from industries, such as manufacturing, food processing and beverage production activities. Due to the difficulty of finding effluent information and permit requirements, non-POTW facilities were not included in this study.

3.3.2. Case 2: Considering potential discharge capacity

Case 2 was established to evaluate the suitability in terms of flow where agricultural areas close to the large WWTPs were given the higher priority. Most of

the larger WWTPs are located near the fall line (Figure 4) where most of the urban areas are located and agricultural lands are minimal. Thus, agricultural areas within close proximity to WWTPs are limited, and "very high" suitable agricultural land was not found (Figure 6b). As a result, only 0.15 km^2 of the agricultural land comprises as "high" suitable, and 30.72 km^2 as a "moderate" category. Most of the WWTPs with low capacity (<1 MGD) is located on the Eastern Shore which resulted in the highest 2,268.38 km^2 (41%) agricultural lands as "very low" suitable category. Approximate 50.9% of the total agricultural land found as non-suitable for recycled water use. In Maryland, most of the permitted well are using less than 0.5 MGD water to irrigate (Appendix B). In that case, adjusted flow classes with a lower range could produce a more comprehensive suitability map in this GIS-MCDA framework. For example, the reclaimed wastewater from medium and small facilities might not be sufficient for large agricultural lands but could be used as supplemental irrigation water for smaller farms.

3.3.3. Case 3: Considering appropriate treatment process

In the next phase, the last suitability map was generated based on Case 3, which includes the treatment process of WWTPs (Figure 6c). According to Maryland's water reuse guideline, recycled water from WWTPs with advanced treatment process is given the priority for all non-food crops and selected food-crops which edible portion doesn't have direct contact with irrigated water. As a result, projected effluent information (treatment process) was collected from the CWNS factsheet and included for suitability analysis. Result shows that, "very high" agricultural areas compromise

34.97 km^2 (0.63%), "high" areas comprise 749.23 km^2 (13.5%) and moderate 1,818.16 km^2 (32.9%) of the total agricultural areas.

Since Maryland has a guideline for water reuse that only recommends the irrigation of food crops where there is no contact with the edible portion of the crop, vegetables and fruits were not included here for the suitability analysis. However, if the regulation is updated in the future then under this decision framework the "very high" suitable area can be increased to 35 km^2, "high" to 751.5 km^2 and "moderate" to 1828.17 km^2 of the total agricultural land.

3.3.4. Composite final map

In the final phase, the composite model was generated to evaluate the suitability of treated water for agricultural irrigation considering availability, capacity, and appropriateness of the treated flow from municipal WWTPs. Thus, the composite suitability map was generated by the two models: Case2 and Case 3. Several hotspots generated within the states with "high" to "very low" suitability index, mostly in western Maryland, western Piedmont, and Eastern Shore (Figure 7). The AHP model mapped 0.5% (26.4 km^2) and 14.44% (798.8 km^2) of the study area as high and moderate suitable areas, respectively. The area of low and very low suitability classes is 45.99%, and 34.1% of the total agricultural area, respectively. Overall, high and moderate suitability classes were clustered in the western region, central Piedmont and the Eastern Shore of Maryland. There are some patches of high and moderate classes in the central part of the western shore where large facilities are located. Another cluster of moderate to low suitability areas is formed along the Atlantic Ocean of the Eastern Shore.

It should be noted that the selection of alternative criteria (different flow category or proximity limit) and suitability indicators (different users) and/or assigning different weights to them could result in different outcomes from the model. For instance, by modifying the regulations (i.e., permitting vegetable irrigation) the "high" suitable area can be increased by 0.01 km^2 (3.21 acres), "moderate" by 2.05 km^2 (506.57) and "low" by 14.23 km^2 (3516.31 acres).

4. Conclusion

In this study, a decision-making framework was defined to evaluate the suitable agricultural land for recycled water use considering wastewater treatment facilities appropriateness (treated effluent volume and quality). The main objective of this study was to demonstrate the application of GIS-MCDA based land suitability evaluation method to solve this spatial problem. The main advantage of the applied GIS-MCDA method is a combination of multiple agricultural, environmental, geographical, and climate criteria within the same land selection framework. It has the ability to define spatial models with specified priorities, classifications, and scenarios to support decision-makers and stakeholders.

The developed decision framework and workflow used in this study will offer a statewide guideline for the decision-makers to adopt and promote the recycled water use for agricultural irrigation. This study is the first of its kind in Maryland to define a set of findings that will determine where large-scale recycled water use for agricultural irrigation is recommended.

5. *Figures*

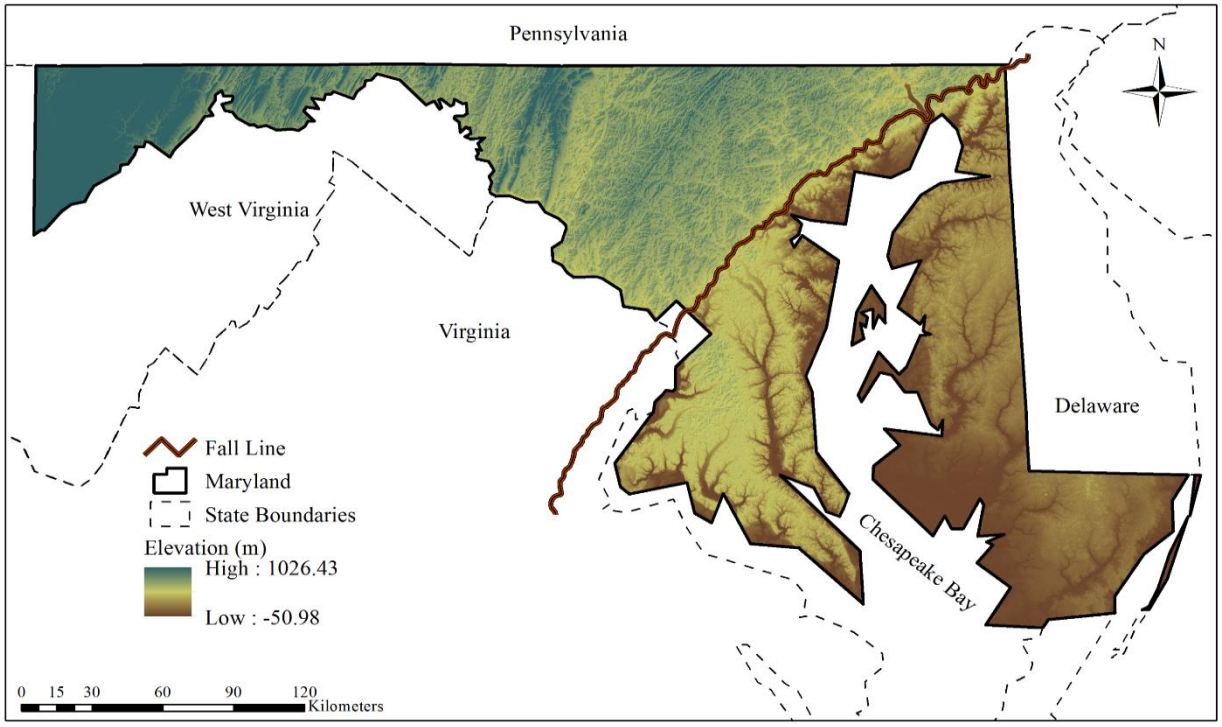

Figure 1: Location of the study area.

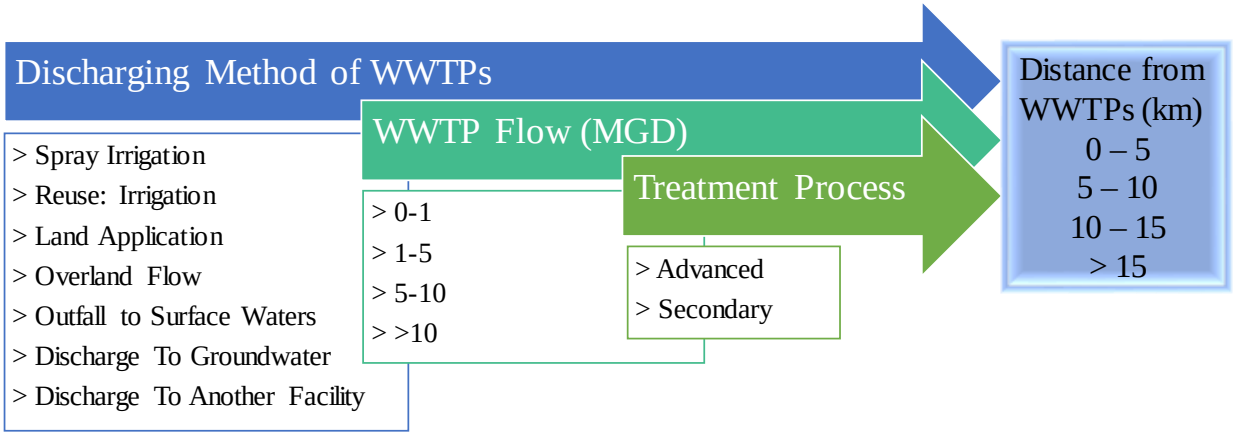

Figure 2: Three-stage classification process for wastewater treatment plants (adapted from Paul et. al., 2020).

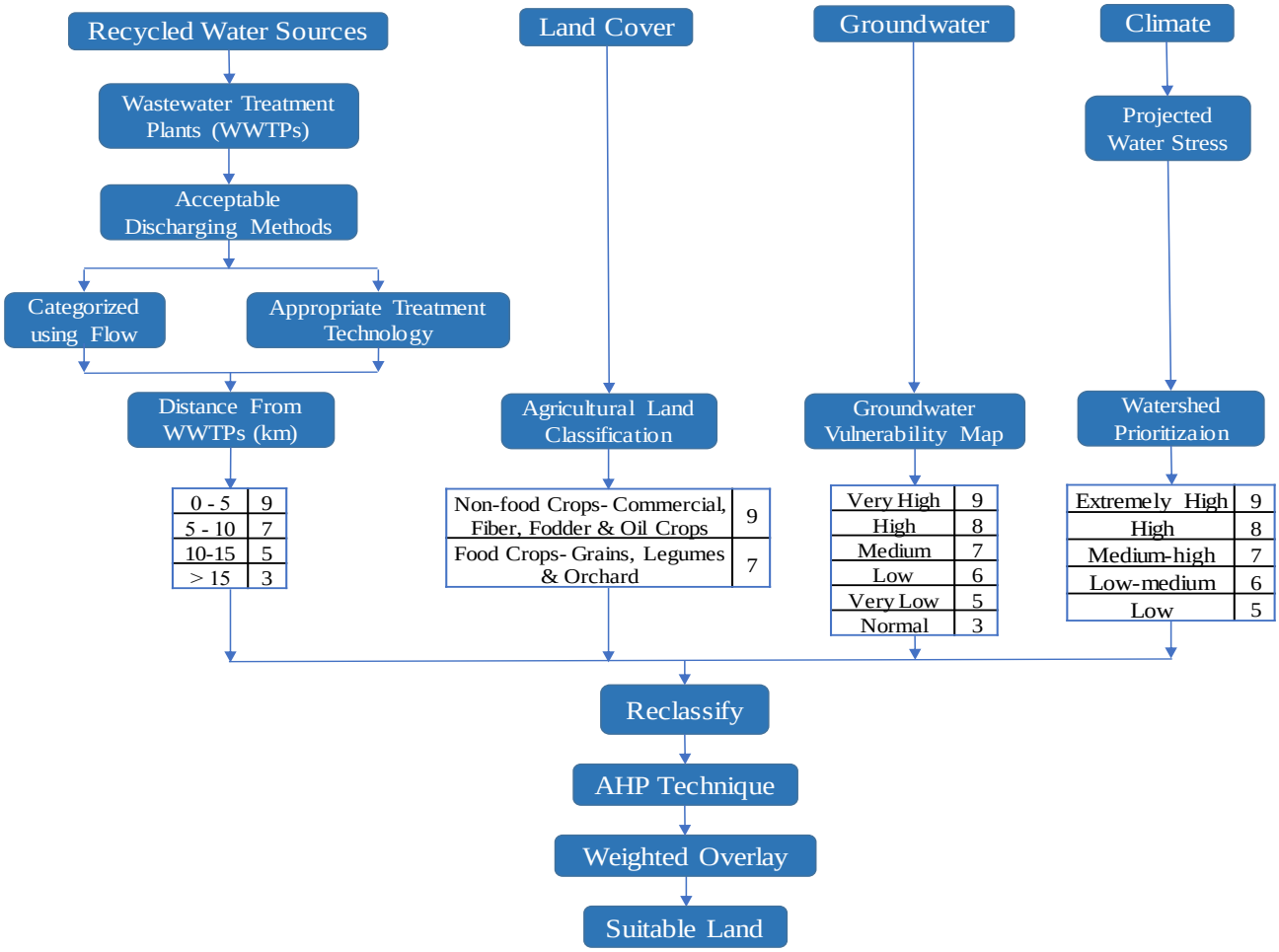

Figure 3: Developed decision hierarchy for the evaluation of suitable agricultural land for irrigation with recycled water.

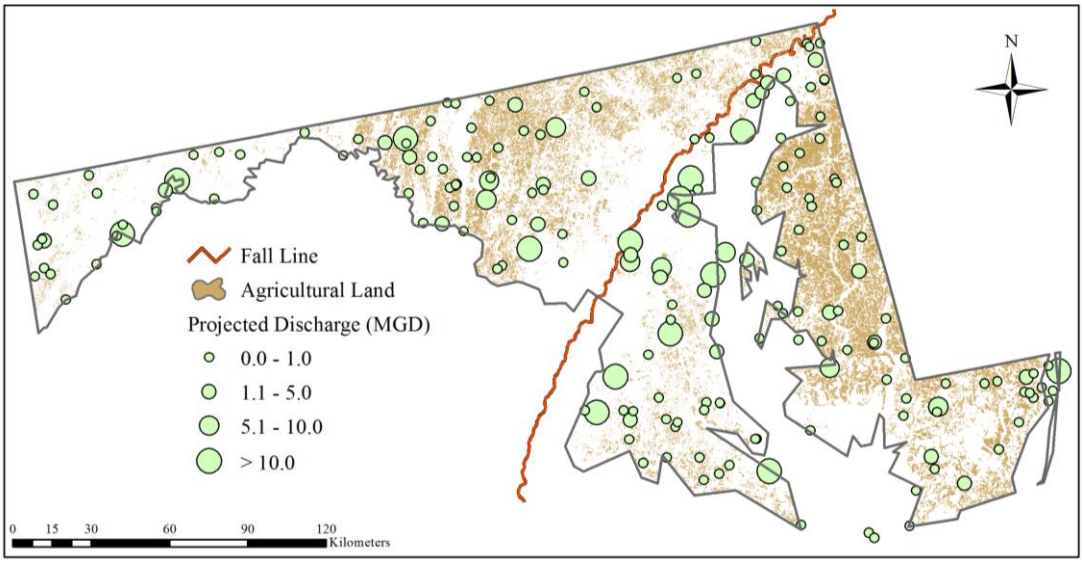

Figure 4: Location of all selected WWTPs within Maryland

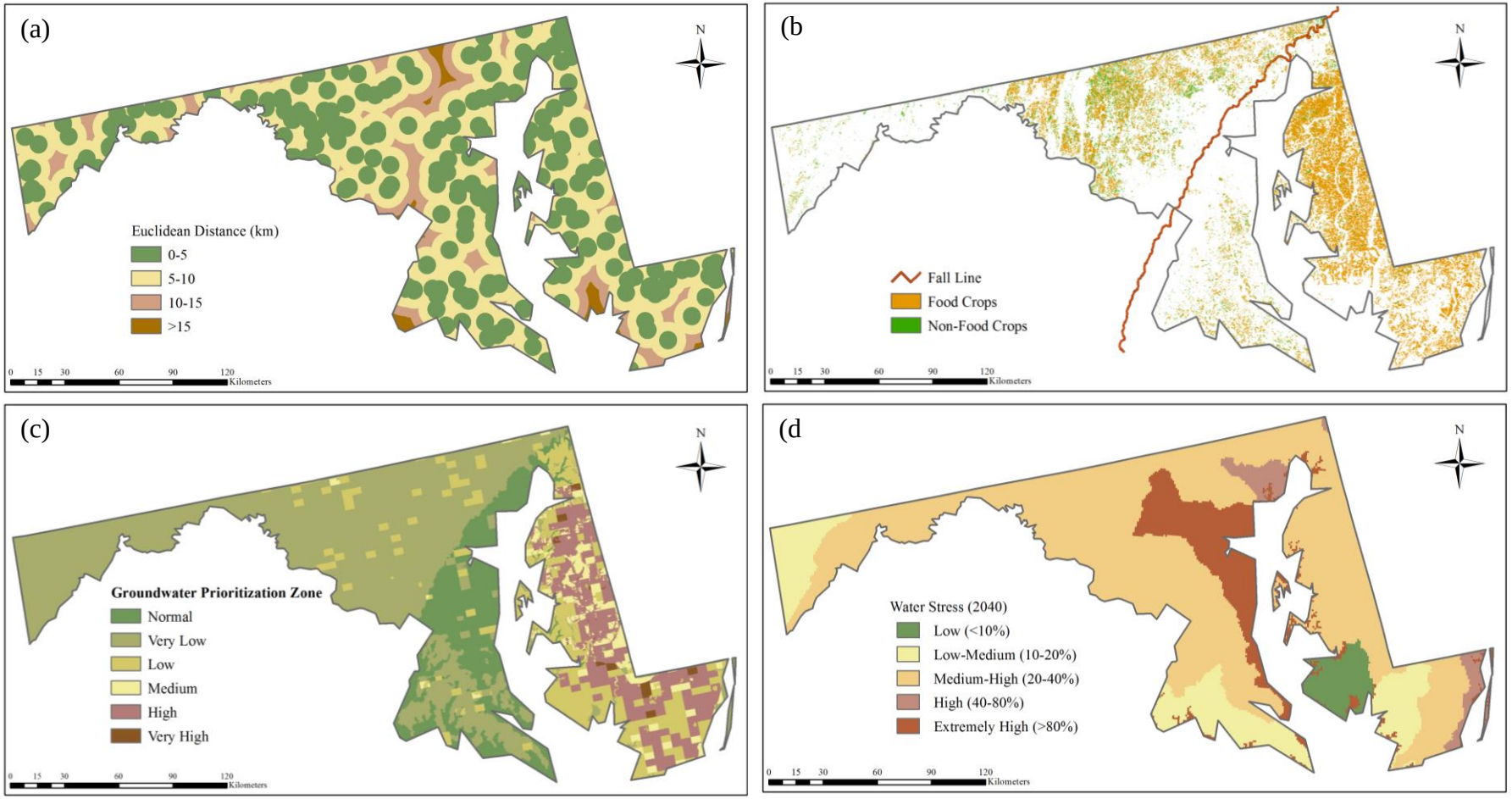

Figure 5: Reclassified maps of the influential criteria: a) distance of WWTPs, b) agricultural land, c) groundwater vulnerability, and d) climate.

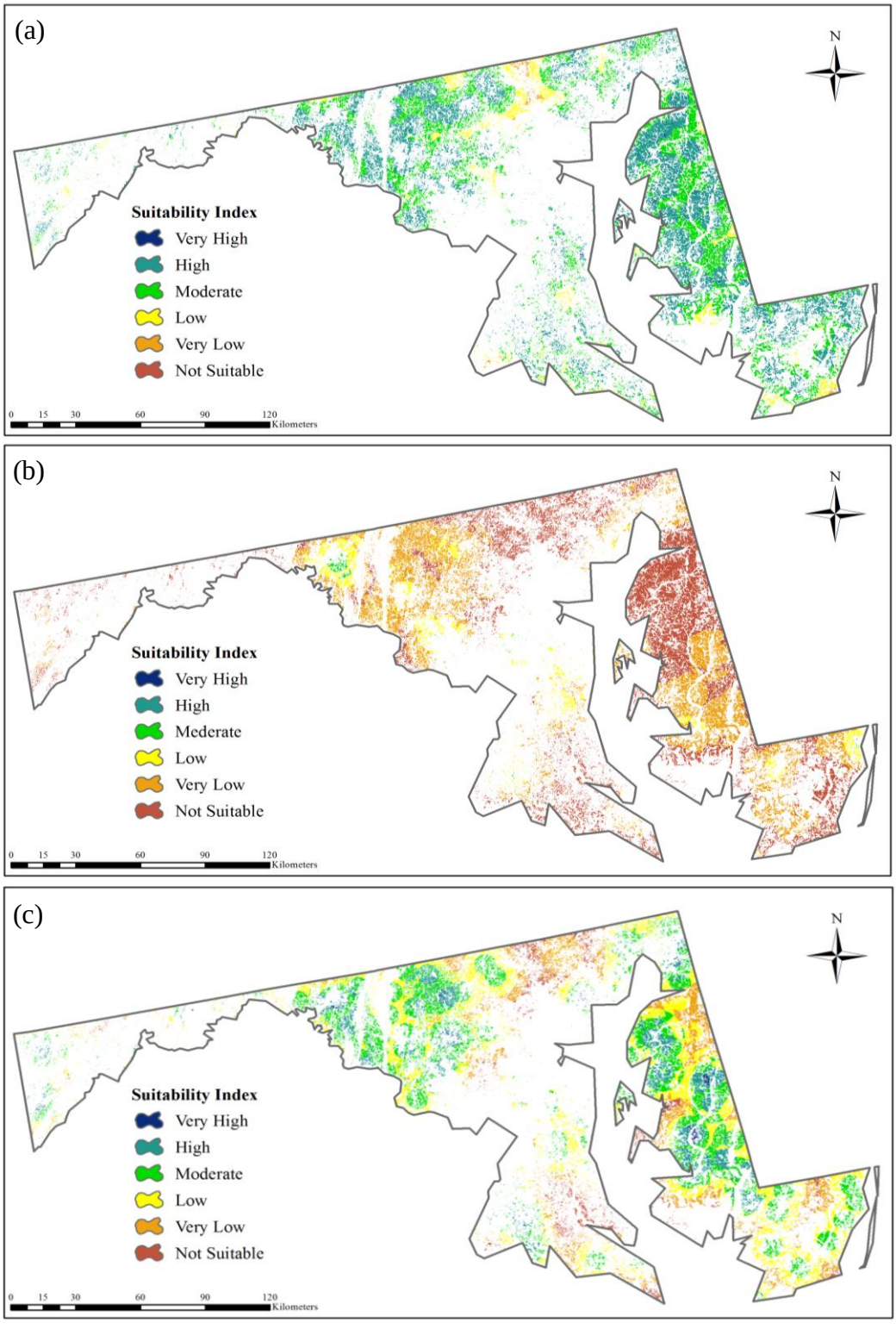

Figure 6: Suitability Map for three cases: a) Case 1: considering selected discharging methods; b) Case 2: considering potential discharge capacity; and c) Case 3: considering appropriate treatment process.

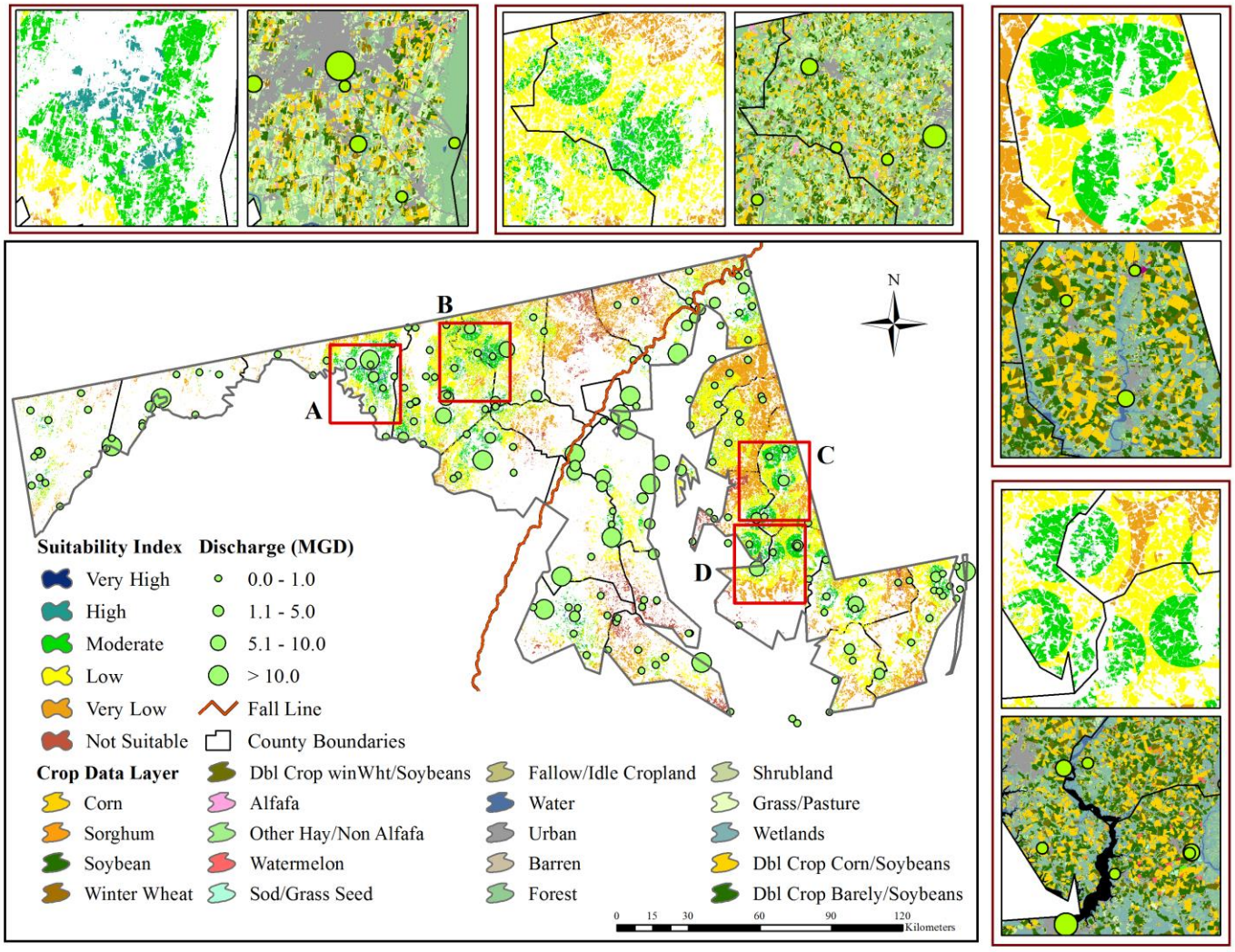

Figure 7: The composite suitability map showing the hotspot of the suitable agricultural lands ranging from “high” to “very low” index for recycled water irrigation. Four clustered suitability zones are showing with existing crops pattern in the boxes.

6. *Tables*

Table 1: Saaty's (1978) nine-point pairwise scale and definition to assign a weight to the criteria.

Intensity of Importance	Definition
1	Equal Importance
3	Weak Importance
5	Strong Importance
7	Very Strong Importance
9	Extremely Importance
2, 4, 6, and 8	Intermediate Values Between Adjacent Scale Values

Table 2: List of datasets used in this study.

Criteria	**Data Type**	**Data Source**
Wastewater Treatment Plants (WWTPs)	Location and discharge information of the facilities	https://www.epa.gov/cwns
	Projected flow and treatment information of the facilities	https://www.epa.gov/npdes https://mde.maryland.gov/Pages/index.aspx
Land Cover	Location and types of crops	https://nassgeodata.gmu.edu/CropScape/
Groundwater	Permitted well information	https://mde.maryland.gov/Pages/index.aspx
	Geological information of aquifer	http://www.mgs.md.gov/groundwater/index.html
	Surficial aquifer thickness map	https://www.usgs.gov/media/images/thickness-surficial-aquifer-sediments-delmarva-peninsula-md
Climate	Aqueduct water stress projections data	https://www.wri.org/resources/data-sets/aqueduct-water-stress-projections-data

Table 3: The list of main criteria and sub-criteria threshold used in the GIS-MCDA model.

Criteria- Thematic Layer	Sub criteria- Feature Class	Rank
Agricultural Land	Non-food Crops- Commercial, Fiber, Fodder & Oil Crops	9
	Food Crops- Grains, Legumes & Orchard	7
Distance from WWTP (km)	0 - 5	9
	5 - 10	7
	10 - 15	5
	>15	3
Groundwater Basin Prioritization	Very High	9
	High	8
	Medium	7
	Low	6
	Very Low	5
	Normal	3
Watershed Prioritizations	Very High	9
	High	8
	Medium	7
	Low	6
	Very Low	5

Table 4: Pairwise matrix for the decision criteria for Case 1: considering selected discharging methods.

	Proximity to WWTPs	Agricultural Land Cover	GW Basin Prioritization	Watershed Prioritization	Weights	Rank	CR
Proximity to WWTPs	1.00	3.00	5.00	7.00	55.6%	1	
Agricultural Land Cover	0.33	1.00	3.00	5.00	25.9%	2	
GW Basin Prioritization	0.20	0.25	1.00	5.00	13.6%	3	8.8%
Watershed Prioritization	0.14	0.20	0.20	1.00	4.9%	4	

Table 5: Pairwise matrix for the decision criteria for Case 2: considering potential discharge capacity.

	Proximity to WWTPs				Agricultural Land Cover	Watershed Prioritization	GW Basin Prioritization	Weights	Rank	CR
	Flow>15	5≤Flow≤15	1≤Flow≤5	Flow<1						
Flow>15	1.00	2.00	3.00	4.00	5.00	7.00	8.00	33.4%	1	
5≤Flow<15	0.50	1.00	2.00	3.00	5.00	7.00	8.00	24.3%	2	
1≤Flow<5	0.33	0.50	1.00	2.00	5.00	7.00	8.00	18.1%	3	
Flow<1	0.25	0.33	0.50	1.00	3.00	5.00	7.00	11.6%	4	
Agricultural Land Cover	0.20	0.20	0.20	0.33	1.00	5.00	5.00	7.0%	5	9.2%
GW Basin Prioritization	0.14	0.14	0.14	0.20	0.20	1.00	5.00	3.6%	6	
Watershed Prioritization	0.12	0.12	0.12	0.14	0.20	0.20	1.00	2.0%	7	

Table 6: Pairwise matrix for the decision criteria for Case 2: considering the appropriate treatment process.

	Proximity to WWTPs		Agricultural Land Cover	GW Basin Prioritization	Watershed Prioritization	Weights	Rank	CR
	Advanced Treatment	Secondary Treatment						
Advanced Treatment	1.00	3.00	5.00	7.00	9.00	51.3%	1	
Secondary Treatment	0.33	1.00	3.00	5.00	7.00	26.2%	2	
Agricultural Land Cover	0.20	0.33	1.00	3.00	5.00	12.9%	3	5.3%
GW Basin Prioritization	0.14	0.20	0.33	1.00	3.00	6.3%	4	
Watershed Prioritization	0.11	0.14	0.20	0.33	1.00	3.3%	5	

Appendix A

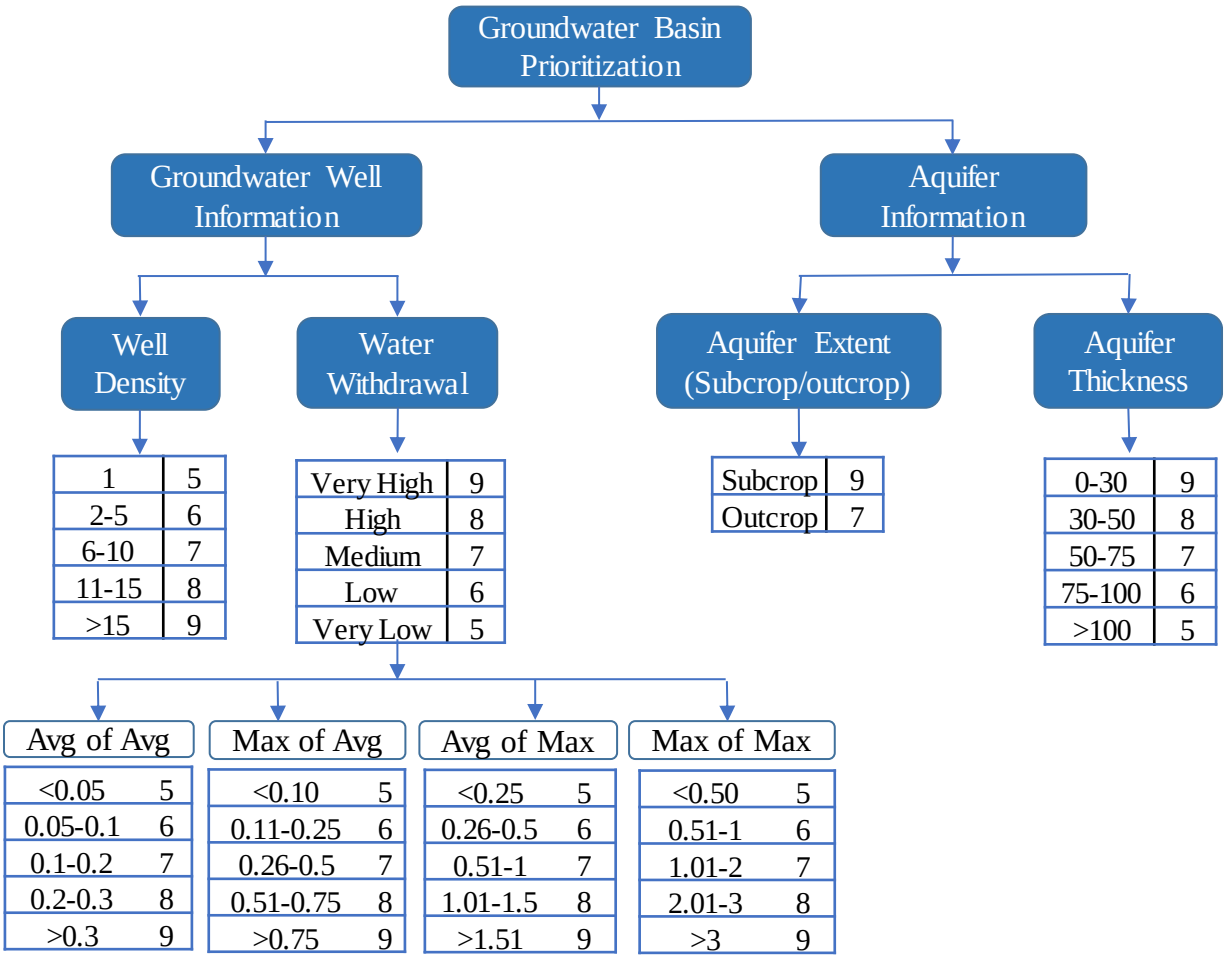

Appendix B:

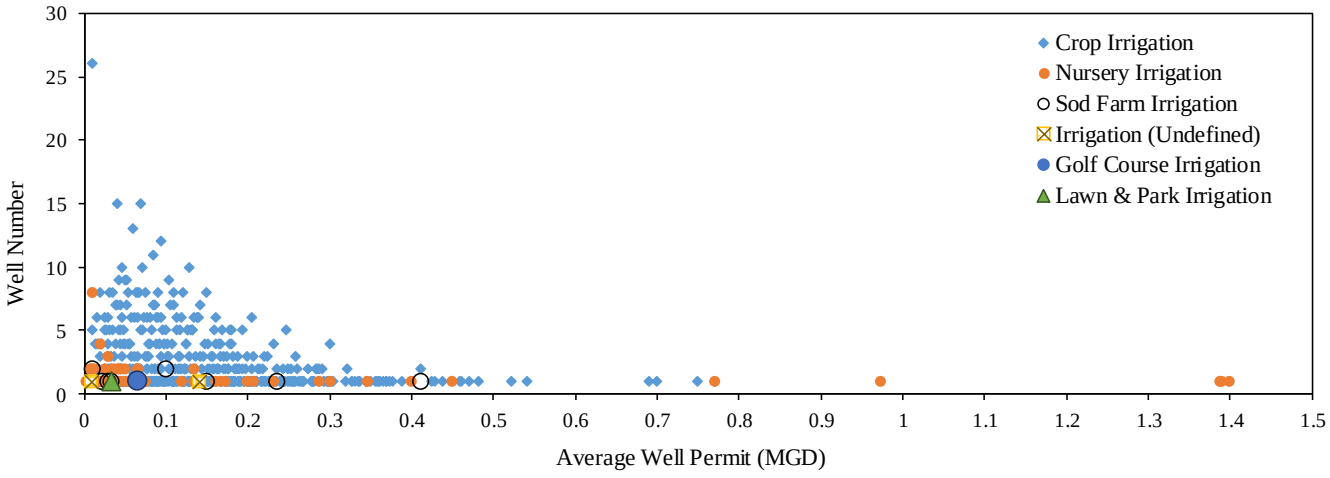

Appendix C:

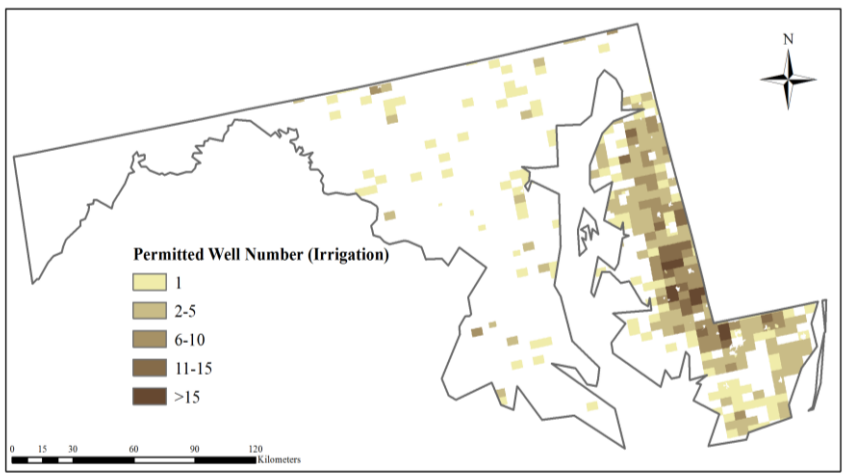
N
Permitted Well Number (Irrigation)
1
2-5
6-10
11-15
>15
0 15 30 60 90 120
Kilometers

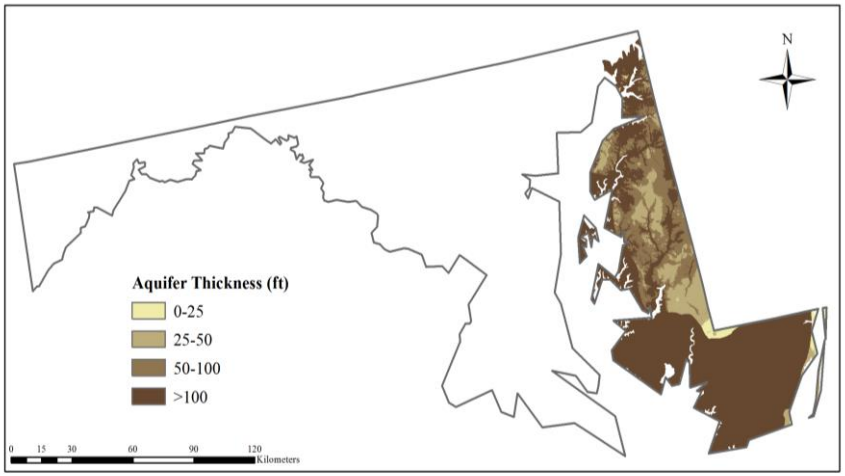
N
Aquifer Thickness (ft)
0-25
25-50
50-100
>100
0 15 30 60 90 120
Kilometers

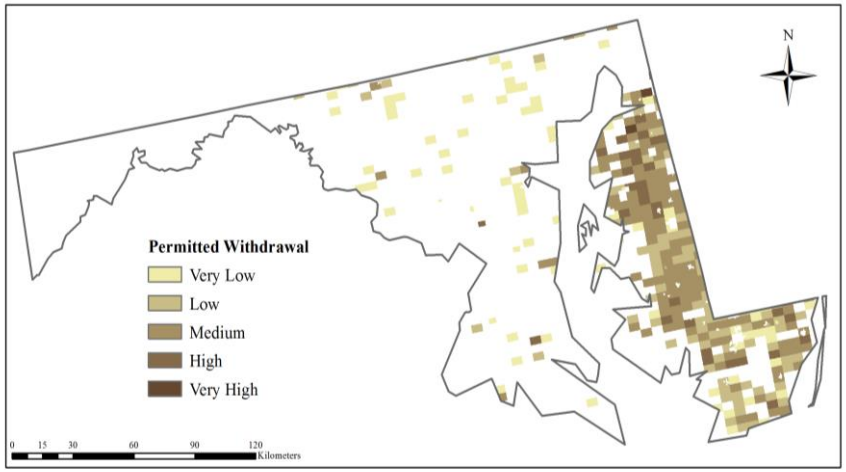
N
Permitted Withdrawal
Very Low
Low
Medium
High
Very High
0 15 30 60 90 120
Kilometers

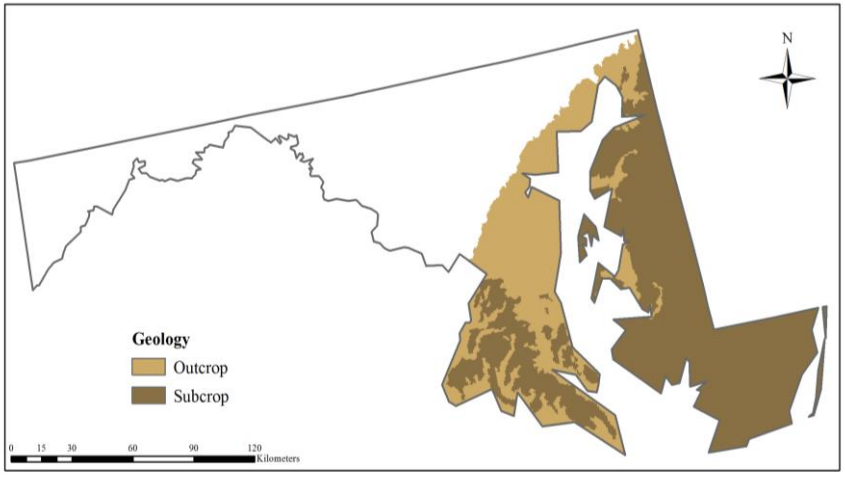
N
Geology
Outcrop
Subcrop
0 15 30 60 90 120
Kilometers

Chapter 8: Evaluating Crop Water Productivity Using a Hydrological Model for Monocacy River Watershed, Maryland

Abstract

Providing efficient water use will ensure sustained crop yields and water saving. However, water productivity is often excluded from policy discussions. The water productivity is a useful index that assesses agricultural water use efficiency. The main objective of this study was to assess crop water productivity from different irrigation sources using the hydrological process in Monocacy River Watershed (MRW), in Maryland. For this purpose, the Soil and Water Assessment Tool (SWAT) was used to simulate the watershed hydrology. The model was calibrated using a sequential uncertainty fitting (SUFI-2) algorithm for 10 years (2005-2014) with a 5 years' warm-up period and validated for another 5 years (2015-2019). For the monthly streamflow simulations, the correlation coefficient (R^2), Nash-Sutcliffe coefficients (NSE), and percent bias (PBIAS) were found with values of 0.0.61, 0.56, and 10.3% during calibration and 0.85, 0.83, and 3.9% during validation respectively. After streamflow calibration, the model was calibrated and validated for crop yield (corn and soybean). The calibrated model was used to estimate the corn and soybean water productivity using different irrigation sources, including treated wastewater from adjacent WWTP. Simulated crop water productivities for corn and soybean were estimated as 0.617 kg/m^3 and 0.173 kg/m^3, respectively. Analysis suggests that maximization of the area by provision of supplemental irrigation from treated wastewater can provide opportunities for improving water productivity. The

This chapter will be submitted for publication in *Water Resources Planning and Management*

outcomes of this study will provide information regarding enhancing water management in the MRW, especially in those areas where crop productivity is low.

1. Introduction

Maryland state uses 97% of its freshwater withdrawals to meet the growing intersectoral demands for hydropower, industry, agriculture, and drinking water supplies (Wheeler, 2003). Despite the rapid urbanization and population growth, over the years, the total water consumption in Maryland has not increased (Boesch, 2008; Wheeler, 2003). However, a complex set of changes in water consumption among different sectors, such as industrial and commercial use, declined over the years while domestic use, public supply, and irrigation use significantly increased. This water demand is expected to rise in the future with increasing suburban land development that affecting the groundwater recharge area and increasing irrigation needs on agricultural land during summer droughts (Boesch, 2008).

In recent years the Mid-Atlantic region experiencing intermittent rainfall with higher temperatures, especially during the growing season. As a result, recurrent short-term droughts are becoming more frequent, and the evaporation rate increased during the summer. Researchers projected more increase in temperature and less summer precipitation in this region. According to the Intergovernmental Panel on Climate Change (IPCC) estimation, average temperatures might increase from 1.34 to 5.78 ºC before 2100 with moderate precipitation increase compared to baseline conditions ((CBF), 2007). Despite moderate increases in precipitation, a higher temperature may lead to more evaporation loss and a decrease in soil moisture (Boesch, 2008). As a result of reductions in soil moisture, this region is expected to

experience more water demand for crop irrigation (CBF, 2007; Boesch, 2008). It is predicted that within the 2040 decade, the Mid-Atlantic USA might experience medium to high water stress driven by high water demand (Luck et al., 2015). The water permit database in the state of Maryland, located in the Mid-Atlantic, indicated that.

Currently, the agricultural sector consumed a high amount of groundwater to meet increased crop water demand due to intermittent precipitation and warmer climate. Historical data indicated that the amount of groundwater withdrawal increased in those years when annual average precipitation was below the normal (838.2-1397 mm) during the growing season (Wheeler, 2003).

The alternatives for freshwater demand reduction during summer exist; however, they have not been fully explored yet in this region. For Maryland, water resource management should focus on a reduction of freshwater water consumption to minimize groundwater withdrawals. This can be achieved by using treated wastewater from the adjacent wastewater treatment plant (WWTP) for irrigation to increase water productivity due to its constant reliability.

Improving the water management should focus on (a) increasing the production per unit of freshwater consumed (water productivity), or (b) maintaining the production with reduced water use or increasing efficiency (Immerzeel et al., 2008). Therefore, the water resource managers and policymakers need to have a better knowledge of freshwater consumption and crop production patterns throughout the watershed.

Generally, water management practices focus on water saving at field scale by reducing irrigation water allocation to the plots. However, a plot level water saving is not enough to get the significant improvement of water use efficiency at the watershed scale (Immerzeel et al., 2008; Keller and Keller, 1995). Few studies found where researchers analyzed the water stress and crop water productivity under different water managements using both field experiments and watershed modelling (Garg et al., 2012; Han et al., 2018; Luan et al., 2018). These studies provided evidence of using water productivity as a useful tool to evaluate the performance of agricultural production systems and recommend best management practices (BMPs) at any scale, ranging from field to watershed.

With this background, this study aimed to apply a systematic approach to assess the agricultural water use and crop yield at fine temporal and spatial resolution to estimate water productivity for a Maryland watershed. To obtain this goal, a distributed hydrological model was used to evaluate the water use efficiency of irrigated areas and provide information for the improvement of freshwater-saving in these areas. The main objectives were: i) to calibrate and validate the model for watershed streamflow and crop yield considering both rainfed and irrigated systems, ii) to assess the spatial and temporal variability of crop consumptive water use (irrigation) at a subbasin level, and iii) to calculate crop water productivity from the model simulation, and iv) to provide the information of treated wastewater use potentiality for future policy implications.

2. *Data and Methodology*

2.1. Study Area

The Monocacy River Watershed (MRW) was selected as a representation of Maryland, USA. MRW is a tributary of the Potomac River Basin and located in western Maryland and south-central Pennsylvania (Figure 1). This watershed is situated within three counties: Frederick and Carroll Counties in Maryland and Adams County in Pennsylvania. According to the long-term average (1901-2001), in Maryland, annual average precipitation was about 1092.2 mm (43 in/yr), or 25,000 MGD (million gallons per day), where water lost by evapotranspiration was about 711 mm (28 in/yr) or 17,000 MGD (NOAA, 2002). The average temperature of this region is approximately 24ºC during the summer and 3ºC during the winter (CCBRM), 2016). Based on the current climate data (2005-2014), the average annual precipitation is approximately 1135 mm, with monthly averages ranging from 72.2 to 122.1 mm. In this region, most of the rainfall event occurs in May-July and September-October, and snow accumulation occurs in December to January.

The MRW is in the Western Piedmont physiographic province where the sub-surface of the watershed consists of a layer of unconsolidated material or composed of soil, clay, sand, and pieces of weathered bedrock. The west side of the watershed is characterized by steep slopes consisted of highly erodible soil and the rest of the valley is mainly constituting prime agricultural soils. The watershed is dominated by C soil group (46.48%) which have low infiltration rates followed by A (23.21%) and B (23.51%) soil groups with high and moderate infiltration rates, respectively.

The land use and land cover of MRW is dominated by agricultural land (51.1%), followed by forested (36.2%), and urban areas (12.1%) (USDA-NASS, 2007). In agricultural land, the most prominent crops are hay (14.5%), corn (13.1%), and soybean (10.8%) (Table 1). Among these crops, irrigation mainly used for corn to maintain high yield goals (Lewis, 2014). Over the years, land acreage for corn and soybean are varied due to suburban expansion. Figure 2 gives an overview of the MRW's historical corn and soybean yield and planted acreage for the last 30 years. It is clear that despite a slight decrease in planted acreage, the corn yields increase considerably. On the other hand, soybean acreage and yield both increases in 30 years; however, increasing trend for soybean production is very mild compared to corn.

2.2. SWAT Model

The process-based models are often used for accurate simulation for the hydrological process and crop yield of the watershed. In this study, the Soil and Water Assessment Tool (SWAT) was used to assess the MRW hydrology and crop yield and calculate the water productivity from the model simulations.

During model development, the watershed is divided into a number of sub-basins and categorized into hydrological response units (HRUs) based on homogeneous soil types, land-use types, and slope classes. SWAT model computes the hydrological process and crop yield at HRU that allow for a high level of spatially detailed simulations. The SWAT model uses a water balance equation to estimate the different water balance components of water resources (e.g., blue and green waters) at both the subbasin and the HRU level (Neitsch et al., 2011). Blue water includes water flows

through or below the land surface and stored in lakes, reservoirs, and aquifers, and green water includes the portion of precipitation that infiltrates and is stored as soil moisture and then returns to the atmosphere via transpiration and evaporation.

2.3. Model Setup

2.3.1. Model Input and Data Collection

SWAT requires elevation, land use, soil, and climate data (i.e., precipitation and temperature) to simulate the hydrological processes of the watershed. The required input data were collected as follows: Digital Elevation Model (DEM) from USGS National Elevation Dataset (USGS, 2006), land use data from the 2018 Crop data Layer (CDL) (USDA-NASS, 2007), and soil data from State Soil Geographic Data (STATSGO). Daily climate data, precipitation, and maximum and minimum temperature data for 19 years (2001-2019) were collected from the National Climatic Data Center (NCDC). For streamflow simulation, the observed monthly streamflow data were collected for19 years (2001-2019).

Total of 29 subbasins was delineated for MRW, and 1294 HRUs were defined with 2-5-5% thresholds for land use-soil-slope. The watershed was delineated, defining the watershed outlet for USGS 01643000, located at the Jug bridge near Fredrick, Maryland (Figure 1). The hydrological process including evapotranspiration, surface runoff, and the channel routing were computed based on the Penman-Monteith (Monteith, 1965), the modified Soil Conservation Service (SCS) Curve Number (CN) method (Neitsch et al., 2011), and the Muskingum routing methods (Arnold et al., 1998), respectively.

2.3.2. Crop management

For the study purpose, for two major crops, corn and soybean were selected for the evaluation of water reuse potentiality. In western Maryland, planting and harvesting date for corn depends on the number of variables and change from year to year. For example, corn is generally planted end of April through mid-May, and soybean is planted in May. Fertilizer amount is also dependent on the soil condition and varies from field to field. However, nitrogen is applied to corn-based on the targeted yield goal. For example, for 200 bushels/acre of corn, around 200 lbs/acre of nitrogen is applied. After observing the 35 years crop yield trend, it was noticeable that crop yield varied from 65-175 bushels/acre, and more than 150 bushels/acre was observed in the last 8 years. Thus, on average, 150 lbs/acre nitrogen was applied in the study. Harvesting date was fixed after 120 days of growing days suggested by Maryland Cooperative Extension (Lewis, 2014).

2.3.3. Parameter Selection and Streamflow Calibration

Based on a literature review of the existing studies on adjacent regions (Chu et al., 2005; Sadeghi et al., 2007; Sexton et al., 2011; Sexton et al., 2010), total 17 parameters were selected for model calibration (Table 2). The initial ranges of the parameters were defined based on the suggestions from the SWAT 2012 manual (Arnold et al., 2012). Sequential Uncertainty Fitting (SUFI-2) algorithm on SWAT-CUP (SWAT Calibration and Uncertainty Programs) was used for model calibration and validation process (Abbaspour, 2008). The model was calibrated for 10 years (2005-2014), with a 4-year warm-up period and was validated for another 5 years

(2015-2019). Model performance was evaluated based on the evaluation matrix described on the (Moriasi et al., 2015).

2.3.4. Crop yield Calibration

After streamflow calibration and validation, the SWAT model was calibrated and validated for annual corn and soybean yield. Observed crop yields were collected for 2005–2019 from the USDA National Agricultural Statistics Service (USDA-NASS). NASS reported the grain crop yields at the county level and in bushels/ac unit. However, SWAT estimates the crop yield at the HRU scale and presents in kg/ha with 20% moisture content at harvest time (Srinivasan et al., 2010). Thus, crop yields were estimated in kg/ha following the method used in Srinivasan et al., (2010). For crop yield simulation evaluation, Percent Bias (PBIAS) and Root Mean Square Error (RMSE) were used as the evaluation criteria. For crop yield calibration, five sensitive crop yield parameters related to harvest and leaf area were selected based on the literature review (Lee et al., 2018; Palazzoli et al., 2015; Uniyal et al., 2019).

2.4. Scenarios Analysis

On the western side of the Chesapeake Bay, there is very little irrigation so all crops are defined as rainfed. So, at the beginning model was run with rainfed irrigation condition and crop yield was assessed for this scenario. Although frequent irrigation practices are evident in Eastern Shore, according to the MDE water permit database, several groundwater wells assigned for crop irrigation are identified within this watershed. Irrigation amount, timing and frequency are determined by the farmers based on the weather conditions, soil moisture and growth stage.

Therefore, three scenarios were developed in this study to understand the impact on water productivity (WP):

Scenario 1: Model run with the rainfed condition.

Scenario 2: Model run with "auto irrigation" from the shallow aquifer was assigned as a source of irrigation, which is required for each HRU. Here, an automatic irrigation event is triggered based on a plant-stress threshold.

Scenario 3: Model run with updated management files considering irrigation source "outside" of the watershed. This scenario developed considering treated wastewater reuse for irrigation purposes to match the expected high crop yield. Modified scenarios were applied for selected HRUs computing maximized irrigated areas based on WWTP capacity.

The WP was calculated for each HRU using SWAT simulated crop yield, and the irrigation amount was used to calculate WP (kg/m^3). To understand the impact of freshwater consumption (irrigation with groundwater) and treated wastewater use on crop water productivity (WP) (kg/m^3) two indices were calculated:

$$WP_{IP} = \frac{Crop\ yiled\ (kg)}{Irrigation\ (m^3) + Effective\ Rainfall(m^3)} \quad (1)$$

$$WP_P = \frac{Crop\ yiled\ (kg)}{Effective\ Rainfall(m^3)} \quad (2)$$

Here, WP_{IP} can be defined as total crop water productivity, consists of both rainfall and irrigation during the crop growth period. On the other hand, WP_P can be defined as green water (rainfall) productivity, where the volume of precipitation consumed during the crop growth period (Luan et al., 2018). The assumption of WP_P

was that for additional irrigation water demand, freshwater withdrawal would be replaced by the unlimited treated wastewater from nearby WWTP.

3. *Results and Discussion*

3.1. Streamflow

SWAT model was calibrated and validated for both irrigation and rainfed management conditions, and the very minimal difference was found between these two simulations. SWAT model was able to capture the observed monthly streamflow during both calibration and validation periods (Figure 3). During calibration periods (2005-2014), the scores of the goodness of fit R^2, NSE, KGE, and PBIAS were 0.61, 0.56, 0.60, and 10.32%, respectively, and categorized as "satisfactory" (Moriasi et al., 2015; Paul and Negahban-Azar, 2018). Average monthly streamflow was well estimated during validation periods (2015-2019) with high R^2, NSE, KGE, and PBIAS values of 0.85, 0.83, 0.79, and 3.92%, respectively. Thus, the high values of NSE ($\geq$0.80) and PBIAS ($\leq\pm$5%) values indicate a "very good" correlation between daily observed and simulated flows and R^2 (>0.75) and KGE ($\geq$0.75) demonstrated a "good" agreement between these. Continuous daily climate data were available after 2008 for all climate stations (Figure 1). This data quality resulted in better model performances with higher scores of the goodness of fit indices during the validation period.

3.2. Crop Yield

Table 3 is showing the adjustment of the parameters for crop yield calibration. Very few parameter modifications were needed to match the observed corn and soybean yield. As mentioned in section 2.4, the model was simulated for both rainfed

and irrigation management. Table 4 showed that the model with irrigation application was able to capture both corn and soybean yield well. Thus, outcomes from this model were considered as a baseline for the analysis.

Figure 4 is showing the comparison between observed and simulated crop yields for calibration (2005-2014) and validation (2015-2019) periods. During calibration, the simulated average crop yields for corn (7817.3 kg/ha) and soybean (2282.3 kg/ha) were higher than the observed yield, 6553.9 kg/ha, and 2123.5 kg/ha for corn and soybean, respectively. As a result, during calibration, the RMSE for corn and soybean was 1596.8 kg/ha and 373.2 kg/ha, respectively. However, the simulated corn and soybean yield during validation was closer to observed data with a smaller relative yield reduction of 8.78% and 6.23%, respectively. Thus, RMSE was much lower during validation than the calibration period, 610.4 kg/ha, and 191.3 kg/ha for corn and soybean, respectively. The relative yield reduction for corn and soybean indicates that the SWAT model overestimated the crop yield during calibration and underestimated during the validation period (Table 3). This result also indicates that applied auto irrigation with a defined fertilizer amount was able to capture recent crop management well.

3.3. Irrigation Requirement

In Maryland, irrigation needs are varied from year to year that depends on rainfall. Based on the SWAT model, the average irrigation for a growing season was simulated as 5.24 mm/ha (0.51 acre-ft) for corn and 6.88 mm/ha (0.65 acre-ft) for soybean production. Within the simulation periods, four dry years (2005, 2007, 2010, and 2013) were selected to estimate the required irrigation demands for corn and

soybean production. Figure 5 shows the applied irrigation amount for corn and soybean production at the HRU scale. Irrigation amount was varied with the HRUs and also differed year to year (Figure 5). However, it was noticeable that the south-eastern part of the watershed required a higher amount of irrigation compared to the other region.

It is estimated that for high yield goal (200 bushels/acre), 15 inches of seasonal water might need, which resulted in an annual average of 128,666 GPD water withdrawal. It is noted that, for more than 10,000 GPD, farmers required Maryland water permit from MDE. Even with zero rain and dry summer may have required up to 25 acre-inches (27,154 gallons) of water to maintain the expected corn production. Based on this, the simulated irrigation amount was much lower than the field application. It is also noted that for more than 10,000 GPD water use Maryland farmers required water permits from MDE.

Within MRW, 18 publicly owned WWTPs are selected, which have high water reuse potentiality with a discharge capacity from 0.04 to 6.5 MGD (Figure 6 and Table 5). All the WWTPs are almost uniformly distributed within the watershed. In this study, only publicly owned WWTPs were considered to wastewater reuse for irrigation. Required irrigation water for 120 growing days was calculated for each crop, and the detailed estimation is presented in Table 5. Since it was difficult to identify the exact amount of irrigation for specific lands, 10 km buffer zones were created from each WWTP to locate the potential corn and soybean acreage.

3.4. Water Productivity

Water productivity for both indices, $WP_{IP,}$ and WP_P, was estimated based on model simulated crop yield and irrigation amount. All the analysis was done at HRU scale and for the 2005-2014 period. Total water productivity (rainfall and irrigation) varied across crops. The estimated WP_{IP} for the corn was relatively high compared to soybean. During 2005-2014, the average irrigation water productivity for corn and soybean found as 0.617 kg/m^3 and 0.173 kg/m^3, respectively. Under the recycled water use scenario, the green water productivity (only rainfall) improved up to 0.713 kg/m^3 for corn and 0.37 kg/m^3 for soybean.

For a better understanding of irrigation use during dry years, four dry years were selected from the (2005-2014) time period. Subbasin scale spatial variability of the corn and soybean water productivity are shown in Figure 7. From Figure 7, it is clear that the distribution of WP_{IP} and WP_P was different for each year. The water productivity of total water consumption (rainfall and irrigation) varied across crops. In MRW, WP_{IP} for both corn and soybean were higher on the western side of the watershed.

The green water productivity (only rainfall) also varied across crops. From Figure 7, it is clear that the overall distribution of the WP_P of corn and soybean was higher on those subbasins where precipitation amount was lower. Again, higher productivity estimated for 2007 when average annual precipitation was much lower (906.6 mm) than in other years. For this year, the largest green water productivity for corn (>0.95 kg/m^3) and soybean (>0.3 kg/m^3) found in southern subbasins where precipitation was lower than 800 mm. Thus, it was clear that instead of groundwater, the treated

wastewater uses for irrigation resulted in higher $WP_{P,}$ especially where the rainfall amount was low.

4. Conclusion

In this study, a quantitative method for computing the crop productivity for corn and soybean was established based on a distributed hydrological model (SWAT). The results demonstrated that the SWAT could be a useful tool in calculating water productivity at the watershed scale. The water productivities for corn and soybean have spatial variability within subbasins, which mainly influenced by precipitation variability. The overall distribution of the total and green water productivity showed that treated wastewater use for crop irrigation has a higher potentiality to increase water use efficiency compared to the baseline condition (groundwater use). The results from this study can be used to assess the water consumption volumes by water source and type. Another important outcome is the SWAT model is able to calculate water productivity both at subbasin and HRU scale rather than the administrative or political boundary (e.g., county). This could be useful for agricultural water managers to manage and allocate freshwater resources within the region properly.

5. *Figures*

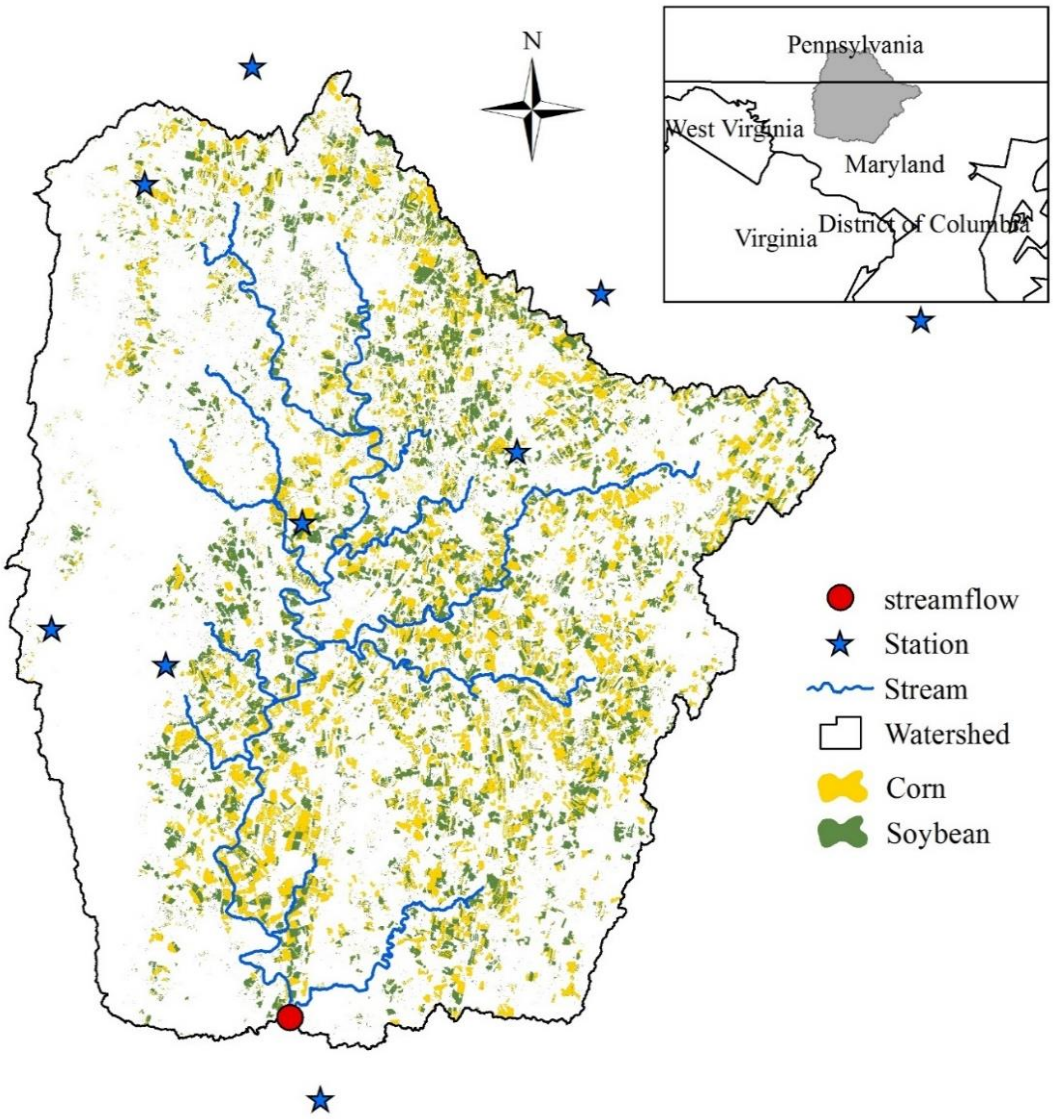

Figure 1: Location of Monocacy River Watershed.

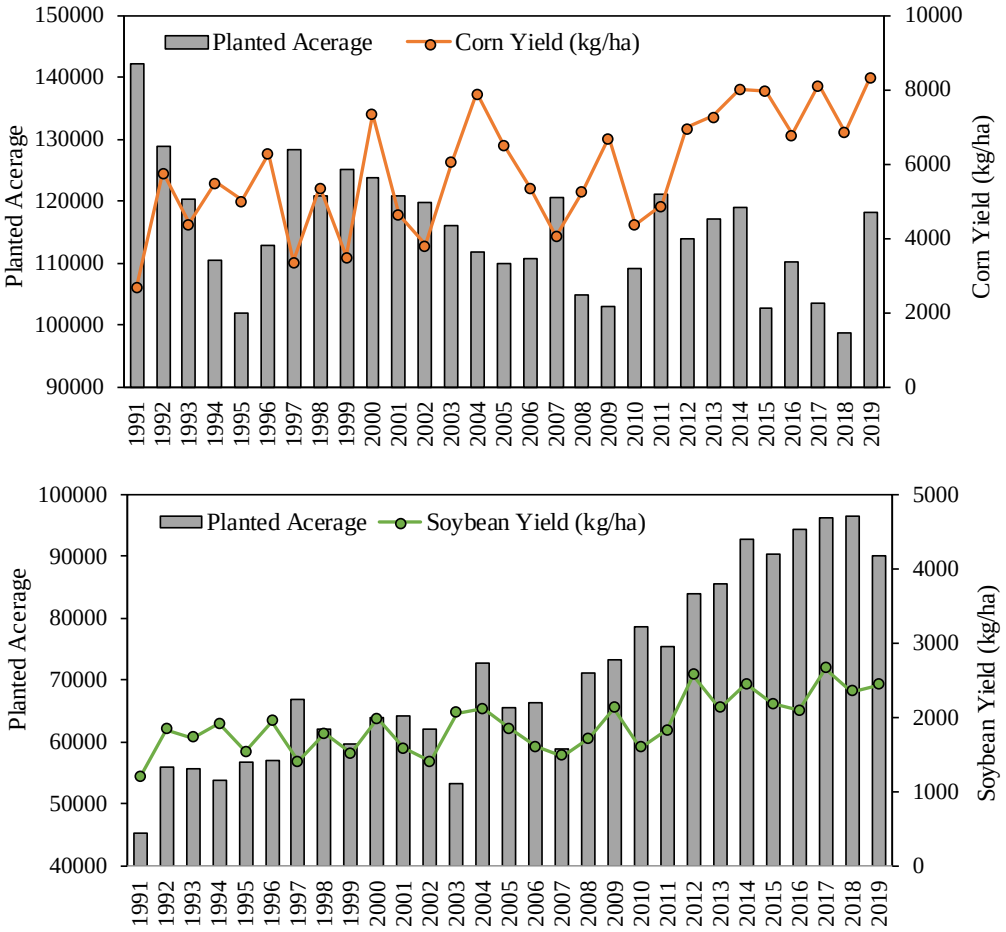

Figure 2: Historical crop yield and planted acreage for (a) corn, and (b) soybean. Data collected from USDA-NASS for 29 years (1991-2019).

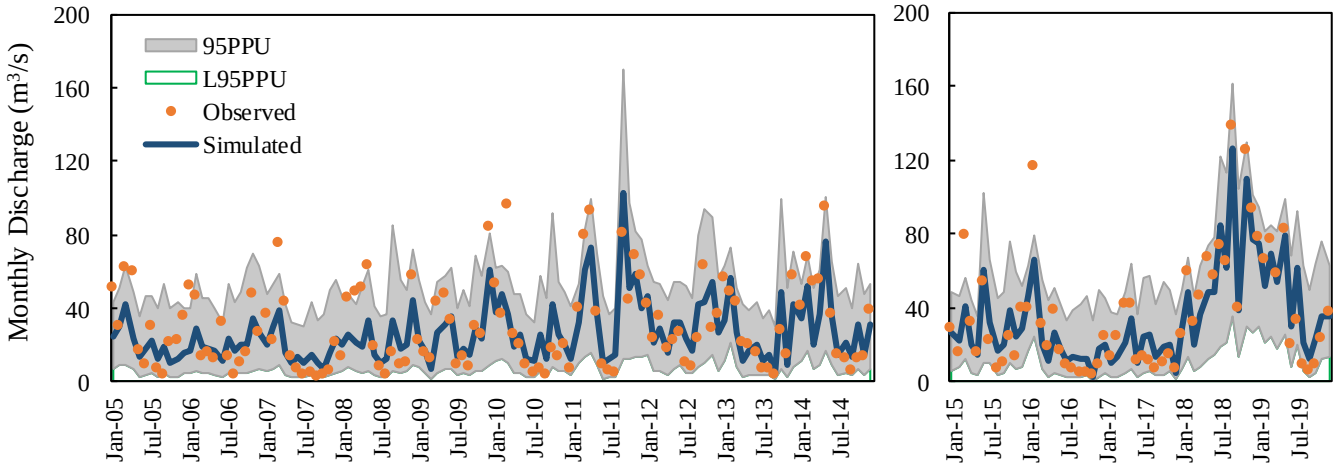

Figure 3: The hydrograph of average monthly observed and simulated discharge during a) calibration (2005-2014) and b) validation (2015-2019).

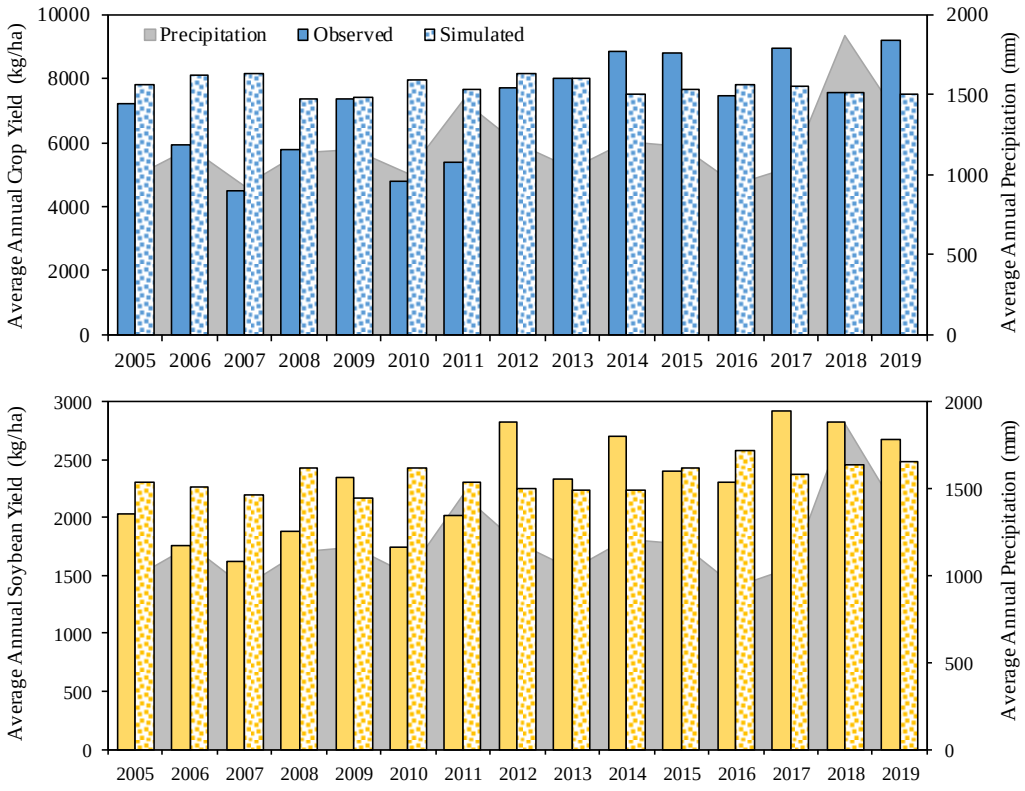

Figure 4: Comparison of observed (NASS) and simulated (SWAT) crop yield for corn (i) and soybean (ii) for the (a) calibration (2005-2014) and (b) validation (2015-2019) period.

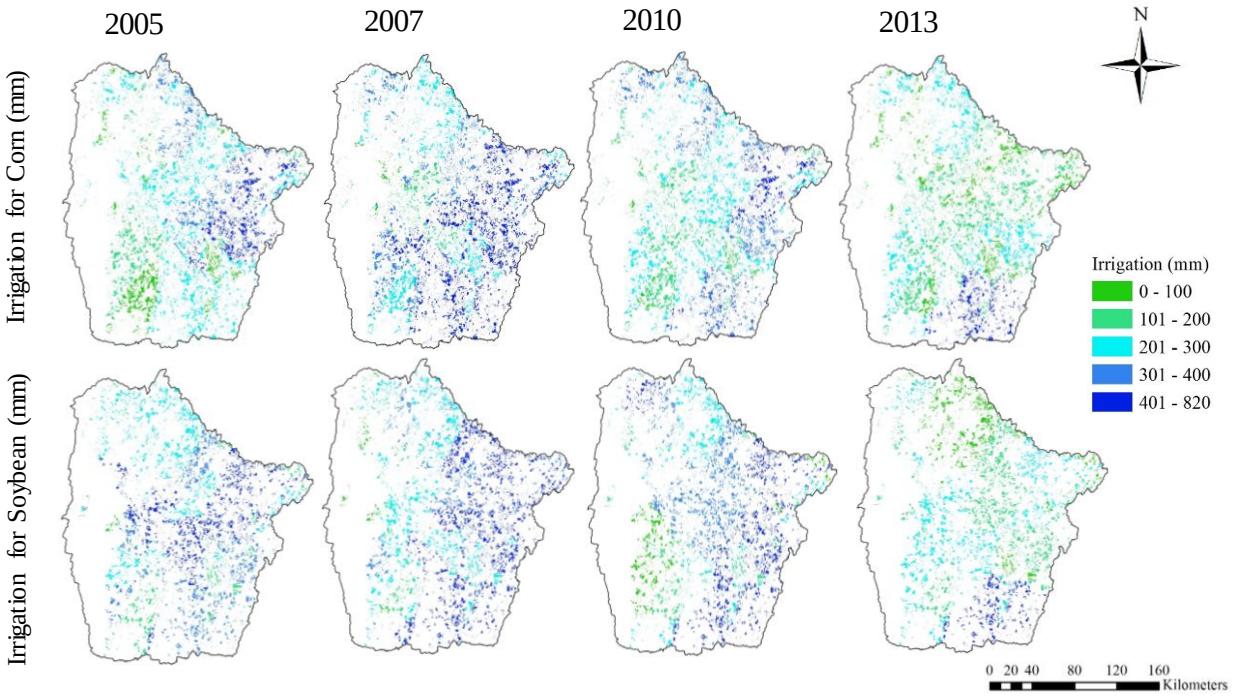

Figure 5: Simulated irrigation amount for corn and soybean production. Maps are presented for four dry years -2005, 2007, 2010, 2013.

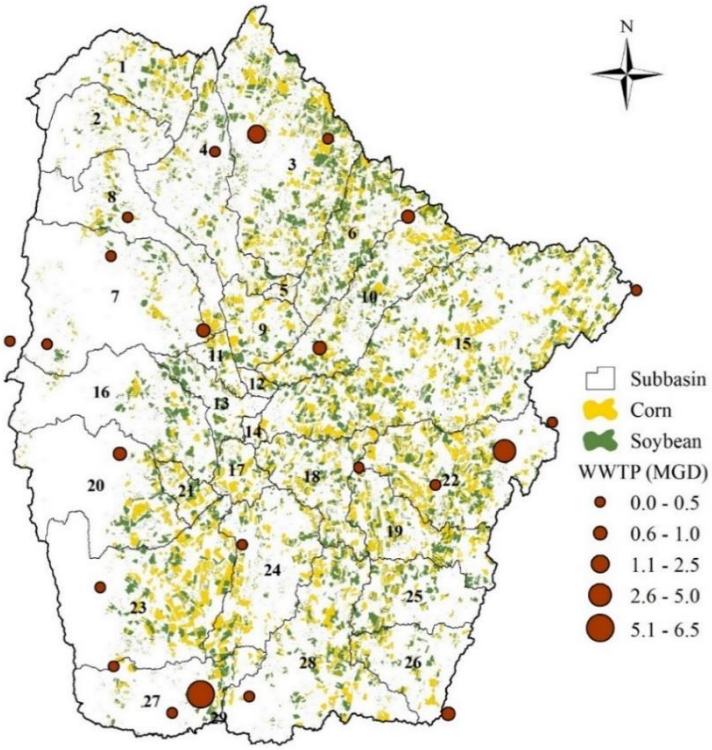

Figure 6: Location of WWTPs, corn and soybean acreage within watershed. Size of the point is showing the capacity of the WWTP.

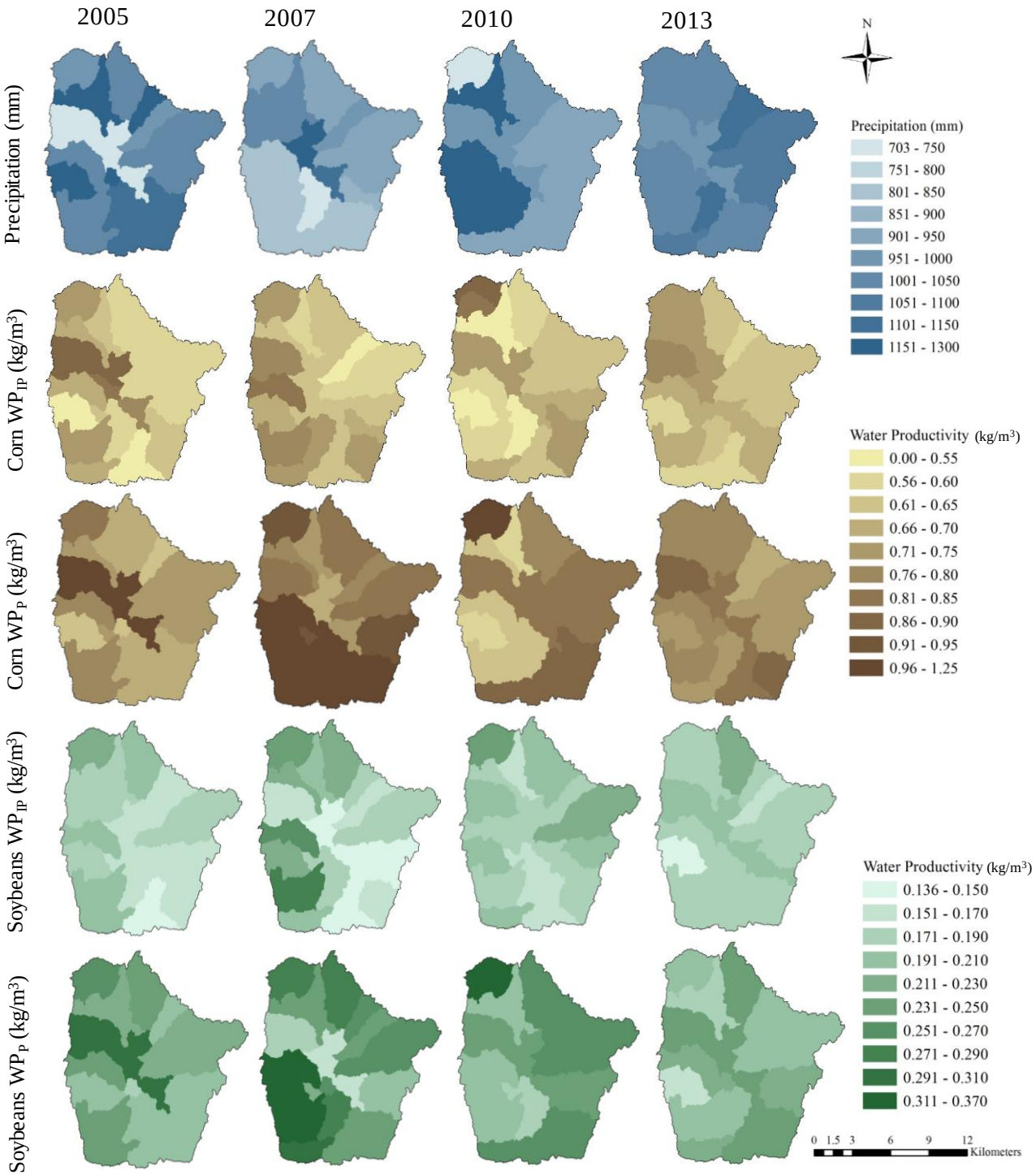

Figure 4: Spatial variability of the total (WPIP) and green water productivity (WPP) for (a) corn and (b) soybean for four dry years: 2005, 2007, 2010, and 2013.

6. Tables

Table 1: Dominant land use and land cover in Monocacy River Watershed.

Land Use & Land Cover	Area (acres)	Area (km^2)	% of Watershed Area
Forest	189307.88	766.10	36.24
Urban Area	68957.65	255.12	12.07
Grassland	1243.05	5.03	0.24
Water	662.31	2.68	0.13
Agricultural Land	76200.67	1085.06	51.33
Hay	75540.25	305.70	14.46
Corn	68321.40	276.49	13.08
Pasture	58279.52	235.85	11.16
Soybean	56368.50	228.12	10.79
Winter Wheat	8315.58	33.65	1.59
Alfalfa	935.82	3.79	0.18
Apple	362.05	1.47	0.07

Table 2: List of parameters used for model calibration and validation.

Parameter	Definition	Initial Range	Calibrated Value
SOL_K	Soil saturated hydraulic conductivity (mm/hr)	-25 to 25	10.95
SOL_AWC	Available soil water capacity (mm H_2O/mm soil)	-25 to 25	3.95
ALPHA_BF	Baseflow recession constant (days)	0.01 to 1	0.680
GW_DELAY	Groundwater delay (days)	1 to 500	113.5
GW_REVAP	Groundwater "revap" coefficient	0.01 to 0.2	0.011
REVAPMN	Re-evaporation threshold (mm H_2O)	0.01 to 500	273.5
GWQMN	Threshold groundwater depth for return flow (mm H_2O)	0.01 to 5000	115.0
CN2	Curve number for moisture condition II	-0.3 to 0.3	0.011
EPCO	Plant uptake compensation factor	0.01 to 1	0.855
ESCO	Soil evaporation compensation factor	0.01 to 1	0.717
CH_N(2)	Main channel Manning's n	0.01 to 0.15	0.059
CH_K(2)	Main channel hydraulic conductivity (mm/hr)	5 to 500	165.2
SFTMP	Snowfall temperature (^oC)	0 to 5	2.1
SMFMN	Melt factor for snow on December 21 (mm H_2O/ ^oC-day)	0 to 10	7.1
SMFMX	Melt factor for snow on June 21 (mm H_2O/ ^oC-day)	0 to 10	7.3
SMTMP	Snow melt base temperature (^oC)	-2 to 5	3.1
TIMP	Snow pack temperature lag factor	0 to 1	0.35

Table 3: Default and adjusted crop yield parameters for corn and soybean applied at HRU scale.

Parameter	Unit	Parameter definition	Corn		Soybean	
			Default	Calibrated	Default	Calibrated
BIO_E	(kg/ha)/(MJ/m^2)	Radiation use efficiency or biomass energy ratio	39	40	25	25
HVSTI	(kg/ha)/(kg/ha)	Harvest index for optimal growing season	0.5	0.5	0.31	0.3
WSYF	(kg/ha)/(kg/ha)	Lower limit of harvest index	0.3	0.3	0.01	0.01
BLAI	(m^2/m^2)	Maximum potential leaf area index	6	6	3	3
DLAI		Fraction of growing season when growth declines	0.7	0.7	0.6	0.5

Table 4: Comparison of model performance for crop yield simulations between rainfed and irrigated conditions.

		With Irrigation		Without Irrigation	
		RYR (%)	RMSE (kg/ha)	RYR (%)	RMSE (kg/ha)
Corn	Calibration	-18.97	1596.8	-24.08	1863.5
	Validation	8.78	610.4	-11.64	873
Soybean	Calibration	-7.48	373.2	23.81	501.8
	Validation	6.23	191.3	32.74	512.2

Table 5: Estimated area of corn and soybean (in km^2) where reclaimed wastewater can be applied from neighboring WWTPs. A list of existing publicly owned WWTPs is included with capacity and discharge method information.

Subbasin No	Area (km^2)		Wastewater Treatment Plant	
	Corn	Soybean	Flow (MGD)	Discharge method
3	3.70	3.06	2.00	Outfall to Surface waters
			0.16	
4	1.22	0.93	0.31	
6	1.79	0.77	0.67	
7	0.19	0.17	0.06	
			0.02	
8	0.43	0.62	0.18	
10	1.45	0.52	0.63	
11	1.65	1.17	0.56	Spray Irrigation
18	0.66	0.36	0.11	Outfall to Surface waters
20	1.03	0.83	0.91	
22	5.8	4.01	3.28	
			0.09	
23	1.91	1.48	0.04	
			0.56	Spray Irrigation
24	0.24	0.17	0.08	Outfall to Surface waters
26	0.85	0.63	0.63	
27, 29	4.52	4.71	6.50	
28	4.41	3.56	3.97	

Chapter 9: Conclusion

1. Summary of Findings

This research provides a decision-making framework that includes both knowledge-based and model-based Decision Support System (DSS) for reclaimed wastewater use in agricultural irrigation. To do so, it has employed a systematic multidisciplinary approach including different disciplines such as hydrology, agricultural science, geography, crop science, and remote sensing.

1.1. MCDA framework

First, suitability areas for recycled water use in irrigation were identified for California (Chapter 3) and Maryland (Chapter 7) using the GIS-MCDA technique. Suitable agricultural lands for reclaimed wastewater irrigation were classified with five classes of Least to Most Suitable. Multiple criteria and sub-criteria were selected based on existing information about water reuse policy, suggested uses, water demand, and environmental-climate conditions for agricultural irrigation. Selected main criteria were: i) agricultural land information including crop types and location, ii) WWTP information including location, flow capacity, and treatment appropriateness, iii) climate condition, iv) groundwater vulnerability, and v) freshwater consumption by the agriculture sector. Based on WWTPs' proximity, sufficient water availability, the "Most Suitable" and "Moderately Suitable" agricultural areas were found to be approximately 145.5 km2, and 276 km2 for California and, 26.4 km2 and 798.8 km2 for Maryland, respectively.

A similar GIS-MCDA framework was applied for Maryland. However, the selection of alternative criteria (different flow category or proximity limit) and

suitability indicators (different users) and assigning weights were different from the California case study. Another difference was that instead of "freshwater consumption" criteria, a groundwater vulnerability map was generated for Maryland. To generate the groundwater vulnerability map, well density, withdrawal rate, and aquifer characteristics were considered. The generated geospatial vulnerability map was used to classify the suitable agricultural lands for reclaimed wastewater use for irrigation (Figure 3 and 7 in Chapter 7). For Maryland, 0.5% (26.4 km2) and 14.44% (798.8 km2) of total agricultural lands were selected as high and moderate suitable areas for reclaimed wastewater use. However, future modifications on water reuse regulations (i.e., permitting vegetable irrigation) can increase the suitable areas. This study also showed the evidence that modifications in irrigation practices and water reuse policies could change the amount of suitable areas.

1.2. Hydrologic Model

In the next phase of this study, hydrologic modelling was used in the decision-making framework to evaluate the different irrigation management scenarios to assess the optimal management solution. Two hydrologic models were developed using the Soil and Water Assessment Tool (SWAT) for two watersheds representing both study areas. The objective was to explore the reclaimed wastewater use potentiality for agriculture irrigation and compare its cost-effectiveness with baseline condition.

1.2.1. Calibration and Validation Process:

San Joaquin Watershed (SJW) was selected within California state, which has a diverse crop pattern with an extensive irrigation operation that features very complex hydrology phenomena. Therefore, an extensive calibration technique with the

quantification of parameter uncertainty was performed for this watershed to predict the streamflow (Chapter 4). Chapter 4 described the model calibration, uncertainty, and sensitivity analysis in detail. This chapter focuses on the California watershed, which has the most complex hydrological process because it is influenced by unregulated water management through intricate irrigation and reservoirs systems. Even with extended calibration techniques, it was challenging to predict its complex hydrologic and biophysical dynamics with limited observation. As a result, a robust remotely sensed Leaf Area Index (LAI) assimilation technique was applied to improve the models' streamflow and crop yield computation (Chapter 5). This improved model was then used to evaluate the water productivity for different irrigation scenarios, including reclaimed water use as an irrigation source.

The Monocacy River Watershed (MRW) was selected for water productivity analysis in Maryland. Unlike the SJW case study, the calibration technique for MRW was less tedious, and the number of calibrated parameters and their ranges were different than SJW. In addition, the agricultural system of MRW is defined as rainfed with minimal irrigation application. A holistic approach was taken for this watershed, where watershed streamflow and crop yield were simulated, considering both rainfed and irrigated systems (Chapter 8). Calibrated SWAT models were used to analyze the multiple irrigation management scenarios that are best suited for watershed characteristics (i.e., climate, irrigation policy, etc.). These scenarios were developed to explore the best adaptive strategies, including recycled wastewater use.

1.2.2. Reclaimed Wastewater Use

Implemented irrigation scenarios were evaluated by using the "what if" scenarios. The rationale of these "what-if" conditions described in detail in Chapter 6 (SJW, California) and Chapter 8 (MRW, Maryland). Both spatial and temporal variability of irrigation consumptive water use and its water productivity (WP) were analyzed at the Hydrologic Response Unit (HRU) and subbasin level. Based on this, the potential of treated wastewater use was assessed to provide information for future policy implications. The reclaimed wastewater use scenario was developed through treated wastewater from existing WWTPs as a valuable alternative for emergency agricultural water (e.g., drought season) and to reduce freshwater (i.e., groundwater) withdrawal. Due to the limitation of enough economic data, crop water productivity (volume of freshwater consumption for a unit crop production) was estimated for each scenario. By comparing the WP between different irrigation scenarios, this study provides quantitative information indicating where improvements are needed.

In California, using reclaimed wastewater is not only a common practice among farmers in some regions but also competitively sought after by many different users. Therefore, several irrigation saving scenarios were applied for the California watershed based on recommendations from various field studies (Chapter 6, Section 2.2, Table 1). Then, the water reuse scenario was applied coupled with these scenarios. Since large amounts of water are applied as irrigation, a very small number of almond and grape areas were selected for treated wastewater use from the existing WWTP (Chapter 6, Figure 1, Table 2 & 3). The combination of auto irrigation (AI) and regulated deficit irrigation (RDI) resulted in WP more than 0.50 kg/m^3 for both

almond and grape. Across different irrigation applications, productivity related to ET losses (WP_{ET}) varied from 0.35 to 0.78 kg/m^3 for almond and from 0.31 to 1.1 kg/m^3 for grape, respectively. The model simulation also showed that wastewater reuse in separate almond and grape irrigation could reduce groundwater consumption more than 74% and 90% under RDI and AI scenarios, respectively.

However, in Maryland watersheds, the probable irrigation amount was simulated from the model due to sufficient data scarcity. Based on the model outcomes, water reuse potential was calculated for selected corn and soybean areas, especially for dry years (Chapter 8, Figure 6, Table 5). In addition, the priority zones for irrigation application was mapped from the model outcomes. Due to a small amount of irrigation application, a large number of potential corn and soybean farms were selected for reclaimed wastewater use. Unlike California, in Maryland, farmer's perceptions and willingness to use reclaimed wastewater have not been evaluated yet. Therefore, a 10 km buffer was used based on the GIS-MCDA framework to calculate the irrigated area. During the model simulation period (2005-2014), the average WP for corn and soybean found as 0.617 kg/m^3 and 0.173 kg/m^3, respectively. Model simulations suggested that under the reclaimed wastewater use scenario, the green water productivity (only rainfall) can be improved up to 0.713 kg/m^3 for corn and 0.37 kg/m^3 for soybean.

These results provide evidence that how an integrated knowledge-based system (MCDA) with a model-based (hydrologic model) approach can be used as a powerful tool to support decision making by providing quantitative information for reclaimed wastewater use in agricultural irrigation and freshwater conservation.

2. Research Contribution

An integrated systematic approach, considering the interaction among land use and climate conditions, hydrological cycle, and agriculture management, is needed to evaluate the future adaptive strategies from local to regional scale. Similarly, more detailed exploratory research is needed to implement the water reuse project to provide information to the water resource managers and policymakers. However, very few studies have been found on the decision-making that covers all of the important decision criteria, especially considering multiple climate conditions. This research contributes to reducing the knowledge gaps for the successful implementation of water reuse projects by providing fundamental data and knowledge for the decision making process.

This study is innovative in the sense that it investigates the convergence approach, coupling knowledge-based, and model-driven methods, to evaluate the relationship among multiple decision criteria such as hydrology, climate change (i.e. long-term drought index and climate condition of each region) and agricultural management for different watersheds. This study utilizes the standardized indicators (e.g., water productivity) to interpret the complex hydrological information to water resource managers and policymakers. It also provides a set of realistic irrigation scenarios and their interactions with the socio-economic and environmental aspects within the agricultural system.

This study highlights the conceptual framework for the complex decision support system using both spatially explicit and temporally continuous geospatial and remote sensing data. Such decision support systems can provide valuable information to the

policymakers to evaluate the potentiality of reclaimed wastewater use. The results of this research are not only beneficial for decision-makers in agricultural water resource management, but also, other users such as model developers, researchers, and other entities can benefit from the results.

3. *Direction of future research*

To complement the presented research, it is suggested that more research should be conducted in the following areas:

- In this study, for the MCDA, it was assumed that all criteria were independent, and no possible dependency was considered in the decision-making process. A data-driven approach should be taken to explore the interaction within the criteria and sub-criteria. Of note is this approach needs an extensive dataset to analyze. For future research, it is suggested that other ranking methods (such as ANP and fuzzy analysis) should be applied to consider the potential dependency between decision criteria and sub-criteria.
- Implementing the results of this research requires effective communication between scientists and policymakers, ensuring the application of scientific information to political actions. Therefore, economic and social components should be included in future research.
- Maryland is facing the challenge of excess nutrient loading into the surface water. Reclaimed wastewater use for irrigation could be a solution for nutrient management and recovery. Therefore, it is suggested that the impacts of wastewater reuse on nutrients discharge should be explored in future studies.

Bibliography

Abatzoglou, J. T., et al., 2017. The West Wide Drought Tracker: drought monitoring at fine spatial scales. Bulletin of the American Meteorological Society. 98**,** 1815-1820.

Abbaspour, C. K., 2008. SWAT Calibrating and Uncertainty Programs. A User Manual. Eawag Zurich, Switzerland.

Abbaspour, K., et al., 2015a. A continental-scale hydrology and water quality model for Europe: Calibration and uncertainty of a high-resolution large-scale SWAT model. Journal of Hydrology. 524**,** 733-752.

Abbaspour, K. C., 2013. SWAT-CUP 2012. SWAT Calibration and Uncertainty Program—A User Manual.

Abbaspour, K. C., et al., 2004. Estimating uncertain flow and transport parameters using a sequential uncertainty fitting procedure. Vadose Zone Journal. 3**,** 1340-1352.

Abbaspour, K. C., et al., 2015b. A continental-scale hydrology and water quality model for Europe: Calibration and uncertainty of a high-resolution large-scale SWAT model. Journal of Hydrology. 524**,** 733-752.

Ahiablame, L., et al., 2017. Streamflow response to potential land use and climate changes in the James River watershed, Upper Midwest United States. Journal of Hydrology-Regional Studies. 14**,** 150-166.

Ahmadzadeh, H., et al., 2016. Using the SWAT model to assess the impacts of changing irrigation from surface to pressurized systems on water productivity

and water saving in the Zarrineh Rud catchment. Agricultural Water Management. 175**,** 15-28.

Aldababseh, A., et al., 2018. Multi-Criteria Evaluation of Irrigated Agriculture Suitability to Achieve Food Security in an Arid Environment. Sustainability. 10**,** 803.

Alemayehu, T., et al., 2017. An improved SWAT vegetation growth module and its evaluation for four tropical ecosystems. Hydrology and Earth System Sciences. 21**,** 4449-4467.

Allen, R. G., et al., 1998. FAO Irrigation and drainage paper No. 56. Rome: Food and Agriculture Organization of the United Nations. 56**,** e156.

Almeida Carina, P. C.-L., Eduardo Jauch, and Ramiro Neves, SWAT LAI calibration with local LAI measurements. 2011 International SWAT Conference & Workshops, 2011.

Aminu, M., et al., 2017. Analytic network process (ANP)-based spatial decision support system (SDSS) for sustainable tourism planning in Cameron Highlands, Malaysia. Arabian Journal of Geosciences. 10**,** 286.

Anagnostopoulos, K. P., Petalas, C., 2011. A fuzzy multicriteria benefit-cost approach for irrigation projects evaluation. Agricultural Water Management. 98**,** 1409-1416.

Anane, M., et al., 2012. Ranking suitable sites for irrigation with reclaimed water in the Nabeul-Hammamet region (Tunisia) using GIS and AHP-multicriteria decision analysis. Resources, Conservation and Recycling. 65**,** 36-46.

Angelakis, A. N., et al., 2018a. WATER REUSE: FROM ANCIENT TO MODERN TIMES AND THE FUTURE. Frontiers in Environmental Science. 6**,** 26.

Angelakis, A. N., et al., 2018b. Water reuse: from ancient to modern times and the future. Frontiers in Environmental Science. 6**,** 26.

Arnold, J. G., et al., 2012. SWAT: Model use, calibration, and validation. Transactions of the ASABE. 55**,** 1491-1508.

Arnold, J. G., et al., 1998. Large area hydrologic modeling and assessment part I: model development. JAWRA Journal of the American Water Resources Association. 34**,** 73-89.

Ashraf Vaghefi, S., et al., 2014. Analyses of the impact of climate change on water resources components, drought and wheat yield in semiarid regions: Karkheh River Basin in Iran. hydrological processes. 28**,** 2018-2032.

Assefa, T., et al., 2018. Assessment of suitable areas for home gardens for irrigation potential, water availability, and water-lifting technologies. Water. 10**,** 495.

Atroosh, K. B., et al., 2013. Water requirement of grape (Vitis vinifera) in the northern highlands of Yemen. Journal of Agricultural Science. 5**,** 136.

Ayalew, G., 2014. Land Suitability Evaluation for surface and sprinkler irrigation Using Geographical Information System (GIS) in Guang Watershed, Highlands of Ethiopia. system (FAO, 1976, 1983). 4.

Azarnivand, A., Chitsaz, N., 2015. Adaptive policy responses to water shortage mitigation in the arid regions—a systematic approach based on eDPSIR, DEMATEL, and MCDA. Environmental monitoring and assessment. 187**,** 23.

Bagocius, V., et al., 2014. Multi-person selection of the best wind turbine based on the multi-criteria integrated additive-multiplicative utility function. Journal of Civil Engineering and Management. 20**,** 590-599.

Ballestero, E., Romero, C., 1996. Portfolio selection: A compromise programming solution. Journal of the Operational Research Society. 47**,** 1377-1386.

Bauwe, A., Kahle, P., 2019. Evaluating the SWAT model to predict streamflow, nitrate loadings and crop yields in a small agricultural catchment. Advances in Geosciences. 48**,** 1-9.

Bellvert, J., et al., 2018. Monitoring Crop Evapotranspiration and Crop Coefficients over an Almond and Pistachio Orchard Throughout Remote Sensing. Remote Sensing. 10.

Bertolini, M., et al., 2006. Application of the AHP methodology in making a proposal for a public work contract. International Journal of Project Management. 24**,** 422-430.

Beven, K., Binley, A., 1992. The future of distributed models: model calibration and uncertainty prediction. Hydrological processes. 6**,** 279-298.

Beven, K., Freer, J., 2001. Equifinality, data assimilation, and uncertainty estimation in mechanistic modelling of complex environmental systems using the GLUE methodology. Journal of hydrology. 249**,** 11-29.

Bhattacharya, A., 2018. Changing Climate and Resource Use Efficiency in Plants. Academic Press.

Blasone, R.-S., et al., 2008. Generalized likelihood uncertainty estimation (GLUE) using adaptive Markov Chain Monte Carlo sampling. Advances in Water Resources. 31**,** 630-648.

Boesch, D. F., Comprehensive Assessment of Climate Change Impacts in Maryland. Report to the Maryland Commission on Climate Change, Scientific and …, 2008.

Box, G. E., Tiao, G. C., 2011. Bayesian inference in statistical analysis. John Wiley & Sons.

Brans, J.-P., Vincke, P., 1985. Note—A Preference Ranking Organisation Method: (The PROMETHEE Method for Multiple Criteria Decision-Making). Management science. 31**,** 647-656.

Buckley, J. J., 1985. Fuzzy hierarchical analysis. Fuzzy Sets and Systems. 17**,** 233-247.

Burke, W. D., Ficklin, D. L., 2017. Future projections of streamflow magnitude and timing differ across coastal watersheds of the western United States. International Journal of Climatology.

CBF, 2007. *Climate change and the chesapeake bay : Challenges, impacts, and the multiple benefits of agricultural conservation work* (Reports). Annapolis, MD: Chesapeake Bay Foundation. (2007). Retrieved October 30, 2019, from https://umaryland.on.worldcat.org/search?queryString=no%3A+192021227#/oclc/192021227. 2007.

CCBRM, 2016. Upper Monocacy River Watershed Characterization Plan. https://www.carrollcountymd.gov/media/2326/upper-monocacy-river-characterization-plan.pdf, 2016.

Chen, C. T., 2000. Extensions of the TOPSIS for group decision-making under fuzzy environment. Fuzzy Sets and Systems. 114**,** 1-9.

Chen, H., et al., 2017a. Modeling pesticide diuron loading from the San Joaquin watershed into the Sacramento-San Joaquin Delta using SWAT. Water Research. 121**,** 374-385.

Chen, X., et al., 2017b. Improved modeling of snow and glacier melting by a progressive two-stage calibration strategy with GRACE and multisource data: How snow and glacier meltwater contributes to the runoff of the Upper Brahmaputra River basin? Water Resources Research. 53**,** 2431-2466.

Chen, Y., et al., 2017c. Assessing the Efficacy of the SWAT Auto-Irrigation Function to Simulate Irrigation, Evapotranspiration, and Crop Response to Management Strategies of the Texas High Plains. Water. 9.

Chen, Y., et al., 2013. The spatial framework for weight sensitivity analysis in AHP-based multi-criteria decision making. Environmental modelling & software. 48**,** 129-140.

Chen, Z., et al., 2012. A critical review on sustainability assessment of recycled water schemes. Science of the Total Environment. 426**,** 13-31.

Childers, D. L., Pickett, S. T., Grove, J. M., Ogden, L., & Whitmer, A., 2014. Advancing urban sustainability theory and action: Challenges and opportunities. Landscape and urban planning, 125, 320-328.

Chu, T., et al., Watershed level BMP evaluation with SWAT model. 2005 ASAE Annual Meeting. American Society of Agricultural and Biological Engineers, 2005, pp. 1.

Cozzi, M., et al., 2015. A spatial analysis model to assess the feasibility of short rotation forestry fertigated with urban wastewater: Basilicata region case study. Agricultural Water Management. 159**,** 185-196.

CRWUA, 2017. Colorado River Water Users Association, http://www.crwua.org/ (accessed 15 October 2017).

Davis, J., n.d. Soils of the Central Valley of California. Retrived from http://online.sfsu.edu/jerry/geog317/field/CentralValleyAgFood.pdf

Denver, J., Nardi, M., Thickness of the Surficial Aquifer, Delmarva Peninsula, Maryland and Delaware: US Geological Survey data release. 2016.

Dieter, C. A., et al., Estimated use of water in the United States in 2015. US Geological Survey, 2018.

Dokoohaki, H., et al., 2016. Coupling and testing a new soil water module in DSSAT CERES-Maize model for maize production under semi-arid condition. Agricultural Water Management. 163**,** 90-99.

Dong, F., et al., 2016. Uncertainty-based multi-objective decision making with hierarchical reliability analysis under water resources and environmental constraints. Water Resources Management. 30**,** 805-822.

Duan, Q., et al., 1992. Effective and efficient global optimization for conceptual rainfall-runoff models. Water resources research. 28**,** 1015-1031.

Dujmovi'c, J., A method for evaluation and selection of complex hardware and software systems. CMG 96 Proceedings. Citeseer, 1996.

Eberhart, R., Kennedy, J., A new optimizer using particle swarm theory. Micro Machine and Human Science, 1995. MHS'95., Proceedings of the Sixth International Symposium on. IEEE, 1995, pp. 39-43.

Elshaikh, A. E., et al., 2018. Performance evaluation of irrigation projects: Theories, methods, and techniques. Agricultural Water Management. 203**,** 87-96.

EPA, 2012 Guidelines for Water Reuse. U.S. Environmental Protection Agency. 2012a.

EPA, Clean Watersheds Needs Survey: Report to Congress., 2012b.

EPA, Chesapeake Bay Progress: Wastewater Pollution Reduction Leads the Way. Vol. https://www.epa.gov/sites/production/files/2016-06/documents/wastewater_progress_report_06142016.pdf. U.S. Environmental Protection Agency, 2016.

ESRI, A., 2012. ArcGIS 10.1. Environmental Systems Research Institute, Redlands, CA.

Falkenmark, M., et al., 2004. Balancing water for humans and nature: the new approach in ecohydrology. Earthscan.

Feizizadeh, B., Blaschke, T., 2014. An uncertainty and sensitivity analysis approach for GIS-based multicriteria landslide susceptibility mapping. International Journal of Geographical Information Science. 28**,** 610-638.

Ficklin, D. L., et al., 2009. Climate change sensitivity assessment of a highly agricultural watershed using SWAT. Journal of Hydrology. 374**,** 16-29.

Fontela, E., Gabus, A., The DEMATEL observer. Dematel, 1976.

G. Arnold, J., et al., 2012. SWAT: Model Use, Calibration, and Validation. Transactions of the ASABE. 55**,** 1491.

Gao, J., 2002. Integration of GPS with remote sensing and GIS: reality and prospect. Photogrammetric engineering and remote sensing. 68**,** 447-454.

Garcia, F., et al., 2017. Which objective function to calibrate rainfall–runoff models for low-flow index simulations? Hydrological Sciences Journal. 62**,** 1149-1166.

Garg, K. K., et al., 2012. SPATIAL MAPPING OF AGRICULTURAL WATER PRODUCTIVITY USING THE SWAT MODEL IN UPPER BHIMA CATCHMENT, INDIA. Irrigation and Drainage. 61**,** 60-79.

Gebbers, R., et al., 2011. Rapid Mapping of the Leaf Area Index in Agricultural Crops. Agronomy Journal. 103**,** 1532-1541.

Goldhamer, D. A., et al., 2006. Regulated deficit irrigation in almonds: effects of variations in applied water and stress timing on yield and yield components. Irrigation Science. 24**,** 101-114.

Gronberg, J. A. M., Dubrovsky, N. M., & Kratzer, C. R., 1998. Environemntal setting of the San Joaquin- Tualre Basins, California. Water-Resources Investigations Report, 97, 4205.

Grum, B., et al., 2016. A decision support approach for the selection and implementation of water harvesting techniques in arid and semi-arid regions. Agricultural Water Management. 173**,** 35-47.

Gupta, H. V., et al., 2009. Decomposition of the mean squared error and NSE performance criteria: Implications for improving hydrological modelling. Journal of Hydrology. 377**,** 80-91.

Ha, L. T., et al., 2017. SWAT-CUP for calibration of spatially distributed hydrological processes and ecosystem services in a Vietnamese river basin using remote sensing. Hydrology and Earth System Sciences Discussions. 1-35.

Ha, L. T., et al., 2018. Calibration of Spatially Distributed Hydrological Processes and Model Parameters in SWAT Using Remote Sensing Data and an Auto-Calibration Procedure: A Case Study in a Vietnamese River Basin. Water. 10.

Hajkowicz, S., Higgins, A., 2008. A comparison of multiple criteria analysis techniques for water resource management. European journal of operational research. 184**,** 255-265.

Han, X., et al., 2018. Effects of Crop Planting Structure Adjustment on Water Use Efficiency in the Irrigation Area of Hei River Basin. Water. 10.

Hanjra, M. A., et al., Transforming urban wastewater into an economic asset: Opportunities and challenges. Wastewater. Springer, 2015, pp. 271-278.

Harris, J., et al., 2001. Application of GIS processing techniques for producing mineral prospectivity maps—a case study: mesothermal Au in the Swayze Greenstone Belt, Ontario, Canada. Natural Resources Research. 10**,** 91-124.

Hassani, Y., et al., 2019. An economic-operational framework for optimum agricultural water distribution in irrigation districts without water marketing. Agricultural Water Management. 221**,** 348-361.

Hou, J., et al., 2016. Optimal spatial allocation of irrigation water under uncertainty using the bilayer nested optimisation algorithm and geospatial technology. International Journal of Geographical Information Science. 1-24.

Huang, I. B., et al., 2011. Multi-criteria decision analysis in environmental sciences: ten years of applications and trends. Science of the total environment. 409**,** 3578-3594.

Immerzeel, W. W., et al., 2008. Integrating remote sensing and a process-based hydrological model to evaluate water use and productivity in a south Indian catchment. Agricultural Water Management. 95**,** 11-24.

Jaramillo, M. F., Restrepo, I., 2017. Wastewater Reuse in Agriculture: A Review about Its Limitations and Benefits. Sustainability. 9**,** 1734.

Jhorar, R. K., et al., 2011. Calibration of a distribution of a distributed irrigation water management model using remotely sensed evapotranspiration rates and groundwater heads. Irrigation and Drainage. 60**,** 57-69.

Johnson, L. F., et al., 2003. Mapping vineyard leaf area with multispectral satellite imagery. Computers and Electronics in Agriculture. 38**,** 33-44.

Kabir, G., 2012. Multiple criteria inventory classification under fuzzy environment. International Journal of Fuzzy System Applications (IJFSA). 2**,** 76-92.

Kabir, G., et al., 2014. A review of multi-criteria decision-making methods for infrastructure management. Structure and Infrastructure Engineering. 10**,** 1176-1210.

Keller, A., Keller, J., 1995. Effective efficiency: a water use concept for allocating fresh water resources and irrigation division discussion paper 22. Winrock International, Arlington, Virginia.

Kennedy, J., Eberhart, R., 1995. Proceedings of IEEE international conference on neural networks. Perth, Australia.

Keshavarz Ghorabaee, M., et al., 2016. A new combinative distance-based assessment (CODAS) method for multi-criteria decision-making. Economic Computation and Economic Cybernetics Studies and Research. 50**,** 25-44.

Khoi, D. N., Thom, V. T., 2015. Parameter uncertainty analysis for simulating streamflow in a river catchment of Vietnam. Global Ecology and Conservation. 4**,** 538-548.

Kim, Y., et al., 2013. Prioritizing the best sites for treated wastewater instream use in an urban watershed using fuzzy TOPSIS. Resources Conservation and Recycling. 73**,** 23-32.

Kosko, B., 1992. Neural Networks and Fuzzy Systems: A Dynamical Systems Approach to Machine Intelligence/Book, (No. QA76. 76. E95 K86). Vol. 1Prentice hall.

Kouchi, D. H., et al., 2017. Sensitivity of Calibrated Parameters and Water Resource Estimates on Different Objective Functions and Optimization Algorithms. Water. 9**,** 384.

Krause, P., et al., 2005. Comparison of different efficiency criteria for hydrological model assessment. Advances in geosciences. 5**,** 89-97.

Kumar, N., et al., 2017. SWAT Model calibration and uncertainty analysis for streamflow prediction of the Tons River Basin, India, using Sequential Uncertainty Fitting (SUFI-2) algorithm. Modeling Earth Systems and Environment. 3**,** 30.

Kumar, V., et al., 2016. Adaptation strategies for water supply management in a drought prone Mediterranean river basin: application of outranking method. Science of The Total Environment. 540**,** 344-357.

Lee, S., et al., 2018. Impacts of Global Circulation Model (GCM) bias and WXGEN on Modeling Hydrologic Variables. Water. 10.

Lettenmaier, D. P., Gan, T. Y., 1990. Hydrologic sensitivities of the Sacramento-San Joaquin River Basin, California, to global warming. Water Resources Research. 26**,** 69-86.

Lewis, J., Estimating Irrigation Water Requirements to Optimize Crop Growth (FS-447). University of Maryland Extension, 2014.

Liu, Y. W., et al., 2017. Investigating the impact of surface soil moisture assimilation on state and parameter estimation in SWAT model based on the ensemble Kalman filter in upper Huai River basin. Journal of Hydrology and Hydromechanics. 65**,** 123-133.

Luan, X. B., et al., 2018. Quantitative study of the crop production water footprint using the SWAT model. Ecological Indicators. 89**,** 1-10.

Luck, M., et al., 2015. Aqueduct water stress projections: decadal projections of water supply and demand using CMIP5 GCMs. World Resources Institute.

Lund, J. R., 2016. California's agricultural and urban water supply reliability and the Sacramento–San Joaquin Delta. San Francisco Estuary and Watershed Science. 14.

Luo, Y., et al., 2008. Dynamic modeling of organophosphate pesticide load in surface water in the northern San Joaquin Valley watershed of California. Environmental Pollution. 156**,** 1171-1181.

Ma, T. X., et al., 2019. Enhancing SWAT with remotely sensed LAI for improved modelling of ecohydrological process in subtropics. Journal of Hydrology. 570**,** 802-815.

Macharis, C., et al., 2004. PROMETHEE and AHP: The design of operational synergies in multicriteria analysis.: Strengthening PROMETHEE with ideas of AHP. European Journal of Operational Research. 153**,** 307-317.

Machiwal, D., et al., 2015. Integrated knowledge-and data-driven approaches for groundwater potential zoning using GIS and multi-criteria decision making techniques on hard-rock terrain of Ahar catchment, Rajasthan, India. Environmental Earth Sciences. 73**,** 1871-1892.

Madsen, H., 2003. Parameter estimation in distributed hydrological catchment modelling using automatic calibration with multiple objectives. Advances in water resources. 26**,** 205-216.

Mainuddin, M., et al., 1997. Optimal crop planning model for an existing groundwater irrigation project in Thailand. Agricultural Water Management. 33**,** 43-62.

Mallakpour, I., Villarini, G., 2017. Analysis of changes in the magnitude, frequency, and seasonality of heavy precipitation over the contiguous USA. Theoretical and Applied Climatology. 130**,** 345-363.

Mango, L. M., et al., 2011. Land use and climate change impacts on the hydrology of the upper Mara River Basin, Kenya: results of a modeling study to support better resource management. Hydrology and Earth System Sciences. 15**,** 2245-2258.

Marek, G. W., et al., 2017. Modeling long-term water use of irrigated cropping rotations in the Texas High Plains using SWAT. Irrigation Science. 35**,** 111-123.

Martin, D. M., et al., 2017. An objective method to prioritize socio-environmental water management tradeoffs using multi-criteria decision Analysis. River Research and Applications. 33**,** 586-596.

Masterson, J. P., et al., Assessment of groundwater availability in the Northern Atlantic Coastal Plain aquifer system from Long Island, New York, to North Carolina. US Geological Survey, 2016.

Mikhailov, L., Singh, M. G., 2003. Fuzzy analytic network process and its application to the development of decision support systems. Ieee Transactions on Systems Man and Cybernetics Part C-Applications and Reviews. 33**,** 33-41.

Miller-Robbie, L., et al., 2017. Wastewater treatment and reuse in urban agriculture: exploring the food, energy, water, and health nexus in Hyderabad, India. Environmental Research Letters. 12**,** 075005.

Mirajkar, A., Patel, P., 2016. Multiobjective two-phase fuzzy optimization approaches in management of water resources. Journal of Water Resources Planning and Management. 142**,** 04016046.

Molden, D., Sakthivadivel, R., 1999. Water accounting to assess use and productivity of water. International Journal of Water Resources Development. 15**,** 55-71.

Molina-Navarro, E., et al., 2017. The impact of the objective function in multi-site and multi-variable calibration of the SWAT model. Environmental Modelling & Software. 93**,** 255-267.

Molina-Navarro, E., et al., 2016. Hydrological modeling and climate change impacts in an agricultural semiarid region. Case study: Guadalupe River basin, Mexico. Agricultural Water Management. 175**,** 29-42.

Montas, H., Shirmohammadi, A., Azar, M., Leisnham, P., 2019. Relationships Between Coefficients of Determination and Correlation, Bias, and Regression, 2019 ASABE Annual International Meeting. Doi: 10.13031/aim.201901248

Monteith, J., Evaporation and environment. Symp. Soc. Exp. Biol, Vol. 19, 1965, pp. 4.

Monteith, J. L., 1977. Climate and the efficiency of crop production in Britain. Philosophical Transactions of the Royal Society of London. B, Biological Sciences. 281**,** 277-294.

Montgomery, B., et al., 2016. A GIS-based Logic Scoring of Preference method for evaluation of land capability and suitability for agriculture. Computers and Electronics in Agriculture. 124**,** 340-353.

Moriasi, D. N., et al., 2007. Model evaluation guidelines for systematic quantification of accuracy in watershed simulations. Transactions of the ASABE. 50**,** 885-900.

Moriasi, D. N., et al., 2015. Hydrologic and water quality models: Performance measures and evaluation criteria. Transactions of the ASABE. 58**,** 1763-1785.

Morton, L. W., Olson, K. R., 2014. Addressing soil degradation and flood risk decision making in levee protected agricultural lands under increasingly variable climate conditions. Journal of Environmental Protection. 5**,** 1220.

Mount, J., Hanak, E., 2014. Water use in California. Public Policy Institute of California (PPIC).

Muleta, M. K., 2011. Model performance sensitivity to objective function during automated calibrations. Journal of hydrologic engineering. 17**,** 756-767.

Nash, J. E., Sutcliffe, J. V., 1970. River flow forecasting through conceptual models part I—A discussion of principles. Journal of hydrology. 10**,** 282-290.

Neitsch, S. L., et al., Soil and water assessment tool theoretical documentation version 2009. Texas Water Resources Institute, 2011.

Neji, H. B. B., Turki, S. Y., 2015. GIS–based multicriteria decision analysis for the delimitation of an agricultural perimeter irrigated with treated wastewater. Agricultural Water Management. 162**,** 78-86.

NOAA, National Oceanic and Atmospheric Administration, Climatological data annual summary Maryland and Delaware 2001: National Climate Data Center,v.125, no.13, p.3-4., 2002.

NWRI, National Water Research Institute, Review of California's Water Recycling Criteria for Agricultural Irrigation : Recommendations of an NWRI Independent Advisory Panel. https://www.waterboards.ca.gov/drinking_water/certlic/drinkingwater/documents/recharge/NWRI_AgPanelReportforCDPHFINAL-09-2012.pdf (accessed 15 June 2017). 2012.

O'Keefe, T. C., Elliott, S. R., & Naiman, R. J., 2012. Introduction to watershed ecology. Printed Lecture Note, University of Washington, USA.

Opricovic, S., 1998. Multicriteria optimization of civil engineering systems. Faculty of Civil Engineering, Belgrade. 2**,** 5-21.

Opricovic, S., 2011. Fuzzy VIKOR with an application to water resources planning. Expert Systems with Applications. 38**,** 12983-12990.

Palazzoli, I., et al., 2015. Impact of prospective climate change on water resources and crop yields in the Indrawati basin, Nepal. Agricultural Systems. 133**,** 143-157.

Pathak, T. B., et al., 2018. Climate change trends and impacts on california agriculture: a detailed review. Agronomy. 8**,** 25.

Patil, A., Ramsankaran, R., 2017. Improving streamflow simulations and forecasting performance of SWAT model by assimilating remotely sensed soil moisture observations. Journal of Hydrology. 555**,** 683-696.

Paul, M., Impacts of Land Use and Climate Changes on Hydrological Processes in South Dakota Watersheds. 2016.

Paul, M., Negahban-Azar, M., 2018. Sensitivity and uncertainty analysis for streamflow prediction using multiple optimization algorithms and objective functions: San Joaquin Watershed, California. Modeling Earth Systems and Environment. 1-17.

Paul, M., et al., 2020. Assessment of agricultural land suitability for irrigation with reclaimed water using geospatial multi-criteria decision analysis. Agricultural Water Management. 231**,** 105987.

Paul, M., et al., 2017. Spatial and temporal evaluation of hydrological response to climate and land use change in three South Dakota watersheds. JAWRA Journal of the American Water Resources Association. 53**,** 69-88.

Phogat, V., et al., 2017. Evaluation of crop coefficients, water productivity, and water balance components for wine grapes irrigated at different deficit levels by a sub-surface drip. Agricultural Water Management. 180**,** 22-34.

Pritchard, T., 2010. Irrigation management of winegrapes with a limited water supply. UC Cooperative Extension http://ucmanagedrought. ucdavis. edu/PDF/WINE-GRAPE% 20DROUGHT% 20LONG-1. pdf.

Punys, P., et al., 2019. A multi-criteria analysis for siting surface-flow constructed wetlands in tile-drained agricultural catchments: The case of Lithuania. Agricultural Water Management. 213**,** 1036-1046.

Rahman, M. M., et al., Use of recycled water for irrigation of open spaces: benefits and risks. Balanced urban development: options and strategies for liveable cities. Springer, 2016, pp. 261-288.

Rajabi, M., et al., 2014. Comparing Knowledge-Driven and Data-Driven Modeling Methods for Susceptibility Mapping in Spatial Epidemiology: A Case Study in Visceral Leishmaniasis. AGILE Digital Editions.

Rajib, M. A., et al., 2016a. Modeling the effects of future land use change on water quality under multiple scenarios: A case study of low-input agriculture with hay/pasture production. Sustainability of Water Quality and Ecology. 8**,** 50-66.

Rajib, M. A., et al., 2016b. Multi-objective calibration of a hydrologic model using spatially distributed remotely sensed/in-situ soil moisture. Journal of Hydrology. 536**,** 192-207.

Ramos, T. B., et al., 2018. Assessing the Impact of LAI Data Assimilation on Simulations of the Soil Water Balance and Maize Development Using MOHID-Land. Water. 10.

RazaviToosi, S. L., Samani, J. M. V., 2016. Evaluating water management strategies in watersheds by new hybrid Fuzzy Analytical Network Process (FANP) methods. Journal of Hydrology. 534**,** 364-376.

Rees, P. L., 2018. Advancing Agricultural Water Security and Resilience Under Nonstationarity and Uncertainty: Evolving Roles of Blue, Green, and Grey Water. Journal of Contemporary Water Research & Education. 165**,** 1-3.

Rikalovic, A., et al., 2014. GIS based multi-criteria analysis for industrial site selection. Procedia Engineering. 69**,** 1054-63.

Ritchie, J. T., 1972. Model for predicting evaporation from a row crop with incomplete cover. Water Resources Research. 8**,** 1204-&.

Rosati, A., et al., 2004. A simple method to estimate photosynthetic radiation use efficiency of canopies. Annals of Botany. 93**,** 567-574.

Rostamian, R., et al., 2008. Application of a SWAT model for estimating runoff and sediment in two mountainous basins in central Iran. Hydrological Sciences Journal. 53**,** 977-988.

Roy, B., 1978. ELECTRE III: Un algorithme de classement fondé sur une représentation floue des préférences en présence de critères multiples. Cahiers du CERO. 20**,** 3-24.

Ruzgys, A., et al., 2014. Integrated evaluation of external wall insulation in residential buildings using SWARA-TODIM MCDM method. Journal of Civil Engineering and Management. 20**,** 103-110.

Saaty, T. L., 1978. Modeling unstructured decision problems—the theory of analytical hierarchies. Mathematics and computers in simulation. 20**,** 147-158.

Saaty, T. L., 1979. Applications of analytical hierarchies. Mathematics and Computers in Simulation. 21**,** 1-20.

Saaty, T. L., The analytical hierarchy process. New York: McGraw-Hill, 1980.

Saaty, T. L., The analytic network process (ANP). RWS Publications, Pittsburgh, Penn, 1996.

Sadeghi, A. M., et al., Assessing the performance of SWAT and AnnAGNPS models in a coastal plain watershed, Choptank River, Maryland, USA. 2007 ASAE Annual Meeting. American Society of Agricultural and Biological Engineers, 2007, pp. 1.

Sadiq, R., Tesfamariam, S., 2009. Environmental decision-making under uncertainty using intuitionistic fuzzy analytic hierarchy process (IF-AHP). Stochastic Environmental Research and Risk Assessment. 23**,** 75-91.

Schilling, K. E., et al., 2014. The potential for agricultural land use change to reduce flood risk in a large watershed. Hydrological processes. 28**,** 3314-3325.

Schulte, P., 2016. Using Recycled Water on Agriculture: Sea Mist Farms and Sonoma County, Pacific Institute Farm Water Success Stories: Recycled Water and Agriculture. http://agwaterstewards.org/wp-content/uploads/2016/08/recycled_water_and_agriculture3.pdf (accessed 16 July, 2017).

Three Reasons the Colorado River Could Dry Up, 2017. Retrived from https://westernresourceadvocates.org/blog/three-reasons-colorado-river-dry/

Service, U. S. C., Section 4: hydrology. In : National Engineering Handbook. SCS, USDA, USA., 1972.

Service, Y. W., 2017. U.S. Climate Data.

Sexton, A., et al., 2011. Impact of parameter uncertainty on critical SWAT output simulations. Transactions of the ASABE. 54**,** 461-471.

Sexton, A. M., et al., 2010. Using NEXRAD and rain gauge precipitation data for hydrologic calibration of SWAT in a northeastern watershed. Transactions of the Asabe. 53**,** 1501-1510.

Shao, W., et al., 2017. Impact of Water Scarcity on the Fenhe River Basin and Mitigation Strategies. Water. 9**,** 30.

Sheikh, B., Recycled water for irrigation of edible crops, prepared for Denver water. 2015.

Siad, S. M., et al., 2019. A review of coupled hydrologic and crop growth models. Agricultural Water Management. 224.

Siebert, J., 2003. California Agriculture: Dimensions and Issues.

Singh, J., et al., 2005. Hydrological modeling of the Iroquois River watershed using HSPF and SWAT. JAWRA Journal of the American Water Resources Association. 41**,** 343-360.

Singh, V., et al., 2013. Hydrological stream flow modelling on Tungabhadra catchment: parameterization and uncertainty analysis using SWAT CUP. Current Science. 1187-1199.

Sinnathamby, S., et al., 2017. Field-scale calibration of crop-yield parameters in the Soil and Water Assessment Tool (SWAT). Agricultural water management. 180**,** 61-69.

Srinivasan, R., et al., 2010. SWAT Ungauged: Hydrological budget and crop yield predicions in the upper Mississippi River Basin. Transactions of the Asabe. 53**,** 1533-1546.

Srinivasan, V., Shocker, A. D., 1973. Linear programming techniques for multidimensional analysis of preferences. Psychometrika. 38**,** 337-369.

Stevens, R. M., et al., 2008. Effect of reduced irrigation on growth, yield, ripening rates and water relations of Chardonnay vines grafted to five rootstocks. Australian Journal of Grape and Wine Research. 14**,** 177-190.

Stevens, R. M., et al., 2010. Reduced irrigation and rootstock effects on vegetative growth, yield and its components, and leaf physiological responses of Shiraz. Australian Journal of Grape and Wine Research. 16**,** 413-425.

Sun, L., et al., 2017a. Hydrological Effects of Vegetation Cover Degradation and Environmental Implications in a Semiarid Temperate Steppe, China. Sustainability. 9.

Sun, L., et al., 2017b. Hydrological Effects of Vegetation Cover Degradation and Environmental Implications in a Semiarid Temperate Steppe, China. Sustainability. 9**,** 20.

Sun, W., et al., 2017c. Physically based distributed hydrological model calibration based on a short period of streamflow data: case studies in four Chinese basins. Hydrology and Earth System Sciences. 21**,** 251.

Sun, X., et al., 2012. Three complementary methods for sensitivity analysis of a water quality model. Environmental Modelling & Software. 37**,** 19-29.

Talib, A., Randhir, T. O., 2017. Climate change and land use impacts on hydrologic processes of watershed systems. Journal of Water and Climate Change. jwc2017064.

Tanaka, S. K., et al., 2006. Climate warming and water management adaptation for California. Climatic Change. 76**,** 361-387.

Teixeira, A. H. D., et al., 2013. Large-Scale Water Productivity Assessments with MODIS Images in a Changing Semi-Arid Environment: A Brazilian Case Study. Remote Sensing. 5**,** 5783-5804.

Thakur, J. K., et al., 2017. Integrating remote sensing, geographic information systems and global positioning system techniques with hydrological modeling. Applied Water Science. 7**,** 1595-1608.

Thiemig, V., et al., 2013. Hydrological evaluation of satellite-based rainfall estimates over the Volta and Baro-Akobo Basin. Journal of Hydrology. 499**,** 324-338.

Trombetta, A., et al., 2016. Calibration of the Aqua Crop model for winter wheat using MODIS LAI images. Agricultural Water Management. 164**,** 304-316.

Tscheikner-Gratl, F., et al., 2017. Comparison of multi-criteria decision support methods for integrated rehabilitation prioritization. Water. 9**,** 68.

Turskis, Z., et al., 2019a. Hybrid group MCDM model to select the most effective alternative of the second runway of the airport. Symmetry-Basel. 11.

Turskis, Z., et al., 2019b. Information security risk assessment in critical infrastructure: a hybrid MCDM approach. Informatica. 30**,** 187-211.

Turskis, Z., et al., 2019c. A hybrid fuzzy group multi-criteria assessment of structural solutions of the symmetric frame alternatives. Symmetry-Basel. 11**,** 20.

Udias, A., et al., 2018. Identifying efficient agricultural irrigation strategies in Crete. Science of the Total Environment. 633**,** 271-284.

Uniyal, B., et al., 2019. Simulation of regional irrigation requirement with SWAT in different agro-climatic zones driven by observed climate and two reanalysis datasets. Science of the Total Environment. 649**,** 846-865.

Uniyal, B., et al., 2015. Parameter identification and uncertainty analysis for simulating streamflow in a river basin of Eastern India. Hydrological Processes. 29**,** 3744-3766.

USDA-ERS, 2018. U.S. and State Farm Income and Wealth Statistics, United States Department of Agriculture Economic Research Service, https://www.ers.usda.gov/data-products/ (accessed 17 May, 2018).

USDA-NASS, C., 2007. Cropland data layer. National Agricultural Statistics.

USGS, 2006. National elevation dataset. US Department of Interior: United States.

USGS-NED, 2013. National Elevation Dataset: United States Geological Survey National Map Viewer. . Available at: http://viewer.nationalmap.gov/viewer/ (accessed 10 March, 2013).

van Griensven, A., Meixner, T., 2006. Methods to quantify and identify the sources of uncertainty for river basin water quality models. Water Science and Technology. 53**,** 51-59.

Vetschera, R., De Almeida, A. T., 2012. A PROMETHEE-based approach to portfolio selection problems. Computers & Operations Research. 39**,** 1010-1020.

Wang, R., et al., 2016. Estimation of the effects of climate variability on crop yield in the Midwest USA. Agricultural and Forest Meteorology. 216**,** 141-156.

Wheeler, J. C., 2003. Freshwater use trends in Maryland, 1985-2000. US Department of the Interior, US Geological Survey.

Williams, J. R., et al., 1989. The EPIC crop growth-model. Transactions of the Asae. 32**,** 497-511.

Williams, L. E., et al., 2010. The effects of applied water at various fractions of measured evapotranspiration on reproductive growth and water productivity of Thompson Seedless grapevines. Irrigation Science. 28**,** 233-243.

Woltersdorf, L., et al., 2018. Benefits of an integrated water and nutrient reuse system for urban areas in semi-arid developing countries. Resources, Conservation and Recycling. 128**,** 382-393.

Worqlul, A. W., et al., 2015. Assessment of surface water irrigation potential in the Ethiopian highlands: The Lake Tana Basin. Catena. 129**,** 76-85.

Wu, H., Chen, B., 2015a. Evaluating uncertainty estimates in distributed hydrological modeling for the Wenjing River watershed in China by GLUE, SUFI-2, and ParaSol methods. Ecological engineering. 76**,** 110-121.

Wu, H., Chen, B., 2015b. Evaluating uncertainty estimates in distributed hydrological modeling for the Wenjing River watershed in China by GLUE, SUFI-2, and ParaSol methods. Ecological Engineering. 76**,** 110-121.

Wu, Y., et al., 2012. Identifying potential areas for biofuel production and evaluating the environmental effects: a case study of the James River Basin in the Midwestern United States. GCB Bioenergy. 4**,** 875-888.

Xu, X. Z., 2001. The SIR method: A superiority and inferiority ranking method for multiple criteria decision making. European Journal of Operational Research. 131**,** 587-602.

Xue, C., et al., 2013. Parameter uncertainty analysis of surface flow and sediment yield in the Huolin Basin, China. Journal of Hydrologic Engineering. 19**,** 1224-1236.

Yalew, S., et al., 2016. AgriSuit: A web-based GIS-MCDA framework for agricultural land suitability assessment. Computers and Electronics in Agriculture. 128**,** 1-8.

Yang, J., et al., 2008. Comparing uncertainty analysis techniques for a SWAT application to the Chaohe Basin in China. Journal of Hydrology. 358**,** 1-23.

Yapo, P. O., et al., 1996. Automatic calibration of conceptual rainfall-runoff models: sensitivity to calibration data. Journal of Hydrology. 181**,** 23-48.

Yesuf, H. M., et al., 2016. Streamflow prediction uncertainty analysis and verification of SWAT model in a tropical watershed. Environmental Earth Sciences. 75**,** 806.

Yildirim, M., et al., 2017. Radiation Use Efficiency and Yield of Pepper (Capsicum annuum L. cv. California Wonder) under Different Irrigation Treatments. Journal of Agricultural Science and Technology. 19**,** 693-705.

Yoon, K., 1980. Systems selection by multiple attribute decision making [Ph. D. thesis]. Manhattan (KS): Kansas State University.

Zabihi, H., et al., 2015. Land suitability procedure for sustainable citrus planning using the application of the analytical network process approach and GIS. Computers and Electronics in Agriculture. 117**,** 114-126.

Zavadskas, E. K., et al., 2013a. MCDM methods WASPAS and MULTIMOORA: Verification of robustness of methods when assessing alternative solutions. Economic Computation and Economic Cybernetics Studies and Research. 47**,** 5-20.

Zavadskas, E. K., et al., 2013b. Multi-criteria assessment of facades' alternatives: peculiarities of ranking methodology. Modern Building Materials, Structures and Techniques. 57**,** 107-112.

Zavadskas, E. K., et al., 2016. Development of TOPSIS method to solve complicated decision-making problems—An overview on developments from 2000 to 2015. International Journal of Information Technology & Decision Making. 15**,** 645-682.

Zhang, F., et al., 2019. Planning seasonal irrigation water allocation based on an interval multiobjective multi-stage stochastic programming approach. Agricultural Water Management. 223**,** 105692.

Zhang, J., et al., 2015a. The comparative study of multi-site uncertainty evaluation method based on SWAT model. Hydrological Processes. 29**,** 2994-3009.

Zhang, J., et al., 2015b. GIS based land suitability assessment for tobacco production using AHP and fuzzy set in Shandong province of China. Computers and Electronics in Agriculture. 114**,** 202-211.

Zhang, L., et al., 2017a. Spatial and temporal variability of temperature, precipitation, and streamflow in upper Sang-kan basin, China. Hydrological Processes. 31**,** 279-295.

Zhang, Y., et al., 2017b. Development of an Evapotranspiration Data Assimilation Technique for Streamflow Estimates: A Case Study in a Semi-Arid Region. Sustainability. 9.

Zou, M. Z., et al., 2018. A new technique to estimate regional irrigation water demand and driving factor effects using an improved SWAT model with LMDI factor decomposition in an arid basin. Journal of Cleaner Production. 185**,** 814-828.